Gwebu, Sandile (2022) *Photochromic materials for potential application in organic electronics.* PhD Thesis, James Cook University.

PHOTOCHROMIC MATERIALS FOR POTENTIAL APPLICATION IN ORGANIC ELECTRONICS

By

Sandile Gwebu

Submitted in total fulfilment of requirement of the degree

DOCTOR OF PHILOSOPHY

in the College of Science and Engineering

JAMES COOK UNIVERSITY
AUSTRALIA

ABSTRACT

Organic photochromic compounds are promising materials for the development of light controllable electronics. The properties of photochromic compounds such as absorption, photoluminescence, oxidation and reduction potentials can be changed reversibly using light. This unique character can be applied in different types of photonic devices. The development of photochromic molecules has primarily focused on the solution or single crystal photonic properties, which have limited applications in organic electronic devices, since these devices typically require uniform thin films.

The aim of this work was to understand structure-property relationships of photochromic molecules and their application in organic electronics.The first project focused on tuning the morphology, optical and thermal properties of solar cell blends using photochromic molecules as additives. Films were prepared and characterized by UV-Vis spectroscopy, atomic force microscopy (AFM), X-ray diffractometry (XRD) and differential scanning calorimetry (DSC) analysis to study their absorption, morphology, crystallinity and thermal properties. Results showed that addition of photochromic additives into solar cell blends decreases the crystallinity, absorption wavelengths, glass transition and melting temperatures of the host polymer. The properties worsened as the additive concentration increased and no photochromic behavior was observed upon irradiating the blends with UV and visible light.

The second part of this work focussed on the synthesis and characterization of solution processable photochromic polymers for potential application in photoswitchable multifunctional organic electronics. Diarylethene-based mainchain photochromic polymers with various alkyl side chains and conjugation lengths were designed and synthesized to enable understanding of the structural requirements for optimal solubility, thin film formation and quality, and photo switching quantum yields.By co-polymerizing diarylethenes with co-monomers with varying conjugation lengths, it was found that the conjugation length of the polymer could be controlled to match the specific light source required for the application. Side-chain length affected polymer solubility, molecular weight and the glass transition temperature while conjugation length affected photoswitching quantum yields. High photoisomerization quantum yields were observed in both solution and film states with minimal photo- and thermal degradation under ambient conditions.Patterning of these polymers was achieved using chemically amplified soft lithography. Based on the observed results, the synthesized polymers are excellent candidates for multi-functional, light-controlled optoelectronic devices such as phototransistors, optical memories and smart solar cells with the ability to simultaneously provide shed and electric energy.

ACKNOWLEDGEMENTS

I would like to thank the following people and organizations:

- My supervisors Professor George Vamvounis and Dr. Bronson Philippa for motivation and guidance throughout the course of my PhD.
- I am very grateful to my supervisor, Professor George Vamvounis for teaching me lab skills and for providing everything to make this work successful.
- Dr. Mark Robertson for the NMR characterization assistance.
- Professor Prashant Sonar and Dr. David Marshall from Queensland University of Technology for help with mass spectroscopy analysis.
- Dr. Shane Askew for help with AFM characterization.
- Dr. Brendan Jones for assistance with XRD characterization.
- Advanced Analytical Centre at James Cook University and the QUT Central Analytical Research Facility for grant me access to their research facilities.
- James Cook University for financial support.
- I thank my friends and fellow HDR candidates for the good times we had together.
- Great appreciation goes to my family for their everlasting love and unending support during difficult times.

STATEMENT OF THE CONTRIBUTION OF OTHERS

Nature of Assistance	**Contribution**	**Names andaffiliations**
Intellectual support	• Proposal writing • Experiment design • Data Analysis	• Professor George Vamvounis andDr Bronson Philippa (JCU)
Experiments	• Synthesis of photochromic molecules: 1,2-bis(2,5-dimethyl-3-thienyl)perfluorocyclopentene and 1,2-bis(2-methyl-5-phenyl-3-thienyl)perfluorocyclopentene • Assistance with mass spectroscopy analysis	• Professor George Vamvounis and Nicholas Sandery (JCU) • Professor Prashant Sonar and David Marshall (QUT)
Financial support	• Fee offset/waiver • Research costs • Stipend	• College of Science and Engineering (JCU) • JCU Graduate Research School
Editorial support	• Thesis writing advice and proof reading	• Professor George Vamvounis (JCU)

PRESENTATIONS

- Sandile Gwebu, Bronson Philippa and George Vamvounis, "Mainchain photochromic polymers: design, synthesis and structure-property relationships", *Queensland Student Chemistry Symposium*, Townsville, Australia, 13-16 July 2021. **Oral presentation.**

  Winner of best presentation prize.

- Sandile Gwebu, Bronson Philippa and George Vamvounis, "Synthesis and application of dithienylethene-based photochromic mainchain polymers", *2022 Royal Australian Chemical Institute (RACI) National Congress*, Brisbane, Australia, 3-8 July 2022. **Oral presentation.**
- Sandile Gwebu, Bronson Philippa and George Vamvounis, "Soft lithography patterning of a diarylethene-based main chain photochromic polymer", *International conference of additive manufacturing for a better world*, Singapore, 22-25 August 2022. **Oral presentation.**

TABLE OF CONTENTS

LIST OF FIGURES

LIST OF SCHEMES

LIST OF TABLES

LIST OF ABBREVIATIONS

AFM	Atomic Force Microscopy
Azo	Azobenzene
CSA	Camphorsulfonic acid
DAE	Diarylethene
DPP	Diketopyrrolopyrrole
DSC	Differential scanning calorimetry
DTE	Dithienylethene
FRET	Förster Resonance Energy Transfer
FTIR	Fourier-transform infrared spectroscopy
GPC	Gel permeation chromatography
HOMO	Highest Occupied Molecular Orbital
LUMO	Lowest Unoccupied Molecular Orbital
MS	Mass spectroscopy
NBS	N-Bromosuccinimide
NLC	Nematic liquid crystals
NMR	Nuclear magnetic resonance spectroscopy
OFETs	Organic field effect transistors
OLEDs	Organic light emitting diodes
OPVs	Organic photovoltaics

OSCs	Organic solar cells
P3HT	Poly(3-hexylthiophene-2,5-diyl)
PCBM	Phenyl-C61-butyric acid methyl ester
PSS	Photostationary state
SP	Spiropyran
TGA	Thermogravimetric analysis
$\mathbf{T_g}$	Glass transition temperature
$\mathbf{T_m}$	Melting temperature
THF	Tetrahydrofuran
UV-Vis	Ultraviolet-visible

CHAPTER 1

INTRODUCTION

1.1. General introduction and aims

Organic photochromic compounds have become an important and evolving research area attracting interest towards the development of various electronic devices such as optical memories,[1] switches,[2] data storage,[3] organic light emitting diodes,[4] logic gates [5] and organic field effect transistors.[6,7] The worldwide commercialization of dyes which change colour upon exposure to light or heat (t-type photochromes) in photochromic sunglasses is the most notable application where photochromic dyes are added to ophthalmic lenses to provide UV protection. A considerable amount of effort has been devoted to developing synthetic methods of producing photochromes and understanding their properties. The last decade has seen an increase in comprehensive studies describing properties of photochromes particularly the dependence of photochromic properties on molecular structure.[2,8–10] Overall, these studies have promoted a deeper understanding of fascinating properties of various classes of photochromes.

The most common classes of photochromic compounds are azobenzene (AZO), spiropyan (SP), fulgimide (FG) and diarylethene (DAE).[9]Azobenzenes and spiropyans undergo thermal-induced (t-type) isomerization reactions whilst the photoisomerization reactions of fulgimide (FG) and diarylethene (DAE) are driven by light, i.e., photo-induced (*p*-type). Among all types of photochromes, diarylethenes are the most attractive because they exhibit great light fatigue resistance and thermal stability. The synthesis and properties of diarylethenes is extensively covered in literature.[11–20]Unfortunately, an often-overlooked important issue is that of practical utility.

Practical applications of photochromic molecules require materials in solid films. Photochromic films can be achieved by blending/doping organic semiconducting polymers with photochromic molecules.[21,22] Unfortunately, this strategy dilutes the photochromes thus making them less than ideal for practical use. At the same, increasing the photochrome concentration in the polymeric media leads to phase separation and segregation which degrades the host polymer's properties.[23]

Polymers containing photochromic moieties on the side-chains have been developed and can be cast into photoswitchable smooth films. Unfortunately, charge conduction, which is required for organic electronic devices is limited due to the lack of intra-chain charge transport.[14,24]This has led to the development of main chain photochromic polymers. The first main chain photochromic polymer was reported byStellacci*et al.* in 1999.[25] Since then, several polymer designs have emerged.However, majority of these polymers have either poor solubility in most common solvents [26] or low molecular weights [25] or poor photoswitching quantum yields in solid state.[27,28] It is challenging to develop photochromic polymers which fulfil all vital properties such as high molecular weight needed to form high quality films, fatigue resistance upon photoswitching, thermal stabilityand high photoswitchingquantum yields in both solution and solid states.

In this thesis, the original concepts will be extended with new ideas and methodologies to understand design requirements of photochromic molecules and their application in organic electronics. The general aim of this study was to design and synthesize photochromic polymers with various conjugation lengths and alkyl side chains to enable understanding of the structural requirements for optimal solubility, thin film formation and photoswitching quantum yields. The idea is further extended to develop a photochromic polymer that can be patterned using soft lithography.

1.2. Thesis outline

Chapter 2

This chapter reviews the recent progress on the synthesis methods and applications of organic photochromic compounds (small molecules and polymers) inelectronics. It begins with a broad classification of diarylethenes into symmetric and asymmetric molecules. The effect of symmetry on the properties of molecules is discussed citing relevant examples from literature. The chapter further reviews the properties of main chain and side chain photochromic polymers. The second part of this review discusses the utilization of organic photochromic compounds in selected applications such as organic field effect transistors (OFETs), sensors, security inks, logic gates, diodes andsolar cells.

Chapter 3

This chapter investigated the effect of doping organic solar cell blends (poly(3-hexylthiophene) (P3HT): phenyl-C60-butyric acid methyl ester (PCBM)) (P3HT:PCBM) with photochromic molecules: azobenzene , 1,3,3-Trimethylindolino-6'-nitrobenzopyrylospiran and 1,2-bis(2,5-dimethyl-3-thienyl)perfluorocyclopentene. Thermal, morphological and optical properties were studied using various techniques to understand if they can be tuned and enhanced using light.

Chapter 4

This chapter covers the design, synthesis and characterization of solution processable fluorene-based photochromic polymers with alkyl side chains of various lengths. A series of alternating copolymers of a dithienylethene with di-*n*-alkyl-fluorene was synthesized by Suzuki-Miyaura cross-coupling polycondensation reactions and their properties were investigated as a function of alkyl chain length. The photochromism of the synthesized polymers was studied in both solution and solid state. The chapter also covers the effect of molecular structure on the thermal properties of the polymers.

Revised manuscript under review (Macromolecules).

Chapter 5

This chapter investigated the effect of conjugation length on optical and photochromic properties of diarylethene-based mainchain polymers. Comonomers with various conjugation lengths were copolymerized with 5-bromo-3-[2-(5-bromo-2-methyl-3-thienyl)-3,3,4,4,5,5-hexafluoro-1-cyclopenten-1-yl]-2-methylthiophene. Optical and photochromic properties were studied as a function of conjugation length. The thermal properties of these polymers are also discussed.

Revised manuscript under review (Macromolecules).

Chapter 6

This chapter covers the synthesis and characterization of an acid-labile diarylethene based mainchain photochromic polymer bearing tetrahydropyran (THP) groups as side chains. THP groups were eliminated *via* an acid-catalyzed reaction to reduce the length of the side chains. This also resulted in the formation of terminal hydroxyl (-OH) groups and the resulting polymer was insoluble. The optical and photochromic properties in solid state before and after deprotection were studied. As proof of concept, soft lithography was used to demonstrate that the polymer film can be patterned using a PDMS stamp.

Manuscript ready for submission to Advanced materials journal.

Chapter 7

This chapter collectively summarizes results obtained in all experimental chapters and recommendations for future work.

THESIS OUTLINE

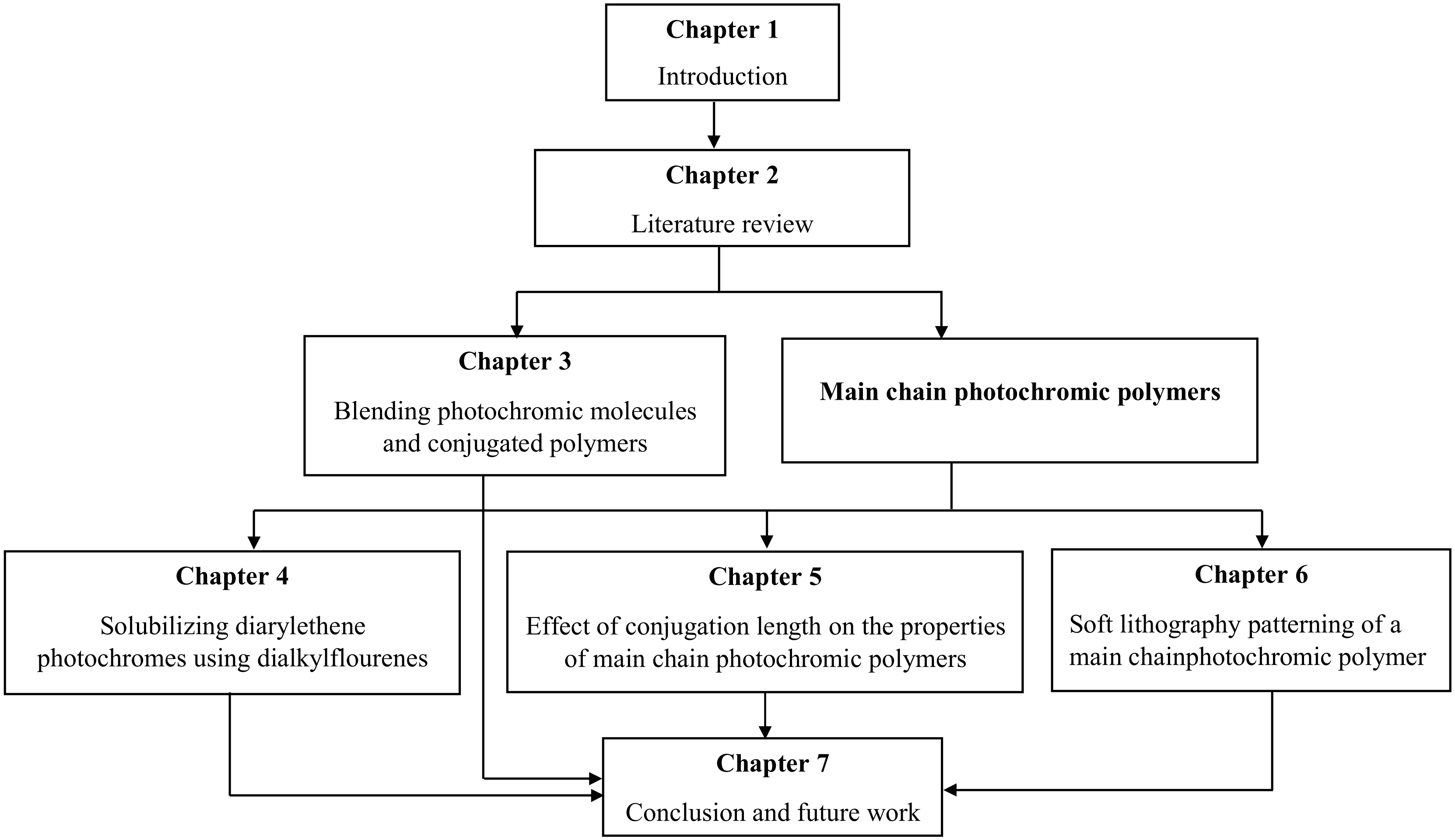

1.3. References

[1] R. C. Shallcross, P. Zacharias, A. Köhnen, P. O. Körner, E. Maibach, K. Meerholz, *Adv. Mater.***2013**, *25*, 469.

[2] M. Irie, T. Fukaminato, K. Matsuda, S. Kobatake, *Chem. Rev.***2014**, *114*, 12174.

[3] H. Qiu, Z. Liu, Y. Yao, M. Herder, S. Hecht, P. Samorì, *Adv. Mater.***2020**, *32*, 1.

[4] Y. Qian, X. Xu, W. Li, J. Wang, B. Wei, Q. Wei, X. Yan, W. Hu, Y. Lu, L. Xie, X. Zhang, W. Huang, *Org. Electron.***2015**, *26*, 476.

[5] X. Chai, Y. X. Fu, T. D. James, J. Zhang, X. P. He, H. Tian, *Chem. Commun.***2017**, *53*, 9494.

[6] L. N. Fu, B. Leng, Y. S. Li, X. K. Gao, *Chinese Chem. Lett.***2016**, *27*, 1319.

[7] M. Carroli, D. T. Duong, E. Buchaca-Domingo, A. Liscio, K. Börjesson, M. Herder, V. Palermo, S. Hecht, N. Stingelin, A. Salleo, E. Orgiu, P. Samorì, *Adv. Funct. Mater.***2020**, *30*, 1907507.

[8] S. Pu, G. Liu, G. Li, R. Wang, T. Yang, *J. Mol. Struct.***2007**, *833*, 23.

[9] A. Fihey, A. Perrier, W. R. Browne, D. Jacquemin, *Chem. Soc. Rev.***2015**, *44*, 3719.

[10] Y. Yokoyama, *Chem. Rev.***2002**, *100*, 1717.

[11] J. C. Micheau, C. Coudret, O. I. Kobeleva, V. A. Barachevsky, V. N. Yarovenko, S. N. Ivanov, B. V. Lichitsky, M. M. Krayushkin, *Dye. Pigment.***2014**, *106*, 32.

[12] H. Xu, S. Wei, C. Fan, G. Liu, S. Pu, *Tetrahedron***2017**, *73*, 6479.

[13] O. Galangau, Y. Kimura, R. Kanazawa, T. Nakashima, T. Kawai, *European J.*

*Org. Chem.***2014**, *2014*, 7165.

[14] H. Nishi, T. Namari, S. Kobatake, *J. Mater. Chem.***2011**, *21*, 17249.

[15] G. Liu, S. Pu, R. Wang, *Org. Lett.***2013**, *15*, 980.

[16] L. Gundogdu, M. Kose, S. Takeuchi, Y. Yokoyama, E. Orhan, *J. Lumin.***2018**, *203*, 568.

[17] G. Liao, D. Xue, C. Zheng, R. Wang, S. Pu, *J. Braz. Chem. Soc.***2016**, *27*, 1989.

[18] A. G. Lvov, M. M. Khusniyarov, V. Z. Shirinian, *J. Photochem. Photobiol. C Photochem. Rev.***2018**, *36*, 1.

[19] Y. Liang, R. Wang, G. Liu, S. Pu, *Spectrochim. Acta Part A Mol. Biomol. Spectrosc.***2018**, *205*, 470.

[20] Q. Zou, X. Li, J. Zhang, J. Zhou, B. Sun, H. Tian, *Chem. Commun.***2012**, *48*, 2095.

[21] M. El Gemayel, K. Börjesson, M. Herder, D. T. Duong, J. A. Hutchison, C. Ruzié, G. Schweicher, A. Salleo, Y. Geerts, S. Hecht, E. Orgiu, P. Samorì, *Nat. Commun.***2015**, *6*, 1.

[22] Y. Li, H. Zhang, C. Qi, X. Guo, *J. Mater. Chem.***2012**, *22*, 4261.

[23] Y. Ishiguro, R. Hayakawa, T. Chikyow, Y. Wakayama, *ACS Appl. Mater. Interfaces***2014**, *6*, 10415.

[24] T. Saika, T. Shimidzuc, M. Irie, *J. Chem. Soc.***1994**, 2123.

[25] F. Stellacci, C. Bertarelli, F. Toscano, M. C. Gallazzi, G. Zotti, G. Zerbi, *Adv. Mater.***1999**, *11*, 292.

[26] C. Bertarelli, A. Bianco, V. Boffa, M. Mirenda, M. C. Gallazzi, G. Zerbi, *Adv. Funct. Mater.***2004**, *14*, 1129.

[27] T. Kawai, T. Kunitake, M. Irie, *Chem. Lett.***1999**, *28*, 905.

[28] H. Choi, H. Lee, Y. Kang, E. Kim, S. O. Kang, J. Ko, *J. Org. Chem.***2005**, *70*, 8291.

CHAPTER 2

LITERATURE REVIEW

2.1. Introduction

Photochromic molecules are compounds that change color due to a reversible conformational isomerism which occurs when the molecule is irradiated with ultraviolet (UV) or visible light. This conformational isomerism causes a change in electronic patterns responsible for properties such as color, luminescence, electronic conductance, refractive index, optical rotation and absorbance.[1,2] Photochromic molecules are promising materials for organic electronics because they are conjugated and their optoelectronic properties can be tuned using light. The most common classes of photochromic compounds are azobenzene (Azo),spiropyan (SP), fulgimide (FG) and diarylethene (DAE), and their isomerization reactions are show in **Figure 2.1**.[3]

Azobenzene-based photochromes undergo structural isomerization at the azo bond, transforming the molecule from trans to cis configuration when irradiated with UV light. Azobenzenes undergo fast, efficient and fully reversible isomerization reactions. The stable linear isomer absorbsin the UV region between 300 nm-400 nm whilst the cis isomer absorbs visible light between 425 nm and 500 nm.[4–7]Spiropyrans absorb in the UV region and undergo 6-π-electrocyclization ring opening reaction toform a highly colored conjugated merocyanine (MC) which absorbs in the visible region.[3] In contrast, fulgimide (FG) and diarylethenes undergo electrocyclization ring closure and opening reactions upon radiation with UV and visible light, respectively.[8–13]Diarylethenes photoisomerization reactions are similar to those of FG.DAEs are the most attractive photochromes for organic electronic applications because they exhibit outstanding light fatigue resistance and thermal irreversibility.[14]

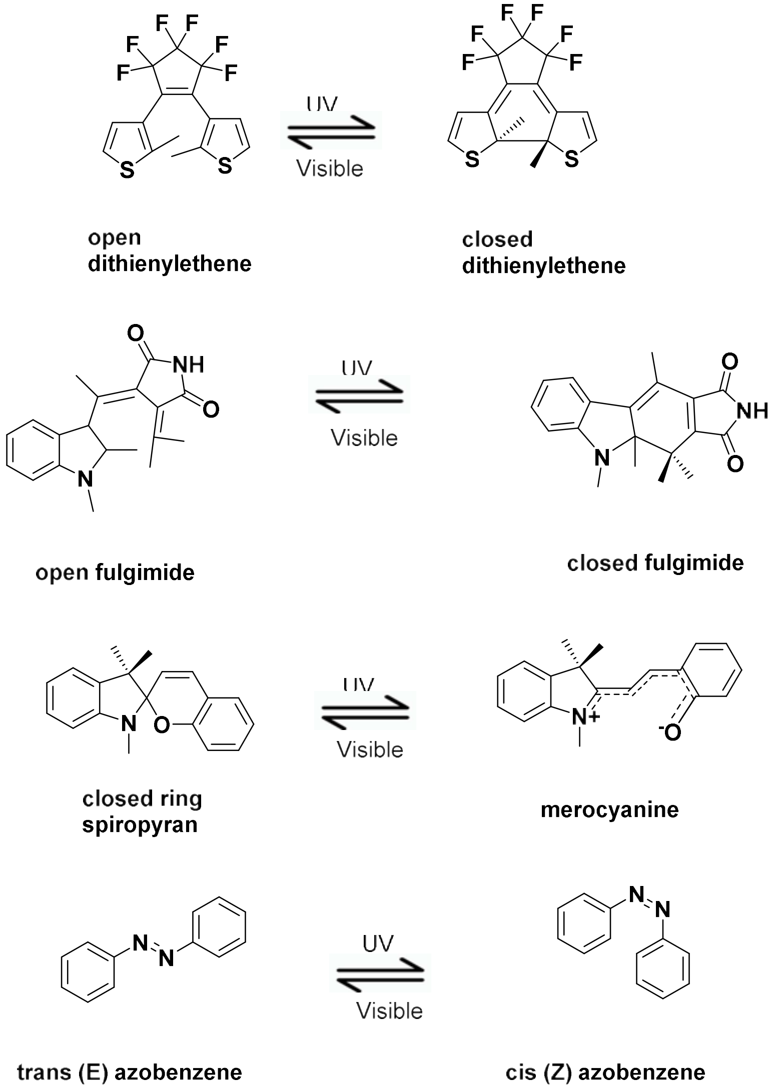

Figure 2.1: Common photochromic molecules and their photoisomerization reactions.[3]

Photochromic materials are utilized as polymers or small molecules in organic electronics. Polymers are classified as either mainchain or sidechain systems depending on the position of the photochromic units in the polymer backbone.[15]If photochromism arises from the main polymer backbone the material is referred to as a mainchain photochromic polymer. Photochromic units can also be attached as side chains on the polymer backbone. The position of the photochromic unit within the polymer backbone influences the properties of the entire polymer such as absorption and photochromic behavior. Small molecule DAEs are either symmetrical or asymmetrical and these structural differences have a significant effect on the properties.Therefore, structural design is the foundation of tuning properties of photochromic compounds. Molecular structure-property relationships and applications of photochromic compounds are discussed in the next sections.

2.1.1. Diarylethenes photochromic molecules

2.1.1.1. Asymmetrical diarylethenes molecules: effect of structure and substituent groups on properties

The symmetry of photochromic molecules has been found to have a significant effect on the absorption and photoswitching properties. For instance, in electronic logic devices asymmetrical diarylethenes have been reported to exhibit better optical performance and faster response to various stimuli compared to symmetrical counterparts.[16–18]Selected examples of asymmetrical diarylethenes molecules are shown in **Figure 2.2**. Triangular terthiophene molecules shown in **Figure 2.2a** were developed to understand the effect of symmetry on the optical properties of DAEs. The maximum absorption of the open-ring isomers displayed a systematic red shift from 1a and 3a due to the introduction of phenyl groups at the 5- and 5″ positions of the thiophene rings. The spectral shifts shown in **Figure 2.2b** and **c** indicate that the π conjugation pathway is connected between position 5- and 5″ of the thiophene ring and is disconnected between the 5- and 5″ positions as shown **Figure 2.2a**. Cycloreversion quantum yields decreased as the conjugation length increased.[19]

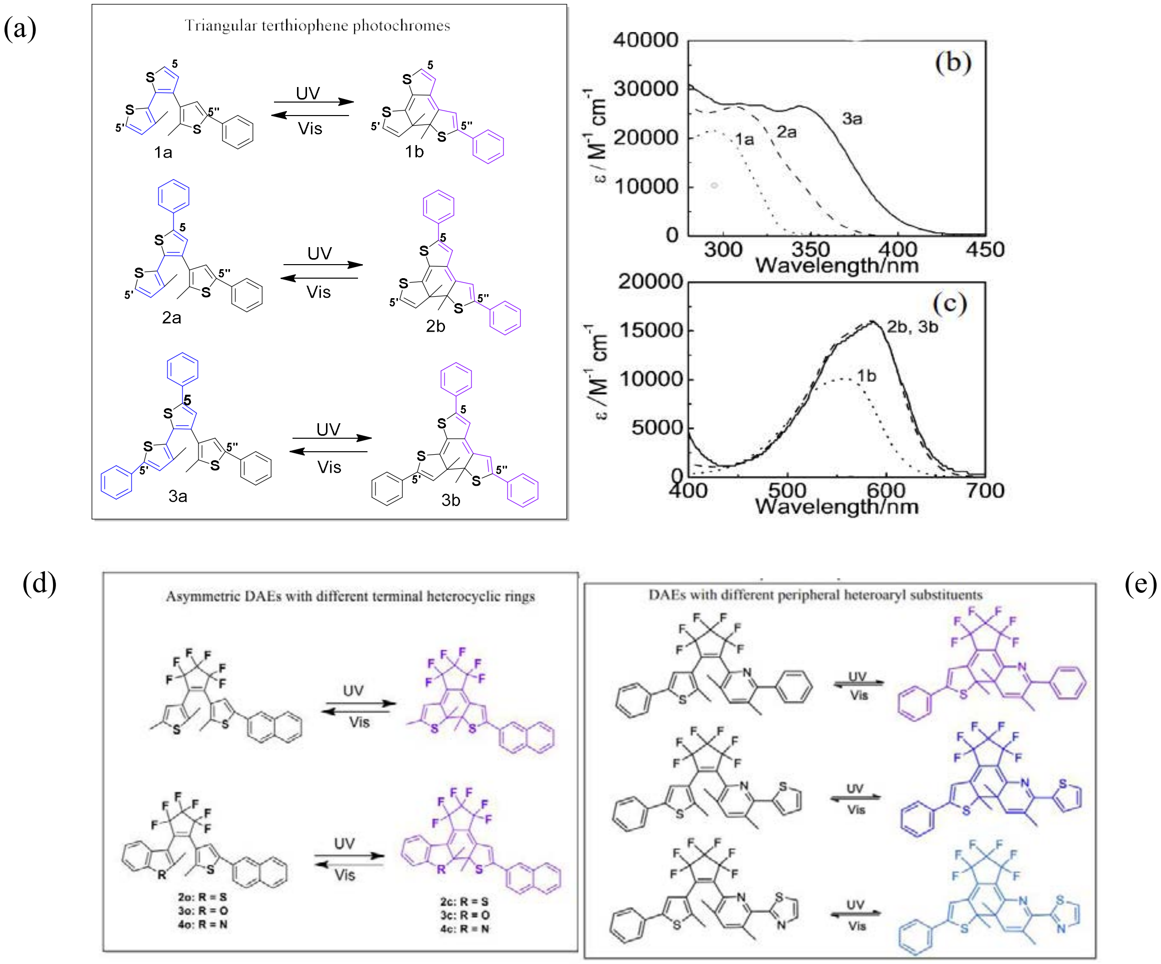

Figure 2.2: Structures of triangular photochromic DTE molecules 1a-3a (a). Absorption spectra of open ring isomers **1a–3a** (b). Absorption spectra of closed ring isomers **1b–3b** (c) Modified with permission from ref.[19] Photochromism of molecules with differentheteroaryl rings (d). Modified with permission from ref.[20]. Structures of diarylethenes with different heteroaryl rings as peripheral substituents (e). Modified with permission from ref.[21]

Asymmetric DAEs are designed by using different terminal heterocyclic rings on either side of the switching motif. The nature of these heterocyclic rings determines the properties of the resulting molecules. Selected structures of asymmetric diarylethenes are presented in **Figure 2.2d and e**. Liang *et al.* investigated the effect of the heteroaryl ring on the photochromism of diarylethene molecules with benzofuran, benzothiophene, indole and thiophene rings. All the four molecules shown in **Figure 2.2d**were photochromic. Notably, the molecules bearing benzothiophene and indole rings showed high cyclization quantum yields in solution and improved fluorescent modulation efficiency in solid state because these heterocycles have low stabilization energies.[20]The properties of asymmetric DAEs can be further tuned by attaching different heteroaryl rings or atoms to the terminal rings as shown in **Figure 2.2e**. Attaching a substituent group at the reactive carbon atom increases the conjugation of the molecules and modulates the optoelectronic and physical properties such as color, photoswitching quantum yields and photoconversion ratios.[21,22]From the structures shown in **Figure 2.2e**, the molecule with a phenylene terminal ring had the lowest cyclization quantum yield of 0.32 which is half that of the other two molecules containing thienyl and thiazyl heteroarlys.High quantum yields of thienyl and thiazyl based molecules were attributed to nitrogen-sulphur heteroatom-contact interactions which stabilized the molecules.

2.1.1.2. Symmetrical diarylethenes molecules: effect of structure and substituent groups on properties

The open form diarylethene isomer has two spatial arrangements in which two aryl groups have C2 and mirror symmetries which are called parallel and antiparallel conformations, respectively, as shown in **Figure 2.3a**.The parallel derivative has low cycloreversion and cyclization quantum yieldswhilst the antiparallel derivative has a higher reaction. Therefore, antiparallel derivatives have promising potential for designing highly photosensitive materials.Symmetricdiarylethenes with various heterocyclic aryl groups such as thiophene, indole, or benzothiophene have been extensively studied owing to their excellent thermal stability, rapid response and fatigue resistance.[14,23–28]Different heterocycles are used to change the conjugation length of the molecules, subsequently the absorption wavelengths and photoswitching quantum yields. Various substituent groups are also attached to the terminal rings to furthertune the properties ofDAEs. Modifying these substituent groups changes the distribution of electrons in the conjugated system in the closed-form isomers resulting in changes in absorption, fluorescence and photochromic properties of DAE molecules. Pu *et al.*[27] investigated the influence of F atom,-OCH_2CH_3 and -$N(CH_3)_2$ groups on the fluorescence and absorption properties of the moleculesshown in **Figure 2.3b**. It was observed that the molecule substituted with a fluorine atom exhibited the highest quantum yields owing to the high electronegativity of the F atom. Changing the substitution position of the F atom also had a significant effect on the properties. Pu *et al.*[29] further investigated the effect of substituent position on the optical properties of molecules shown in **Figure 2.3c**. The highest maxima absorptions of the open-ring and closed-ring isomers were observed for the *meta*-substituted derivative, but its quantum yields of cyclization and cycloreversion reactions were the lowest while the opposite was observed for the *para*- substituted derivative. The values of the *ortho*-substituted derivative were in between those of the *para*-and *meta*-substituted derivatives. The results were attributed to the different electron withdrawing effects when the fluorine atoms were substituted on different carbon atoms of the terminal phenyl rings.

Morimitsu *etal.*[28] investigated the optoelectronic properties of DAE molecules with alkoxy substituents at 2- and 2′- positions of the thiophene rings (**Figure 2.3d**) and the properties were compared to those of an unsubstituted DAE molecule. All the moleculesexhibited photochromic behavior, high quantum yields and thermal irreversibility at high temperatures above 100 °C. There were no significant differences in cyclization quantum yields of molecules 1a, 2a, 3a, and 4a as they were found to be 0.44, 0.48, 0.46 and 0.43, respectively. The cycloreversionquantum yields of molecules 1b, 2b, 3b and 4b were estimated to be1.7×10^{-5}, 2.5×10^{-4}, 6.6×10^{-4} and 6.4×10^{-4}, respectively. These figures are lower than that of an unsubstituted molecule by a factor of 10^{2}-10^{3} implying bulking substituents suppresses cycloreversion quantum yields. It was also observed that the alkoxy substituents negatively impacted the thermal stability of the colored closed ring isomers at high temperatures as the colors of the molecules faded in less than 60 seconds.[28] Therefore, substituent/functional groups and their positioning must be carefully chosen when designing photochromic molecules.

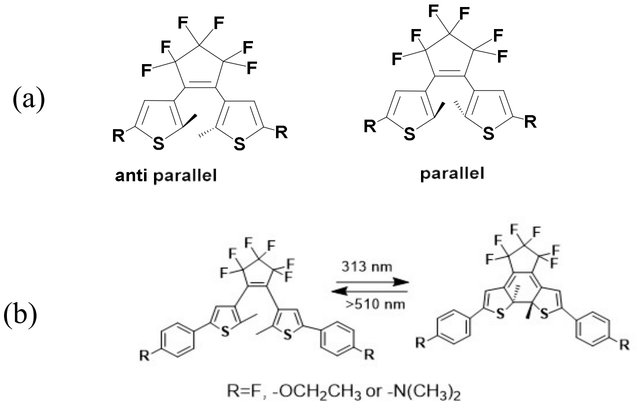

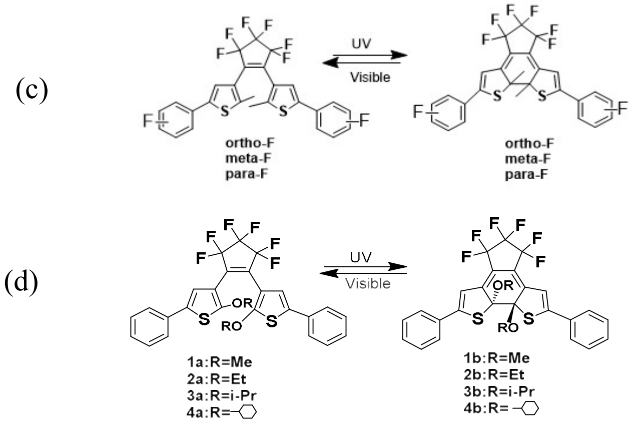

Figure 2.3: General structure of a symmetric DAE molecule (a), structures of symmetric DAE molecules with various substituents groups on the terminal ring (b). Modified with permission from ref. [27]Structures of diarylethene molecules with F substituents on ortho, meta and para positions of the terminal rings (c).[29] Structures of symmetric DAE molecules with various pedant groups (d) Reprinted (adapted) with permission from ref. [28] Copyright 2002 American Chemical Society.

2.1.1.3. Diarylethene polymers with photochromic units in the mainchain: synthesis procedures and properties

Incorporating photochromic switches directly in the conjugated polymer backbone changes the conjugation pathway and subsequently the optoelectronic properties of molecules.[1,30] A handful of mainchain photochromic polymers synthesized by various methods such as Wittig,Honer, Friedländer condensation, ring opening metathesis polymerization (ROMP) and palladium catalyzed cross coupling polymerization have been reported in literature.[1,14,31–33]

The first main chain DTE based polymer shown in **Figure 2.4a** was synthesized by Stellacci*etal.*by $FeCl_3$ oxidative polymerization.[34] The photochromism and thermal stability of the synthesized polymer was found to be higher than that of its monomer. A high cyclization quantum yield of 86% was observed, however, the cycloreversion quantum yield was low at 0.15%. Bertarelli *et al.*[35] used Horner and Wittig polycondensation reactions to prepare conjugated polymers incorporating hexafluorocyclopentene-based switching units and dialkoxyphenylene derivatives:dihexyloxyphenylenevinylene (**Figure 2.4b**)anddidodecyloxyphenylenevinylene(**Figure 2.4c**).High cyclization quantum yields close to 1 were observed for both polymers, unfortunately, cycloreversion quantum yields were very low at 0.005. Moreover, the hexyloxyphenylenevinylene-basedpolymer showed low solubility in chloroform.

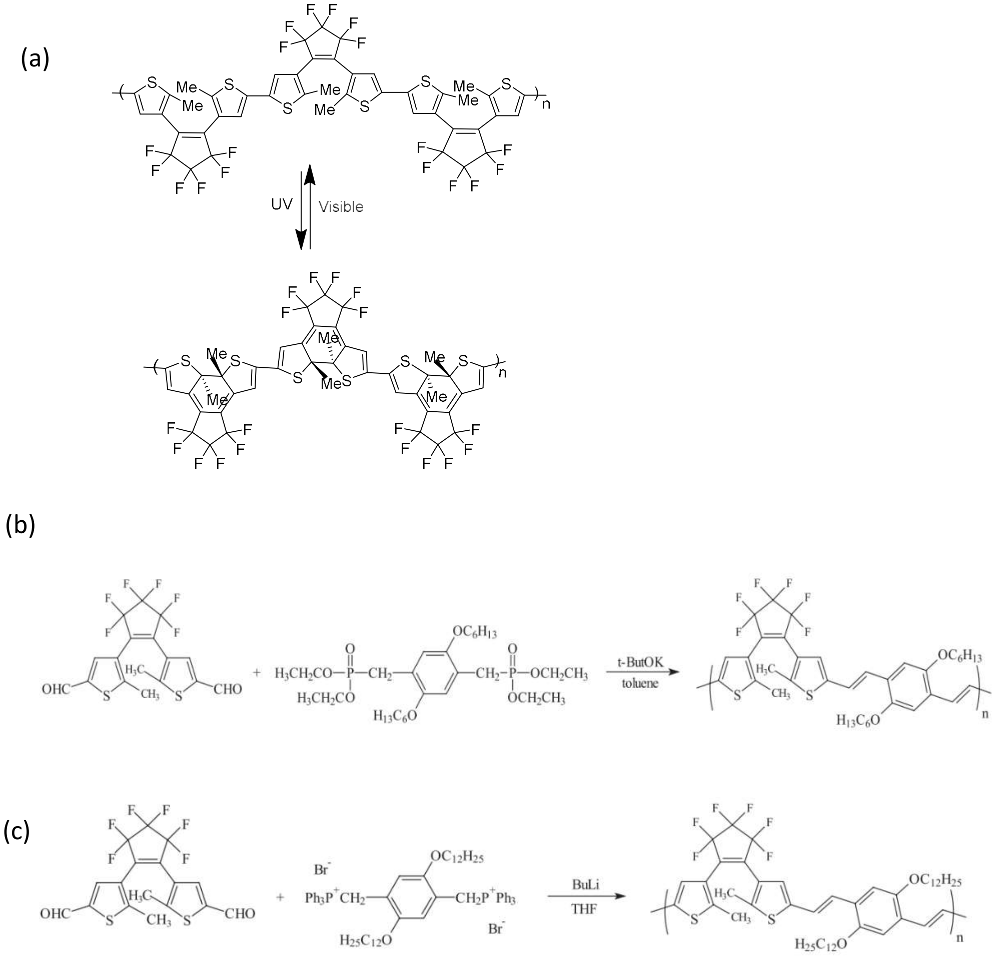

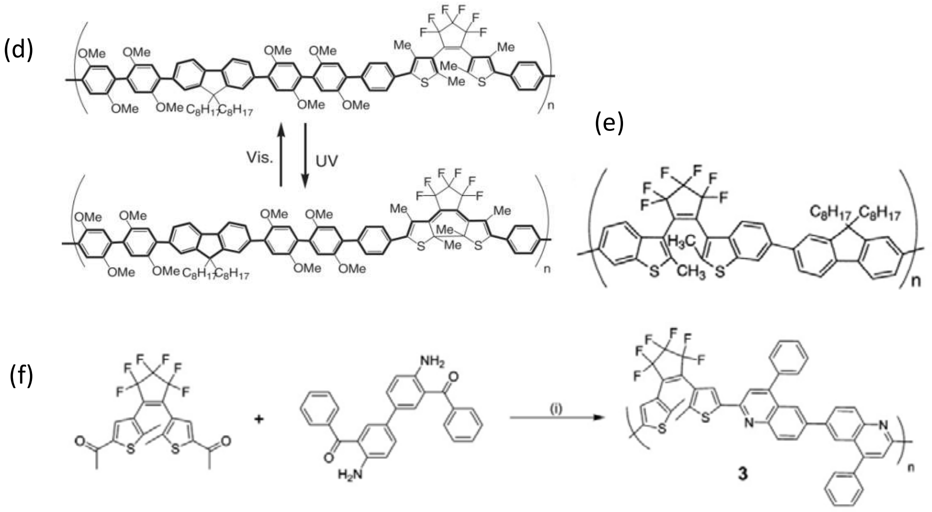

a Reagents and conditions: (i) diphenyl phosphate, *m*-cresol, 135 °C (74%).

Figure 2.4: Selected examples of photochromic DTE mainchain polymers prepared by various polymerization methods: $FeCl_3$ oxidative polymerization[34] (a); Horner reaction[35] (b);Wittig polycondensation reaction[35] (c); Palladium-catalyzed cross coupling polymerization[36–37] (d and e); Friedländer condensation (f).[38]

Kawai and coworkers[36–37]have used palladium-catalyzed coupling reaction to prepare soluble diarylethene-based mainchain photochromic polymers (**Figure 2.4d** and **e**).One example isa main chain photochromic copolymer comprised of benzothiophene switching unit and dioctylfluorene derivative (**Figure 2.4e**). Upon irradiating the polymer solution with UV light, the absorption peak at 340 nm decreased and two new absorption peaks corresponding to closed-ring appeared between 400 nm and 560 nm. The polymer film also exhibited photochromism but the quantum yield was lower than that in solution indicating that the benzothiophene switches do not close readily in solid state. The molecular weight of the polymer shown in **Figure 2.4e**was low at ~6500 g/mol thus making it less ideal for practical application.

Hexafluorocyclopentene-*alt*-phenylquinoline main chain polymer (**Figure 2.4f**) was synthesized by Friedländer condensation method. In solution, high quantum yields of cyclization over 60% were observed, while the corresponding quantum yield of cycloreversion was less 1%.[38] The poor photochromic response of main chain photochromic polymers has been attributed to intramolecular interactions between the dithienylethene units which inhibits the photoswitching action due to large changes in macromolecular conformations required.[1]

2.1.1.4. Diarylethene polymers with photochromic units as the side-chains

Photochromic motifs can be incorporated on polymer backbone as side chain to modulate polymer properties such as absorption and fluorescence.[39,40]**Figure 2.5**shows the structure of a conjugated polymer bearing photochromic DAE units as side chains.

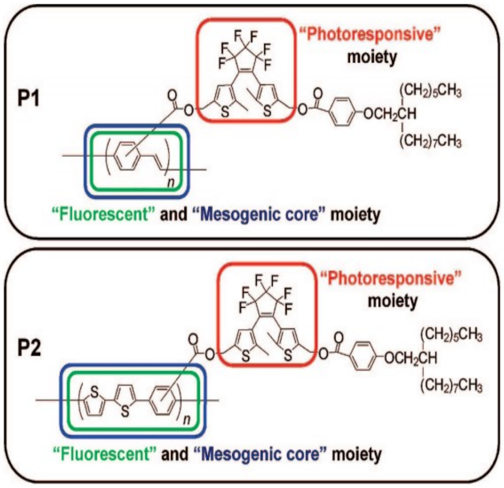

Figure 2.5: Example of a photochromic polymer with DAE side chains.[40]

In this design, the π-conjugated main chain is responsible for the fluorescence behavior, the chiral alkyl groups control the polarization of light and DAE side chains provide the photochromic properties. The fluorescence properties could be modulated by alternate irradiating the molecule with UV and visible light.[41,42]Photoresponsive conjugated polymers have been synthesized by condensation reactions between conjugated polymer backbones and photochromic DTEs as side chains. Unfortunately, intra-chain charge transport is limited in these materials thus making them less than ideal for realistic application.[34,43]

2.1.2. Other types of photochromic molecules: azobenzenes, spiropyrans and fulgides/fulgimides (FG)

2.1.2.1. Azobenzenes

Azobenzenes are the most studied class of photochromic compounds and are important components of thermotropic, lyotropic and polymeric liquid crystals (LCs). The isomerization mechanisms and applications of azobenzene and its derivatives have been reviewed.[3,44–46] Recent research progress demonstrate that ferrocene-based complexes containing azobenzene photochromic units offer greater electrochemical, thermal and photochemical stability compared to pure azobenzene or ferrocene compounds.[44,47,48] Therefore, researchers are now focusing on developing novel ferrocene-azobenzene based photochromic compounds. Polymerizing a ferrocene and an azobenzene results in a polymer containing repeating units of both ferrocene and azobenzene in the main chain. The ratio of ferrocene to azobenzene can be manipulated to produce a polymer with desired properties. It has also been reported that the intramolecular interactions between ferrocenylcentre and the azo group has an effect on the isomerization reactions of ferrocene-azobenzene systems.[49]

Side chain azobenzene polymers are preferred over main chains because they are easy to synthesize, and the distribution sequence of photochromic units can be easily controlled. Azobenzenes units have been incorporated as side-chains on polymer backbones to enhance orientation switching of nematic liquid crystals (NLCs).[50–52] The influence of side-chain azobenzene photochromic units on the properties of liquid crystal block copolymers was reviewed by Shusaku Nagano.[53]

Azobenzene units can be covalently bonded to a conjugated polymer backbone to make materials for fabricating photoresponsive electronics. Tian *et al.*[54] reported a (diketopyrrolopyrrole)-quaterthiophene (DPP) polymer with azobenzene side chains (**Figure 2.6**). The azobenzene groups in the side chains of the DPP polymer could undergo fully reversible trans/cis photoisomerization upon irradiation with UV and visible light. This enabled fabrication of optically tunable field effects transistors.

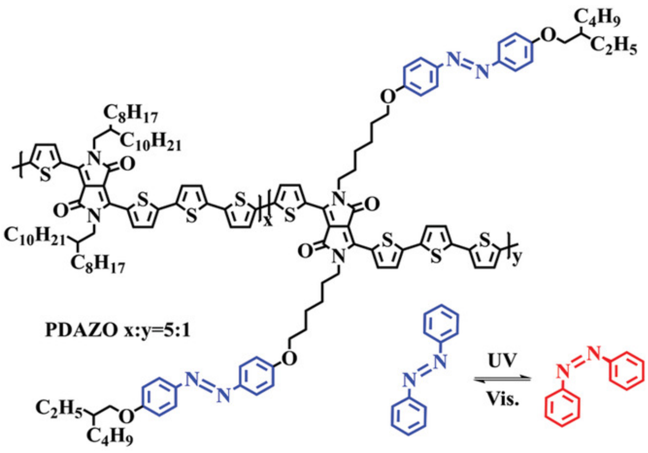

Figure 2.6: Thechemical structure of PDAZO showing randomly distributed azobenzene groups along the conjugated backbone.[54]

2.1.2.2. Spiropyrans (SP) photochromes

A spiropyran is made up of two heteroaromatic rings of which one is a pyran ring **(Figure 2.7)**. The two rings are connected by a sp^3 hybridized spiro carbon atom.

Spiropyrans can maintain their photochromism both in solution and solid matrices such as gels, resins and membranes. Spiropyran-based molecules are usually prepared by condensation reactions involving methylene bases (or their derivatives) and ortho hydroxyl aromatic aldehydes.[54–56] Various synthetic routes for preparing spiropyranmoleculesare discussed in Lukyanov *et al*'s comprehensive review.[56]

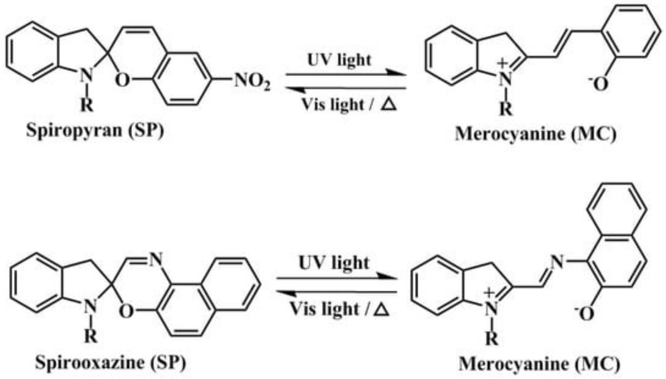

Figure 2.7: Photochromism of a spiropyran molecule.[57]

Spiropyrans are utilized in both monomeric and polymeric form. Their structures can be functionalized to include functional groups which enable them to respond to various stimuli such as pH, temperature, metal ions and redox potentials.[58–60] The influence of spiropyran structure on the photochromic mechanisms and application in chemical sensing, fluorescence probes, data storage, optical and modulators were thoroughly reviewed by Xia *et al.*[57] The most appealing advantage of spiropyran-based composites is their solubility in aqueous media which has enabled their application in biological processes. The major disadvantage of spiropyrans is their poor resistance to light and thermal fatigue.[61]

2.1.2.3. Fulgimides (FG) photochromes

Photochromism of fulgimide is based on a 6π electrocyclic rearrangement (**Figure 2.8**) The properties of FG are similar to those of diarylethenes. FG have been used in holographical and optical data storages owing to their outstanding optical properties, thermal and light fatigue resistance.[62,63]

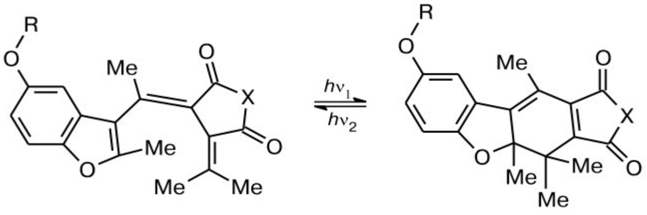

Figure 2.8: Photochromism of fulgimides.

Synthesis of FG depends on the Stobbe condensation reaction for preparing fulgides which are then reacted with primary amines. The Stobbe condensation reaction produces poor yields of fulgides, hence, mass production of FG is challenging and this has hindered practical application of fulgides and fulgimides in electronic devices.[11,62,64]

2.2. Application of photochromic materials in organic electronics

2.2.1. Diarylethenes photochromes in organic field effect transistors (OFETs)

Organic field-effect transistors (OFETs) are one of the most important elements for organic electronics owing to their unique characteristics of flexibility, lightweight, optical transparency and low cost. They are used in diverse electronic applications such as electronic papers, radio frequency identification tags, flexible large area displays, smart memory and sensors devices. OFETs based on conjugated *p*-type and *n*-type organic semiconductors have been developed, their carrier mobilities and electrical characteristics have surpassed that of amorphous silicon.[65–68] However, the commercial application of OFETs is still hindered by the relatively low device performance and long-term stability due to lack of high-performance and air-stable conjugated polymers. These drawbacks can be solved by molecular tailoring OFETs components. Combining traditional OFETs with functional molecular building blocks has attracted too much research interest towards the development of multi-functional OFETs such as phototransistors and light-emitting transistors.[68–70]

Bi-functional OFETs based on photochromic molecules are promising candidates for light sensing and optical memory applications because their switching can becontrolled using light. OFETs are composed of an active layer (also known as the channel layer), dielectric layer and the three electrodes (gate, source and drain electrodes). They also have interfaces such as the electrode/channel layer interface and dielectric/channel layer interface. Both the interfacial and functional layers have great influence on the device performance. Photochromic materials have been used as self-assembled or hybrid channel layers,[71–73] dielectric layers,[74,75] interface materials [67,76] and dopants in OFET channel layers.[71,72] Applications of some photochromes in organic field-effect transistors are extensively discussed in Fu *et al'*s review.[68] Since then, photochromic materials have continued to attract attention towards the development multifunctional OFETs. The next section discusses the recent advances in applications of diarylethenes photochromic molecules in organic transistors.

2.2.1.1. Diarylethenes as OFET active layer components

Photochromes have been investigated as pristine semiconducting components in OFETs. However, the devices suffer from poor charge-transport properties due to low conductivity of photochromes.[71,76] Blending organic semiconducting polymers with a suitable photochromic molecule has been considered as an effective strategy to achieve dual functionalities in OFETs. Carrolli*et al.*[77] investigated the influence of diarylethene photochromes on the morphology and optoelectronic performance of organic thin-film transistors. Film blends of photochromic DAE and P3HT were prepared by mixing P3HT with various regioregularities (regiorandom and regioregular) and molecular weights (M_w = 20–100 kDa) with an open form DAE molecule in chloroform. It was observed that M_w higher or lower than 50 kDanegatively impacts field-effect mobility and results in low device current switchability. The films made with regioregularP3HT exhibited enhanced electrical performance yet accompanied by highphotoresponse. Annealing temperature also had an effect on the photoresponse of the P3HT/DAE-Me blend because the presence of the open form DAE-Me_o loweredthe melting temperature of P3HT, thus assisting in increasing the lamellar crystal thickness without necessarily affecting the overall degree of crystallinity. The ability of DAE-Me to trap the holes transported within the P3HT matrix when in the closed isomer and to detrap them when switched back to the open form depended on the phase separation between the two components. This study proved that regioregularity and annealing temperature must be carefully chosen/controlled during the fabrication process in order to tune the resulting device properties.

Diaryethenes photochromes have recently attracted interest towards the development of ambipolar transistors.[78–80]Ambipolar transistors are a class of transistors in which holes and electrons can transport simultaneously within the channel layer. Kurokawa and coworkers[80] developed an optically switchable OFET composed of a benzothienothiophene-substituted diarylethene (BTT-DAE) channel. The device architecture and photoisomerization of the photochrome is shown in **Figure 2.9.**

In this design, the benzothienothiophene ring is intentionally attached to the switching unit to control the band gap of the molecule. It was observed that the closed-ring isomer formed upon UV light irradiation allows the injection of both holes and electrons from source-drain electrodes into the BTT-DAE layer. The drain current (I_D) – drain voltage (V_D) characteristics of a DAE transistor with a closed-ring isomer for *p*-type and *n*-type operation are shown in **Figure 2.9b**and**c**. The I_D-V_D curve shown in **Figure 2.9b** represents a *p*-type transistor operation.The drain current linearly increased when negative gate voltages were applied. Interestingly, the transistor also displayed a *n*-type operation (**Figure 2.9c**) when a positive V_D was applied. The effect of light irradiation on both electron and hole currents was investigated by measuring drain current while simultaneously applying gate voltages and irradiation with visible light for 30 min. As shown in **Figure 2.9d**and**e**, both I_D-V_D curves indicates typical ambipolar transistor operation. The injection of both holes and electrons was well modulated by controlling the gate voltages. After irradiation with visible light for 30 minutes the drain currents were suppressed due to the cycloreversion of the molecule from closed form to open-ring form.

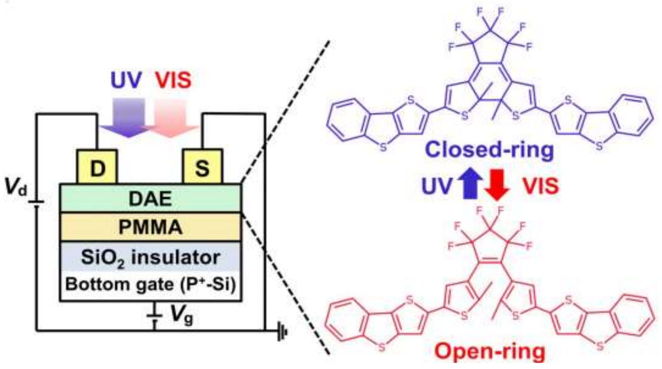

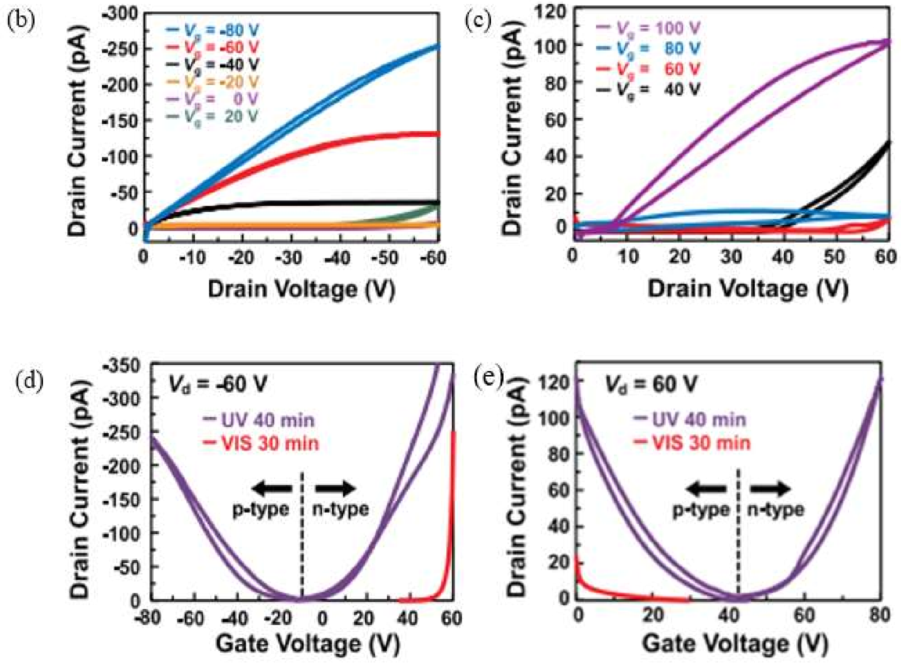

Figure 2.9: Device architecture and photoisomerization of DAE photochrome (a), drain current-drain voltage curves in a BTT-DAE transistor for (b) *p*-type operation and (c) *n*-type operation. The drain current-gate voltage characteristics were measured at (d) $V_D = -60$ V and (e) $V_D = 60$ V.[80]

The modulation of *p*-type and *n*-type charge transport in ambipolar transistors can be enhanced by tuning the energy levels of the semiconducting components. Rekab*et al.*[79] developed a ternany channel by blending a diketopyrrolopyrrole-based polymer with two structurally different photochromic DAE molecules with *ad hoc* energy levels. The photochromic molecules had complementary functions within the polymer matrix thus allowing selective phototuning of holes and electrons. These breakthroughs in ambipolar transistors pave a way towards the development of artificial synaptic transistors, light-emitting transistors and logic devices.

2.2.1.2. Diarylethenes as OFET interfaces

The performance of OFETs is highly dependent on the properties of the interfaces between the layers of the device. The interface trap density affects the device mobility and threshold voltage dramatically.[81] The dielectric/active layer interface is a very important interface in OFETs because it is the site for carrier injection from the semiconductor channel to the dielectric layer. Modification of dielectric/active layer interface by photochromic monolayer is another way for developing photoresponsive OFETs. DAE molecules have been used as OFET interfaces,[71,78,79,82]however, there is limited literature on the influence of DAE structure on OFET performance. Dashitsyrenova*et al.*[83] investigated the effect of the carbonyl group and its position in the ethene bridge of the diarylethene molecule on the electrical performance and stability of OFETs devices. Three photochromes shown in **Figure 2.10a** were used as dielectric/active interfacial self-assembled monolayers in OFET devices with structure shown in **Figure 2.10b.** The difference between TO-1 and TO-2 is the position of the carbonyl group but its effect on the molecule's optoelectronic properties is significant. There were no significant differences in the absorption maxima of the open-form isomers. However, upon irradiation with UV light, the absorption wavelength of photochromes with carbonyl groups shifted to longer wavelengths indicating that introducing a carbonyl functional group in the structure of TO-0 (with λ_{max}=452 nm)results in a strong bathochromic shift as the closed isomers of TO-1 (λ_{max}= 523 nm) and TO-2 (549 nm). All the devices incorporating photochrome TO-0, TO-1 and TO-2 indicated photoresponsiveness upon irradiation with UV and visible light.

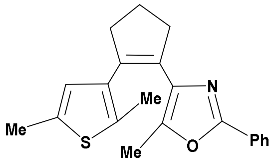

TO-0

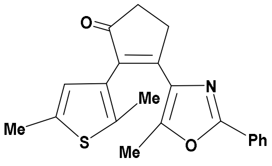

TO-1

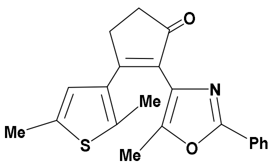

TO-2

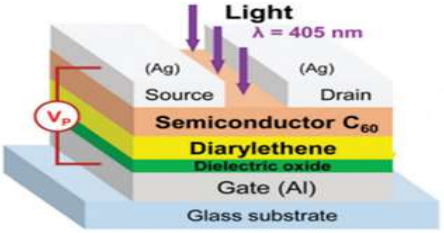

Figure 2.10: Chemical structures of dihetarylethene compounds TO-0, TO-1 and TO-2 (a) and OFET device architecture (b).[83]

The memory characteristics were studied by simultaneously applying an electric bias (programming voltage V_P) between the source and gate electrodes, and irradiating with a laser diode at 405 nm for some time interval (tp). The devices incorporating TO-1 and TO-2 had wider memory windows (~4V) compared to the one with the cyclopentene derivative (TO-0) which had a memory window of ~1.7V. Under negative and positive programming bias, TO-1 had the highest switching coefficients of 5000 compared to 1000 for TO-2 and 600 for TO-0. However, stability studies revealed that devices with TO-0 are the most stable because they retained the highest drain current over 100 000 seconds time interval. Clearly, modifying the chemical structure of the photochrome is an alternative approach for tuning the characteristics of photoswitchable OFETs.

Diaryethene molecules can also be incorporated as interfaces of ambipolar OFETs to modulate the concurrent transportation of hole and electrons from the semiconductor to the electrodes. Qui *et al.*[82] developed an ambipolar transistor in which WSe_2 semiconductor was interfaced with a DAE molecules. The device could simultaneously modulate the transportation of electrons and holes upon stimulation by light. The photo modulation was found to be efficient and reversible with negligible switching fatigue after 20 illumination cycles.

2.2.2. Diarylethenes as sensors

Photochromic molecules are versatile in chemical sensing through colorimetric and fluorometric analysis. Chemical sensors have high sensitivity, simple operation and low cost compared to conventional methods such as inductively coupled plasma emission spectroscopy (ICP-OES) and atomic absorption spectroscopy (AAS) which require expensive instruments, high operating costs, and complicated operating procedures. Photochromes are responsive towards different stimuli such as light, ions, temperature, pH or electric fields.[84] They can also respond to multiple stimuli resulting in multiple signal outputs; hence, they are ideal candidates for multiple analyte sensing. The photoinduced process generates isomers with several recognition units, which can bind with different analytes. Different classes of photochromic materials have been used for various sensing applications. The applications of photochromic molecules in different sensing areas such as metal ions, anions, biomolecules, pH, temperature, multi-analyte discrimination, gas and vapor are discussed in Qin *et al.*'s detailed review.[85]

A wide range of organic molecules such as explosives, toxic vapors and many more pose threats to human lives. For the reason that, the demand for highly sensitive chemo sensors has increased over the past decade. Efficient photoswitcable gas and biological molecule sensors have been developed using photochromic compounds. Wang *et al.*[86] prepared a photochromic diarylethene with a 2-(1H-dithienobenzoimidazole)phenol unit for ion sensing. Its photochromism and fluorescence switching behavior was induced by the presence of either an acid or base. Addition of an acid activated its photochromism enhanced its fluorescence intensity. Upon addition of Al^{3+} the fluorescence intensity of the diarylethene increased by a factor of six and the peak blue-shifted from 500 nm to 469 nm. The photochromic compound also exhibited a "turn-off" fluorescence switching property upon addition of CN^- ions and a color change from blue to dark. A similar photochromic diarylethene with a 2-hydroxybenzhydrazide moiety was reported by Lv*et al.*[87] Its fluorescent switching characteristics were induced by Al^{3+}/EDTA and UV/vis light. Interestingly, it exhibited specific recognition of Al^{3+} and the sensing ability was not affected by interference from other cations and anions.

DTE molecules can beused a single molecules or combined with porous materials or polymer matrices to develop sensing platforms.[85,88]Vamvounis and Sandery[89] developed a colorimetric sensor for nitroaromatics using a single DTE molecule. Upon exposure to UV light the molecule could switch from colorless to pink. Addition of nitroaromatic derivatives suppressed the photoswitchingbehavior of the DTE molecule. However, the molecule could not detect the presence of toluene. The DTE molecule was highly selective and sensitive towards nitroaromatics due to their high molar absorptivity and the good absorption overlap with the DTE.Li *et al.*[90] designed three novel dithienylethene bridged difluoroboron β-diketonate dyes for sensing amine vapors. The structures of the molecules are shown in **Figure 2.11.**

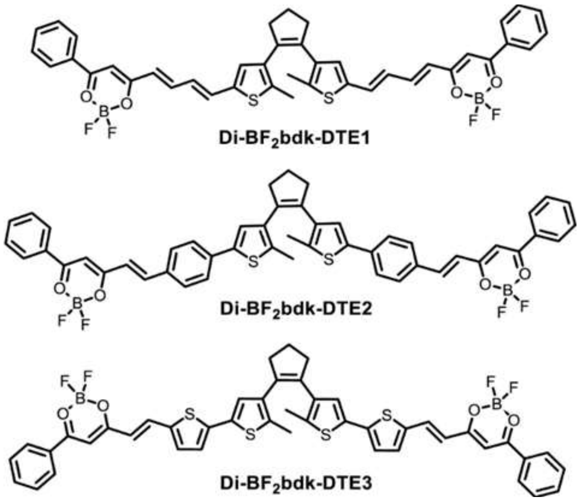

Figure 2.11: Structures of DAE molecules with bridged difluoroboron β-diketonate groups.[90]

In each structure the BF2bdk group acts as an electron acceptor and binding site for amines. The photoisomerization behaviors of the dyes were explored in both solution and solid sates using toluene as a solvent and PMMA as solid film. Upon alternating irradiating with blue light (460–470 nm) and near-infrared light (760–770 nm) all the molecules displayed excellent photochromism and fluorescent switching behaviors in toluene and PMMA film. The differences in conjugated group between the BF2bdk and dithienylethene groups had a significant effect on their photochromic properties. The absorption maxima of open form Di-BF2bdk-DTE1, Di-BF2bdk-DTE2 and Di-BF2bdk-DTE3 were 490, 466 and 516 nm, respectively. Di-BF2bdk-DTE1 displayed the fastest optical response rates to blue light compared to the other two molecules. This was attributed to the antiparallel conformation of the Di-BF2bdk-DTE1 based on electron densities and molecular geometries calculated using the density functional theory (DFT). The dyes also exhibited an outstanding sensing performance for volatile *n*-propylamine vapor in solid state. Upon exposure to *n*-propylamine vapor the NIR absorption peak (at 816 nm) of the closed Di-BF2bdk-DTE1(c) isomer gradually decreased and a new peak at 542 nm appeared. The color changed from yellowish-brown to purple. Changes in UV–Vis absorption and fluorescence spectral of the PMMA films of Di-BF2bdk-DTE2 and Di-BF2bdk-DTE3 towards *n*-propylamine vapor were also observed. The sensitivities of the PMMA dyes towards *n*-propylamine vapor decreased in the following order Di-BF2bdk-DTE1 > Di-BF2bdk-DTE2 > Di-BF2bdk-DTE3.

Glutathione (GSH) sensors based on spiropyran are quite common,[91–93] however, there is a need to simplify the sensor design and further increase the availability, stability, sensitivity and selectivity. Therefore, researchers are now focusing on developing diarylethene-based glucose sensors. Chai[94] developed a simple glycosheet hybrid sensor (Glyco-DTE@MnO_2) for sensing intracellular GSH. The glyco-DTE@MnO_2 sensor was prepared by assembling Glyco-DTE molecules onto the surface of two dimensional MnO_2 nanosheets which quench fluorescence from the Glyco-DTE reporter. The hybrid sensor also had β-ᴅ-galactoside cell-targeting moiety linked with Glyco-DTE which enhanced water solubility and the cell targetability of the Glyco-DTE@MnO_2 sensor. The sensor could undergo decomposition when an overexpressed intra-cellular GSH was detected in HepG2 cell lines following the recovery of the photoswitchable fluorescence signal regulated by Glyco-DTE.

2.2.3. Diarylethenesfor security measures: security inks, molecular keypad locks and logic gates

Protecting information at the molecular level is one of the most effective ways of curbing forgery and fraud. Molecular systems encode, encrypt, conceal and protect data. All these activities lead to improved data security for safe communication and transportation. A molecular keypad is a photochemical device which authorizes password entries whereas a molecular logic gate is a molecule that can perform a logical operation based on physical or chemical inputs and resulting in a single output. The two molecular devices are similar, the major difference is that output signals of a molecular keypad lock are dependent not only on the proper combination of the inputs but also on the correct order by which these inputs are introduced.[95–97] Security inks are one example of molecular keypads for implementing anti-counterfeiting measures, for example in banknotes and passport. Photochromic security inks offer two layers of protection: the use of an external light trigger to make the ink visible and the chemical identity of the compound itself. Various types of photochromes such as the dithienylethenes, fulgimides and azobenzenes have been used to develop keypad locks [97,98] and logic gates.[99–103]Applications and working mechanisms of keypad locks and logic gates are discussed in Andréasson and Pischel's well written tutorial review.[95]

The exclusive use of light to control inputs has been demonstrated before and it has led to further development of photochrome-based security inks [95]. In 2017, Ritchie *et al.*[104] developed photochrome-doped-PMMA polymer films blends for potential application in security inks. The films blends were composed of a green-fluorescent diarylethene molecule with sulfonyl groups (P1) with either a non-fluorescent diarylethene (P2) or a red-fluorescent spiropyran molecule (P3). Förster Resonance Energy Transfer (FRET) occurred between the colored isomers in the films indicating that the diarylethene is working as an intermolecular FRET donor aided by elevation of its excited state lifetime from the sulfonyl modification and polymer environment. FRET is the mechanism of quenching between the fluorophore and chromophore. It is a physical process by which energy is transferred non-radiatively from the excited donor to an acceptor molecule (with overlapping absorbance) by means of long-range dipole-dipole coupling. It was observed that the blend composed of P1+P2 behaved as a photonic keypad lock whereby UV and green light are inputs and green fluorescence is the output as shown in **Figure 2.12 a** and **b**. The main advantage of doping a polymer matrix with a photochrome is that it eliminates some synthetic steps for coupling the photochromes together.[3,96,105] This strategy easily permits the fluorescent FRET donor to be surrounded with multiple nonfluorescent FRET acceptors producing a superior on/off fluorescence ratio. The blends composed of P1+P3 molecules operated as a three-state fluorescent system producing either no fluorescence, green fluorescence or red fluorescence as shown in **Figure 2.12b**.

A tri-component security ink system consisting of a fluorescent donor molecule and two photochromic acceptor molecules encapsulated in polymer micelles was reported by Naren*et al.*[106] Its function relies on orthogonally controlled FRET processes between perylene (a blue emitter) and two diarylethene (DAE) photoswitches emitting green and red light. In this system, UV and blue light are inputs whilst green or red fluorescence are outputs. In molecular logic gates absorption or emission change is recorded as output in response to various inputs such as light irradiation or chemicals. The differences in nature of inputs enable application of molecular logic gates in various fields such as biochemistry, electronics and many more. Redox reactions can also be used as an additional input because electrochromic reactions also trigger the cyclization or cycloreversion of diarylethenes.[99,100]

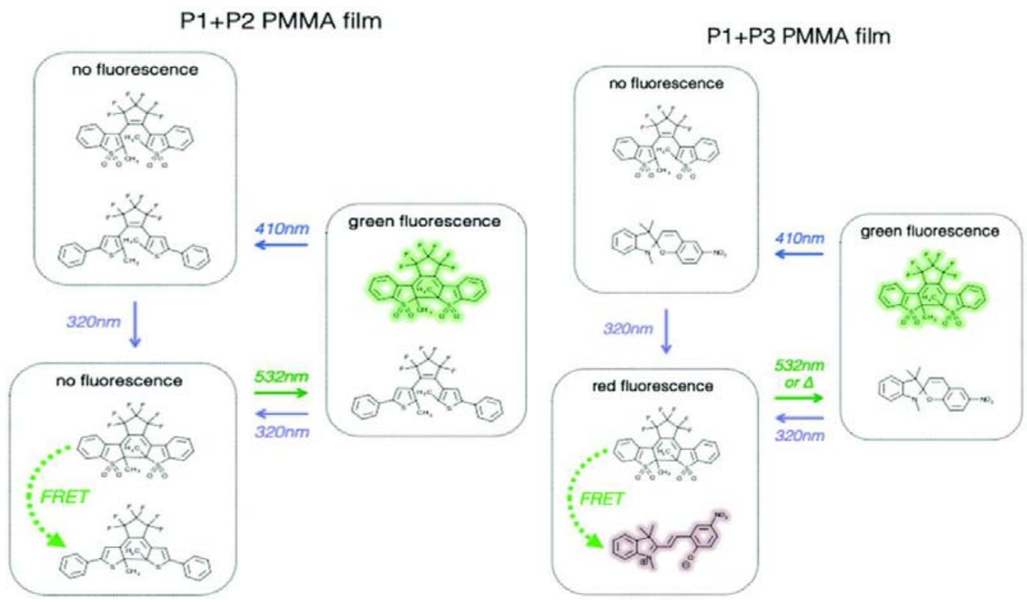

Figure 2.12: Fluorescence characteristics and FRET pathways for the P1+P2 (left panel) and P1+P3 (right panel) PMMA films after irradiation with light of various wavelengths.[104]

Most logic gates reported in literature are based on monomeric diarylethenes and this limits their solubility and multifunctionality.[96,97,100] Polymeric DAE based logic gates have been reported.[99,107]Chai *et al.*[99] reported a water-soluble photochromic bis-glycosyl diarylethene system with a logic gate operation. The polymer was synthesized by a Suzuki coupling reaction between a piperazine group, naphthalimide derivative and a diarylethene molecule.The resulting conjugate was coupled with two β-D-galactosides by a click reaction. The maximum absorption peak was observed at 260 nm. After illumination with UV light (254 nm), the maximum absorption peak at 260 nmdecreased. A new peak at 535 nm was observed and its intensity at 535 nm increased with irradiation time until a photostationary state was reached. The initial yellow color of the aqueous solution gradually turned red, indicating the occurrence of a cyclization process. The initial yellowish was recovered upon irradiation with visible light (>500 nm) indicating a photocycloreversion from closed form to open form. A control compound without a bis-galactoside group was tested under the same conditions. Its aqueous solution did not show any photochromism upon irradiation with UV light. To understand the molecules' response to chemicals, trifluoroacetic acid (TFA) was added to the yellow aqueous solution. The absorbance maxima of the yellow solution blue-shifted from 405 nm to 390 nm and turned colorless. The fluorescence spectrum also showed a blue shift from 525 nm to 515 nm. Neutralization of this solution with triethylamine (TEA) converted the molecule back to its initial state and regenerated low fluorescence. The combination of these independent stimuli led to the development of an aqueous logic gate composed of one molecule. Since the fluorescence of this molecule could be independently stimulated by UV/Vis and TFA/TEA cycling, four stimuli namely; visible light, TFA, UV light and TEA could be used as inputs. The output signal was the change of fluorescence intensity at 520 nm. The limitations of most DAE molecules used for constructing logic gates is that their solid-state properties are not well studied and it is difficult to develop polymeric DAEs due to high structural constrain.

Singh *et al.*[107] developed a photochromic conjugated microporous polymer with logic gate functions. The photochromic conjugated microporous polymer (pcCMP) was synthesized by coupling photochromic dithienylethene aldehyde and benzene-1,3,5-tricarbohydrazide molecules. The synthesized pcCMP showed solid state photochromism upon irradiation with light of different intensities as illustrated in **Figure 2.13**. The UV−vis absorption spectra for the open-form isomer showed two intense absorption bands at 320 nm and 366 nm. These two peaks were also observed in the absorption spectrum of the closed-form isomer and an additional low absorption peak at 622 nm was present. The photoreversibility of the isomers was investigated for 10 cycles and found to be equally faster without any color fading. The pcCMP-C also exhibited some thermo response upon heating at 130°C for 2 minutes. Since the polymer could be stimulated by heat and light, a logic gate with two inputs (UV light and heat) and an output in the form of absorbance at 625 nm could be constructed.

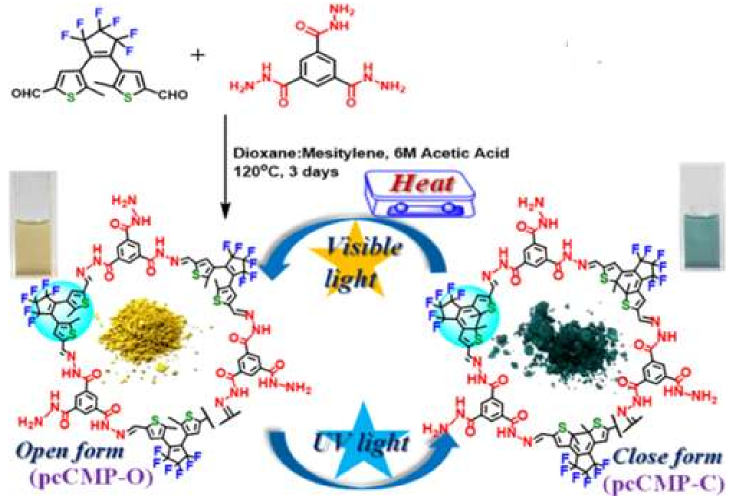

Figure 2.13: Synthetic scheme for the pcCMP and color changes in photo-isomers.[107]

2.2.4. Diarylethenesin diodes

Diodes are semiconductor devices that allow current to flow only in one direction. They act as rectifiers in electronic circuits and emitters in LEDs. The basic structure of a diode is composed of a junction between a *p*-type and a *n*-type semiconductor. Diodes are generally made from a single semiconductor crystal doped with *p*- and *n*-type materials. Photochromic molecules have been utilized as independent light-controlled carrier switches in memory diodes [109–111]and OLEDs.[108,113–116] Photo irradiation changes the $I_p$of DAE molecules which then affectscurrent injection into the emitting layer. When the DAE molecule is in open form the barrier for charge injection is large and current injection is difficult, but upon irradiation with UV light the closed-ring isomers enhances the I_p of the devices which then facilitate carrier injection from the photochromic layer to the emitting layer allowing the devices to be switched on. However, it is still a challenge to obtain large current on/off ratios when using pristine DAE molecules as independent light-controlled carrier switches. To improve the switching ratios, an additional cross-linking over layer is usually included on top of thehole injection layer but this results in low photo absorption which decreases the photoisomerization efficiency.[116]Doping or functionalizing the emitting layers with DAE photochromes has proven useful in improving on/off ratios of luminescence and current densities. Qian *et al.*[116], developed light-emitting devices (OLEDs) with the single emitting layers doped with a photochromic diarylethene-based compound (*N,N'E,N,N'E)-N,N'*-(4,4'-(cyclopentene-1,2-diyl)bis (5-methylthiophene-4,2-diyl))bis(methan-1-yl-1-ylidene)bis(3-(benzo[d]thiazol-2-yl)aniline) (BMTA). The photochrome was blended with methyl-9,10-bis(naphthalen-2-yl)anthracene (MADN) and *N*-(3-(benzo[d]thiazol-2-yl)-4-hydroxyphenyl)-4-tert-butylbenzamide (T4TB) to make a photoactive light emitting layer. The device structure of the OLED fabricated is shown in **Figure 2.14a**.

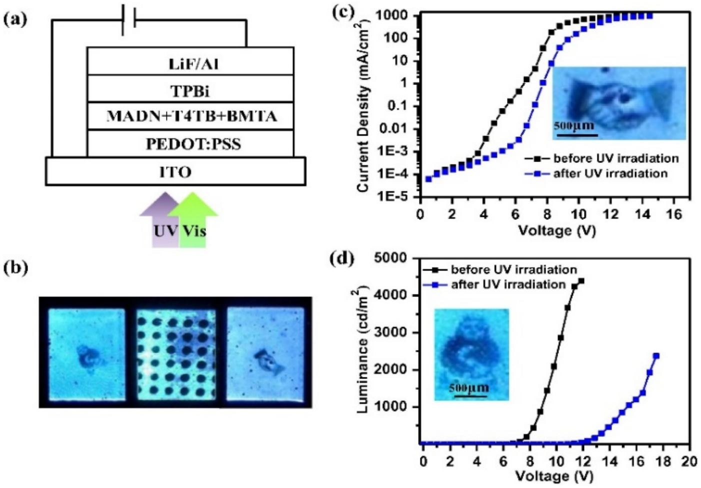

Figure 2.14: OLED device structure (a); photo-lithographed images of the emissive OLED (b); current density–voltage (c); and luminance–voltage (d) change in luminance of the devices before and after UV irradiation.[116]

PEDOT: PSS and TPBi were used as hole and electron transporting layers, respectively. Micro-photolithography was used to study the memory and optical characteristics of the devices. Different images were inputted, the corresponding micro-patterning and optical information storage of the OLED was recorded using a mask-free DMD micro-photolithography system to obtain image processed programmable OLEDs illustrated in **Figure 2.14b**. When irradiated with UV light, the OLED current density changed from 0.46 to 0.003 mA/cm^2 as shown in **Figure 2.14c** and a remarkable current on/off ratio of 1.4 x 10^2 was recorded. Without irradiation the turn-on voltage was 6.2 V and the luminescence increased as the applied operating voltage increased. Upon irradiation with UV light, the turn-on voltage increased to 9.7 V and the device suddenly turned dark. The recorded luminance decreased from 4398 to 45 cd/m^2 as shown in **Figure 2.14d.** A maximum luminescence on/off ratio of 1.9 x 10^3 was obtained which is a quite attractive non-destructive readout of light-written information.

In contrary, a study conducted by Ligorio*et al.*[114] revealed that when a DAE photochrome is used to modify the ITO electrode the current density is not influenced by DAE switching but the luminescence doubles when the DAE photochrome is switched from closed-form to open-form. To fabricate the OLED devices, clean ITO substrates were immersed in a 2 mM DAE-ethanol solutionfor 8 hours resulting a DAE self-assembled monolayer (SAM). Agreen emitting polymer (poly(9,9-dioctylfluorene-co-benzothiadiazole) (F8BT)) was deposited by spin coating.Calcium and aluminum were thermally evaporated as electrode and capping layer, respectively. Irradiating the devices with UV light doubled the electroluminescence and the original value could be restored reversibly by irradiating with visible light. This expanded functionality is brought by the changes in electronic structure of the diarylethene molecules upon irradiation which affect the confinement of charge carriers within the emissive layer. It is worth mentioning that the DAE photochrome used in this study had a phosphonic acid group to facilitate the formation of a chemically bond molecular film onto the ITO electrode. Further developments are still needed to achievephotoswitchable devices with large current on/off ratios and luminescence.

2.2.5. Diarylethenesin solar cells

Solar cells are similar to photodiodes, the major difference is that photodiodes are optimized for light detection while solar cells are optimized for energy conversion efficiency. In solar cells, photochromes are usually used to produce “smart” windows which darken upon irradiation with sunlight and generate electricity at the same time. Such devices are attractive for building integrated photovoltaics. Dye sensitized solar cells incorporating photochromes have been reported in literature.[117–120]Dithienylethenes have excellent resistance to light fatigue and great thermal stability in both isomeric forms. They also have wide absorption spectra (300 nm -800 nm) which overlaps well with the solar irradiance spectrum thus making them potential photo harvesting materials for solar cells. Dithienylethene-based dye sensitized solar cells with a basic D-π-A structure was reported by Wu *et al.*[112] Two DTE photochromes (**Figure 2.15a**) with different acceptor units were employed as sensitizing dyes. Interestingly, sensitizers with an open-ring isomer gave better photovoltaic performances in DSSCs.[112]This was linked to the location of the HOMO orbitals in the π –framework as modelled in **Figure 2.15**. The HOMO orbitals of open isomers (CAO and CNO) were found to be primarily located at π-framework of the donor part and the electron density of the LUMOs were delocalized over the DTE and anchoring group.

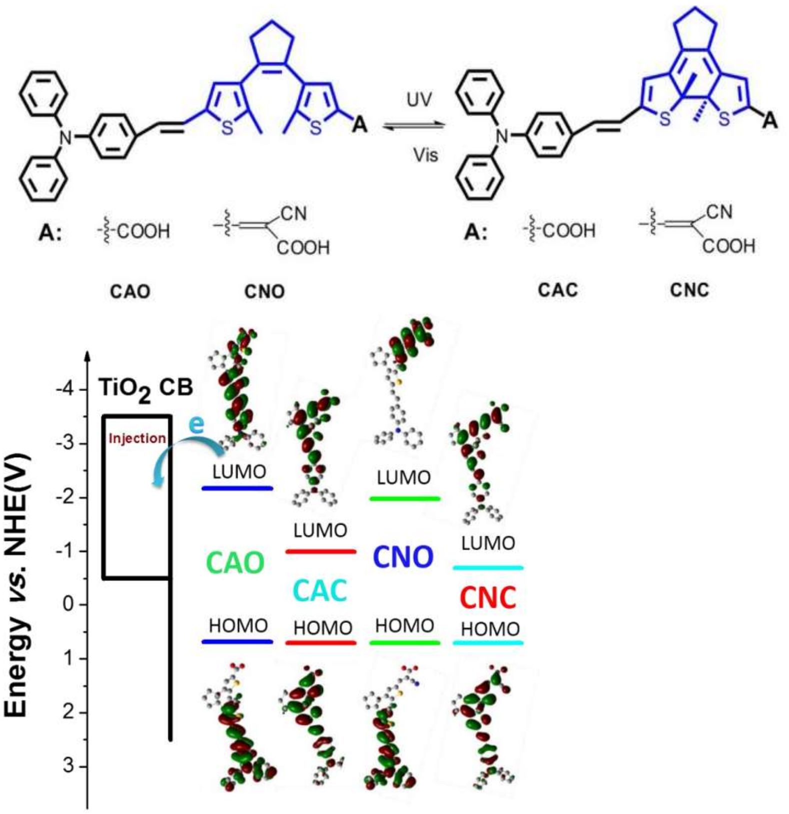

Figure 2.15: Structures of DTE photochromes used in dye-sensitized solar cells (a) and calculated frontier molecular orbitals of HOMO and LUMO diagram for CAO, CAC, CNO and CNC (b).[112]

The distinct location of the HOMO and LUMO orbitals enabled good charge separation thus resulting in improved photovoltaic performance. As shown in **Figure 2.15**, the electron density of HOMO or LUMO orbital of (CAC and CNC) are located at the conjunction bridges (DTE unit) and acceptors suggesting that there is a strong electron-donating ability of the closed-ring thus leading to poor charge separation. Saes*et al.*[34] reported photochromic organic solar cell based on a ternary blend bulk heterojunction (poly-TPD:PC61BM) binary using DAE dyes. Inclusion of photochromesdecreased the short-circuit current (J_{SC}), fill factor (FF) and overall power conversion efficiency (PCE) of poly-TPD:PC61BM. Upon illumination with UV light, a small increase in J_{SC} was observed suggesting that the conjugated closed-form DAE contributes to photocurrent generation. The contribution of DAE towards PCE was low although the weight ratio of DAE:poly-TPD:PC61BM was high at 10 : 1 : 4.

2.3. Conclusion and future directions

The role of photochromic polymers in organic electronics is to control properties such absorption, ionization potentials and fluorescence by thermal or light irradiation. Material properties are dependent photochrome structure. The properties can be tailored to suit the desired application by structurally modifying or functionalizing the photochrome. Challenges and opportunities co-exist in fundamental research of photoresponsive organic electronics.

In OFETs, photochromic molecules act as charge traps. High switching ratios have been obtained for both *p*-type and *n*-type transistors using various strategies for incorporating photochromes in OFET components.However, the low photo-modulated current on/off ratio, low device performance and stability obtained using some photochromes still need to be improved. This could be achieved by designing and synthesizing of new photochromic materials with excellent cycloreversibility, rapid response, low fatigue and stability for both isomers.

Photochromic sensors show high selectivity and sensitivity towards various analytes such toxic ions, vapors and gases. However, sensors still need to be further developed to ensure availability, portability and low detection levels. A lot of work has been done towards the development of photochromic molecules for security measures, especially logic gates. But single component security ink systems still need to be developed to simplify the synthesis procedures and real-life use of the ink. Molecular logic gates with many inputs are attractive for fabricating logic devices with multiple functions. Opportunities exist towards developing photochromic molecules which can respond to numerous independent stimuli.

Photochromes have proven useful in developing organic diode devices with large on/off current ratios and high luminescence. There is limited literature in photochrome-based solar cells. From this literature survey, a few dye-sensitised solar cells utilizing photochromic dyes have been reported. The development of photostable mainchain photochromic polymers could solve issues related to poor charge transport and poor photo switching in solid state. Furthermore, design and synthesis of patternable mainchain photochromic polymers could enable the realization of light-controllable printable electronics such as organic solar cells, transistors and light emitting diodes.

2.4. References

[1] T. J. Wigglesworth, A. J. Myles, N. R. Branda, *European J. Org. Chem.***2005**, *2005*, 1233.

[2] M. Irie, in *Encycl. Polym. Nanomater.* (Ed.: K. Kobayashi, Shiro, Müllen), Springer-Verlag, Berlin Heidelberg, **2013**, pp. 1–10.

[3] A. Fihey, A. Perrier, W. R. Browne, D. Jacquemin, *Chem. Soc. Rev.***2015**, *44*, 3719.

[4] A. S. Angeloni, D. Caretti, C. Carlini, E. Chiellini, G. Galli, A. Altomare, R. Solaro, M. Laus, *Liq. Cryst.***1989**, *4*, 513.

[5] C. Y. Gong Linbo, Gong Shuling, Dong Haiqing, Zhang Chunlei, *Front. Chem. China***2007**, *2*, 292.

[6] H.L. Z. and E.-Q. C. He-Lou Xie, Shao-Jie Wang, Guan-Qun Zhong, Yi-Xin Liu, *Macromolecules***2011**, *44*, 7600.

[7] A. Kitano, R. Ichikawa, H. Nakano, *Opt. Mater. (Amst).***2018**, *86*, 51.

[8] N. I. Islamova, X. Chen, C.-J. Fan, R. S. Andino, W. J. Lees, *Polym. Degrad. Stab.***2013**, *98*, 1662.

[9] B. Otto, K. Rück-Braun, *European J. Org. Chem.***2003**, *2003*, 2409.

[10] S. I. Luyksaar, I. V. Platonova, M. M. Krayushkin, V. A. Barachevskii, S. P. Molchanov, *Russ. Chem. Bull.***2011**, *60*, 861.

[11] S. I. Luyksaar, V. A. Migulin, B. V. Nabatov, M. M. Krayushkin, *Russ. Chem. Bull.***2010**, *59*, 446.

[12] S. Faulkner, L. S. Natrajan, W. S. Perry, D. Sykes, *Dalt. Trans.***2009**, 3890.

[13] Y. Yokoyama, *Chem. Rev.***2002**, *100*, 1717.

[14] M. Irie, T. Fukaminato, K. Matsuda, S. Kobatake, *Chem. Rev.***2014**, *114*, 12174.

[15] M. J. Marsella, Z.-Q. Wang, R. H. Mitchell, *Org. Lett.***2002**, *2*, 2979.

[16] G. Liu, S. Pu, R. Wang, *Org. Lett.***2013**, *15*, 980.

[17] Z. Li, X. Li, H. Chen, C. He, L. Wang, Y. Yang, S. Wang, H. Guo, S. H. Liu,

*Dye. Pigment.***2019**, *162*, 712.

[18] Q. Zou, X. Li, J. Zhang, J. Zhou, B. Sun, H. Tian, *Chem. Commun.***2012**, *48*, 2095.

[19] T. Kawai, T. Iseda, M. Irie, *Chem. Commun. (Camb).***2004**, 72.

[20] Y. Liang, R. Wang, G. Liu, S. Pu, *Spectrochim. Acta Part A Mol. Biomol. Spectrosc.***2018**, *205*, 470.

[21] G. Liao, D. Xue, C. Zheng, R. Wang, S. Pu, *J. Braz. Chem. Soc.***2016**, *27*, 1989.

[22] R. Wang, X. Zhang, S. Pu, G. Liu, Y. Dai, *Spectrochim. Acta - Part A Mol. Biomol. Spectrosc.***2017**, *173*, 257.

[23] A. Fihey, D. Jacquemin, *Chem. Sci.***2015**, *6*, 3495.

[24] A. G. Lvov, M. M. Khusniyarov, V. Z. Shirinian, *J. Photochem. Photobiol. C Photochem. Rev.***2018**, *36*, 1.

[25] H. Xu, S. Wei, C. Fan, G. Liu, S. Pu, *Tetrahedron***2017**, *73*, 6479.

[26] G. Pariani, M. Quintavalla, L. Colella, L. Oggioni, R. Castagna,

F. Ortica, C. Bertarelli, A. Bianco, *J. Phys. Chem. C***2017**, 23592.

[27] S. Pu, T. Yang, J. Xu, L. Shen, G. Li, Q. Xiao, B. Chen, *Tetrahedron***2005**, *61*, 6623.

[28] K. Morimitsu, K. Shibata, S. Kobatake, M. Irie, *J. Org. Chem.***2002**, *67*, 4574.

[29] S. Pu, T. Yang, G. Li, J. Xu, B. Chen, *Tetrahedron Lett.***2006**, *47*, 3167.

[30] C. P. Harvey, J. D. Tovar, *Polym. Chem.***2011**, *2*, 2699.

[31] B. Carsten, F. He, H. J. Son, T. Xu, L. Yu, *Chem. Rev.***2011**, *111*, 1493.

[32] M. Morimoto, S. Kobatake, M. Irie, *Chem. Rec.***2004**, *4*, 23.

[33] K. Altenhöner, J. H. Lamm, J. Mattay, *European J. Org. Chem.***2010**, *1*, 6033.

[34] F. Stellacci, C. Bertarelli, F. Toscano, M. C. Gallazzi, G. Zotti, G. Zerbi, *Adv. Mater.***1999**, *11*, 292.

[35] C. Bertarelli, A. Bianco, V. Boffa, M. Mirenda, M. C. Gallazzi, G. Zerbi, *Adv. Funct. Mater.***2004**, *14*, 1129.

[36] T. Kawai, Y. Nakashima, M. Irie, *Adv. Mater.***2005**, *17*, 309.

[37] T. Kawai, T. Kunitake, M. Irie, *Chem. Lett.***1999**, *28*, 905.

[38] H. Choi, H. Lee, Y. Kang, E. Kim, S. O. Kang, J. Ko, *J. Org. Chem.***2005**, *70*, 8291.

[39] A. J. Myles, N. R. Branda, *Macromolecules***2003**, *36*, 298.

[40] H. Hayasaka, T. Miyashita, K. Tamura, K. Akagi, *Adv. Funct. Mater.***2010**, *20*, 1243.

[41] K. Watanabe, K. Suda, K. Akagi, *J. Mater. Chem. C***2013**, *1*, 2797.

[42] L. A. P. Kane-Maguire, G. G. Wallace, *Chem. Soc. Rev.***2010**, *39*, 2545.

[43] T. J. Wigglesworth, N. R. Branda, *Adv. Mater.***2004**, *16*, 123.

[44] X. Zhai, H. Yu, L. Wang, Z. Deng, Z. U. Abdin, R. Tong, X. Yang, Y. Chen, M. Saleem, *Appl. Organomet. Chem.***2016**, *30*, 62.

[45] K. G. Yager, C. J. Barrett, *J. Photochem. Photobiol. A Chem.***2006**, *182*, 250.

[46] K. G. Yager, C. J. Barrett, in *Smart Light. Mater.* (Ed.: T.I. Yue Zhao), John Wiley & Sons, **2009**, pp. 1–46.

[47] A. Khan, L. Wang, H. Yu, M. Haroon, R. S. Ullah, A. Nazir, T. Elshaarani, M. Usman, S. Fahad, K.-R. Naveed, *J. Organomet. Chem.***2019**, *880*, 124.

[48] X. Xia, H. Yu, L. Wang, Z. Ul-Abdin, *RSC Adv.***2016**, *6*, 105296.

[49] X. Xiaa, H. Yua, L. Wanga, Z. Denga, K. J. Sheab, Zain-ul-Abdin, *Eur. Polym. J.***2018**, *100*, 103.

[50] A. Bobrovsky, V. Shibaev, A. Piryazev, D. V. Anokhin, D. A. Ivanov, O. Sinitsyna, V. Hamplova, M. Kaspar, A. Bubnov, *Macromol. Chem. Phys.***2017**, *218*, DOI 10.1002/macp.201700127.

[51] K. Mukai, K. Imai, M. Hara, S. Nagano, T. Seki, *ChemPhotoChem***2019**, *3*, 495.

[52] K. Ichimura, Y. Suzuki, T. Seki, A. Hosoki, K. Aoki, *Langmuir***1988**, *4*, 1214.

[53] S. Nagano, *Langmuir***2019**, *35*, 5673.

[54] J. Tian, L. Fu, Z. Liu, H. Geng, Y. Sun, G. Lin, X. Zhang, G. Zhang, D. Zhang, *Adv. Funct. Mater.***2019**, *29*, 1807176.

[55] S. B. Schmidt, F. Kempe, O. Brügner, M. Walter, M. Sommer, *Polym.*

*Chem.***2017**, *8*, 5407.

[56] B.S Lukyanov and M.B. Lukyanova, *Chem. Heterocycl. Compd.***2005**, *41*, 281.

[57] H. Xia, K. Xie, G. Zou, *Molecules***2017**, *22*, 2236.

[58] I. V. Ozhogin, V. V. Chernyavina, B. S. Lukyanov, V. I. Malay, I. A. Rostovtseva, N. I. Makarova, V. V. Tkachev, M. B. Lukyanova, A. V. Metelitsa, S. M. Aldoshin, *J. Mol. Struct.***2019**, *1196*, 409.

[59] S. Chng, M. G. Moloney, L. Y. L. Wu, *ACS Omega***2018**, *3*, 15554.

[60] S. Bhattacharyya, M. Maity, A. Chowdhury, M. L. Saha, S. K. Panja, P. J. Stang, P. S. Mukherjee, *Inorg. Chem.***2020**, *59*, 2083.

[61] R. Klajn, *Chem. Soc. Rev.***2014**, *43*, 148.

[62] D. Lachmann, R. Lahmy, B. König, *European J. Org. Chem.***2019**, *2019*, 5018.

[63] B. Yao, Y. Wang, N. Menke, M. Lei, Y. Zheng, L. Ren, G. Chen, Y. Chen, M. Fan, *Mol. Cryst. Liq. Cryst.***2005**, *430*, 211.

[64] V. P. Rybalkin, N. I. Makarova, S. Y. Pluzhnikova, L. L. Popova, A. V. Metelitsa, V. A. Bren’, V. I. Minkina, *Russ. Chem. Bull.***2014**, *63*, 1780.

[65] X. Gao, Z. Zhao, *Sci. China Chem.***2015**, *58*, 947.

[66] S. Brixi, O. A. Melville, N. T. Boileau, B. H. Lessard, *J. Mater. Chem. C***2018**, *6*, 11972.

[67] H. Chen, W. Zhang, M. Li, G. He, X. Guo, *Chem. Rev.***2020**, *120*, 2879.

[68] L. N. Fu, B. Leng, Y. S. Li, X. K. Gao, *Chinese Chem. Lett.***2016**, *27*, 1319.

[69] X. Zhang, L. Hou, P. Samorì, *Nat. Commun.***2016**, *7*, 11118.

[70] M. El Gemayel, K. Börjesson, M. Herder, D. T. Duong, J. A. Hutchison, C. Ruzié, G. Schweicher, A. Salleo, Y. Geerts, S. Hecht, E. Orgiu, P. Samorì, *Nat. Commun.***2015**, *6*, 1.

[71] R. Hayakawa, K. Higashiguchi, K. Matsuda, T. Chikyow, Y. Wakayama, *ACS Appl. Mater. Interfaces***2013**, *5*, 3625.

[72] Y. Ishiguro, R. Hayakawa, T. Yasuda, T. Chikyow, Y. Wakayama, *ACS Appl. Mater. Interfaces***2013**, *5*, 9726.

[73] K. Börjesson, M. Herder, L. Grubert, D. T. Duong, A. Salleo, S. Hecht, E. Orgiu, P. Samorì, *J. Mater. Chem. C***2015**, *3*, 4156.

[74] Q. Shen, L. Wang, S. Liu, Y. Cao, L. Gan, X. Guo, M. L. Steigerwald, Z. Shuai, Z. Liu, C. Nuckolls, *Adv. Mater.***2010**, *22*, 3282.

[75] H. Zhang, J. Hui, H. Chen, J. Chen, W. Xu, Z. Shuai, D. Zhu, X. Guo, *Adv. Electron. Mater.***2015**, *1*, 1.

[76] R. Hayakawa, M. Petit, K. Higashiguchi, K. Matsuda, T. Chikyow, Y. Wakayama, *Org. Electron.***2015**, *21*, 149.

[77] M. Carroli, D. T. Duong, E. Buchaca-Domingo, A. Liscio, K. Börjesson, M. Herder, V. Palermo, S. Hecht, N. Stingelin, A. Salleo, E. Orgiu, P. Samorì, *Adv. Funct. Mater.***2020**, *30*, 1907507.

[78] Y. Kurokawa, R. Hayakawa, S. Shimada, K. Higashiguchi, Y. Noguchi, K. Matsuda, Y. Wakayama, *Org. Electron.*__2019__, *64*, 205.

[79] W. Rekab, T. Leydecker, L. Hou, H. Chen, M. Kirkus, C. Cendra, M. Herder, S. Hecht, A. Salleo, I. McCulloch, E. Orgiu, P. Samorì, *Adv. Funct. Mater.*__2020__, *30*, 1.

[80] Y. Kurokawa, R. Hayakawa, S. Shimada, K. Tanaka, K. Higashiguchi, Y. Noguchi, K. Matsuda, Y. Wakayama, *Jpn. J. Appl. Phys.*__2019__, *58*,3.

[81] X. Wu, R. Jia, J. Pan, X. Zhang, J. Jie, *Nanoscale Horizons*__2020__, *5*, 454.

[82] H. Qiu, Z. Liu, Y. Yao, M. Herder, S. Hecht, P. Samorì, *Adv. Mater.*__2020__, *32*, 1.

[83] D. D. Dashitsyrenova, A. G. Lvov, L. A. Frolova, A. V. Kulikov, N. N. Dremova, V. Z. Shirinian, S. M. Aldoshin, M. M. Krayushkin, P. A. Troshin, *J. Mater. Chem. C*__2019__, *7*, 6889.

[84] X. Xie, G. Mistlberger, E. Bakker, *J. Am. Chem. Soc.*__2012__, *134*, 16929.

[85] M. Qin, Y. Huang, F. Li, Y. Song, *J. Mater. Chem. C*__2015__, *3*, 9265.

[86] R. Wang, N. Wang, S. Pu, X. Zhang, G. Liu, Y. Dai, *Dye. Pigment.*__2017__, *146*, 445.

[87] J. Lv, Y. Fu, G. Liu, C. Fan, S. Pu, *RSC Adv.*__2019__, *9*, 10395.

[88] K. Fries, S. Samanta, S. Orski, J. Locklin, *Chem. Commun.*__2008__, 6288.

[89] G. Vamvounis, N. Sandery, *Aust. J. Chem.*__2015__, *68*, 1723.

[90] Z. Li, Y. Pei, S. Hou, Y. Dai, D. Liu, J. Zhu, Y. P. Zhu, X. Liu, *Dye. Pigment.***2020**, *179*, 108419.

[91] N. Shao, J. Jin, H. Wang, J. Zheng, R. Yang, W. Chan, Z. Abliz, *J. Am. Chem. Soc.***2010**, *132*, 725.

[92] J. Garcia, J. B. Addison, S. Z. Liu, S. Lu, A. L. Faulkner, B. M. Hodur, E. I. Balmond, V. W. Or, J. H. Yun, K. Trevino, B. Shen, J. T. Shaw, N. L. Frank, A. Y. Louie, *J. Phys. Chem. B***2019**, *123*, 6799.

[93] S. Heng, X. Zhang, J. Pei, A. D. Abell, *Biosensors***2017**, 7, 36.

[94] X. Chai, H. H. Han, Y. Zang, J. Li, X. P. He, J. Zhang, H. Tian, *Beilstein J. Org. Chem.***2019**, *15*, 2380.

[95] J. Andréasson, U. Pischel, *Chem. Soc. Rev.***2018**, *47*, 2266.

[96] J. Andréasson, U. Pischel, S. D. Straight, T. A. Moore, A. L. Moore, D. Gust, *J. Am. Chem. Soc.***2011**, *133*, 11641.

[97] S. Chen, Z. Guo, S. Zhu, W. E. Shi, W. Zhu, *ACS Appl. Mater. Interfaces***2013**, *5*, 5623.

[98] K. D. Renuka, C. L. Lekshmi, K. Joseph, S. Mahesh, *ChemistrySelect***2017**, *2*, 11615.

[99] X. Chai, Y. X. Fu, T. D. James, J. Zhang, X. P. He, H. Tian, *Chem. Commun.***2017**, *53*, 9494.

[100] Q. Ai, K. H. Ahn, *RSC Adv.***2016**, *6*, 43000.

[101] M. F. Budyka, V. M. Li, *High Energy Chem.***2017**, *51*, 338.

[102] M. F. Budyka, V. M. Li, *ChemPhysChem***2017**, *18*, 260.

[103] J. C. Chaplin, N. A. Russell, N. Krasnogor, *BioSystems***2012**, *109*, 35.

[104] C. Ritchie, G. Vamvounis, H. Soleimaninejad, T. A. Smith, E. J. Bieske, V. Dryza, *Phys. Chem. Chem. Phys.***2017**, *19*, 19984.

[105] J. Andréasson, S. D. Straight, T. A. Moore, A. L. Moore, D. Gust, *Chem. - A Eur. J.***2009**, *15*, 3936.

[106] G. Naren, C. W. Hsu, S. Li, M. Morimoto, S. Tang, J. Hernando, G. Guirado, M. Irie, F. M. Raymo, H. Sundén, J. Andréasson, *Nat. Commun.***2019**, *10*, 1.

[107] A. Singh, P. Verma, S. Laha, D. Samanta, S. Roy, T. Maji, *ACS Appl. Mater. Interfaces***2020**, 18, 20991.

[108] Z. Zhang, X. Liu, Z. Li, Z. Chen, F. Zhao, F. Zhang, C. H. Tung, *Adv. Funct. Mater.***2008**, *18*, 302.

[109] R. C. Shallcross, P. Zacharias, A. Köhnen, P. O. Körner, E. Maibach, K. Meerholz, *Adv. Mater.***2013**, *25*, 469.

[110] T. Tsujioka, T. Sasa, Y. Kakihara, *Org. Electron.***2012**, *13*, 681.

[111] R. C. Shallcross, P. O. Körner, E. Maibach, A. Köhnen, K. Meerholz, *Adv. Mater.***2013**, *25*, 4807.

[112] W. Wu, J. Wang, Z. Zheng, Y. Hu, J. Jin, Q. Zhang, J. Hua, *Sci. Rep.***2015**, *5*,8592.

[113] M. Taguchi, T. Nakagawa, T. Nakashima, C. Adachi, T. Kawai, *Chem. Commun.***2013**, *49*, 6373.

[114] G. Ligorio, G. F. Cotella, A. Bonasera, N. Zorn Morales, G. Carnicella, B. Kobin, Q. Wang, N. Koch, S. Hecht, E. J. W. List-Kratochvil, F. Cacialli, *Nanoscale***2020**, *12*, 5444.

[115] P. Zacharias, M. C. Gather, A. Köhnen, N. Rehmann, K. Meerholz, *Angew. Chemie - Int. Ed.***2009**, *48*, 4038.

[116] Y. Qian, X. Xu, W. Li, J. Wang, B. Wei, Q. Wei, X. Yan, W. Hu, Y. Lu, L. Xie, X. Zhang, W. Huang, *Org. Electron.***2015**, *26*, 476.

[117] S. Ma, H. Ting, Y. Ma, L. Zheng, M. Zhang, L. Xiao, Z. Chen, *AIP Adv.***2015**, *5*, 057154.

[118] N. M. Johnson, Y. Y. Smolin, D. Hagaman, M. Soroush, K. K. S. Lau, H. F. Ji, *Phys. Chem. Chem. Phys.***2017**, *19*, 2981.

[119] N. M. Johnson, Y. Y. Smolin, C. Shindler, D. Hagaman, M. Soroush, K. K. S. Lau, H.-F. Ji, *AIMS Mater. Sci.***2015**, *2*, 503.

[120] L. Wang, Y. Liu, X. Zhan, D. Luo, X. Sun, *J. Mater. Chem. C***2019**, *7*, 8649.

CHAPTER 3

TUNING PROPERTIES OF POLYMER SOLAR CELL BLENDS USING PHOTOCHROMIC COMPOUNDS

3.1.Introduction

Organic photochromic compounds are fascinating materials for the development of light controllable electronics.[1–3] The properties of photochromic compounds such as color, geometry, absorption, photoluminescence, oxidation and reduction potentials can be changed reversibly during photoswitching.[4–6] This unique character can be applied in different types of photonic devices. Electronic changes can be applied to optical memory and transistor devices whereas geometrical structural changes can be potentially applied to actuators.[7]

Blending/doping organic semiconductor materials with photochromic molecules have been considered as an effective strategy to improve device performance and achieve dual functionalities in organic light emitting diodes (OLEDs) [8–10] and field effect transistors (OFETs).[11–15]Optically controllable OFETs have been developed by doping photochromic molecules such as spiropyrans (SP) [16,17] and diarylethenes[14,18] which controlled the morphology of the channel layer, optical and electrical properties *via* photoisomerization. In addition, these molecules have been used to fabricate ambipolar OFETs in which both hole and electron transport could be simultaneously modulated using light.[19–21] This strategy may be used to control the properties of organic photovoltaics (OPVs) since solar cells and transistors have similar characteristics.

Generally, OPVs suffer from low power conversion efficiency (PCE) and poor device stability .[22,23] The stability of OPVs is often governed by the morphology of the active layer which is determined by the nature of its donor and acceptor components. One method of improving morphology involves the use of additives.[24–27] Unfortunately, most additives reported in literature are either unstable under UV light [28] or reduce device stability if they remain in the active layer unless they are deliberately volatilized *via* post treatment methods such as thermal annealing, vacuum drying and hot-substrate casting.[29,30] However, these post treatment methods are not effective in removing residual additives and could damage the active layer. It has been reported that annealing at temperatures higher than the optimum may have detrimental effect on the active layer crystallinity of OPV active layers.[31,32] Therefore, it is crucial to discover UV stable additives which do not require post treatment or volatilization. Organic photochromic compounds are potential additives for OPVs since they are photostable and absorb light in both UV and visible regions of the electromagnetic spectrum which can contribute to photocurrent generation.

Photoisomerization of azobenzene results in molecular movement and a significant geometric change from an elongated trans form to a bent cis form with the molecular length changing from ~0.9 nm to ~0.55 nm.[33] On the other hand, diarylethene molecules shrinks (from ~1.01 nm to ~0.90 nm) upon cyclization and expands (from ~0.49 nm to ~0.56 nm) upon cycloreversion.[7] Photoexcitation of spiropyrans with UV light gradually cleaves the C-O bond of the colorless, non-polar and orthogonally shaped closed-form isomer to produce a colored, charged and planar conjugated open-form.[34] The photoswitching actions of these molecules could help control the properties of OPVs blends. Moreover, these molecules are conjugated, may interact with the donor and the acceptor through intermolecular π-π interactions. These interactions together with photochromism could facilitate ordered molecular arrangements, enhance absorptivity, morphology and thermal stability of OPVs blends. Therefore, this study investigated the effect of doping solar cell (P3HT: PCBM) blends with organic photochromes. The structures of P3HT, PCBM and photochromic additives (azobenzene, 1,3,3-Trimethylindolino-6'-nitrobenzopyrylospiran and 1,2-bis(2,5-dimethyl-3-thienyl)perfluorocyclopentene) are shown in **Scheme 3.1.** Morphology, crystallinity, optical and thermal properties of photochrome-processed P3HT: PCBM blends were studied. Unfortunately, undesirable results were obtained. The crystallinity of the blends decreased upon addition of photochromes. Thermal and optical properties of P3HT: PCBM blends diminished upon addition of photochromic additives and worsened as the concentration of the additives increased. The goal of improving the properties of organic solar cell blends using photochromic additives was not achieved.

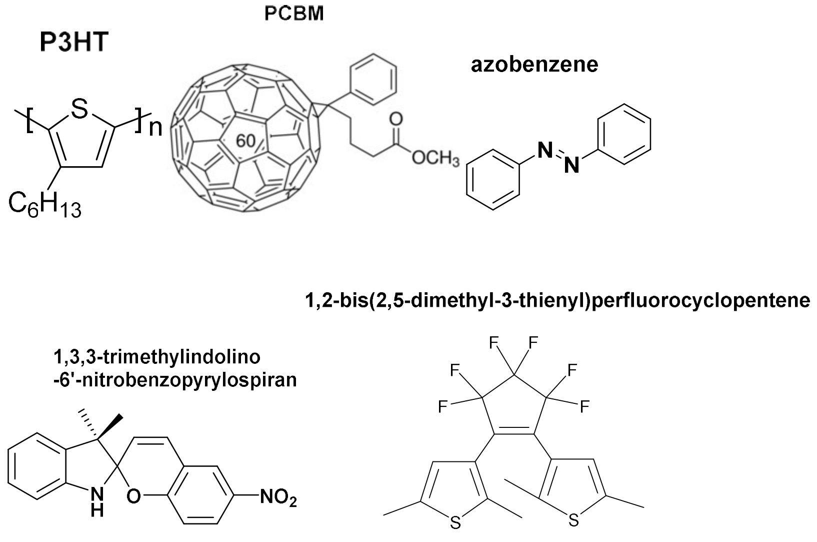

Scheme 3.1: Chemical structures of P3HT, PCBM and photochromic additives (azobenzene, 1,3,3-trimethylindolino-6'-nitrobenzopyrylospiran and 1,2-bis(2,5-dimethyl-3-thienyl)perfluorocyclopentene).

3.2.Experimental

3.2.1. Chemicals and reagents

P3HT (average M_n 54 000 – 75 000, electronic grade, head-to-tail regioregularity: >98%) and Azobenzene were purchased from Sigma-Aldrich. Chlorobenzene, [6,6]-Phenyl C61 butyric acid methyl ester (PCBM) (99.5%) and 1,3,3-Trimethylindolino-6'-nitrobenzopyrylospiran were purchased from RCI Labscan Limited, Nano-C Products and Tokyo Chemical Industry, respectively, and used as received. 1,2-bis(2,5-dimethyl-3-thienyl)perfluorocyclopentenewas obtained from previous work.[35]

3.2.2. Methods

Blends were prepared following a procedure reported in literature with modification.[36] P3HT: PCBM (1:1 wt.%) blend solutions with a total concentration of 12 mg/mL were dissolved in chlorobenzene. In a typical procedure, P3HT was dissolved in a suitable solvent and stirred for 2 hours. PCBM was added to the solution and the blend was stirred for 24 hours at 50 ºC to ensure complete mixing. 1 mL portions were extracted from this blend and 1,3,3-trimethylindolino-6'-nitrobenzopyrylospiran, azobenzene and 1,2-bis(2,5-dimethyl-3-thienyl)perfluorocyclopentene were added in various weight fractions of 0%, 0.5%, 1%, 1.5% and 2% (wt./wt.) in each portion. The additive concentrations were kept low because photochromes act as charge traps [12] and high additive levels lead to phase separation and segregation which can degrade the host polymer's properties.[37]

Glass substrates were cleaned in an ultrasound bath for 20 minutes using soapy water, acetone and ethanol, respectively, and dried under nitrogen. Each blend was drop casted on a glass substrate and allowed to dry at room temperature. The dry films were used for UV-Vis spectroscopy, X-ray difractometry (XRD) and differential scanning calorimetry (DSC) analysis. A handheld UVGL-58 lamp (6W) and visible light Cole-ParmerFiber Optic Illuminator (150 W) were used as the light sources for the photoisomerization of the films. The light irradiation time was fixed at 10 minutes to inhibit photocurrent or photo-oxidation, but to still induce photochrome isomerization in the blends.[37]

3.2.3. Characterization

The optical properties of the film blends were measured using a UV-Vis spectrophotometer (Shimadzu, UV2600). Surface roughness and morphology were studied using AFM (NT-MDT NTEGRA). Thermal properties were investigated using SDT 650 (TA instruments) and DSC 250 (TA instruments). The heating/ cooling rates were equal at 10 ºC min^{-1}. TGA ramp rate was 10 ºC min^{-1}. Each test was repeated three times. XRD patterns were acquired using a Siemens D5000 diffractometer with Cu Kα (λ = 1.5406 Å) as the incident beam at a scan rate of 0.2°min^{-1}.

3.3.Results and discussion

3.3.1. Thermal properties of solar cell blends processed with photochromic additives

P3HT and PCBM are the most studied *p*- and *n*-type materials, respectively and are relatively stable under thermal stress, ambient air and continuous illumination, hence, were chosen for this study. Thermal behaviors of pure PCBM, P3HT, Azo, SP and DAE were investigated by TGA and DSC, and the results are presented in the Appendix of Chapter 3. The glass transition temperatures (T_g) of pure PCBM and P3HT were found to be 124.62 ºC and 14.68 ºC, respectively. These values are similar to those reported in literature.[38,39] The $T_g$of P3HT: PCBM (1:1 wt.%) blend was found to be 49.49 ºC.

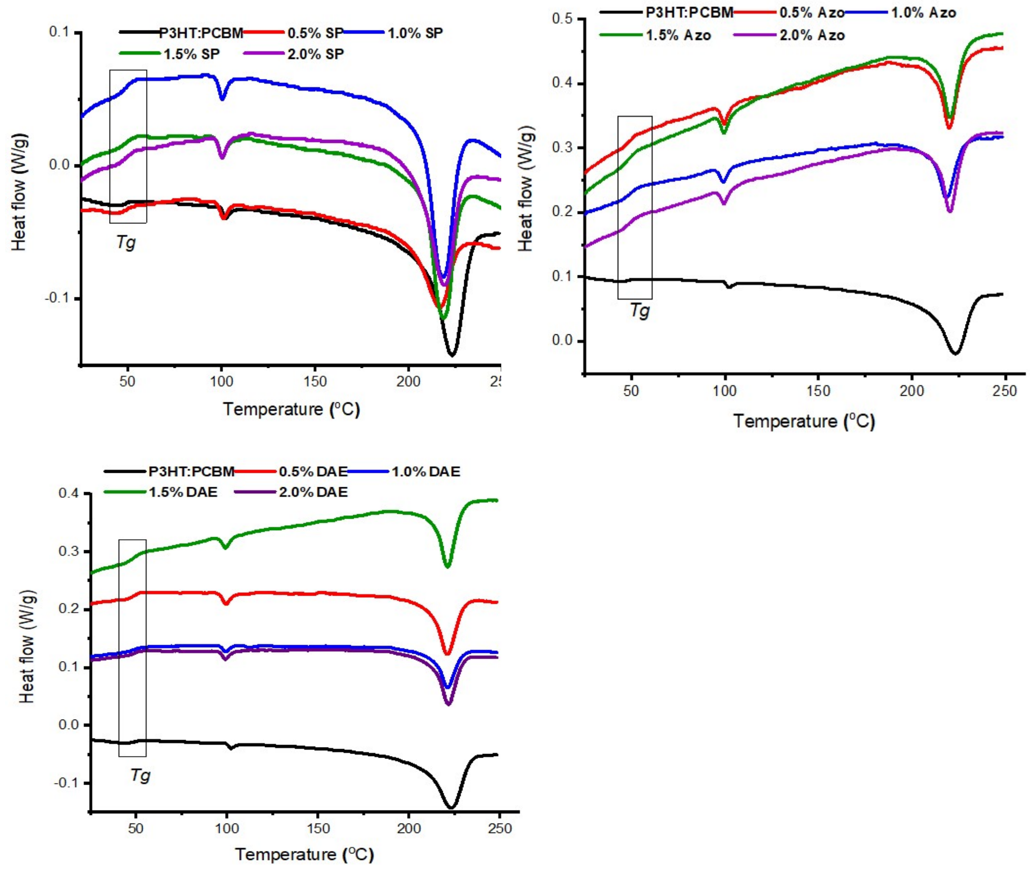

Figure 3.1:DSC heating curves of P3HT: PCBM processed with different amounts of spiropyran (a), Azobenzene (b)and DAE (c).

The thermal stability of OPV blends is governed by the $T_g$and crystallinity of the donor polymer. It has been reported that under thermal stress it is difficult for the acceptor material to diffuse from the polymer matrix if the T_g of the polymer is high, thus making the morphology of the active layer thermally stable.[40–42]**Figure 3.1** shows the DSC heating curves of OPV blends processed with photochromic additives. Upon addition of SP additive, the T_g and T_m of the blends decreased implying that this additive acts as a plasticizer.[43] The amount of each photochrome was varied to understand the effect of photochrome concentration on the thermal properties of OPV blends. Both T_g and Tm of the blend decreased as the amount of SP additive increased suggesting that the presence of additive molecules increases the mobility of polymers chains which is disadvantageous to thermal stability.[43] Therefore, the concentration of the processing additive must be kept low to avoid compromising thermal stability.[16,44]Thermal properties of blends processed with DAE and Azo were unchanged even when the concentration was increased to 2% implying that these additives do not interact strongly with P3HT.

3.3.2. Effect of adding additives on the crystallinity of solar cell blends

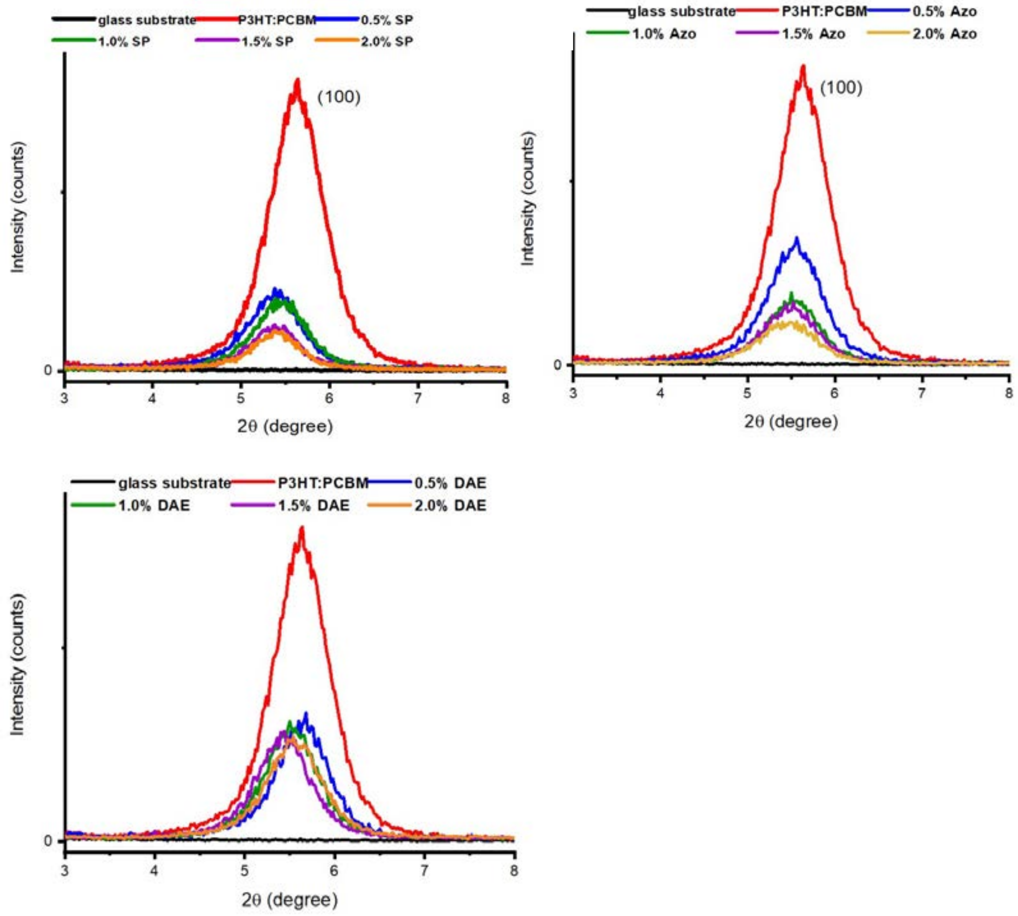

Figure 3.2:XRD patterns of P3HT: PCBM blends processed with SP (a), Azo (b) and DAE (c).

XRD is a powerful technique for investigating crystallinity of polymeric materials. **Figure 3.2** shows the XRD profiles of P3HT: PCBM blends processed with different photochromic additives. The XRD patterns of the P3HT: PCBM blend films showed an intense diffraction peak at $2\theta = 5.6^{\circ}$. This peak corresponds to the (100) plane of an ordered and self-organized lamellar structure of P3HT formed by parallel stacking of P3HT chains separated by regions filled with the alkyl side chains. The area under this peak is often used to determine the crystallinity of OPV blends. A greater peak area indicate that the material is highly crystalline.[45,46] Upon addition of photochromic molecules, the position of the (100) peak shifted to lower 2θ values and the intensity of the peak gradually decreased as the concentrations of additives increased. This result indicates that addition of solid additives disturbs the alignment of the P3HT chains thus decreasing the crystallinity of the blend.[37] This was further confirmed by significant increments in interlayer spacing of P3HT chains (**Table 3.1**) calculated using equation**3.1**.

$$d = \frac{\lambda}{2\,sin(\Theta)} \qquad (3.1)$$

where d is the distance between the layer distance between P3HT adjacent chains, λ is the wavelength of the X-ray beam (0.154 nm) and ϴ is the diffraction angle.

Upon addition of photochromic molecules, interlayer spacing between P3HT chains increased from 1.571 nm to 1.640 nm. An increase in interlayer spacing is unfavorable for charge transport because a long hopping distance of the charge carriers between P3HT backbones could have a negative impact on the short-circuit current (J_{SC}) and PCE of solar devices.[45]

Table 3.1. Interlayer spacing of P3HT chains in the blend films processed with different additives

Sample	Interlayer spacing (nm)	RMS (nm)
P3HT: PCBM	1.571	10.203 ±1.376
0.5% SP	1.640	12.254 ±1.012
1.0% SP	1.640	12.398 ±1.271
1.5% SP	1.640	15.254 ±2.105
2.0% SP	1.640	14.176 ±2.632
0.5% Azo	1.590	14.532 ±1.407
1.0% Azo	1.590	16.231 ±1.631
1.5% Azo	1.590	17.027 ±1.329
2.0% Azo	1.590	18.324 ±1.362
0.5% DAE	1.571	11.381 ±1.208
1.0% DAE	1.580	13.206 ±2.097
1.5% DAE	1.600	13.745 ±1.876
2.0% DAE	1.620	13.975 ±1.193

Surface roughness is another important feature of OPV active layers because the optimal domain size for exciton dissociation is 10-20 nm [27,47]. Therefore, it is important to maintain a suitable polymer aggregate size to achieve high exciton dissociation. **Figure 3.3** shows AFM images of OPV blends containing 1.0% of SP, Azo and DAE. A finely dispersed structure was observed for P3HT: PCBM blends with no additive.Films processed with DAE and Azo show good coverage and closely packed aggregates with a finer, fibrous morphology indicating a large interpenetrating network across the film.[25] In addition, the surface roughness increased as the amount of additives increased due to formation of larger domain sizes (**Figure S3.3in the**

Appendix).[16] The blends processed with SP additive had smooth surfaces suspected to be caused by segregation of SP molecules to the bottom of the film.[37]

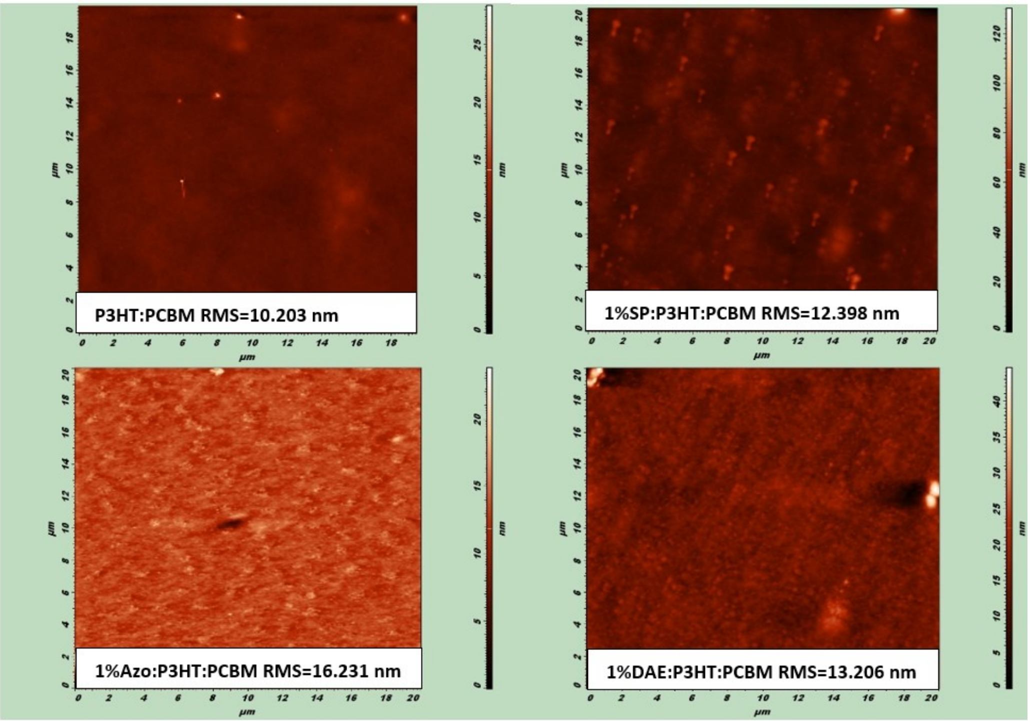

Figure 3.3:AFM images of P3HT: PCBM (a), P3HT: PCBM blends processed with SP (a), Azo (b) and DAE (c).

3.3.3. Optical properties of OPV blends processed with photochromic additives

The absorption spectrum of P3HT: PCBM blend film showed a dominant absorption peak at 520 nm and shoulder peaks at 555 nm and 603nm characteristic of transitions related to P3HT vibration modes. The peak at 520 nm is assigned to the intrachain π–π transitions of P3HT blocks. The two vibronic shoulders at 550 nm and 603 nm can be attributed to the π-π inter-chain packing of P3HT molecules.[27,48,49]In general, the optical absorption maxima of a conjugated polymer increases with increasing crystallinity and conjugation chain length.[27,38,50]

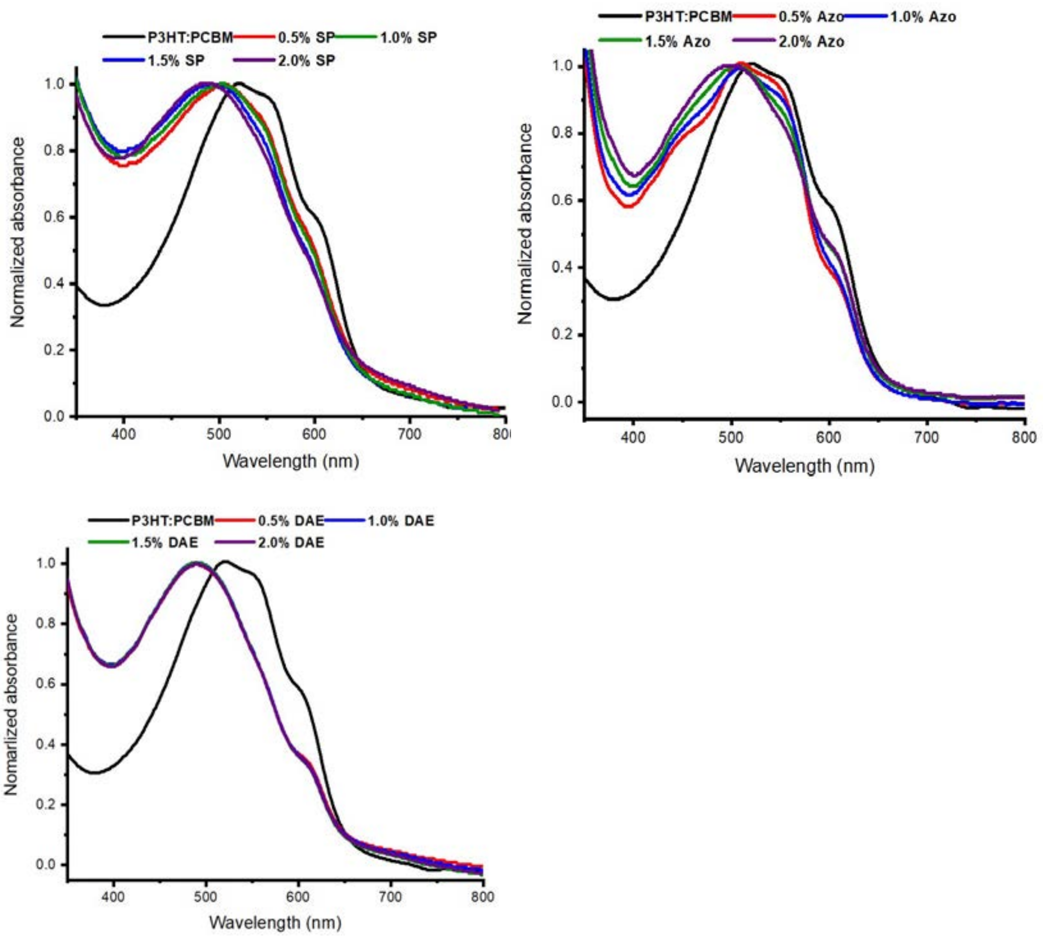

Figure 3.4: UV-Vis absorption spectra of P3HT: PCBM blends processed with SP (a), Azo (b) and DAE (c).

The absorption spectra of films processed with photochromic molecules (**Figure 3.4**) are blue shifted to ~490 nm and shoulder peaks at 555 nm and 603 nm are absent. This suggests that the addition of photochromic molecules disrupts molecular ordering of blend components and weakens the secondary interactions between P3HT polymer segments.[51,52]The photochromic behaviors of the blends were also investigated. Photoswitching spectra of pristine photochromes in both solution and film state are shownin **Figure S3.4** (Appendix of Chapter 3).The absorption spectra ofP3HT: PCBM films processed with azobenzene did not change irradiation with UV and Vis light because azobenzenes are difficult to switch in solid solution because their photoisomerization from the elongated trans form to the bent cis form requires a large volume change.[53,54]

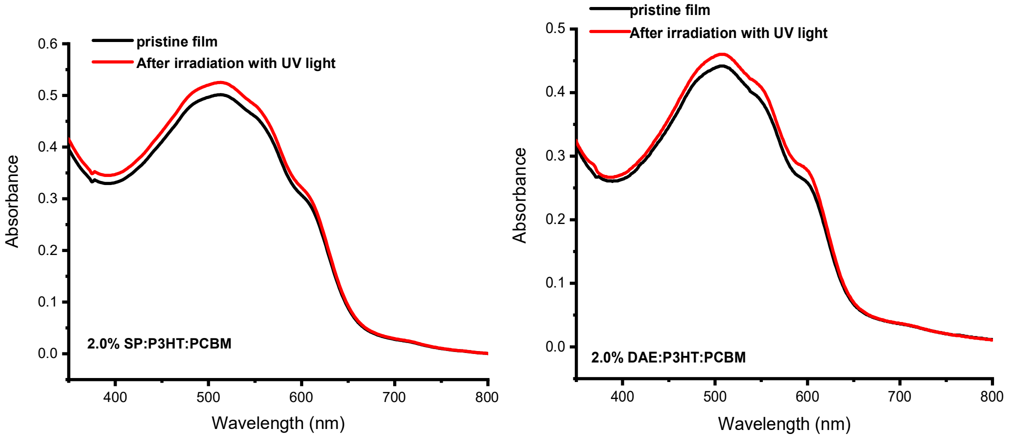

Figure 3.5: Absorption spectra of P3HT: PCBM blends processed with SP (a) and DAE (b) additives.

Figure 3.5 shows the absorption spectra of P3HT: PCBM processed with different SP and DAE after alternating irradiation with UV light and Vis light for 10 minutes. The absorption intensity slightly increased upon irradiation with UV light and decreased to the original intensity upon irradiation with Vis light due to the photoisomerization of SP and DAE molecules in the blend. The absorption intensity of DAE processed blends could be cycled numerous times upon alternate irradiation with UV and Vis light with minimal fatigue (**Figure 3.6**). Fatigue was observed after five cycles for SP-processed blends owing to the spiropyran's poor resistance to illumination.[55] For all the blend films, no color change was observed due to low photochrome concentration.

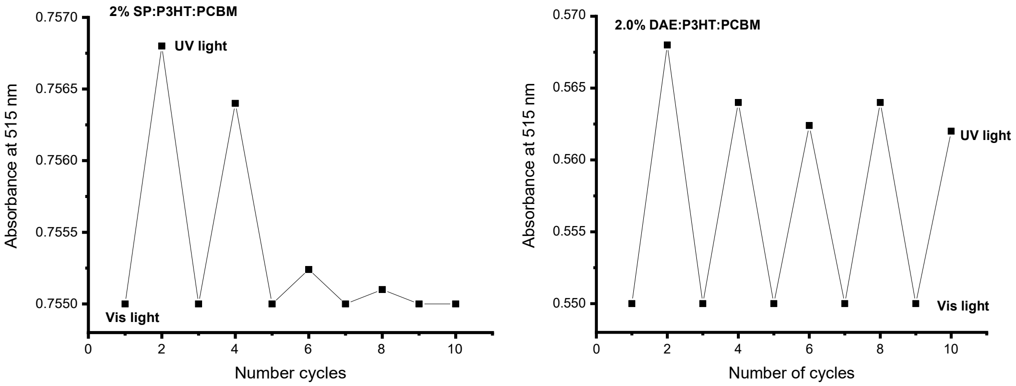

Figure 3.6: Absorption intensity of OPV blends at 515 nm after alternate UV and Vis light irradiation over many cycles.

3.4.Conclusion

Optical, morphological and thermal properties of OPV blends processed with azobenzene, spiropyran and diarylethene molecules as additives were examined. Addition of azobenzene and diarylethene molecules did not alter the thermal properties of P3HT: PCBM blends. Thermal properties of blends processed with spiropyran molecules decreased due to plasticization. The crystallinity of the blend decreased and the interlayer spacings between P3HT chain increased upon addition of photochromic additives implying that these molecules disturbs the alignment of the P3HT chains. The absorption spectra of films processed with photochromic molecules were blue shifted compared to that of P3HT: PCBM due to reduced interactions between P3HT polymer segments. The properties worsened as the concentrations of additives gradually increased. Photoswitching was observed for films processed with spiropyran and diarylethene molecules. Fatigue was observed for the blends processed with SP. This study demonstrated that doping semiconducting materials with photochromes is not an ideal strategy for tuning properties of OPV blends. Development of photochromic polymers could enable realization of photoswitchable OPVs and other organic electronic devices. Therefore, the scope of the project focussed on the development of mainchain photochromic polymers.

3.5.References

[1] M. Lahikainen, K. Kuntze, H. Zeng, S. Helantera, S. Hecht, A. Priimagi, *ACS Appl. Mater. Interfaces***2020**, *12*, 47939.

[2] P. Lutsyk, K. Janus, J. Sworakowski, A. Kochalska, S. Neprek, *Chem. Phys.***2012**, *404*, 22.

[3] M. Irie, M. Morimoto, *Photochemistry,***2020***, 47,* 457.

[4] J. Frisch, M. Herder, P. Herrmann, G. Heimel, S. Hecht, N. Koch, *Appl. Phys. A Mater. Sci. Process.***2013**, *113*, 1.

[5] F. M. Raymo, M. Tomasulo, *Chem. Soc. Rev.***2005**, *34*, 327.

[6] N. Matsui, T. Tsujioka, *Org. Electron.***2014**, *15*, 2264.

[7] M. Irie, *Proc. Japan Acad. Ser. B Phys. Biol. Sci.***2010**, *86*, 472.

[8] G. Ligorio, G. F. Cotella, A. Bonasera, N. Zorn Morales, G. Carnicella, B. Kobin, Q. Wang, N. Koch, S. Hecht, E. J. W. List-Kratochvil, F. Cacialli, *Nanoscale***2020**, *12*, 5444.

[9] P. Zacharias, M. C. Gather, A. Köhnen, N. Rehmann, K. Meerholz, *Angew. Chemie - Int. Ed.***2009**, *48*, 4038.

[10] Z. Zhang, X. Liu, Z. Li, Z. Chen, F. Zhao, F. Zhang, C. H. Tung, *Adv. Funct. Mater.***2008**, *18*, 302.

[11] A. R. Tuktarov, R. B. Salikhov, A. A. Khuzin, I. N. Safargalin, I. N. Mullagaliev, O. V. Venidiktova, T. M. Valova, V. A. Barachevsky, U. M. Dzhemilev, *Mendeleev Commun.***2019**, *29*, 160.

[12] M. Carroli, D. T. Duong, E. Buchaca-Domingo, A. Liscio, K. Börjesson, M.

Herder, V. Palermo, S. Hecht, N. Stingelin, A. Salleo, E. Orgiu, P. Samorì, *Adv. Funct. Mater.***2020**, *30*, 1907507.

[13] A. R. Tuktarov, R. B. Salikhov, A. A. Khuzin, N. R. Popod'Ko, I. N. Safargalin, I. N. Mullagaliev, U. M. Dzhemilev, *RSC Adv.***2019**, *9*, 7505.

[14] M. El Gemayel, K. Börjesson, M. Herder, D. T. Duong, J. A. Hutchison, C. Ruzié, G. Schweicher, A. Salleo, Y. Geerts, S. Hecht, E. Orgiu, P. Samorì, *Nat. Commun.***2015**, *6*, 1.

[15] M. Kang, A. N. Cha, S. A. Lee, S. K. Lee, S. Bae, D. Y. Jeon, J. M. Hong, S. Fabiano, M. Berggren, T. W. Kim, *Org. Electron.***2019**, *78*, 105554.

[16] Y. Li, H. Zhang, C. Qi, X. Guo, *J. Mater. Chem.***2012**, *22*, 4261.

[17] Q. Shen, L. Wang, S. Liu, Y. Cao, L. Gan, X. Guo, M. L. Steigerwald, Z. Shuai, Z. Liu, C. Nuckolls, *Adv. Mater.***2010**, *22*, 3282.

[18] E. Orgiu, N. Crivillers, M. Herder, L. Grubert, M. Pätzel, J. Frisch, E. Pavlica, D. T. Duong, G. Bratina, A. Salleo, N. Koch, S. Hecht, P. Samorì, *Nat. Chem.***2012**, *4*, 675.

[19] H. Qiu, Z. Liu, Y. Yao, M. Herder, S. Hecht, P. Samorì, *Adv. Mater.***2020**, *32*, 1.

[20] W. Rekab, T. Leydecker, L. Hou, H. Chen, M. Kirkus, C. Cendra, M. Herder, S. Hecht, A. Salleo, I. McCulloch, E. Orgiu, P. Samorì, *Adv. Funct. Mater.***2020**, *30*, 1.

[21] Y. Kurokawa, R. Hayakawa, S. Shimada, K. Higashiguchi, Y. Noguchi, K. Matsuda, Y. Wakayama, *Org. Electron.***2019**, *64*, 205.

[22] W. Wang, L. Song, D. Magerl, D. Moseguí González, V. Körstgens, M. Philipp, J. F. Moulin, P. Müller-Buschbaum, *Adv. Funct. Mater.***2018**, *28*, 1.

[23] T. H. Lee, S. Y. Park, B. Walker, S. J. Ko, J. Heo, H. Y. Woo, H. Choi, J. Y. Kim, *RSC Adv.***2017**, *7*, 7476.

[24] R. Yu, H. Yao, L. Hong, Y. Qin, J. Zhu, Y. Cui, S. Li, J. Hou, *Nat. Commun.***2018**, *9*, 1.

[25] G. Sai-Anand, A. Dubey, A. I. Gopalan, S. Venkatesan, S. Ruban, K. M. Reza, J. Choi, K. S. Lakhi, B. Xu, Q. Qiao, A. Vinu, *Sol. Energy Mater. Sol. Cells***2018**, *182*, 246.

[26] B. Xu, G. Sai-Anand, G. E. Unni, H. M. Jeong, J. S. Kim, S. W. Kim, J. B. Kwon, J. H. Bae, S. W. Kang, *Appl. Surf. Sci.***2019**, *484*, 825.

[27] B. Xu, G. Sai-Anand, A. I. Gopalan, Q. Qiao, S. W. Kang, *Polymers (Basel).***2018**, *10*, 1.

[28] N. Y. Doumon, G. Wang, X. Qiu, A. J. Minnaard, R. C. Chiechi, L. J. A. Koster, *Sci. Rep.***2019**, *9*, 1.

[29] H. Waters, N. Bristow, O. Moudam, S. W. Chang, C. J. Su, W. R. Wu, U. S. Jeng, M. Horie, J. Kettle, *Org. Electron.***2014**, *15*, 2433.

[30] I. E. Jacobs, F. Wang, Z. I. Bedolla Valdez, A. N. Ayala Oviedo, D. J. Bilsky, A. J. Moulé, *J. Mater. Chem. C***2018**, *6*, 219.

[31] N. D. Treat, C. G. Shuttle, M. F. Toney, C. J. Hawker, M. L. Chabinyc, *J. Mater. Chem.***2011**, *21*, 15224.

[32] Z. Abada, A. Mellit, M. Benghanem, *Int. J. Green Energy***2020**, *17*, 101.

[33] D. Liu, D. J. Broer, *Nat. Commun.***2015**, *6*, 8334.

[34] J. Keyvan Rad, Z. Balzade, A. R. Mahdavian, *J. Photochem. Photobiol. C Photochem. Rev.***2022**, *51*, 100487.

[35] G. Vamvounis, N. Sandery, *Aust. J. Chem.***2015**, *68*, 1723.

[36] H. N. Tran, D. H. Kim, S. Park, S. Cho, *Curr. Appl. Phys.***2018**, *18*, 534.

[37] Y. Ishiguro, R. Hayakawa, T. Chikyow, Y. Wakayama, *ACS Appl. Mater. Interfaces***2014**, *6*, 10415.

[38] J. Zhao, A. Swinnen, G. Van Assche, J. Manca, D. Vanderzande, B. Van Mele, *J. Phys. Chem. B***2009**, *113*, 1587.

[39] T. T. Ngo, D. N. Nguyen, V. T. Nguyen, *Adv. Nat. Sci. Nanosci. Nanotechnol.***2012**, *3*, 045001.

[40] C. Zhang, A. Mumyatov, S. Langner, J. D. Perea, T. Kassar, J. Min, L. Ke, H. Chen, K. L. Gerasimov, D. V. Anokhin, D. A. Ivanov, T. Ameri, A. Osvet, D. K. Susarova, T. Unruh, N. Li, P. Troshin, C. J. Brabec, *Adv. Energy Mater.***2017**, *7*, 1601204.

[41] Z. M. Beiley, E. T. Hoke, R. Noriega, J. Dacuña, G. F. Burkhard, J. A. Bartelt, A. Salleo, M. F. Toney, M. D. McGehee, *Adv. Energy Mater.***2011**, *1*, 954.

[42] I. T. Sachs-Quintana, T. Heumüller, W. R. Mateker, D. E. Orozco, R. Cheacharoen, S. Sweetnam, C. J. Brabec, M. D. McGehee, *Adv. Funct. Mater.***2014**, *24*, 3978.

[43] J. Yin, W. Zhou, L. Zhang, Y. Xie, Z. Yu, J. Shao, W. Ma, J. Zeng, Y. Chen, *Macromol. Rapid Commun.***2017**, *38*, 1.

[44] Y. Ishiguro, R. Hayakawa, T. Chikyow, Y. Wakayama, *ACS Appl. Mater. Interfaces***2014**, *6*, 10415.

[45] A. Solanki, B. Wu, T. Salim, Y. M. Lam, T. C. Sum, *Phys. Chem. Chem. Phys.***2015**, *17*, 26111.

[46] M. S. Park, F. S. Kim, *Polymers (Basel).***2019**, *11*, 1.

[47] B. Kim, B. Ma, V. R. Donuru, H. Liu, J. M. J. Fréchet, *Chem. Commun.***2010**, *46*, 4148.

[48] B. Lim, J. Jo, S. I. Na, J. Kim, S. S. Kim, D. Y. Kim, *J. Mater. Chem.***2010**, *20*, 10919.

[49] G. Kalonga, *J. Chem. Eng. Mater. Sci.***2013**, *4*, 93.

[50] H. Kim, S. Ok, H. Chae, Y. Choe, *Nanoscale Res. Lett.***2012**, *7*, 56.

[51] C. Scharsich, R. H. Lohwasser, M. Sommer, U. Asawapirom, U. Scherf, M. Thelakkat, D. Neher, A. Köhler, *J. Polym. Sci. Part B Polym. Phys.***2012**, *50*, 442.

[52] R. Steyrleuthner, M. Schubert, I. Howard, B. Klaumünzer, K. Schilling, Z. Chen, P. Saalfrank, F. Laquai, A. Facchetti, D. Neher, *J. Am. Chem. Soc.***2012**, *134*, 18303.

[53] U. Bhattacharjee, D. Freppon, L. Men, J. Vela, E. A. Smith, J. W. Petrich, *ChemPhysChem***2017**, *18*, 2526.

[54] A. Gonzalez, E. S. Kengmana, M. V. Fonseca, G. G. D. Han, *Mater. Today Adv.***2020**, *6*, 100058.

[55] R. Klajn, *Chem. Soc. Rev.***2014**, *43*, 148.

CHAPTER 4

EFFECT OF ALKYL CHAIN LENGTH ON THE PROPERTIES OF DIARYLETHENE-BASED MAINCHAIN PHOTOCHROMIC POLYMERS

4.1.Introduction

Organic electronics, such as field effect transistors(OFETs), [1–3] light emitting diodes (OLEDs),[4] actuators,[5] and photovoltaics (OPV),[6] have the potential to revolutionize the semiconductor industry with ultra-thin, flexible, efficient and long-lasting devices. Solution processable conjugated polymers have been used as the active semiconductor layer in these devices because of their cost-effective simple processing to form uniform thin-films. To broaden the foot-print of these devices, multi-functional conjugated materials are on demand to allow for instance smart solar cell windows [6] and non-destructive memory devices.[7] Organic photochromic materials are of great interest because they are conjugated and their optoelectronic properties can be tuned using light. Organic photochromic materials developed so far have been primarily limited to crystalline small molecule materials which are not solution processable or side-chain photochromic polymers which would limit intra- and inter-chain charge transport.[8] This study explores synthetic strategies to produce solution-processable photochromic polymers in the mainchain. The quality of the films and their photoswitchable properties were investigated as a function of alkyl chain length.

Photochromic materials can be broadly classed as thermally-reversible or light-reversible materials.[9] For organic electronic devices, light-reversible materials are of interest because of the thermal stability of both colorless and colored states.[10,11] One class of light-reversible materials is based on the dithienylethenes (DTE) motif which undergo an efficient 6-π electrocyclization and cycloreversion process in the presence of UV and visible light to switch from their colorless open-isomeric form to their colored closed-isomeric form.[11,12] Furthermore, DTEs have been shown to be fatigue resistant for over30000 cycles in the single crystalline phase showing great promise for robust organic electronic devices.[13,14] However, studies to date have primarily focused on the solution or single crystal photonic properties of these photochromic molecules, which has limited application to organic electronic devices as these devices require uniform thin films.[15–17]

Photochromic materials that are solution-processable to form uniform thin films have been achieved by dispersing the photochromic molecules into semiconducting polymer matrices such as poly(3-hexylthiophene) (P3HT) and poly(9,9-dioctylfluorene-alt-bithiophene). These dispersed materials have successfully controlled the dielectric constant in the channel layer in field effect transistors to control the charge mobility of these devices.[18–20] They have also been used as photoactive layers of OPV devices that change color and light absorption when illuminated with UV or Vis light.[6] Unfortunately, the photoswitching quantum yields are reduced as the polymer matrix hinders the change in the molecular configuration. Furthermore, the photochrome concentration should be as high as possible to maximize the doping effect. However, there is an upper limit to the photochrome concentration to avoid phase separation or segregation, which can affect charge transport. For instance, Li *et al.*[21] had to restrict the photochrome concentration in host P3HT <10 wt.% to suppress phase separation. Polymers containing photochromic materials on the side-chain have shown photoswitching in the neat thin film state.[22,23] These side-chain polymers are excellent materials for photonic applications; however, charge conduction, which is required for organic electronic devices, may be limited due to the lack of intra-chain charge transport.

Mainchain photochromic materials are ideal multi-functional materials for organic electronic devices due to their inter- and intra-charge transport properties, however, their solubility can be a significant issue for DTE type polymers because of the lack of alkyl chains required for solubilization.[24,25] To overcome insolubility, aromatic comonomers containing solubilizing alkyl-chains based on fluorene,[26] phenylene [8,27,28] and quinolone [29] can be used however most designs have either have poor solubility,[8] low molecular weights,[26,30] poor photoswitching quantum yields in solid state [26] or photochemical instability.[28] For instance, Stellaci*et al.*[30] reported poly(1,2-bis(2-meth- yl-3-thienyl)perfluorocyclopentene) with a low molecular weight of 3000 g/mol. In addition, Kawai *et al.*[26] reported a main chain photochromic copolymer comprised of hexafluorocyclopentene-benzothiophene switching unit and dioctylfluorene derivatives which were found to have low photoswitching quantum yields in solid state and photo-chemically unstable.Solubility and polymer molecular weights are interrelated to the solubilizing group, and the switching ability has been attributed to steric encumbrance.[31] Film quality is often linked to polymer molecular weight.[32,33] Therefore, the design of mainchain photochromic polymers with improved thin-film photochromic properties requires a fundamental understanding of the structural requirements for optimal solubility, thin film formation and photoswitching quantum yields.This study, therefore, explores the effect of the alkyl side-chain length to understand the design requirements for efficient and solution processable mainchain photoswitchable polymers.

4.2.Experimental

4.2.1. Chemicals and reagents

2-Methylthiophene, N-bromosuccinimide (NBS), trimethylsilyl chloride (TMSCl), *n*-butyllithium, fluorene, bromine, tetrabutylammonium bromide, 1-bromopropane, bromobenzene and phenylboronic acid, tetrakis(triphenylphosphine)palladium(0) ($Pd(PPh_3)_4$) and 2-isopropoxy-4,4,5,5-tetramethyl-[1,3,2]dioxaborolane were purchased from Sigma Aldrich. 9,9-di-*n*-hexylfluorene-2,7-diboronic acid bis(pinacol) ester and 9,9-di-*n*-octylfluorene-2,7-diboronic acid bis(pinacol) ester were purchased from Boron Molecular. Octafluorocyclopentene was supplied by TCI chemicals. Sodium hydroxide pellets, anhydrous sodium sulfate, sodium chloride and potassium carbonate were purchased from Univar. Tetrahydrofuran (THF) was dried over sodium/benzophenone and then distilled under argon atmosphere immediately before use. Dichloromethane (DCM) and petroleum ether were distilled prior to use.

4.2.2. Characterization

^1H NMR spectra were acquired using a Bruker AscendTM 400 MHz spectrometer for samples in $CDCl_3$. Chemical shifts are reported in parts per million (ppm) and are referenced to the residual solvent peak (chloroform, ^1H = 7.26 ppm). Peak multiplicities are designated in the following manner: singlet (s), doublet (d), triplet (t), doublet and multiplet (m). The polymer molecular weights were determined using gel permeation chromatography (GPC) (Agilent Technologies 1260 Infinity Series) using THF as eluent and polystyrene narrow standards. The PLgel 5 μm Mixed–C columns (300×7.5 mm)×2 were calibrated using polystyrene narrow standards in tetrahydrofuran. Infrared spectra were recorded on Nicolet 6700 FT-IR spectrometer equipped with an attenuated total reflection (ATR) crystal. Absorption spectra were recorded using a Shimadzu UV2600 spectrophotometer. Surface roughness and morphology were studied using AFM (NT-MDT NTEGRA).

Molar absorption coefficients of closed-form isomers were determined by linear fitting concentrations and absorption values of polymer solutions after all the open isomers have been fully converted to closed isomers by UV irradiation. The conversion from open-form to closed-form was calculated to be 99% for all the polymers. Solution quantum yields of cyclization ($\Phi_{o\rightarrow c}$) and cycloreversion ($\Phi_{c\rightarrow o}$) were measured by a relative method in THF using 1,2-bis(2-methyl-5-phenyl-3-thienyl)perfluorocyclopentene as the reference standard/actinometer, which has quantum yields of cyclization of 0.574 at 365 nm and quantum yield of cycloreversion of 0.013 at $\lambda>492$ nm.[34,35] The quantum yield was calculated using the equation below:

$$\Phi_{o\rightarrow c} = \frac{\Delta \mathrm{A} \times \mathrm{V}}{\mathrm{I_o} \times (1 - 10^{-\mathrm{A}\lambda}) \times \varepsilon \times \Delta \mathrm{t}} \tag{4.1}$$

$\Delta A$is the increase of absorbance at λ_{max} of the closed-form isomer; Δt is the irradiation time required to reach photostationary state; V is the volume (L) of irradiated solution; $\varepsilon$is the molar absorption coefficient of the closed-form isomer obtained using a linear fit between concentration and absorption (reported in **Table 4.2**); A is the absorbance of the solution at the irradiation wavelength (mean value during the irradiation period) and $I_o$is the photon flux determined using the actinometer (reference molecule) 1,2-bis(2-methyl-5-phenyl-3-thienyl)perfluorocyclopentene. The photon flux was measured as previously reported.[36] The expression for the ring-opening quantum yield $\Phi_{c\rightarrow o}$is the same as equation 1 but in this case ΔA is the decrease in absorbance at λ_{max} of the closed-form isomer. Conversion was calculated using **equation (4.2)**.[8]

$$C(\lambda) = \frac{\varepsilon_o(\lambda)\Phi_{o\to c}}{\varepsilon_c(\lambda)\Phi_{c\to o} + \varepsilon_o(\lambda)\Phi_{o\to c}} \qquad (4.2)$$

where ε_o and ε_c is the molar absorption coefficient of the open-form and closed-form isomers, respectively.$\Phi_{o\to c}$ and $\Phi_{c\to o}$ is cyclization and cycloreversion quantum yield, respectively.

The relative rates of solid state photoswitching were measured relative to poly(3-[3,3,4,4,5,5-hexafluoro-2-(2-methyl-3-thienyl)-1-cyclopenten-1-yl]-2-methylthiophene)-*alt*-(di-*n*-hexylphenylene) (P4) (discussed in Chapter 5) and calculated using the **equation 4.3**.

$$\frac{\chi_i}{\chi_4} = \frac{S_i}{S_4}\frac{\epsilon_4}{\epsilon_i}, \qquad (4.3)$$

where χ_i is the rate of photoswitching of polymer i (representing P1, P2 and P3), χ_4 is the rate for P4, $S_i = \frac{dA}{dt}$ is the slope of the absorbance-vs-time plot for polymer i as shown in **Figure 4.7a** and **b**, S_4 is the slope for P4, ϵ_i is the molar absorption coefficient of polymer i and ϵ_4 is the same for P4. The reference values for poly(3-[3,3,4,4,5,5-hexafluoro-2-(2-methyl-3-thienyl)-1-cyclopenten-1-yl]-2-methylthiophene)-alt-(di-n-hexylphenylene) were taken to be $\chi_{o\to c} = 1$ and $\chi_{c\to o} = 0.1$.Concentrations were calculated using the molar masses of the repeating units.

Thin films for measuring UV–Vis absorption spectroscopy and atomic force microscopy were prepared on glass (Sail Brand) by spin coating 10 mg/mL (for UV-Vis) and 20 mg/mL (for AFM) in toluene at 1500 rotations per minute for 45 s using a Chemat KW-4A spincoater. Glass substrates were cleaned prior to use in an ultrasound bath for 10 minutes using soapy water, acetone and ethanol, respectively, and dried under nitrogen. The surface morphology and thickness of the films was measured using an NTEGRA TS-150 atomic force microscope (AFM) in semi contact mode. Molar absorption coefficients in solid state were evaluated by UV-Vis spectroscopy from linear fits of absorbance of films of different thicknesses. In a typical procedure, four films of the same polymer were prepared by spin coating solutions with different concentrations. The absorbance of each film was recorded before and after switching the polymers. The absorbance values were plotted against film thickness (cm) to estimate the absorption coefficients and reported in **Table 4.3**. Thermal properties were investigated using an SDT 650 (TA instruments) and DSC 250 (TA instruments). The DSC was equipped with a refrigeration cooling system (RCS) and the heating/ cooling rates were equal at 10 ºC min^{-1}. TGA ramp rate was maintained at 10 ºC min^{-1}. Degradation temperatures were estimated at 5% weight loss. Photochemical stability measurements were performed by switching repeatedly between the colored and colorless isomeric forms of the polymers using a handheld UVGL-58 lamp at 365 nm (6W) and visible light Cole-ParmerFiber Optic Illuminator (150 W) and measuring the absorption spectra. A cut-off filter was used for cycloreversion experiments to eliminate UV light. Polymer films (~20 nm) were irradiated with alternate UV and visible light for 600s in air and absorbance was measured and recorded after each switching cycle. Switching experiments were optimised up to 20 cycles using fluorene-based polymers. Switching cycles were optimized, it took ~600 s to convert a polymer from open form to closed form and for the reverse reaction. No signs of fatigue were observed after 20 cycles. To compare all the polymers, switching cycles were reduced to 12 to save time.

4.2.3. Synthesis of comonomers

The dibromide monomer was synthesized following a procedure shown in **Scheme 4.1.**

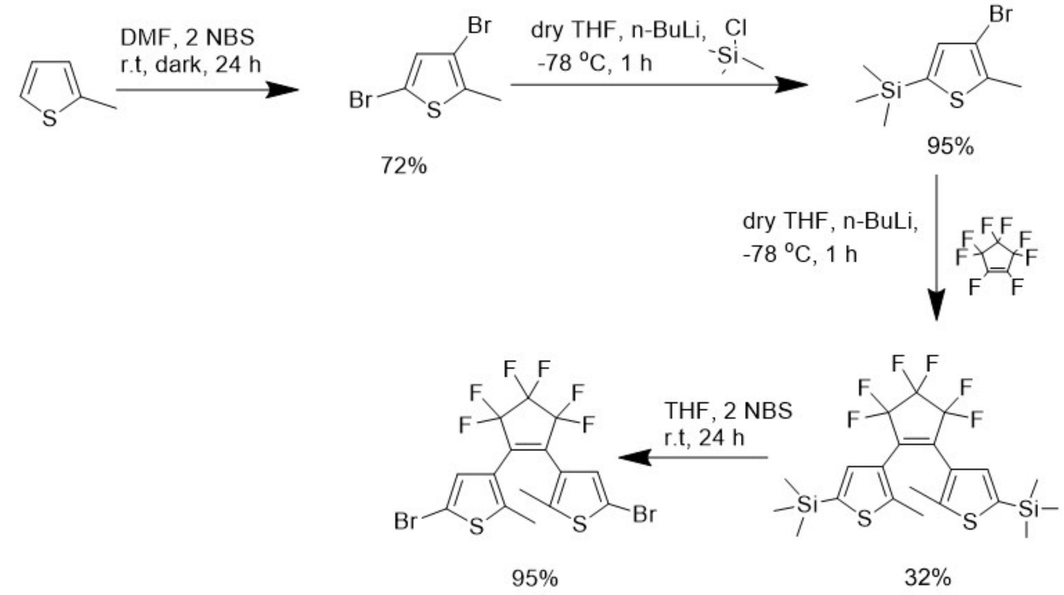

Scheme 4.1: Synthesis of 5-bromo-3-[2-(5-bromo-2-methyl-3-thienyl)-3,3,4,4,5,5-hexafluoro-1-cyclopenten-1-yl]-2-methylthiophene.

Synthesis of 3,5-dibromo-2-methylthiophene

A 250 mL round bottom flask was charged with 2-methylthiophene (10.0 g, 104 mmol, 1.0 eq.) dissolved in dimethylformamide (200 mL). N-Bromosuccinimide (NBS) (36.84 g, 206 mmol, 2.0 eq.) was slowly added to this solution at r.t. and stirred for 24 h at room temperature. The solution was quenched with NH_4Cl (5 mL) and extracted with diethyl ether(3 x 50 mL). The combined organic layers were washed with water (2 x 50 mL) and brine (20 mL). The organic phase was dried over anhydrous sodium sulfate,filtered, and the solvent was removed using a rotary evaporator to afford a light brown oil.[37,38] The crude product was purified by vacuum distillation and column chromatography (column height 17.0 cm, diameter ~4.0 cm) over petroleum ether to afford a yellow oil (18.896 g, 72.09%). ^1H NMR (400 MHz, $CDCl_3$) δ: 2.36 (3H, s); 6.88 (1H, s). υ_{max}/cm^{-1} 783, 816, 951, 1023, 1142, 1304, 1449, 1533, 2918, 3096; MS (*m/z*) Cald for $[C_4H_5Br_2S]^+$:253.8395, found:253.8394.

Synthesis of 3-bromo-2-methyl-5- trimethylsilylthiophene

A 250 mL flame dried round bottom flask was charged with 3,5-dibromo-2-methylthiophene (20.192 g, 78.9 mmol, 1.0 eq.) and dry THF (100 mL) under argon and cooled to -78 °C. n-Butyllithium (1.6 M in hexane, 49 mL, 78.9 mmol, 1.0 eq.) was slowly added resulting in a yellow-brown solution. The reaction for stirred for 0.5 hours at −78 °C. Trimethylsilyl chloride (10.5 mL, 82.8 mmol, 1.05 eq.) was added dropwise to the reaction mixture. The temperature of reaction was allowed to rise to room temperature and the reaction mixture was left to stir overnight. The resulting mixture was poured into 100 mL of ice-cold water and extracted with diethyl ether (3 x 50 mL). The combined organic layers were washed with water (2 x 50 mL) and brine (20 mL). The organic layer was dried over anhydrous sodium sulfate, filtered, and the solvent was removed under reduced pressure to afford a yellow oil. The crude product was purified using column chromatography (silica, petroleum ether, column height 25 cm, diameter ~4.0 cm) to obtain 3-bromo-2-methyl-5-trimethylsilylthiophene as a light yellow oil (18.764 g, 95.16%).[39,40] ^{1}H NMR (400 MHz, $CDCl_3$) δ: 7.03 (s, 1H, Ar-H); 2.44 (s, 3 H, $-CH_3$); 0.30 (s, 9 H, $Si-(CH_3)_3$); υ_{max}/cm^{-1}: 784, 843, 974, 1023, 1143, 1304, 1449, 1534, 2918, 3097; MS (*m/z*) Cald for $[C_4H_{13}SiBrS]^+$: 247.9685, found: 247.9685.

Synthesis of thiophene,3,3'-(3,3,4,4,5,5-hexafluoro-1-cyclopentene-1,2-diyl)bis[2-methyl-5-(trimethylsilyl)-(ACI)

A 250 mL flame dried round bottom flask was charged with 3-bromo-2-methyl-5-trimethylsilylthiophene (15.95 g, 64.0 mmol, 1.0 eq.) and dry THF (130 mL) under argon and cooled to -78 °C. n-Butyllithium(1.6 M in hexane solution, 42 mL, 69.1 mmol, 1.05 eq.) was added dropwise and the reaction was further stirred for 0.5 h while temperature was maintained at -78 °C. Octafluorocyclopentene (4.30 mL, 32.0

mmol, 0.5 eq.) was then added dropwise and the reaction mixture was kept stirring for another 2 h at -78 °C. After that, the reaction was left stirring overnight allowing the temperature to rise to room temperature. The reaction was quenched with water (50 mL) and the aqueous layer was extracted with chloroform (3 x 100 mL) washed with water (2 x 200 mL) and brine (50 mL). The combined organic phase was dried over anhydrous Na_2SO_4, filtered, and the solvent was removed using a rotary evaporator to afford a thick yellow oil. The crude product was purified by column chromatography (column height 15.0 cm, diameter ~4.0 cm) on silica gel with petroleum ether as an eluent to afford a pale yellow oil which was recrystallized from methanol (10 mL) to yield a white waxy powder (4.02 g, 12%).[39] λ_{max} (open isomer) (THF)/nm 280 [log(ε/dm^3 mol^{-1} cm^{-1}) (4.01)]; λ_{max} (closed isomer) (THF)/nm 550 [log(ε/dm^3 mol^{-1} cm^{-1}) (3.85)]; ^{1}H NMR (400 MHz, $CDCl_3$) δ: 7.06 (s, 2H); 1.92 (s, 6H); 0.28 (s, 18H); υ_{max}/cm^{-1} 754, 833, 974, 1091, 1189, 1316, 1438, 1540, 2956; MS (*m/z*) Cald for $[C_{21}H_{26}Si_2F_6S_2]^+$: 512.0913, found: 512.0910; T_m =89.05 ^oC.

Synthesis of 5-bromo-3-[2-(5-bromo-2-methyl-3-thienyl)-3,3,4,4,5,5-hexafluoro-1-cyclopenten-1-yl]-2-methylthiophene

Thiophene,3,3'-(3,3,4,4,5,5-hexafluoro-1-cyclopentene-1,2-diyl)bis[2-methyl-5-(trimethylsilyl)-(ACI)(1.630 g, 3.2 mmol, 1.0 eq.)was dissolved in 50 mL of THF and a solution of NBS (1.132 g, 6.4 mmol, 2.0 eq.) (in THF) was slowly added. The reaction mixture was covered with aluminium foil and stirred in an ice-water bath overnight. The reaction quenched with acetone (10 mL) and the mixture was extracted with chloroform (3 x 30 mL). The combined organic layers were washed with water (2 x 50 mL) and brine (30 mL). The organic layer was dried over anhydrous sodium sulfate, filtered, and the solvent was removed under reduced pressure to afford a pink solid. The crude product was purified by column chromatography on silica gel (column height 15.0 cm, diameter ~3.0 cm) with petrol ether as an eluent to afford a pale-pink powder (1.512 g, 90%)[39].λ_{max} (open isomer) (THF)/nm 306 [log(ε/dm^3 mol^{-1} cm^{-1}) (3.06)]; λ_{max} (closed isomer) (THF)/nm 540 [log(ε/dm^3 mol^{-1} cm^{-1}) (3.15)];^{1}H NMR (400 MHz, $CDCl_3$) δ: 7.03 (s, 2H); 1.91 (s, 6H);υ_{max}/cm^{-1}: 660, 749, 823, 987, 1056, 1186, 1328, 1437, 2956; MS (*m/z*) Cald for $[C_{21}H_{26}Br_2F_6S_2]^+$: 523.8333, found: 523.8329; T_m =149.73 ^{o}C.

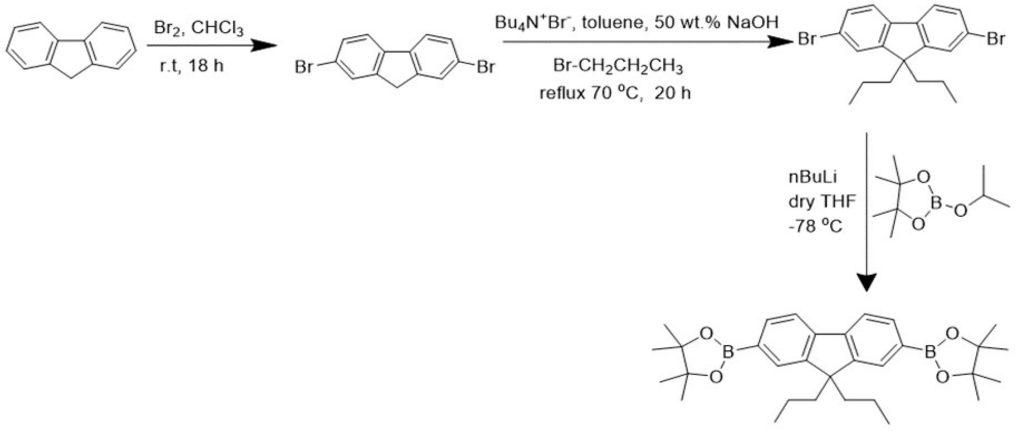

Scheme 4.2: Synthesis of 9,9-dipropylfluorene-2,7-diboronic acid bis(pinacol) ester.

Synthesis of 2,7-dibromofluorene

A 250 mL round bottom flask was charged with fluorene (10.0 g, 60 mmol, 1.0 eq.) and chloroform (150 mL). The mixture was stirred at room temperature for 30 minutes to dissolve all the solid. Anhydrous ferric chloride (150 mg, 0.92 mmol, 0.015 eq.) was then added to the solution, and the flask was wrapped in aluminium foil. The reaction was then cooled to 0 °C in an ice water bath. Bromine (6.4 mL, 123 mmol, 2.05 eq.) was slowly added using a dropping funnel. The ice water bath was removed and the reaction was left stirring overnight at room temperature. To quench the reaction, saturated sodium thiosulfate solution was slowly added until the red color of the solution completely disappeared. The mixture was extracted with dichloromethane (3 x 50 mL) and washed with water (2 x 50 mL) and brine (20 mL).

The combined organic layers were dried over anhydrous sodium sulfate, filtered, and the solvent was removed under reduced pressure to afford a pale yellow solid. The crude product was purified by recrystallization in ethanol (300 mL) to afford an off-white solid (11.04 g; 56.79%)[41,42]. ^{1}H NMR (400 MHz, $CDCl_3$) δ: 7.69 (s, 2H), 7.63 (d, 2H), 7.53 (d, 2H), 3.90 (s, 2H); υ_{max}/cm^{-1} 684, 809, 840, 1003, 1052, 1158, 1388, 1397, 1453; MS (*m/z*) Cald for $[C_{13}H_8Br_2]^+$: 321.8987, found: 321.8986; T_m =162.65 °C.

2,7-dibromo-9,9-dipropylfluorene

A 50 mL round bottom flask was charged with 2,7-dibromofluorene (2 g, 6.17 mmol, 1.0 eq.), tetrabutylammonium bromide (0.169 g,0.525 mmol, 0.085 eq.) as a phase-transfer catalyst and in toluene (10 mL). Aqueous NaOH solution (7.5 mL of 50 wt.%) was added to the mixture and the reaction was allowed to stir for 1 hour at room temperature. 1-bromopropane (1.897 g, 15.425 mmol, 2.5 eq.) was then added and the reaction mixture was thenheated at 70 °C under reflux for 20 h. The reaction mixture was cooled to room temperature and quenched with saturated sodium bicarbonate (100 mL) and extracted with DCM (2 x 50 mL). The combined organic layers were washed with water (2 x 50 mL) dried over anhydrous sodium sulfate, filtered and the solvent was removed under reduced pressure. The crude product was recrystallized twice in ethanol (10 mL) to afford a white solid (1.341g; 53%) [42,43]. ^{1}H NMR (400 MHz, $CDCl_3$) δ: 7.45-7.54 (m, 6H), 1.90-2.01 (m, 4H), 0.62-0.64 (m, 10H); υ_{max}/cm^{-1} 746, 805, 884, 1055, 1268, 1413, 1449, 2865, 2924, 2947; MS (*m/z*) Cald for $[C_{19}H_{20}Br_2]^+$: 405.9926, found: 405.9925; T_m = 135.53 °C.

9,9-dipropylfluorene-2,7-diboronic acid bis(pinacol) ester

A flame dried 100 mL round bottom flask was charged with 2,7-dibromo-9,9-dipropylfluorene (1.0 g, 2.45 mmol, 1.0 eq.) and dry THF (40 mL) under argon and cooled to -78 ^{o}C.*n*-Butyllithium (3.21 mL, 5.1 mmol, 2.1 eq.) was addedand the mixture was stirred for 1 h at -78 ^{o}C.2-Isopropoxy4,4,5,5-tetramethyl-[1,3,2]dioxaborolane(0.9486 g, 5.0 mmol, 2.05 eq.) was added and the mixture was left stirring overnight. The reaction was quenched with 20 mL of cold water and the mixture was extracted with chloroform (3 x 50 mL). The combined organic layers were washed with water (2 x 50 mL). The organic phase was dried over anhydrous sodium sulfate, filtered, and the solvent was removed using a rotary evaporator to afford a light green solid. The crude product was recrystallized twice in ethanol (10 mL) to yield an off-white solid (0.65 g; 58%). ^{1}H NMR (400 MHz, $CDCl_3$) δ: 7.72-7.81 (m, 6H), 1.99-2.03 (m, 4H), 1.40 (s, 24H), 0.60-0.87 (m, 10H); υ_{max}/cm^{-1} 710, 837, 865, 1079, 1111, 1265, 1346, 1423, 1473, 1607, 2834, 2932, 2959; MS (*m/z*) Cald for $[C_{31}H_{44}B_2O_4]^+$: 502.3421, found: 502.3416; T_m = 271.49 ^{o}C.

4.2.4. Synthesis of polymers

Poly(3-[3,3,4,4,5,5-hexafluoro-2-(2-methyl-3-thienyl)-1-cyclopenten-1-yl]-2-methylthiophene)-*alt*-(9,9-di-*n*-propyl-9H-fluorene) (P1)

A 50 mL Schlenk tube was charged with 5-bromo-3-[2-(5-bromo-2-methyl-3-thienyl)-3,3,4,4,5,5-hexafluoro-1-cyclopenten-1-yl]-2-methylthiophene (0.1050 g, 0.194 mmol), 9,9'-*n*-propylfluorene-2,7-diboronic acid bis(pinacol) ester (0.09 g, 0.194 mmol), THF(3.5 mL) and aqueous potassium carbonate (2 ml, 2 M). This mixture was purged with nitrogen for 10 min and $Pd(PPh_3)_4$ (0.0022 g, 0.0019 mmol) was added. The mixture was then degassed three times using freeze-pump thaw cycles then covered with a blanket of argon. The mixture was stirred at 60 °C for 120 h. To remove the reactive end-groups, the resultant polymer was treated bromobenzene and phenylboronic acid after 72 and 84 h, respectively. The reaction was quenched with water (10 mL), and the mixture was extracted with dichloromethane (3 x 20 mL). The combined organic layers were washed with water (2 x 50 mL) and brine (20 mL). The organic layer was dried over anhydrous sodium sulfate, filtered, and the solvent was removed using a rotary evaporator to afford a teal green colored oil. The oil was dissolved in 5 ml of chloroform and precipitated into 25 mL methanol to afford a teal green solid (0.08 g, 76%). λ_{max} (open isomer) (THF)/nm 365 [log(ε/dm^3 mol^{-1} cm^{-1}) (4.64)], λ_{max} (closed isomer) (THF)/nm 625 [log(ε/dm^3 mol^{-1} cm^{-1}) (4.38)];^{1}H NMR (400 MHz, $CDCl_3$) δ: 7.22-7.44 (m, 8H), 1.84-1.93 (m, 10H), 0.52-0.81 (m, 10H); υ_{max}/cm^{-1} 853, 990, 1008, 1053, 1113, 1135, 1198, 1216, 1228, 1270, 1365, 1455, 1738, 2968; T_d = 344 °C; GPC: M_w = 10.73 kg/mol, PDI = 3.53.

Poly(3-[3,3,4,4,5,5-hexafluoro-2-(2-methyl-3-thienyl)-1-cyclopenten-1-yl]-2-methylthiophene)-*alt*-(9,9-di-*n*-hexyl-9H-fluorene) (P2)

A 50 mL Schlenk tube was charged with 5-bromo-3-[2-(5-bromo-2-methyl-3-thienyl)-3,3,4,4,5,5-hexafluoro-1-cyclopenten-1-yl]-2-methylthiophene (0.1020 g, 0.194 mmol, 1.0 eq.), 9,9-di-*n*-hexylfluorene-2,7-diboronic acid bis(pinacol) ester (0.114 g, 0.194 mmol, 1.0 eq.), toluene (3.5 mL) and aqueous potassium carbonate (2 ml, 2 M). This mixture was purged with nitrogen for 10 min and $Pd(PPh_3)_4$ (0.0021 g, 0.0019 mmol) was added. The mixture was then degassed three times using freeze-pump thaw cycles and then covered with a blanket of argon. The mixture was stirred at 100 °C for 120 h. To remove the reactive end-groups, the resultant polymer was treated bromobenzene and phenylboronic acid after 72 and 84 h, respectively. The reaction was quenched with water (10 mL), and the mixture was extracted with dichloromethane (3 x 20 mL). The combined organic layers were washed with water (2 x 50 mL) and brine (20 mL). The organic layer was dried over anhydrous sodium sulfate, filtered, and the solvent was removed using a rotary evaporator to afford a teal green colored oil. The oil was dissolved in 5 ml of chloroform and precipitated into 25 mL methanol to afford a teal green solid (0.09 g, 68%). λ_{max} (open isomer) (THF)/nm 365 [log(ε/dm^3 mol^{-1} cm^{-1}) (4.56)], λ_{max} (closed isomer) (THF)/nm 625 [log(ε/dm^3 mol^{-1} cm^{-1}) (4.38)]; ^{1}H NMR (400 MHz, $CDCl_3$) *δ*: 7.71 ppm (d, 2H), 7.58 ppm (d, 2H), 7.49 ppm (s, 2H), 7.38 ppm (s, 2H), 2.06 ppm (m, 9H), 1.10 ppm (m, 13H), 0.77 ppm (m, 10H); υ_{max}/cm^{-1} 812, 856, 898, 990, 1031, 1054, 1116, 1133, 1202, 1216, 1228, 1272, 1351, 1364, 1454, 1737, 2855, 2055, 2968; T_d = 389 °C; GPC: M_w = 13.27 kg/mol, PDI = 2.28.

Poly(3-[3,3,4,4,5,5-hexafluoro-2-(2-methyl-3-thienyl)-1-cyclopenten-1-yl]-2-methylthiophene)-*alt*-(9,9-di-*n*-propyl-9H-fluorene) (P3)

A 50 mL Schlenk tube was charged with 5-bromo-3-[2-(5-bromo-2-methyl-3-thienyl)-3,3,4,4,5,5-hexafluoro-1-cyclopenten-1-yl]-2-methylthiophene (0.1010 g, 0.194 mmol, 1.0 eq.), 9,9-di-*n*-octylfluorene-2,7-diboronic acid bis(pinacol) ester (0.123 g, 0.194 mmol, 1.0 eq.), toluene (3.5 mL) and aqueous potassium carbonate (2 ml, 2 M). This mixture was purged with nitrogen for 10 min and $Pd(PPh_3)_4$ (0.0022 g, 0.0019 mmol) was added. The mixture was then degassed three times using freeze-pump thaw cycles and then covered with a blanket of argon. The mixture was stirred at 100 °C for 120 h. To remove the reactive end-groups, the resultant polymer was treated bromobenzene and phenylboronic acid after 72 and 84 h, respectively. The reaction was quenched with water (10 mL), and the mixture was extracted with dichloromethane (3 x 20 mL). The combined organic layers were washed with water (2 x 50 mL) and brine (20 mL). The organic layer was dried over anhydrous sodium sulfate, filtered, and the solvent was removed using a rotary evaporator to afford a teal green colored oil. The oil was dissolved in 5 ml of chloroform and precipitated into 25 mL methanol to afford a teal green solid(0.110 g, 76%). λ_{max} (open isomer) (THF)/nm 365 [log(ε/dm^3 mol^{-1} cm^{-1}) (4.70)], λ_{max} (closed isomer) (THF)/nm 625 [log(ε/dm^3

mol^{-1} cm^{-1}) (4.45)]; ^{1}H NMR (400 MHz, $CDCl_3$) δ: 7.12-7.44 (m, 8H), 1.90-2.01 (m, 10H), 0.78-0.87 (m, 20H), 0.61-0.70 (m, 10H); υ_{max}/cm^{-1} 813, 898, 989, 1053, 1116, 1204, 1216,1228, 1271, 1364, 1454, 2852, 2925, 2968, 3014; T_d = 404 °C; GPC: M_w = 20.21 kg/mol, PDI = 2.18.

4.3.Results and discussion

4.3.1. Polymer synthesis

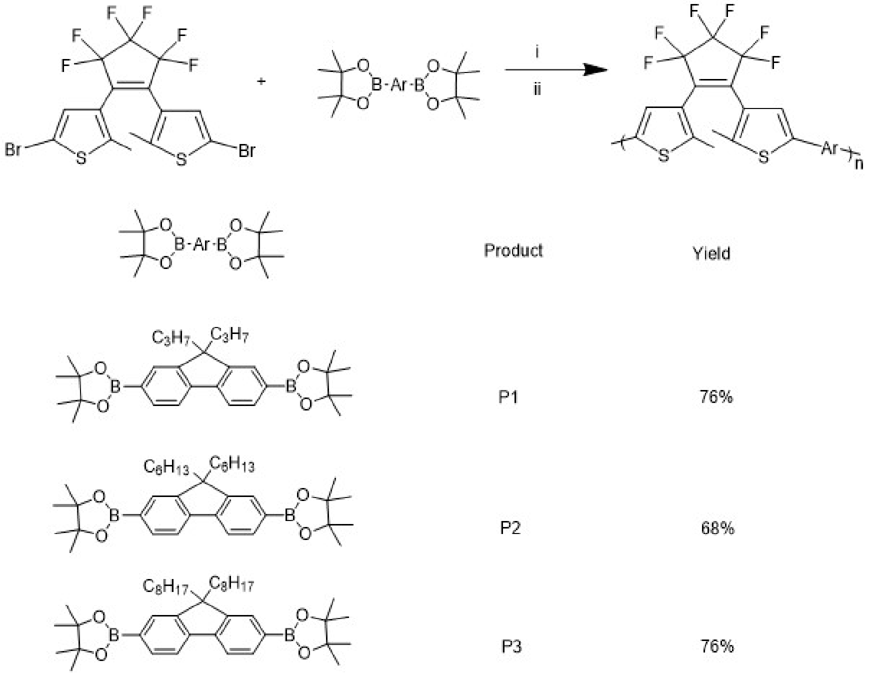

Scheme 4.3: Synthetic protocol for preparation of photochromic polymers. Reagents and conditions: (i) tetrahydrofuran or toluene, 2 M K_2CO_3, $Pd(PPh_3)_4$,60 ºC or 90 ºC, 96-120 h, (ii) phenylboronic acid and bromobenzene.

The syntheses of these polymers were attempted using direct arylation [44]Stille coupling[45] and Suzuki-Miyaura cross-coupling reactions.[46] It was found that Suzuki-Miyaura polycondensation reactions between 5-bromo-3-[2-(5-bromo-2-methyl-3-thienyl)-3,3,4,4,5,5-hexafluoro-1-cyclopenten-1-yl]-2-methylthiopheneand the corresponding diboronic acid bis(pinacol) esters resulted in the highest molecular weight polymers, as shown in **Scheme 4.3**. The dibromide monomer was prepared according to a modified procedure as described by Liu *et al.*[39] This monomer was chosen as a building block to prepare the corresponding polymers as there are many diboronic acid bis(pinacol) esters (or other dimetal cross-coupling reagents) available to co-polymerize with this comonomer. The reactive end-groups of the polymers were replaced with phenylene units using phenyl boronic acid and bromobenzene to avoid unwanted post-polymerization reactions/degradation [47,48] of the polymers during photoswitching. The polymer structure was confirmed using ^{1}H-NMR and FT-IR and their spectra are given in the Appendix of Chapter 3. The polymer's average molecular numbers (M_n) ranged from 2890 to 9308 Daltons and are summarized in **Table 4.1**. The M_n of P1 to P3 increased with alkyl sidechain length and may be attributed to enhanced solubility in the polymerization solvent.[49] All polymers were thermally stable ≥ 344 ˚C (**Figure 4.3b**).

Table 4.1. Molecular weight, glass transition (T_g) and degradation temperatures (T_d) of P1-P3.

Polymer	**M_w (kg/mol)**	**PDI**	**T_g °C**	**T_d °C**
P1	10.73	3.53	170	344
P2	13.27	2.28	108	389
P3	20.21	2.17	96	404

4.3.2. Solution physicochemical properties

The solution properties of the photochromic polymers are depicted in **Figure 4.1** and summarized in **Table 4.2**. The photostationary state (PSS) of all the polymers under ambient conditions were dominated by the open isomer of the photochromic polymer (**Figure 4.2**). The polymer's photostationary properties are similar to isolated DTE photochromic molecules and indicates that the long-range conjugation of the polymer backbone does not affect the PSS of these polymers.[50] The open isomers of P1-P3 showed a strong peak centered at 365 nm in THF due to a π-π* transition and not related to the alkyl side-chain length.[51,52] The maximum absorption of P1 was red-shifted compared to a model compound reported by Woodland *et al*. indicating an extension of the conjugation in both the open (336 vs. 365 nm) and closed (618 vs 625 nm) isomeric forms of the polymers (**Figure 4.3**).[53] The 6-π electrocyclization quantum yield were measured with reference to 1,2-bis(2-methyl-5-phenyl-3-thienyl)perfluorocyclopentene and ranged from 0.524 to 0.594indicating that alky chain length does not affect switching ability. Cycloreversion quantum yields of P1-P3 were similar and ranged from 0.007 to 0.009. Analogues of P1and P3 with lower molecular weight distributions were prepared and their quantum yields were measured (**Table 4.3**). It was found that the quantum yields of cyclization were not dependent on the molecular weight.

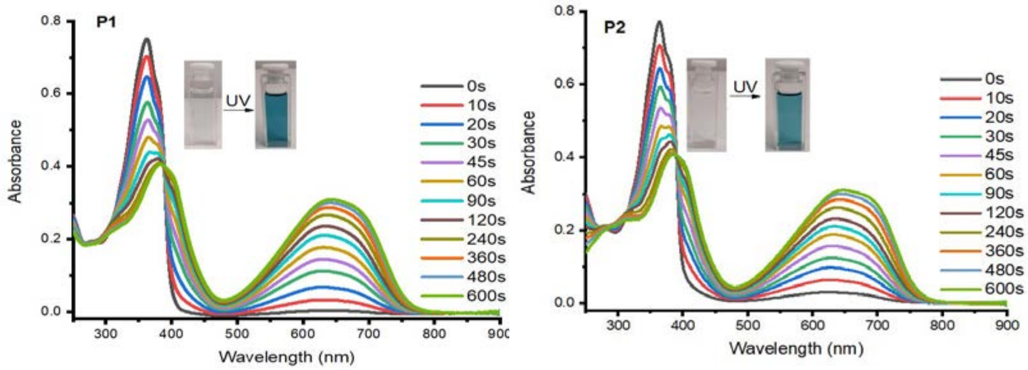

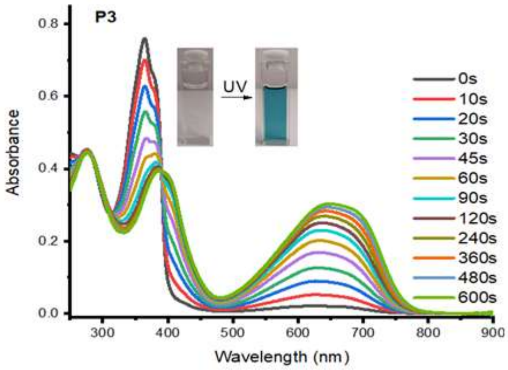

Figure 4.1:UV-Vis absorption spectra of 1x10^{-5} M solutions of P1-P3 in THF upon irradiation with 365 nm monochromatic light.

Table 4.2. Summary of solution properties of P1-P3

	λ$_{max}$; ε (M^{-1} cm^{-1}) (open-form)	**λ$_{max}$; ε (M^{-1} cm^{-1}) (closed-form)**	**$\Phi_{o\rightarrow c}$**	**$\Phi_{c\rightarrow o}$**	**Conversion (%)**
P1	365; 43606	625; 24054	0.594 ± 0.002	0.009 ± 0.001	99
P2	365; 36141	625; 24087	0.591 ± 0.001	0.008 ± 0.001	99
P3	365; 50264	625; 28506	0.524 ± 0.002	0.007 ± 0.001	99

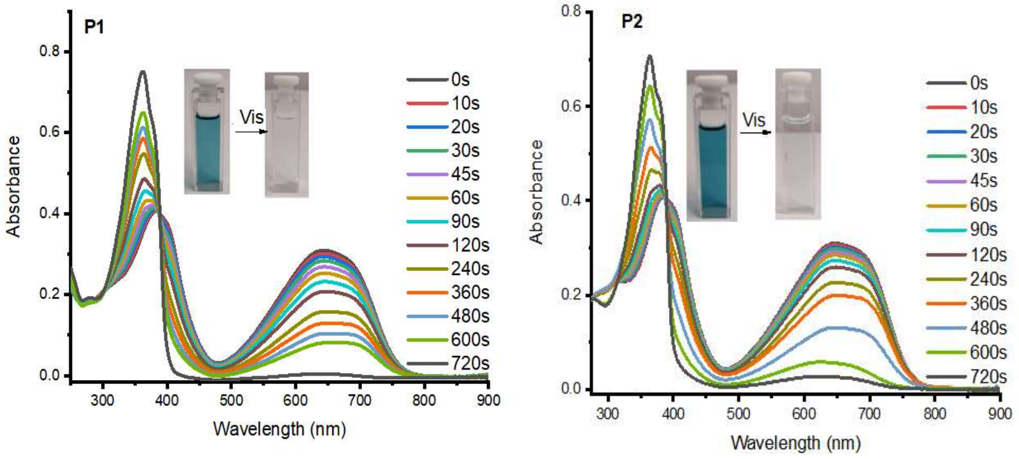

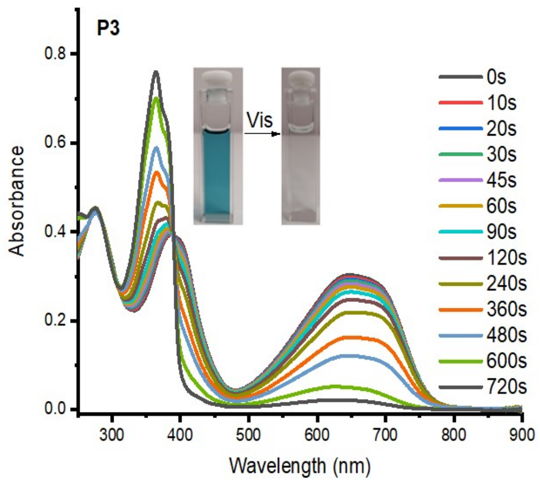

Figure 4.2: Changes in UV-Vis absorption spectra of P1-P3 in THF upon irradiation with Vis light (>550 nm). The solution concentration was 1x10^{-5} M.

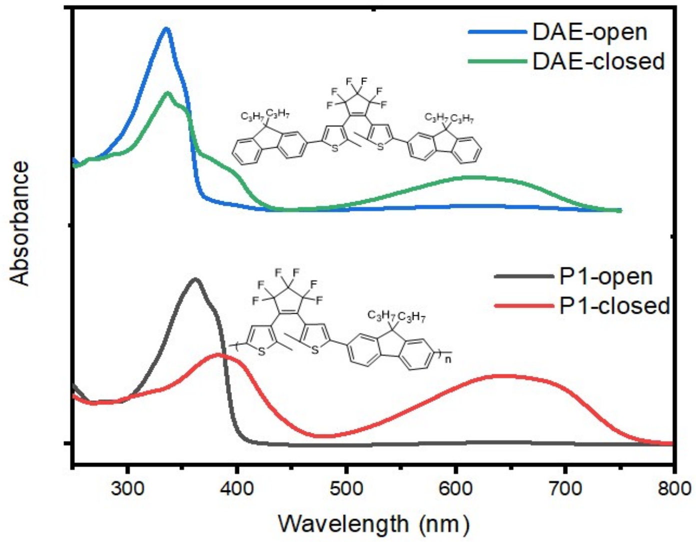

Figure 4.3: Absorption profile of a model diarylethene compound (DAE) and P1 in both open ring and closed ring isomeric forms.

Table 4.3. Dependence of quantum yield on molecular weight.

Polymer	**M_w (kg/mol)**	**ε (M^{-1} cm^{-1}) (closed-form)**	$\Phi_{o\to c}$	$\Phi_{c\to o}$
P1	10.73	24054	0.594 ± 0.002	0.009 ± 0.001
P1-1	6.40	24209	0.590 ± 0.002	0.009 ± 0.001
P3	20.27	28506	0.524 ± 0.002	0.007 ± 0.001
P3-1	8.24	26788	0.520 ± 0.001	0.008± 0.001

4.3.3. Thin film physicochemical properties

Solutions of P1-P3 in toluene (20 mg/mL) were cast onto glass substrates to form 20 nm thick polymer films. These films were characterized using Atomic Force Microscopy (AFM) and Differential Scanning Calorimetry (DSC) to determine the quality of the film and the thermal properties of the resultant films, respectively. **Figure 4.4** depicts the AFM of the six polymer films and their corresponding root mean square (RMS) roughness are reported in **Table 4.4**. All the polymer films were smooth with low RMS roughness; however, small grains could be clearly seen from the micrograph of P1 with an RMS roughness of>2 nm. The micrographs of P2 and P3 were smoother with RMS values <1 nm. This study suggests that the smaller alkyl solubilizing group in P1 may form slightly smaller crystallites due to aggregation.[54–56]

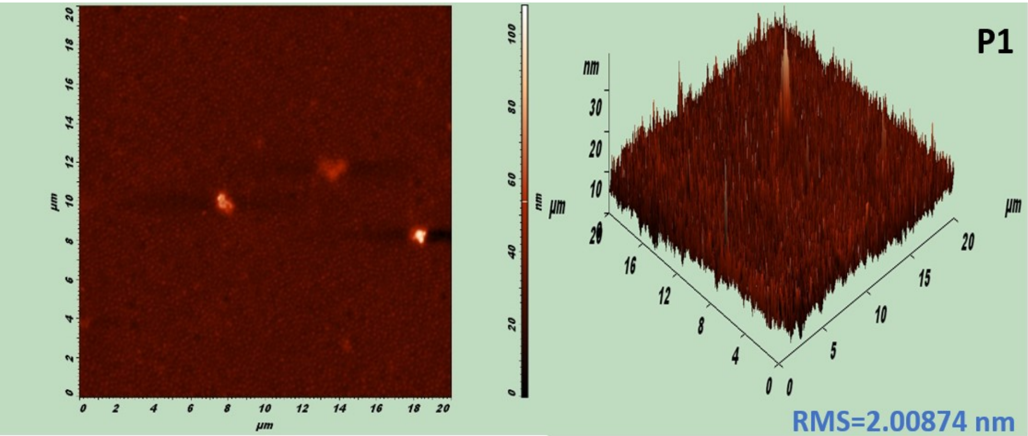

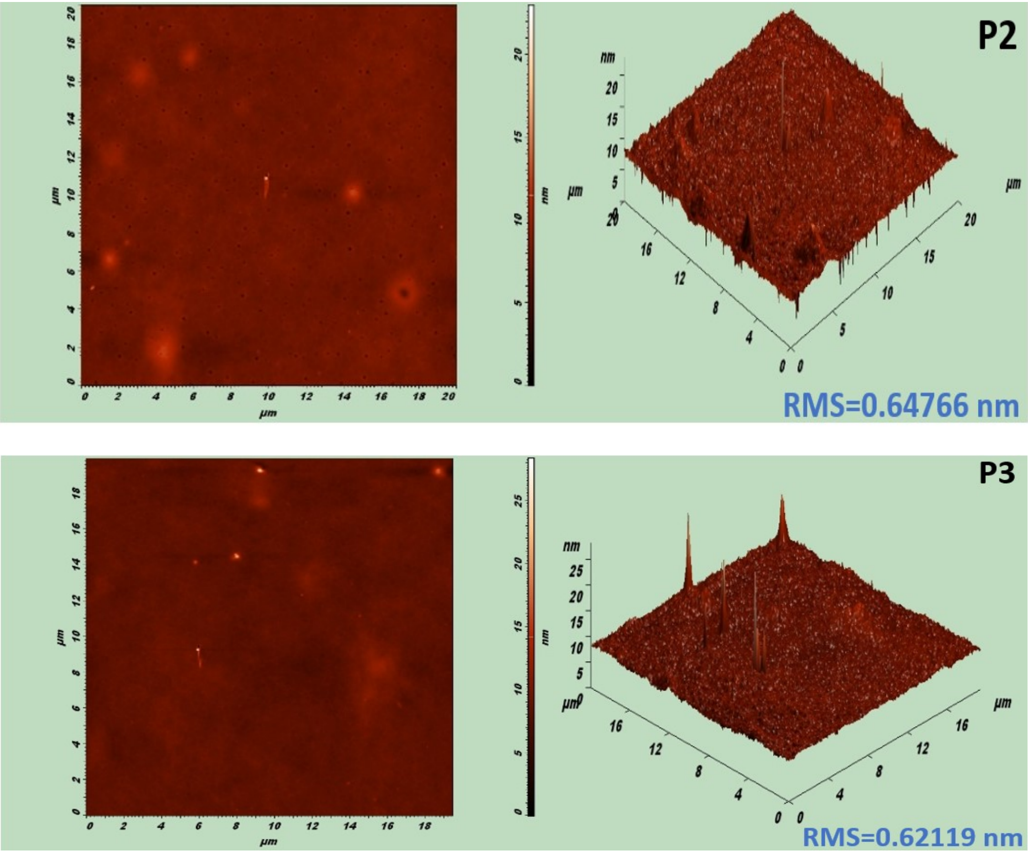

Figure 4.4:AFM micrographs of P1-P3.

Another important property of polymer films is their thermal stability towards change of state (glass transition). **Figure 4.5a** depicts the DSC traces of P1-P3.All polymers show a weak glass transition temperature, and a melting point was not observed, implying all polymers are amorphous. The films were flexible and showed no signs of cracking or fragility. As the alkyl chain length increased from P1-P3, the glass transition temperature decreased from 165 ºC to 96 ºC with enthalpies ranging between 0.3 J/g and 0.9J/g, which has been related to an increase in internal plasticization.[57,58] The transitions are weak as it has been reported for polyfluorenes.[59]

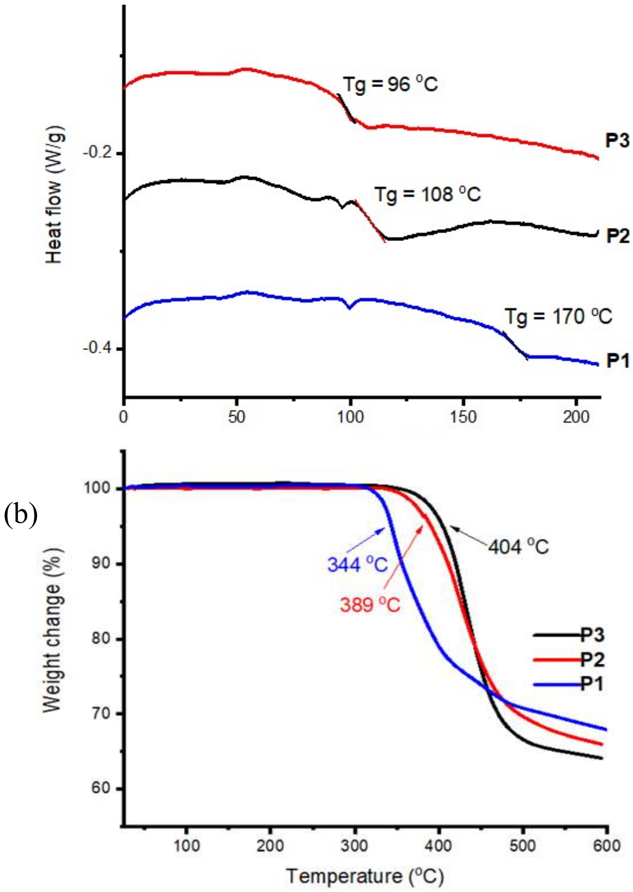

Figure 4.5:DSC traces of P1-P3 (Heating rates were 10 ºC min^{-1}) (a) and TGA thermograms of P1-P3 (Ramp rates were equal 10ºC/min) (b).

The absorption and photochromic properties of the polymer films are depicted in **Figures 4.6** and **4.7** and summarized in **Table 4.4**. The maximum and onset of absorption of the open and closed isomeric form of all the polymers were similar to their solution properties, indicating that planarization of the polymer backbone does not occur in the thin film state regardless of alkyl chain length. This lack of planarization is consistent of conjugated polymers composed of fluorene-*alt*-thiophene based polymers.[60,61]

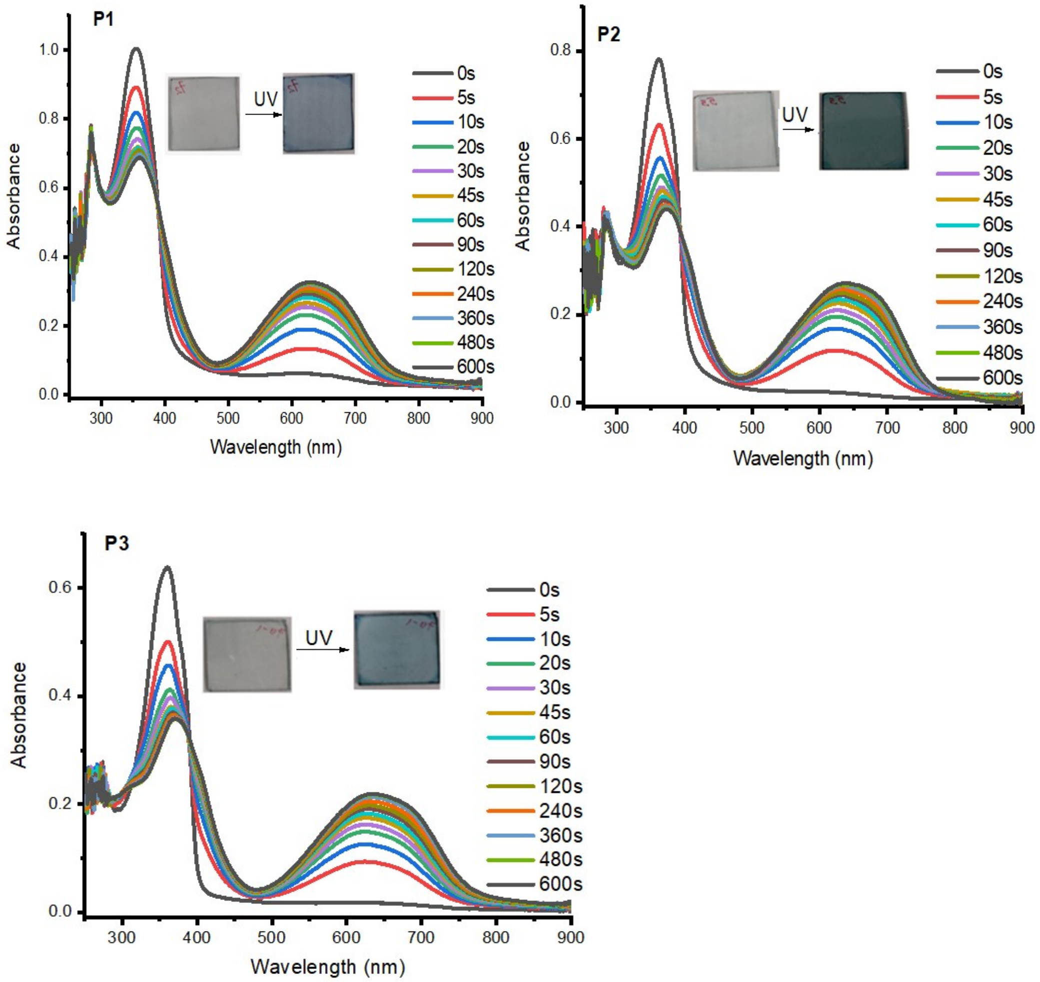

Figure 4.6: Absorption spectra of thin films of P1- P3 upon irradiation with UV light.

To understand the differences in the photoswitching efficiency between the polymers, the relative rates of electrocylization and cycloreversion were measured rather than the quantum yield as an appropriate reference was not available. The rates of cyclization were related to poly(3-[3,3,4,4,5,5-hexafluoro-2-(2-methyl-3-thienyl)-1-cyclopenten-1-yl]-2-methylthiophene)-alt-(di-*n*-hexylphenylene) and set to 1 as a reference point for ring-closing and 0.1 as a reference point for ring opening. As the alkyl chain length increased for P1-P3, the relative ring-closing rate decreased indicating that morphological differences and/or steric interactions played a role in the efficiency of electrocyclization.[62] The cycloreversion rate trend is similar to the electrocyclization, however P3 is significantly lower than P1, and P2 and the reason for this is not understood.

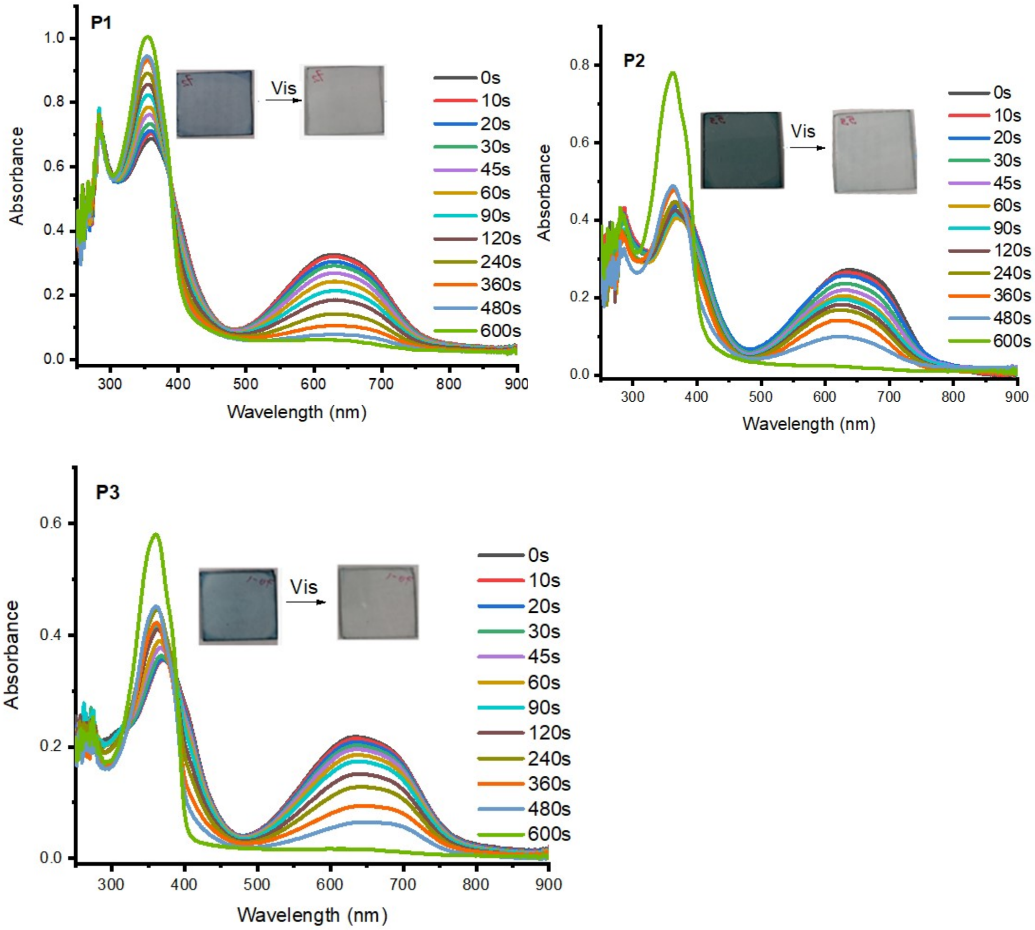

Figure 4.7: Absorption spectra of thin films of P1- P3 upon irradiation with Vis light (>550 nm). The film thickness was ~20 nm.

Table 4.4. Summary of optical and photochromic properties of P1-P3 films

	λ_{max}; ε (M^{-1} cm^{-1}) (open-form)	**λ_{max}; ε (M^{-1} cm^{-1}) (closed-form)**	**$\chi_{o\to c}$**	**$\chi_{c\to o}$**	**RMS (nm)**
P1	355; 23158	630; 10945	0.57 ± 0.05	0.23 ±0.01	2.01 ± 0.281
P2	361; 21774	635; 10157	0.44 ± 0.04	0.21 ± 0.02	0.65 ± 0.04

P3	362; 29820	637; 13761	0.41 ± 0.03	0.08 ± 0.03	0.62 ± 0.08

An important parameter in organic photonics and electronics is the photostability of the active layers.[63–65] The photochemical stability of these polymers were investigated by irradiating the polymer thin films with UV light for 600 s followed by visible light for 600 s 12 times in air (**Figure 4.8**). It can be seen that electrocyclization and cycloreversion was observed after 12 cycles without fatigue.The photochemical stability observed indicates that photooxidation of the polymers to form fluorenones, often observed in polyfluorenes, and/or photo-chain scission and diels-alder [2+4] cycloaddition with singlet oxygen does not occur, regardless of the alkyl chain length.[66–69]

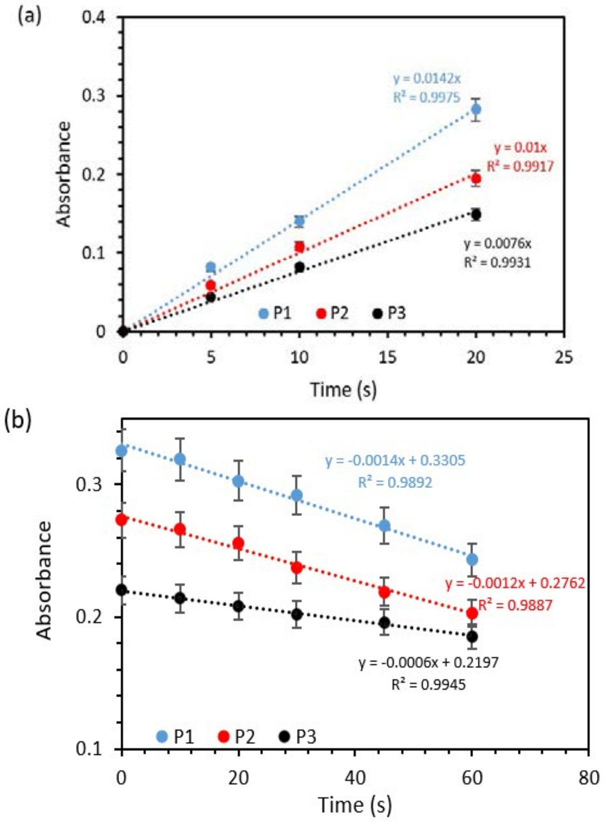

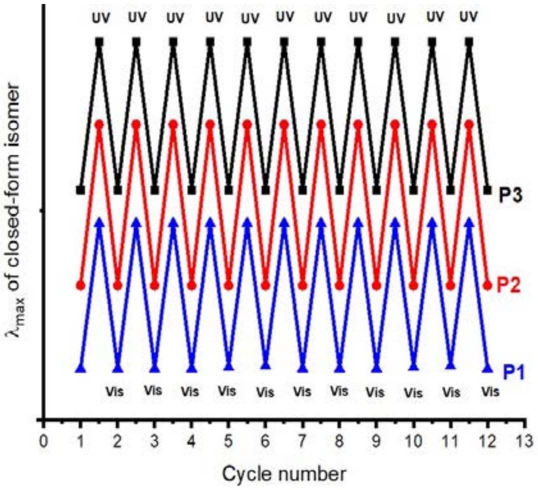

Figure 4.8: Absorption intensity vs time of P1-P3 upon irradiation with UV (a) and Vis light (b). Reversible photoswitching of P1-P3 (c). The films were excited with UV light for 600 s and visible light for 600 s.

4.4.Conclusion

Solution-processable diarylethene-based mainchain photochromic polymers with various chain lengths were successfully synthesized by Suzuki-Miyaura polycondensation reaction. The polymers are soluble in common solvents such as chloroform, THF, dichloromethane and toluene, and can be cast into high quality thin films. Photoisomerization was observed in both solution and film states with minimal photo- and thermal degradation under ambient conditions.Depending on the application, photoswitchable polymers containing short alkyl solubilizing groups would be preferred when high temperature stresses are present while longer alkyl groups resulted in slightly more smooth films, which is important for charge transport characteristics. Based on these exciting results, these polymers are excellent candidates for multi-functional, light-controlled optoelectronic devices such as phototransistors, optical memories and photoswitches.

4.5.References

[1] M. Carroli, D. T. Duong, E. Buchaca-Domingo, A. Liscio, K. Börjesson, M. Herder, V. Palermo, S. Hecht, N. Stingelin, A. Salleo, E. Orgiu, P. Samorì, *Adv. Funct. Mater.***2020**, *30*, 1907507.

[2] E. Orgiu, N. Crivillers, M. Herder, L. Grubert, M. Pätzel, J. Frisch, E. Pavlica, D. T. Duong, G. Bratina, A. Salleo, N. Koch, S. Hecht, P. Samorì, *Nat. Chem.***2012**, *4*, 675.

[3] Y. Kurokawa, R. Hayakawa, S. Shimada, K. Higashiguchi, Y. Noguchi, K. Matsuda, Y. Wakayama, *Org. Electron.***2019**, *64*, 205.

[4] Z. Zhang, X. Liu, Z. Li, Z. Chen, F. Zhao, F. Zhang, C. H. Tung, *Adv. Funct. Mater.***2008**, *18*, 302.

[5] M. Lahikainen, K. Kuntze, H. Zeng, S. Helantera, S. Hecht, A. Priimagi, *ACS Appl. Mater. Interfaces***2020**, *12*, 47939.

[6] B. W. H. Saes, M. M. Wienk, R. A. J. Janssen, *RSC Adv.***2020**, *10*, 30176.

[7] D. D. Dashitsyrenova, A. G. Lvov, L. A. Frolova, A. V. Kulikov, N. N. Dremova, V. Z. Shirinian, S. M. Aldoshin, M. M. Krayushkin, P. A. Troshin, *J. Mater. Chem. C***2019**, *7*, 6889.

[8] C. Bertarelli, A. Bianco, V. Boffa, M. Mirenda, M. C. Gallazzi, G. Zerbi, *Adv. Funct. Mater.***2004**, *14*, 1129.

[9] M. Irie, T. Fukaminato, K. Matsuda, S. Kobatake, *Chem. Rev.***2014**, *114*, 12174.

[10] H. Xu, S. Wei, C. Fan, G. Liu, S. Pu, *Tetrahedron***2017**, *73*, 6479.

[11] K. Morimitsu, K. Shibata, S. Kobatake, M. Irie, *J. Org. Chem.***2002**, *67*, 4574.

[12] S. Pu, T. Yang, J. Xu, L. Shen, G. Li, Q. Xiao, B. Chen, *Tetrahedron***2005**, *61*, 6623.

[13] M. Hanazawa, R. Sumiya, Y. Horikawa, M. Irie, *J. Chem. Soc. Chem. Commun.***1992**, 206.

[14] M. Irie, T. Fukaminato, K. Matsuda, S. Kobatake, *Chem. Rev.***2014**, *114*, 12174.

[15] T. Tsujioka, M. Kume, M. Irie, *Opt. Rev.***1997**, *4*, 655.

[16] T. Tsujioka, Y. Hamada, K. Shibata, A. Taniguchi, T. Fuyuki, *Appl. Phys. Lett.***2001**, *78*, 2282.

[17] K. Shibata, K. Muto, S. Kobatake, M. Irie, *J. Phys. Chem. A***2002**, *106*, 209.

[18] Y. Ishiguro, R. Hayakawa, T. Chikyow, Y. Wakayama, *J. Mater. Chem. C***2013**, *1*, 3012.

[19] Y. Ishiguro, R. Hayakawa, T. Yasuda, T. Chikyow, Y. Wakayama, *ACS Appl. Mater. Interfaces***2013**, *5*, 9726.

[20] P. Lutsyk, K. Janus, J. Sworakowski, G. Generali, R. Capelli, M. Muccini, *J. Phys. Chem. C***2011**, *115*, 3105.

[21] Y. Li, H. Zhang, C. Qi, X. Guo, *J. Mater. Chem.***2012**, *22*, 4261.

[22] H. Nishi, T. Namari, S. Kobatake, *J. Mater. Chem.***2011**, *21*, 17249.

[23] T. Saika, T. Shimidzuc, M. Irie, *J. Chem. Soc.***1994**, 2123.

[24] R. D. McCullough, *Adv. Mater.***1998**, *10*, 93.

[25] M. R. Bryce, A. Chissel, P. Kathirgamanathan, D. Parker, N. R. M. Smith, *J. Chem. Soc. Chem. Commun.***1987**, 466.

[26] T. Kawai, T. Kunitake, M. Irie, *Chem. Lett.***1999**, *28*, 905.

[27] E. Kim, H. W. Lee, *J. Mater. Chem.***2006**, *16*, 1384.

[28] Q. Luo, H. Cheng, H. Tian, *Polym. Chem.***2011**, *2*, 2435.

[29] H. Choi, H. Lee, Y. Kang, E. Kim, S. O. Kang, J. Ko, *J. Org. Chem.***2005**, *70*, 8291.

[30] F. Stellacci, C. Bertarelli, F. Toscano, M. C. Gallazzi, G. Zotti, G. Zerbi, *Adv. Mater.***1999**, *11*, 292.

[31] C. P. Harvey, J. D. Tovar, *Polym. Chem.***2011**, *2*, 2699.

[32] W. Xu, K. Mihhels, N. Kotov, S. Lepikko, R. H. A. Ras, C. M. Johnson, T. Pettersson, E. Kontturi, *J. Colloid Interface Sci.***2022**, *605*, 441.

[33] S. Hayashi, S. I. Yamamoto, T. Koizumi, *Sci. Rep.***2017**, *7*, 1.

[34] K. Higashiguchi, H. Yotsuji, K. Matsuda, *Chem. Lett.***2017**, *46*, 1564.

[35] M. Irie, T. Lifka, S. Kobatake, N. Kato, *J. Am. Chem. Soc.***2000**, *122*, 4871.

[36] A. R. Santos, R. Ballardini, P. Belser, M. T. Gandolfi, V. M. Iyer, L. Moggi, *Photochem. Photobiol. Sci.***2009**, *8*, 1734.

[37] Y. Bai, K. M. Louis, R. Scott Murphy, *J. Photochem. Photobiol. A Chem.***2007**, *192*, 130.

[38] S. Pu, G. Liu, G. Li, R. Wang, T. Yang, *J. Mol. Struct.***2007**, *833*, 23.

[39] R. Liu, Y. Yang, Q. Cui, W. Xu, R. Peng, L. Li, *Chem. - A Eur. J.***2018**, *24*,

17756.

[40] D. Becker, N. Konnertz, M. Böhning, J. Schmidt, A. Thomas, *Chem. Mater.***2016**, *28*, 8523.

[41] Y. Han, J. Zhao, H. Yang, X. Huang, X. Zhou, T. Hui, J. Yan, *J. Mol. Struct.***2020**, *1217*, 128395.

[42] R. Jagarapu, S. Maddala, I. Mahto, P. Venkatakrishnan, *Asian J. Org. Chem.***2020**, *9*, 2144.

[43] M. P. Aldred, R. Hudson, S. P. Kitney, P. Vlachos, A. Liedtke, K. L. Woon, M. O'Neill, S. M. Kelly, *Liq. Cryst.***2008**, *35*, 413.

[44] J. R. Pouliot, F. Grenier, J. T. Blaskovits, S. Beaupré, M. Leclerc, *Chem. Rev.***2016**, *116*, 14225.

[45] B. Carsten, F. He, H. J. Son, T. Xu, L. Yu, *Chem. Rev.***2011**, *111*, 1493.

[46] B. Hohl, L. Bertschi, X. Zhang, A. D. Schlüter, J. Sakamoto, *Macromolecules***2012**, *45*, 5418.

[47] G. L. Gibson, D. Gao, A. A. Jahnke, J. Sun, A. J. Tilley, D. S. Seferos, *J. Mater. Chem. A***2014**, *2*, 14468.

[48] U. Koldemir, S. R. Puniredd, M. Wagner, S. Tongay, T. D. McCarley, G. D. Kamenov, K. Müllen, W. Pisula, J. R. Reynolds, *Macromolecules***2015**, *48*, 6369.

[49] J. Sherwood, J. H. Clark, I. J. S. Fairlamb, J. M. Slattery, *Green Chem.***2019**, *21*, 2164.

[50] A. Fihey, A. Perrier, W. R. Browne, D. Jacquemin, *Chem. Soc. Rev.***2015**, *44*,

3719.

[51] Y. Tokita, M. Katoh, K. Kosaka, Y. Ohta, T. Yokozawa, *Polym. Chem.***2021**, *12*, 7065.

[52] S. N. Islam, N. Gogurla, D. Giri, S. K. Ray, S. K. Patra, *J. Lumin.***2019**, *208*, 509.

[53] W. Woodland, R. Lim, C. Motti, P. Irving, J. Wang, M. Payne, P. C. Junk, G. Vamvounis, *Aust. J. Chem.***2019**, *72*, 874.

[54] M. Suzuki, K. Suzuki, T. Won, H. Yamada, *J. Mater. Chem. C***2022**, *10*, 1162.

[55] G. L. Schulz, X. Chen, S. A. Chen, S. Holdcroft, *Macromolecules***2006**, *39*, 9157.

[56] A. J. Sandee, C. K. Williams, N. R. Evans, J. E. Davies, C. E. Boothby, A. Köhler, R. H. Friend, A. B. Holmes, *J. Am. Chem. Soc.***2004**, *126*, 7041.

[57] S. Pankaj, E. Hempel, M. Beiner, *Macromolecules***2009**, *42*, 716.

[58] R. Xie, A. R. Weisen, Y. Lee, M. A. Aplan, A. M. Fenton, A. E. Masucci, F. Kempe, M. Sommer, C. W. Pester, R. H. Colby, E. D. Gomez, *Nat. Commun.***2020**, *11*, 4.

[59] D.-F. Tang, G.-A. Wen, W. Wei, W. Huang, *Polym. Int.***2008**, *57*, 1235.

[60] G. Vamvounis, S. Holdcroft, *Adv. Mater.***2004**, *16*, 716.

[61] G. Vamvounis, G. L. Schulz, S. Holdcroft, *Macromolecules***2004**, *37*, 8897.

[62] M. El Gemayel, K. Börjesson, M. Herder, D. T. Duong, J. A. Hutchison, C. Ruzié, G. Schweicher, A. Salleo, Y. Geerts, S. Hecht, E. Orgiu, P. Samorì, *Nat. Commun.***2015**, *6*, 1.

[63] A. Tournebize, A. Rivaton, H. Peisert, T. Chassé, *J. Phys. Chem. C***2015**, *119*, 9142.

[64] R. C. Shallcross, P. Zacharias, A. Köhnen, P. O. Körner, E. Maibach, K. Meerholz, *Adv. Mater.***2013**, *25*, 469.

[65] M. J. Deen, M. H. Kazemeini, S. Holdcroft, *J. Appl. Phys.***2008**, *103*, 124509.

[66] A. P. Kulkarni, X. Kong, S. A. Jenekhe, *J. Phys. Chem. B***2004**, *108*, 8689.

[67] Y. Honmou, S. Hirata, H. Komiyama, J. Hiyoshi, S. Kawauchi, T. Iyoda, M. Vacha, *Nat. Commun.***2014**, *5*, 1.

[68] M. S. A. Abdou, S. Holdcroft, *Can. J. Chem.***1995**, *73*, 1893.

[69] B. H. Cumpston, K. F. Jensen, *J. Appl. Polym. Sci.***1998**, *69*, 2451.

CHAPTER 5

EFFECT OF CONJUGATION LENGTH ON THE PROPERTIES OF PHOTOCHROMIC POLYMERS

5.1.Introduction

Chapter 4explored synthetic procedures for producingsolution processable photochromic polymers. These materials are attractive towards the development ofphotoswitchable electronics such as transistors, [1–3] actuators [4,5] and light-emitting diodes (LEDs) [6–8] since their properties are similar properties to those of π-conjugated polymers and can be controlled with light. The most important requirements for the practical application of photochromic materials are fast response, thermal stability of the two isomers and high quantum yields in both solution and solid states, and ability to form high quality films. Studies on photochromes has been primarily limited to low-molecular weight compounds that show high crystallinity in solid state and side-chain photochromic polymers with limited intra- and inter-chain charge transport.[9]

Mainchain photochromic materials are ideal multi-functional materials for organic electronic devices due to their inter- and intra-charge transport properties, however their solubility is still limited due to lack of solubilizing groups. Furthermore, photoswitching quantum yields particularly in solid state are low due to steric encumbrance.[10] Aromatic comonomers containing solubilizing alkyl-chains based on fluorene,[11] phenylene [9,12,13] and phenylquinoline[14] have been used to develop polymers with various conjugation lengths, however most designs have either have poor solubility,[9] low molecular weights,[11,15] poor photoswitching quantum yields in solid state [11] or photochemical instability.[13] Furthermore, the effect of conjugation on the properties on photochromic polymer has not been studied. Choi *et al.*[14]synthesized a polymer comprised of a hexafluorocyclopentene-based dithienylethene switching unit paired with phenylquinoline units byFriedländer condensation method which was found to have low solubility in chloroform and poor photochromism in solid state. In addition, Zerbi and coworkers [9] prepared photo-switchable mainchain conjugated polymers incorporating hexafluorocyclopentene-based switching units and dialkoxyphenylene derivatives (dihexyloxyphenylenevinylene or didodecyloxy-phenylenevinylene), of which the dihexyloxyphenylenevinylene-based polymer showed low solubility in chloroform. The poor response of main chain photochromic polymers has been attributed to intramolecular interactions between the dithienylethene units which inhibits the photochromic switching action of the interacting units due to the large changes in macromolecular conformations required.[16]

Polymer solubility and molecular weight are dependent on the solubilizing group while the photoswitchingspeeddepends on steric bulkiness.[17] Therefore, the design of mainchain photochromic polymers which fulfil vital properties such as high molecular weight, solubility and high photoswitching quantum yields requires a deeper understanding of structural design. Following successful design and synthesis of solubledithienylethene-*alt*-di-*n*-alkyl-fluorene photochromic polymers reported in **chapter 4**, the project was extended to study the effect of conjugation length on the properties of mainchaindithienylethene-based polymers. Photochromic copolymers incorporating hexafluorocyclopentene-based diarylethene switching units coupled with either flourene, carbazole, phenylene or benzodithiophene derivatives (**Figure 5.1**) were designed and synthesized by Suzuki polycondensation reactions.

5.2.Experimental

5.2.1. Chemicals and reagents

2-Methylthiophene, N-bromosuccinimide (NBS), trimethylsilyl chloride (TMSCl), n-butyllithium, fluorene, bromine, tetrabutylammonium bromide, 1-bromopropane, bromobenzene and phenylboronic acid, tetrakis(triphenylphosphine)palladium(0) ($Pd(PPh_3)_4$) and 2-isopropoxy-4,4,5,5-tetramethyl-[1,3,2]dioxaborolane and 4,8-bis(3,5-dioctyl-2-thienyl)-2,6-bis(4,4,5,5-tetramethyl-1,3,2-dioxaborolan-2-yl)benzo[1,2-b:4,5-b′]dithiophene were purchased from Sigma Aldrich. 9,9-dioctylfluorene-2,7-diboronic acid bis(pinacol) ester and 1,4-dibromo-2,5-dihexylbenzene were purchased from Boron molecular. Octafluorocyclopentene and 9-(heptadecan-9-yl)-2,7-bis(4,4,5,5-tetramethyl-1,3,2-dioxaborolan-2-yl)-9H-carbazole were purchased from TCI chemicals and Ossila, respectively. THF was dried over sodium/benzophenone and then distilled under argon atmosphere immediately before use. Dichloromethane and petroleum ether were distilled under vacuum prior to use. All other solvents were used as received.

5.2.2. Characterization

^1H NMR spectra were recorded using a Bruker AscendTM 400 MHz spectrometer for samples in $CDCl_3$. Chemical shifts are reported in parts per million (ppm) and are referenced to the residual solvent peak (chloroform, ^1H = 7.26 ppm). Peak multiplicities are designated in the following manner: singlet (s), doublet (d), triplet (t), doublet and multiplet (m). The polymer molecular weights were determined using gel permeation chromatography (GPC) (Agilent Technologies 1260 Infinity Series) using THF as eluent and polystyrene narrow standards. The PLgel 5 µm Mixed–C columns (300×7.5 mm)×2 were calibrated using polystyrene narrow standards in tetrahydrofuran. Infrared spectra were recorded on Nicolet 6700 FT-IR spectrometer equipped with an attenuated total reflection (ATR) crystal. Absorption spectra were recorded using a Shimadzu UV2600 spectrophotometer.

Solution quantum yields of cyclization ($\Phi_{o\rightarrow c}$) and cycloreversion ($\Phi_{c\rightarrow o}$) were measured by a relative method as described in **Section 4.2.2** 1,2-bis(2-methyl-5-phenyl-3-thienyl)perfluorocyclopentene which has quantum yield of 0.59 and 0.574 at 280 nm and 365 nm, respectively and quantum yield of cycloreversion of 0.013 at λ>492 nm was used an actinometer.[18,19] The relative rates of solid state photoswitching were measured using P4 as a reference and assigning its $\chi_{o\rightarrow c}$to 1 and $\chi_{c\rightarrow o}$to 0.1. Detailed procedure is covered in section **Section 4.2.2**.

Films for measuring UV–Vis absorption spectroscopy and atomic force microscopy were prepared on glass (Sail Brand) by spin coating 10 mg/mL (for UV-Vis) and 20 mg/mL (for AFM) in toluene at 1500 rotations per minute for 45 s using a Chemat KW-4A spincoater. Glass substrates were cleaned prior to use in an ultrasound bath for 10 minutes using soapy water, acetone and ethanol, respectively, and dried under nitrogen. The surface morphology and thickness of the films was measured using an NTEGRA TS-150 atomic force microscope (AFM) in semi contact mode. Molar absorption coefficients in solid state were evaluated by UV-Vis spectroscopy from linear fits of absorbance of films of different thicknesses. In a typical procedure, four films of the same polymer were prepared by spin coating solutions with different concentrations. The absorbance of each film was recorded before and after switching the polymers. The absorbance values were plotted against film thickness (cm) to estimate the absorption coefficients and reported in **Table 5.4**. Thermal properties were investigated using an SDT 650 (TA instruments) and DSC 250 (TA instruments). The DSC was equipped with a refrigeration cooling system (RCS) and the heating/ cooling rates were equal at 10 ºC min^{-1}. TGA ramp rate was maintained at

10 ºC min^{-1}. Degradation temperatures were estimated at 5% weight loss. Photochemical stability measurements were performed following a procedure reported in section **4.2.2.**

5.2.3. Synthesis procedures

2,5-Dihexyl-1,4-phenylene-bis(pinacolato boronate)

A 50 mL round bottom flask was charged with 1,4-dibromo-2,5-dihexylbenzene (0.3 g, 0.74 mmol, 1 eq.), 4,4,4',4',5,5,5',5'-octamethyl-2,2'-bis(1,3,2- dioxaborolane) (0.562 g, 2.22 mmol, 3 eq.), potassium acetate (0.327 g, 3.3 mmol, 3.3 eq.), [1,1'-bis(diphenylphosphino)ferrocene] palladium(II) dichloride complex with dichloromethane (0.03 g, 2.00 mmol 0.05 eq.) and 1,4- dioxane (5 mL). The mixture was stirred at 90 °C for 24 h. The reaction mixture was cooled to room temperature and quenched with water (10 mL). The resulting mixture was extracted with ethyl acetate (3 x 20 mL). The combined organic layers were washed with water (2 x 20 mL). The organic phase was dried over anhydrous sodium sulfate, filtered, and the solvent was removed using a rotary evaporator to afford an off-white solid. The crude product was purified by recrystallization in methanol (5 mL) to obtain a clean colorless solid (0.23 g, 64%)[20]. ^{1}H NMR (400 MHz, $CDCl_3$) δ: 7.51 (s, 2H), 2.81-2.85 (m, 4H), 1.56-1.52 (m, 6H), 1.36-1.31 (m, 36H), 0.91 (t, 6H);υ_{max}/cm^{-1} 707, 859, 962, 1096, 1141, 1165, 1215, 1263, 1314, 1368, 1388, 1406, 1737, 2853, 2952, 2968; MS (*m/z*) Cald for $[C_{30}H_{52}B_2O_4]^+$: 498.4046, found: 498.4041; T_m = 107.58 ºC.

Polymer synthesis

The synthesis of P3 is covered in Section **4.3.1.**

Poly(3-[3,3,4,4,5,5-hexafluoro-2-(2-methyl-3-thienyl)-1-cyclopenten-1-yl]-2-methylthiophene)-*alt*-(di-*n*-hexylphenylene) (P4)

A 50 mL Schlenk tube was charged with 5-bromo-3-[2-(5-bromo-2-methyl-3-thienyl)-3,3,4,4,5,5-hexafluoro-1-cyclopenten-1-yl]-2-methylthiophene(0.113 g, 0.215 mmol, 1.0 eq.), 2,5-di-*n*-hexyl-1,4-phenylene-bis(pinacolato boronate) (0.107 g, 0.215 mmol, 1.0 eq.), THF (4 mL) and aqueous potassium carbonate (2 mL, 2 M). This mixture was purged with nitrogen for 10 min, $Pd(PPh_3)_4$ (0.0023 g, 0.00215 mmol, 0.01 eq.) and Aliquat 336 (0.00096 g, 0.00215 mmol, 0.01 eq.) were added. The reaction was degassed with three freeze-pump thaw cycles and covered with a blanket of argon. The reaction was stirred at 60 °C for 120 h. To remove the reactive end-groups, the resultant polymer was treated bromobenzene and phenylboronic acid after 84 and 96 h, respectively. The reaction was quenched with water (10 mL), and the mixture was extracted with dichloromethane (3 x 20 mL). The combined organic layers were washed with water (2 x 50 mL) and brine (20 mL). The organic layer was dried over anhydrous sodium sulfate, filtered, and the solvent was removed using a rotary evaporator to afford a violet-colored oil. The crude product was purified by column chromatography (chloroform and silica gel; column diameter 3 cm, column height, 10 cm) to afford a violet solid (0.06 g,52%).λ_{max} (open isomer) (THF)/nm 282 [log(ε/dm^3 mol^{-1} cm^{-1}) (4.31)], λ_{max} (closed isomer) (THF)/nm 569 [log(ε/dm^3 mol^{-1} cm^{-1}) (4.20)]; ^{1}H NMR (400 MHz, $CDCl_3$) δ: 7.24-7.08 (m, 4H), 2.48-2.82 (m, 4H), 2.04-1.91 (m, 6H), 1.38-1.28 (m, 16H), 0.90-0.86 (m, 6H);υ_{max}/cm^{-1} 823, 849, 896, 988, 1052, 1114, 1134, 1192, 1216, 1228, 1270, 1340, 1364, 1439, 1737, 2855, 2925, 2968; T_d = 188 °C; GPC: M_w = 6.69 kg/mol, PDI = 5.58.

Poly(3-[3,3,4,4,5,5-hexafluoro-2-(2-methyl-3-thienyl)-1-cyclopenten-1-yl]-2-methylthiophene)-*alt*-(9-(1-octylnonyl)carbazole) (P5)

A 50 mL Schlenk tube was charged with 5-bromo-3-[2-(5-bromo-2-methyl-3-thienyl)-3,3,4,4,5,5-hexafluoro-1-cyclopenten-1-yl]-2-methylthiophene (0.1010 g, 0.192 mmol, 1.0 eq.), 9-(heptadecan-9-yl)-2,7-bis(4,4,5,5-tetramethyl-1,3,2-dioxaborolan-2-yl)-9H-carbazole (0.1262 g, 0.192 mmol, 1.0 eq.), toluene (3.5 mL) and aqueous potassium carbonate (2 mL, 2 M). This mixture was purged with nitrogen for 10 min and $Pd(PPh_3)_4$ (0.0022 g, 0.0019 mmol) was added. The mixture was then degassed three times using freeze-pump thaw cycles then covered with a blanket of argon. The mixture was stirred at 100 °C for 120 h. To remove the reactive end-groups, the resultant polymer was treated bromobenzene and phenylboronic acid after 72 and 84 h, respectively. The reaction was quenched with water (10 mL), and the mixture was extracted with dichloromethane (3 x 20 mL). The combined organic layers were washed with water (2 x 50 mL) and brine (20 mL). The organic layer was dried over anhydrous sodium sulfate, filtered, and the solvent was removed using a rotary evaporator to afford a teal green colored oil. The oil was dissolved in 5 mL of chloroform and precipitated into 25 mL methanol to afford a teal green solid(0.110 g, 76%). λ_{max} (open isomer) (THF)/nm 365 [log(ε/dm^3 mol^{-1} cm^{-1}) (4.46)], λ_{max} (closed isomer) (THF)/nm 622 [log(ε/dm^3 mol^{-1} cm^{-1}) (4.32)];^{1}H NMR (400 MHz, $CDCl_3$) δ: 7.17-8.08 (m, 8H), 4.25-4.67 (m, 1H), 1.92-2.34 (m, 10H), 1.15-1.28 (m, 24H), 0.84 (t, 6H);υ_{max}/cm^{-1} 844, 904, 985, 1052, 1114, 1135, 1203, 1216, 1228, 1271, 1364, 1434, 1454, 1599, 1737, 2853, 2924, 2968; T_d = 359 °C; GPC: M_w = 12.90 kg/mol, PDI = 2.43.

Poly(3-[3,3,4,4,5,5-hexafluoro-2-(2-methyl-3-thienyl)-1-cyclopenten-1-yl]-2-methylthiophene)-alt-(4,8-bis(3,5-dioctyl-2-thienyl)-1,5-dithia-*s*-indacene) (P6)

A 50 mL Schlenk tube was charged with 5-bromo-3-[2-(5-bromo-2-methyl-3-thienyl)-3,3,4,4,5,5-hexafluoro-1-cyclopenten-1-yl]-2-methylthiophene(0.051 g, 0.097 mmol, 1.0 eq.), 4,8-bis(3,5-dioctyl-2-thienyl)-2,6-bis(4,4,5,5-tetramethyl-1,3,2-dioxaborolan-2-yl)benzo[1,2-b:4,5-b′]dithiophene (0.1023 g, 0.097 mmol, 1.0 eq.), toluene (3.5 mL)and aqueous potassium carbonate (2 mL, 2M). This mixture was purged with nitrogen for 10 min and $Pd(PPh_3)_4$ (0.0022 g, 0.0019 mmol) was added. The mixture was then degassed three times using freeze-pump thaw cycles then covered with a blanket of argon. The mixture was stirred at 100 °C for 96 h. To remove the reactive end-groups, the resultant polymer was treated bromobenzene and phenylboronic acid after 72 and 84 h, respectively. The reaction was quenched with water (10 mL), and the mixture was extracted with dichloromethane (3 x 20 mL). The combined organic layers were washed with water (2 x 50 ml) and brine (20 mL). The organic layer was dried over anhydrous sodium sulfate, filtered, and the solvent was removed using a rotary evaporator to afford a lime green colored oil. The oil was dissolved in 5 mL of chloroform and precipitated into 25 mL methanol to afford a teal green solid (0.08 g, 71%). λ_{max} (open isomer) (THF)/nm 381 [log(ε/dm^3 mol^{-1} cm^{-1}) (4.72)], λ_{max} (closed isomer) (THF)/nm 675 [log(ε/dm^3 mol^{-1} cm^{-1}) (4.49)]; ^1H NMR (400 MHz, $CDCl_3$) δ: 7.18-7.24 (m, 4H), 6.83 (s, 2H), 2.88-2.92 (m, 4H), 2.38-2.41 (m, 4H), 1.98-1.76 (m, 10H), 1.30-1.32 (m, 20H), 1.07-1.10 (m, 22H), 0.76-0.90 (m, 14 H); υ_{max}/cm^{-1} 828, 899, 985, 1049, 1090, 1194, 1216, 1271, 1364, 1454, 1737, 2851, 2922, 2968; T_d = 425 °C; GPC: M_w = 12.41 kg/mol, PDI = 2.52.

5.3.Results and discussion

5.3.1. Polymer structure

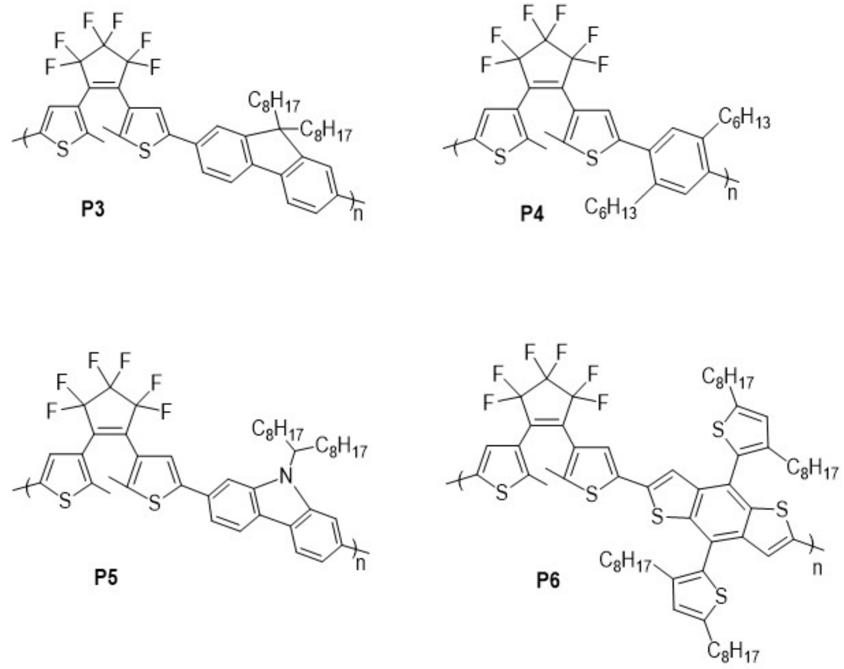

Figure 5.1: Chemical structures of P3-P6.

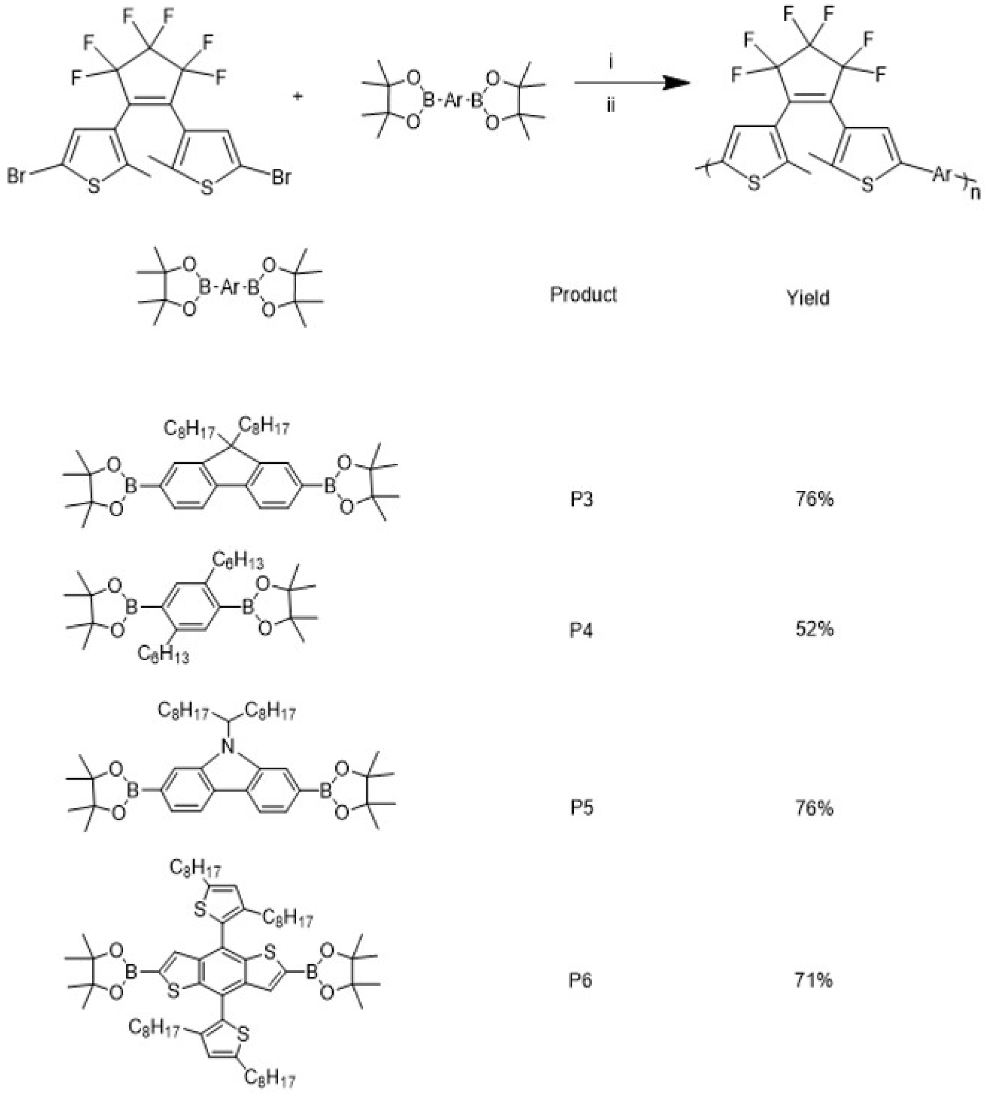

Scheme 5.1: Synthetic protocol for preparation of photochromic polymers P3-P6. Reagents and conditions: (i) tetrahydrofuran or toluene, 2 M K_2CO_3, $Pd(PPh_3)_4$,60 °C or 90 °C, 96-120 h, (ii) phenylboronic acid and bromobenzene.

P3-P6 were synthesized by Suzuki-Miyaura polycondensation reactions between 5-bromo-3-[2-(5-bromo-2-methyl-3-thienyl)-3,3,4,4,5,5-hexafluoro-1-cyclopenten-1-yl]-2-methylthiopheneand the corresponding diboronic acid bis(pinacol) esters as shown in **Scheme 5.1.**Structures of P3-P6 are shown in **Figure 5.1**. The reactive end-groups of the polymers were replaced with phenylene units of phenyl boronic acid and bromobenzene to avoid unwanted post-polymerization reactions/degradation [21,22] of the polymers during photoswitching. Polymer structures were confirmed using ^{1}H-NMR and FT-IR and the spectra are given in the Appendix of Chapter 5. The average molecular numbers (M_n) for P3-P6 ranged 1312 to 9308 Daltons and summarized in **Table 5.1.** P4 had the lowest M_w despite optimizing the reaction parameters such as solvent (toluene or THF), catalyst ($Pd(PPh_3)_4$ or Pd (II) acetate) and base type (K_2CO_3 or Cs_2CO_3). This could be attributed to the use of sterically hindered 2,5-di-*n*-hexyl-1,4-phenylene-bis(pinacolato boronate) monomer. The highest degree of polymerization of P4 was achieved by using 1 mol % of a phase transfer catalyst (Aliquat 336) to the reaction mixture into THF solvent and $Pd(PPh_3)_4$ catalyst. All polymers were thermally stable with degradation temperatures ≥ 188 °C (**Figure 5.5b**).

Table5.1. Molecular weight, dispersity index (PDI), glass transition temperatures(T_g) and degradation temperatures(T_d) of P3-P6.

Polymer	**M_w(kg/mol)**	**PDI**	**T_g(°C)**	**T_d(°C)**
P3	20.27	2.17	96	404
P4	6.69	5.52	49	188
P5	12.90	2.53	94	359
P6	12.41	2.52	58	425

5.3.2. Solution physicochemical properties

The π-conjugation system of a diarylethene is restricted to each side of the open-ring isomer but extends over both sides upon excitation with UV light to form a closed-ring isomer. For that reason, conjugation length has a significant effect on the absorption properties of photochromic molecules. Solution properties of P3-P6 are depicted in **Figure 5.2** and summarized in **Table 5.2**. Under ambient conditions, polymer solutions were dominated by the open form isomers (**Figure 5.3**). The photostationary properties of P3-P6 are similar to those of small molecule diarylethenes indicating extending the conjugation length does not affect the PSS of these molecules.[23] The open isomer of the polymer containing the fluorene comonomer (P3) showed a strong peak centered at 365 nm in THF due to a π-π* transition.[24,25] P5 displayed a maximum absorption at 365 nm, which is similar to P3, and this is expected since polyfluorenes and polycarbazoles have a similar absorption maximum.[26] The emergence of a higher energy peak at 272 nm is also typical to carbazole based polymers and related to π-π* electronic transition of the conjugation.[27] Interestingly, the variation of the HOMO and LUMO levels of carbazole based polymer [28] does not affect the main absorption maximum in the photostationary state when compared to P3. In contrast, P4 displays a hypsochromic shift and P6 displays a bathochromic shift compared to P3 and related to the degree of π-orbital overlap in the polymer backbone.[29,30] Upon photoexcitation using 365 nm light for up to 600 s, the emergence of a peak in the visible area of the electromagnetic spectrum appears and is related to the π-π* transition of the closed isomer of the photochromic polymers. The trend in the closed isomers is the same as the open isomers with P4 having the shortest conjugation length (569 nm) and P6 having the longest conjugation length (662 nm), which were not affected by the alkyl chain length, molecular weight distribution and energy levels. It is worth mentioning thatP6 absorbs upto 450 nm. Both solution and film of P6 are slightly yellow under ambient light. Therefore, P6 was switched to colourless form before doing quantum yield measurements.The 6-π electrocyclization quantum yields were measured with reference to 1,2-bis(2-methyl-5-phenyl-3-thienyl)perfluorocyclopentene and ranged from 0.41 to 0.87 depending on the comonomer. Polymers based on flourene, phenylene and carbazole comonomer showed cyclization quantum yieldsover 0.5 due to the enforced antiparallel conformation of the dithienylethenemoieties.[14,31] Analogues of P3 and P4 were prepared with lower molecular weight distributions and their quantum yields were measured (**Table 5.3**). It was found that the quantum yields of cyclization were not dependent on the molecular weight. Cycloreversion quantum yields varied between 0.004 to 0.011 and are typical for DTE based materials and related to the degree of conjugation, where higher conjugation has been shown to have lower cycloreversion quantum yields.[32,33]

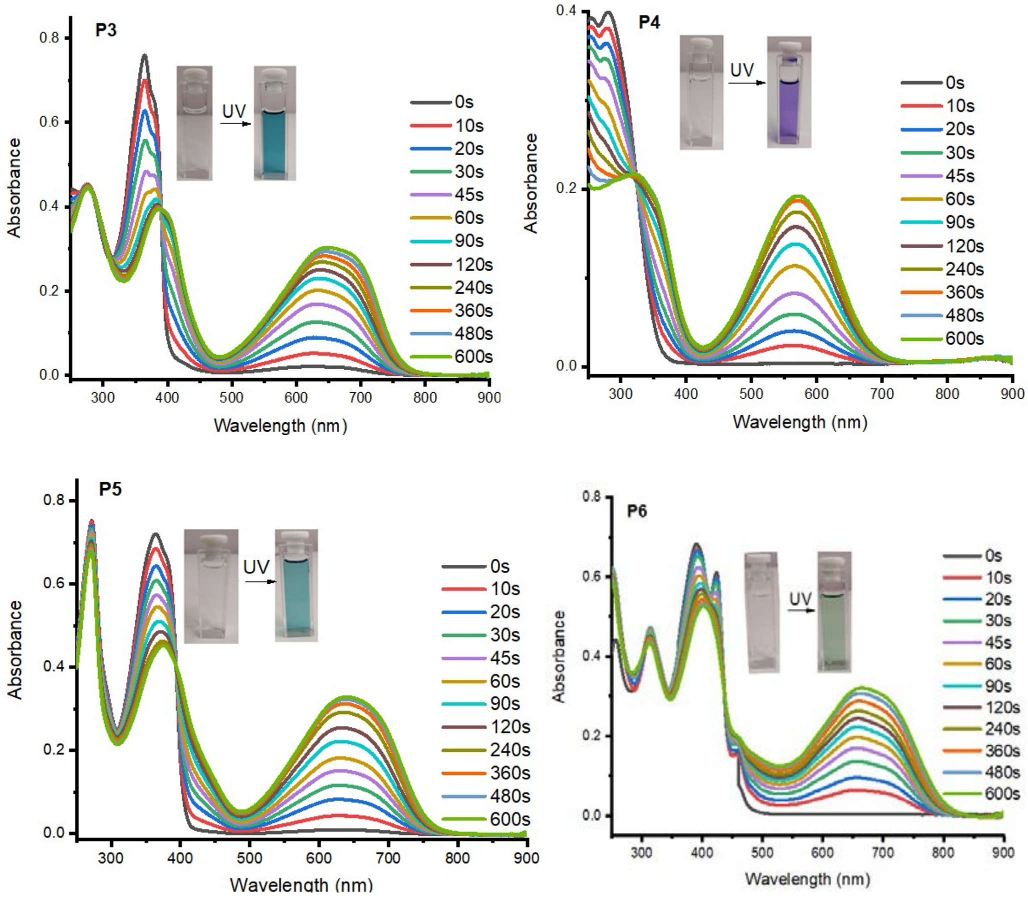

Figure 5.2: UV-Vis absorption spectra of 1x10^{-5} M solutions of P3-P6 in THF upon irradiation with 365 nm monochromatic light.

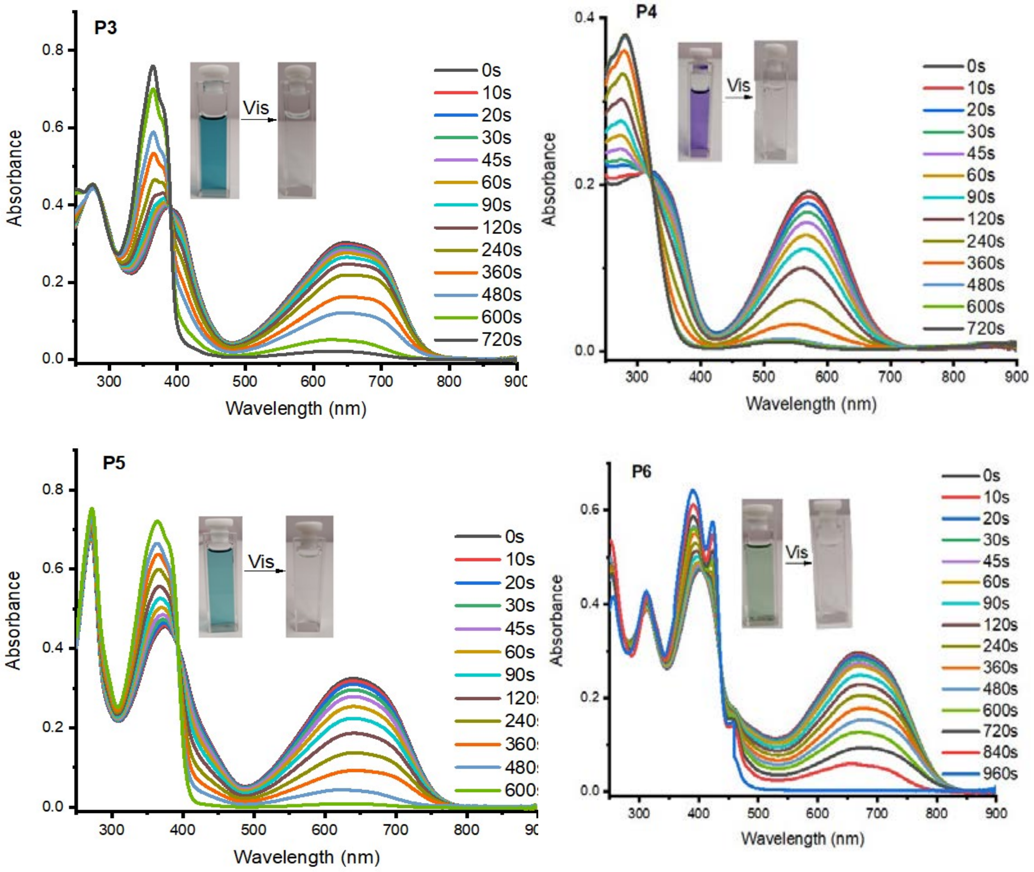

Figure 5.3: Changes in UV-Vis absorption spectra of P4-P6 in THF upon irradiation with Vis light (>550 nm). The solution concentration was $1x10^{-5}$ M.

Table 5.2. Summary of solution properties of P3-P6

	λ_{max}; ε (M^{-1} cm^{-1}) (open-form)	**λ_{max}; ε (M^{-1} cm^{-1}) (closed-form)**	**$\Phi_{o\rightarrow c}$**	**$\Phi_{c\rightarrow o}$**	**Conversion(%)**
P3	365; 50264	625; 28506	0.524 ± 0.002^{a}	0.007 ± 0.001^{c}	99
P4	282; 20336	569; 15712	0.795 ± 0.001^{b}	0.011 ± 0.001^{c}	99
P5	272; 29074 365; 27678	622; 21120 _	0.851 ± 0.002^{a}	0.011 ± 0.001^{c} _	99

			0.866 ± 0.002^a		
P6	381; 53105	675; 30868	0.412 ± 0.003^a	0.004 ± 0.001^c	99

^{a} Upon irradiation with 365 nm UV light; ^{b} Upon irradiation with 280 nm UV light; ^{c} Upon irradiation with visible light >550 nm.

Table 5.3. Dependence of quantum yield on molecular weight

Polymer	**M$_w$ (kg/mol)**	**ε (M^{-1} cm^{-1}) (closed-form)**	$\Phi_{o\rightarrow c}$	$\Phi_{c\rightarrow o}$
P3	20.27	28506	0.524 ± 0.002^a	0.007 ± 0.001^c
P3-1	8.20	26788	0.520 ± 0.001^a	0.008± 0.001^c
P4	6.69	15712	0.795 ± 0.001^b	0.011 ± 0.001^c
P4-1	2.40	16106	0.788 ± 0.001^b	0.011 ± 0.001^c

^{a} Upon irradiation with 365 nm UV light; ^{b} Upon irradiation with 280 nm UV light; ^{c} Upon irradiation with visible light >550 nm.

5.3.3. Thin film physicochemical properties

Thin films of P3-P6 (~20 nm thick) were prepared by spin casting 20 mg/mL polymer solutions onto glass substrates and drying at ambient temperature. These films were characterized using Atomic Force Microscopy (AFM) and Differential Scanning Calorimetry (DSC) to study film and thermal properties, respectively.

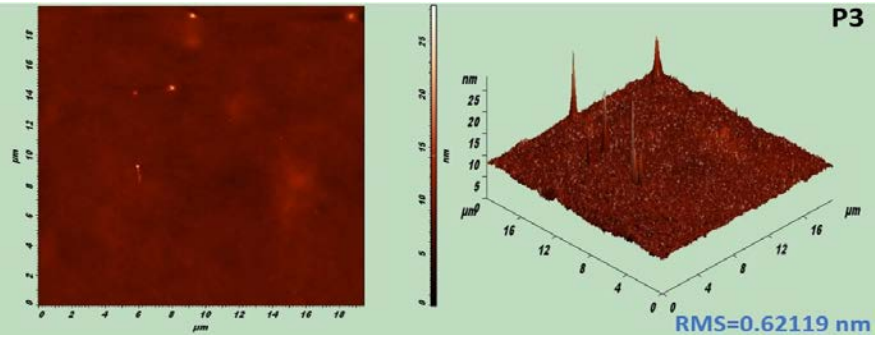

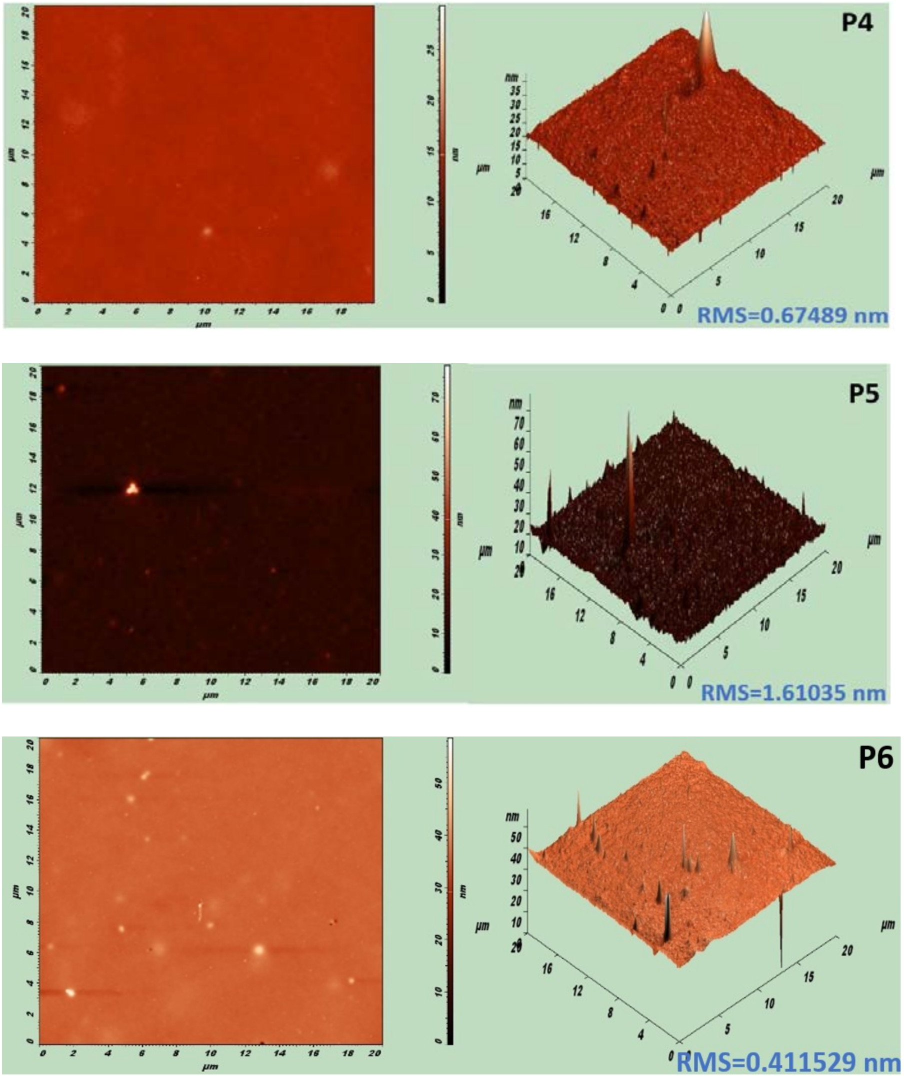

Figure 5.4:AFM micrographs of P3-P6.

AFM micrographs of film of P3-P6 are depicted in **Figure 5.4** depicts and their corresponding root mean square (RMS) roughness are reported in **Table 5.4**. All the polymer films were smooth with low RMS roughness >1.7 nm indicating good film quality. This could be attributed to high molecular weights of these polymers.[34]Thermal stability of polymers is another important property in the development of organic electronics.[34,35]**Figure 5.5a** depicts the DSC traces of P3-P6. All polymers show weak glass transition temperatures and melting points were not observed, implying all polymers are amorphous. The T_g of P3-P6 varied from 49 ºC to 96ºC and show little dependence on conjugation length.

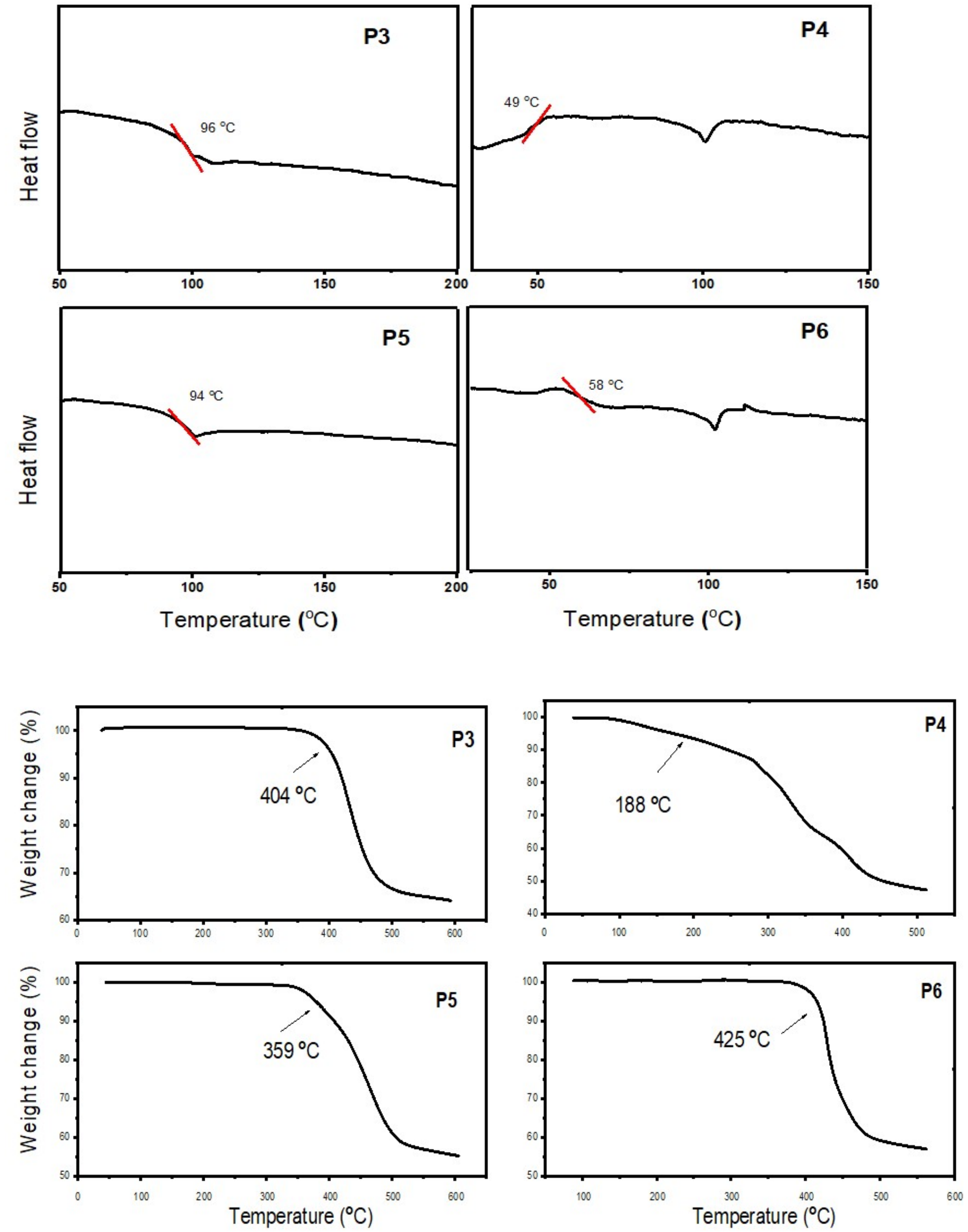

Figure 5.5:DSC traces (a) and TGA thermograms (b) of P3-P6. Heating and ramp rates were equal 10ºC/min.

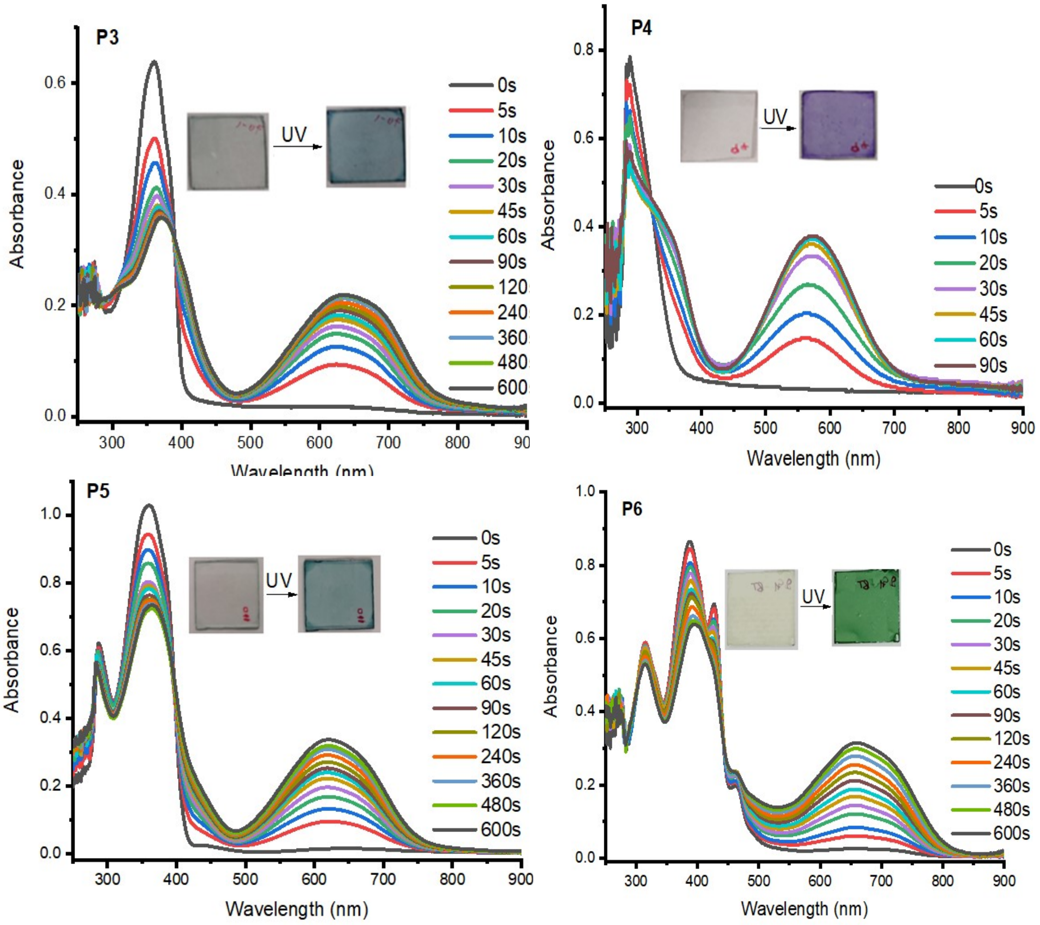

Figure 5.6: Absorption spectra of thin films of P3- P6 upon irradiation with UV light (365 nm). The film thickness was ~20 nm.

The absorption and photochromic properties of the polymer films are depicted in **Figures 5.6**and **5.7** and summarized in **Table 5.4**. The maximum and onset of absorption of the open and closed isomeric form of all the polymers were similar to their solution properties indicating that planarization of the polymer backbone does not occur in the thin film state regardless of their conjugation length. This lack of planarization is consistent of conjugated polymers composed of fluorene-*alt*-thiophene based polymers.[36,37]

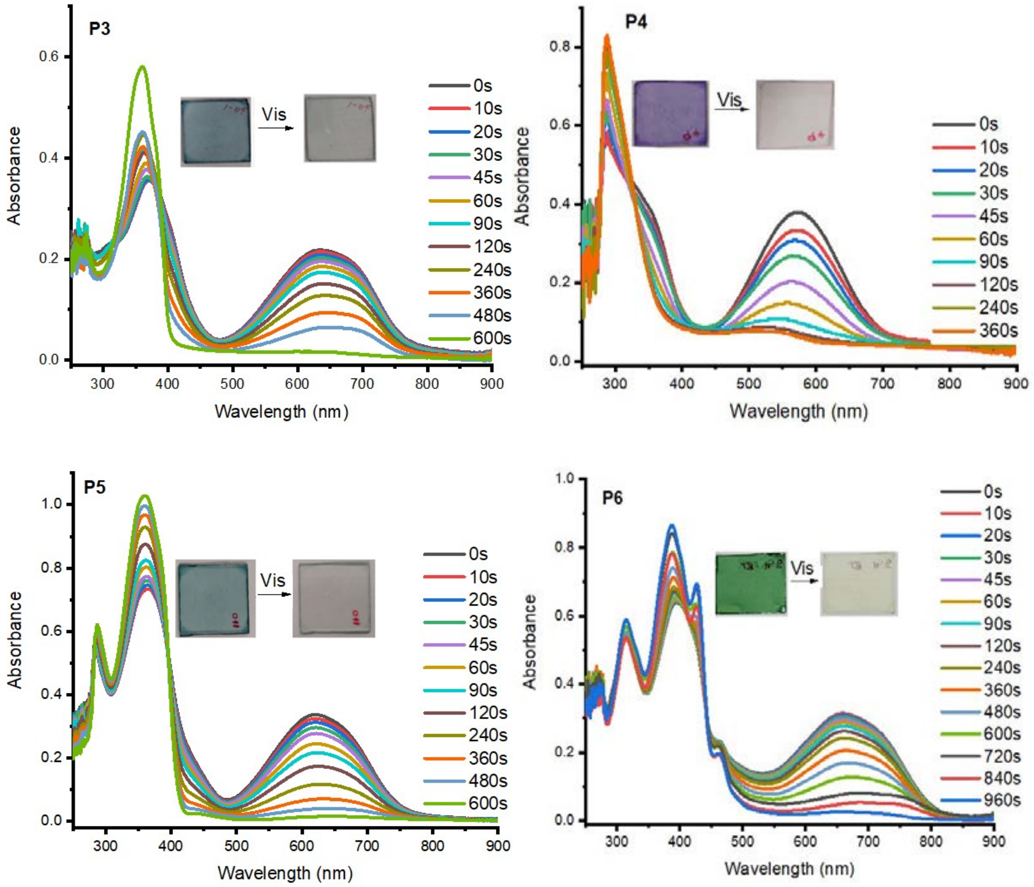

Figure 5.7: Absorption spectra of thin films of P3- P6 upon irradiation with Vis light (>550 nm). The film thickness was ~20 nm.

To understand the differences in the photoswitching efficiency between P3, P5 and P6, the relative rates of electrocylization and cycloreversion (**Figure 5.8a** and **b**) were measured rather than the quantum yield as an appropriate reference was not available. The rates of cyclization were related to P4 and set to 1 as a reference point for ring-closing and 0.1 as a reference point for ring opening. P4 has the fastest switching rate and P6 has the slowest related to differences in conjugation. P3 and P5 had the same relative ring-closing rates and further indicates that the energy levels (fluorene vs. carbazole) do not play a role in the electrocyclization. P6 had the lowest relative electrocyclization rate and could be related to the higher absorptivity (triple that of the P4 reference), differences in the morphology and/or steric interactions. Ring-opening rates ranged between 0.04 to 0.26 relative to P4. The cycloreversion rate trend is similar to the electrocyclization rate.

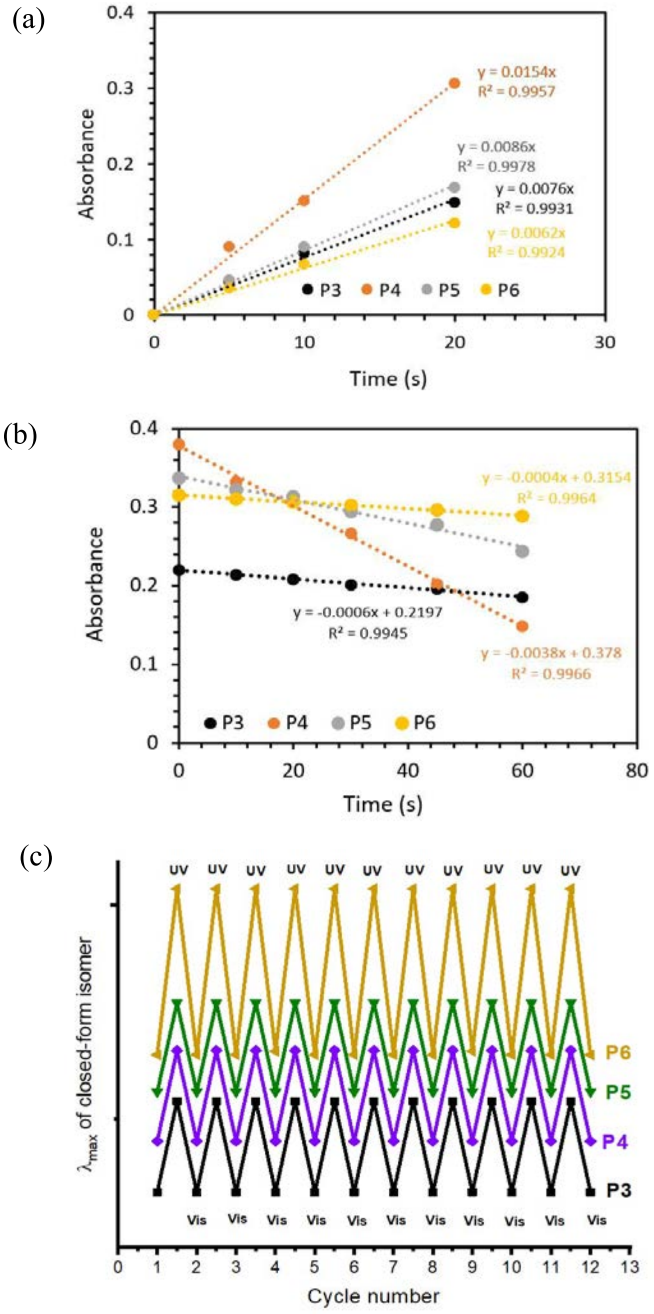

Figure 5.8: Absorption intensity vs time of P3-P6 upon irradiation with UV (a) and Vis light (b). Reversible photoswitching of P3-P6 (c). The films were excited with UV light for 600 s and visible light for 600 s.

Table 5.4. Summary of optical and photochromic properties of P3-P6 films

	λ_{max}; ε (M^{-1} cm^{-1}) (open-form)	λ_{max}; ε (M^{-1} cm^{-1}) (closed-form)	$\chi_{o\rightarrow c}$	$\chi_{c\rightarrow o}$	RMS (nm)
P3	362; 29820	637; 13761	0.408 ± 0.03[a]	0.077 ± 0.03[c]	0.621 ± 0.083
P4	287; 11137	573; 6697	1.000*[b]	0.100*[c]	0.674 ± 0.052
P5	286; 6736	621; 9322	_	0.265 ± 0.02[c]	1.610 ± 0.118
	360; 19090	_	0.404 ± 0.02	_	
P6	387; 35787	662; 16628	0.164± 0.03[a]	0.042 ± 0.02[c]	0.411 ± 0.03

[a] Upon irradiation with 365 nm UV light; [b] Upon irradiation with 280 nm UV light; [c] Upon irradiation with visible light >550 nm; *used as a reference value for relative rate measurements.

Photostability of the active layers is an important parameter in organic photonics and electronics.[38–40] The photochemical stability of P3-P6 was studied by alternate irradiating the polymer thin films with UV light for 600 s followed by visible light for 600 s 12 times in air, which represents 240 min of irradiation. Electrocyclization and cycloreversion was observed for 12 cycles without any signs of fatigue (**Figure 5.8c**). The photochemical stability observed indicates that these polymers do not undergo photooxidation to form fluorenones and/or photo-chain scission and Diels-Alder [2+4] cycloaddition with singlet oxygen, as often observed in polyfluorenes.[41–44]

5.4.Conclusion

Diarylethene-based mainchain photochromic polymers comprised of flourene, carbazole, phenylene or benzodithiophene comonomers were successfully synthesized by Suzuki-Miyaura polycondensation reaction. The polymers are soluble in common solvents and can be cast into high quality smooth thin films. Photoisomerization was observed in both solution and film states with minimal photo- and thermal degradation under ambient conditions. By co-polymerizing comonomers with varying conjugation lengths, it was found that the polymer conjugation length could be controlled to match the specific light source required for the application. Because of these exciting results, these polymers are excellent candidates for multi-functional, light-controlled optoelectronic devices such as phototransistors, security inks, optical memories and smart solar cells.

5.5.References

[1] L. N. Fu, B. Leng, Y. S. Li, X. K. Gao, *Chinese Chem. Lett.***2016**, *27*, 1319.

[2] M. Carroli, D. T. Duong, E. Buchaca-Domingo, A. Liscio, K. Börjesson, M. Herder, V. Palermo, S. Hecht, N. Stingelin, A. Salleo, E. Orgiu, P. Samorì, *Adv. Funct. Mater.***2020**, *30*, 1907507.

[3] H. Qiu, Z. Liu, Y. Yao, M. Herder, S. Hecht, P. Samorì, *Adv. Mater.***2020**, *32*, 1907903.

[4] M. Lahikainen, K. Kuntze, H. Zeng, S. Helantera, S. Hecht, A. Priimagi, *ACS Appl. Mater. Interfaces***2020**, *12*, 47939.

[5] M. Irie, T. Fukaminato, K. Matsuda, S. Kobatake, *Chem. Rev.***2014**, *114*, 12174.

[6] G. Ligorio, G. F. Cotella, A. Bonasera, N. Zorn Morales, G. Carnicella, B. Kobin, Q. Wang, N. Koch, S. Hecht, E. J. W. List-Kratochvil, F. Cacialli, *Nanoscale***2020**, *12*, 5444.

[7] P. Zacharias, M. C. Gather, A. Köhnen, N. Rehmann, K. Meerholz, *Angew. Chemie - Int. Ed.***2009**, *48*, 4038.

[8] Y. Qian, X. Xu, W. Li, J. Wang, B. Wei, Q. Wei, X. Yan, W. Hu, Y. Lu, L. Xie, X. Zhang, W. Huang, *Org. Electron.* **2015**, *26*, 476.

[9] C. Bertarelli, A. Bianco, V. Boffa, M. Mirenda, M. C. Gallazzi, G. Zerbi, *Adv. Funct. Mater.* **2004**, *14*, 1129.

[10] M. El Gemayel, K. Börjesson, M. Herder, D. T. Duong, J. A. Hutchison, C. Ruzié, G. Schweicher, A. Salleo, Y. Geerts, S. Hecht, E. Orgiu, P. Samorì, *Nat. Commun.* **2015**, *6*, 1.

[11] T. Kawai, T. Kunitake, M. Irie, *Chem. Lett.* **1999**, *28*, 905.

[12] E. Kim, H. W. Lee, *J. Mater. Chem.* **2006**, *16*, 1384.

[13] Q. Luo, H. Cheng, H. Tian, *Polym. Chem.* **2011**, *2*, 2435.

[14] H. Choi, H. Lee, Y. Kang, E. Kim, S. O. Kang, J. Ko, *J. Org. Chem.* **2005**, *70*, 8291.

[15] F. Stellacci, C. Bertarelli, F. Toscano, M. C. Gallazzi, G. Zotti, G. Zerbi, *Adv. Mater.* **1999**, *11*, 292.

[16] T. J. Wigglesworth, A. J. Myles, N. R. Branda, *European J. Org. Chem.* **2005**, *2005*, 1233.

[17] C. P. Harvey, J. D. Tovar, *Polym. Chem.* **2011**, *2*, 2699.

[18] K. Higashiguchi, H. Yotsuji, K. Matsuda, *Chem. Lett.* **2017**, *46*, 1564.

[19] M. Irie, T. Lifka, S. Kobatake, N. Kato, *J. Am. Chem. Soc.* **2000**, *122*, 4871.

[20] R. Ammenhäuser, A. Helfer, U. Scherf, *Org. Mater.* **2020**, *02*, 159.

[21] G. L. Gibson, D. Gao, A. A. Jahnke, J. Sun, A. J. Tilley, D. S. Seferos, *J. Mater. Chem. A* **2014**, *2*, 14468.

[22] U. Koldemir, S. R. Puniredd, M. Wagner, S. Tongay, T. D. McCarley, G. D. Kamenov, K. Müllen, W. Pisula, J. R. Reynolds, *Macromolecules***2015**, *48*, 6369.

[23] A. Fihey, A. Perrier, W. R. Browne, D. Jacquemin, *Chem. Soc. Rev.***2015**, *44*, 3719.

[24] Y. Tokita, M. Katoh, K. Kosaka, Y. Ohta, T. Yokozawa, *Polym. Chem.***2021**, *12*, 7065.

[25] S. N. Islam, N. Gogurla, D. Giri, S. K. Ray, S. K. Patra, *J. Lumin.***2019**, *208*, 509.

[26] M. Irfan, K. D. Belfield, A. Saeed, *RSC Adv.***2015**, *5*, 48760.

[27] K. Panthi, P. Z. El-Khoury, A. N. Tarnovsky, T. H. Kinstle, *Tetrahedron***2010**, *66*, 9641.

[28] Z. G. Zhang, H. Fan, J. Min, S. Zhang, J. Zhang, M. Zhang, X. Guo, X. Zhan, Y. Li, *Polym. Chem.***2011**, *2*, 1678.

[29] H. Meier, J. Gerold, H. Kolshorn, B. Mühling, *Chem. - A Eur. J.***2004**, *10*, 360.

[30] E. W. Muller, A. A. Burney-Allen, J. Shaw, D. L. Wheeler, V. Duzhko, M. Jeffries-EL, *J. Polym. Sci.***2020**, *58*, 1299.

[31] W. Woodland, R. Lim, C. Motti, P. Irving, J. Wang, M. Payne, P. C. Junk, G. Vamvounis, *Aust. J. Chem.***2019**, *72*, 874.

[32] O. Galangau, Y. Kimura, R. Kanazawa, T. Nakashima, T. Kawai, *European J. Org. Chem.***2014**, *2014*, 7165.

[33] C. Fan, S. Pu, G. Liu, *Spectrochim. Acta - Part A Mol. Biomol. Spectrosc.***2014**,

131, 235.

[34] W. Xu, K. Mihhels, N. Kotov, S. Lepikko, R. H. A. Ras, C. M. Johnson, T. Pettersson, E. Kontturi, *J. Colloid Interface Sci.***2022**, *605*, 441.

[35] J. Sun, D. Wu, L. Gao, M. Hou, G. Lu, J. Li, X. Zhang, Y. Miao, H. Wang, B. Xu, *RSC Adv.***2018**, *8*, 1638.

[36] G. Vamvounis, S. Holdcroft, *Adv. Mater.***2004**, *16*, 716.

[37] G. Vamvounis, G. L. Schulz, S. Holdcroft, *Macromolecules***2004**, *37*, 8897.

[38] A. Tournebize, A. Rivaton, H. Peisert, T. Chassé, *J. Phys. Chem. C***2015**, *119*, 9142.

[39] R. C. Shallcross, P. Zacharias, A. Köhnen, P. O. Körner, E. Maibach, K. Meerholz, *Adv. Mater.***2013**, *25*, 469.

[40] M. J. Deen, M. H. Kazemeini, S. Holdcroft, *J. Appl. Phys.***2008**, *103*, DOI 10.1063/1.2942400.

[41] A. P. Kulkarni, X. Kong, S. A. Jenekhe, *J. Phys. Chem. B***2004**, *108*, 8689.

[42] Y. Honmou, S. Hirata, H. Komiyama, J. Hiyoshi, S. Kawauchi, T. Iyoda, M. Vacha, *Nat. Commun.***2014**, *5*, 1.

[43] M. S. A. Abdou, S. Holdcroft, *Can. J. Chem.***1995**, *73*, 1893.

[44] B. H. Cumpston, K. F. Jensen, *J. Appl. Polym. Sci.***1998**, *69*, 2451.

CHAPTER 6

SYNTHESIS, OPTICAL PROPERTIES AND SOFT LITHOGRAPHY PATTERNING OF A DIARYLETHENE-BASED MAIN CHAIN PHOTOCHROMIC POLYMER

6.1. Introduction

Organic optical microelectronics such as memory diodes,[1] light-emitting diodes [2,3] and organic field effect transistors [3,4] are growing in demand due to rapid innovations in the development of consumer electronics. π-conjugated polymers are a foundation for the fabrication of these electronics because they are light in weight and can be easily cast into patternable flexible thin films. A new class of conjugated polymers has been developed using photochromics and has shown potential towards the development of light switchable electronics.[5–7] Traditionally, organic electronic devices are switched electrically, where the device is toggled between a high (ON or '1' state) and low (OFF or '0' state) conductance state via application of a suitable electric field.[8]Photoswitchable devices offer an extension of these devices with the ability to modulate the change in conductivity with light. In this chapter, the synthesis and soft lithography patterning of an acid labile diarylethene-based mainchain photochromic polymer is reported.

In organic microelectronics, patterning of active/insulating layers in thin-film form is necessary to tune morphology and promote device performance. Common fabrication techniques for printing/patterning conjugated polymers include ink-jet printing,[9] screen printing,[10] aerosol printing,[11,12] electrochemical patterning,[13,14] and lithography.[15–17] Unfortunately, these conventional techniques have limitations, such as low resolutions (e.g., over 100 μm), complex and high-cost procedures involving alignments, masks, etchings and post-assemblies[18–20] which have hindered rapid innovations and broad applications of conjugated polymers.

Photolithography and soft lithography are the most robust fabrication approaches for patterning microelectronics. Nonetheless, photolithography is not ideal for printing conjugated polymers because harsh processing conditions cause significant damages to the polymers.[21] Chemically amplified photolithography and soft lithography involving deposition of acid onto the surface of a polymer film followed by heating and development are novel techniques for patterning conjugated polymers bearing 2-tetrahydropyranyl (THP) groups.[16,21–23]Chemically amplified soft lithography is a convenient, low-cost and non-photolithographic method based on elastomeric polydimethylsiloxane (PDMS) molds that prevents photochemical damage to the conjugated polymer. This technique would be ideal for patterning photoswitchable polymers.

This chapter reports the synthesis, characterization of an acid-labile diarylethene-based main chain photochromic polymer and its patterning using chemically amplified soft lithography. This polymer contains THP side chains and undergoes solid state acid-catalyzed reaction as shown in **Scheme 6.1**. The polymer retains its optical and photochromic properties in solid state after deprotection. Intriguingly, the polymer can be patterned using a PDMS stamp resulting in micropatterns with high resolutions. Based on these interesting results this polymer can find potential application in photoswitchable microelectronics.

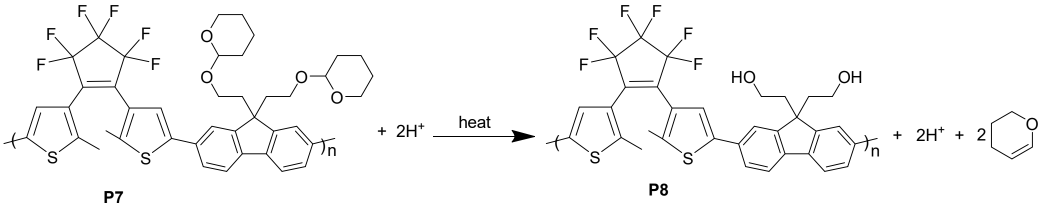

Scheme 6.1: Acid-catalyzed elimination of dihydropyran from P7.

6.2. Experimental

6.2.1. Chemicals and reagents

2-Methylthiophene, *N*-Bromosuccinimide (NBS), trimethylsilyl chloride (TMSCl), n-butyllithium, fluorene, bromine, tetrabutylammonium bromide, 2-bromoethanol, 3,4-dihydro-2H-pyran, bromobenzene and phenylboronic acid, tetrakis(triphenylphosphine)palladium(0) ($Pd(PPh_3)_4$), camphorsulfonic acid (CSA) and 2-isopropoxy4,4,5,5-tetramethyl-[1,3,2]dioxaborolane were all purchased from Sigma Aldrich. Tetrahydrofuran (THF) was dried over sodium/benzophenone and then distilled under argon atmosphere immediately before use. Dichloromethane (DCM) and petroleum ether were distilled under vacuum prior to use. The dibromide photochrome was synthesized following a method reported in Chapter 4. An elastomeric stamp of PDMS was fabricated by the Australian National Fabrication Facility-Queensland Node.

6.2.2. Synthesis procedures

2-(2-Bromoethoxy)tetrahydro-2H-pyran

A 250 mL round bottom flask was charged with 2-bromoethanol (10.00 g, 80 mmol, 1.0 eq.) and dichloromethane (100 mL) and cooled to ^{o}C in an ice bath. 3,4-dihydro-2*H*-pyran (8.06 g, 96 mmol, 1.2 eq.) and *p*-toluene sulfonate (20 mg, 0.12 mmol, 0.0015 eq.) was added. The mixture was stirred for 5 hours and quenched with aqueous solution of $NaHCO_3$(10 wt.%, 100 mL). The mixture was extracted with dichloromethane (3 x 50 mL) and washed with water (2 x 50 mL). The combined organic layers were dried over anhydrous sodium sulfate, filtered, and the solvent was removed under reduced pressure to afford a brown liquid. The crude product was purified by column chromatography (column height=15 cm, diameter =4.0 cm) on silica gel using ethyl acetate/*n*-hexane mixture (*v*/*v* = 1/15) as eluent to afford light yellow liquid of (13.44 g, 80.4%).[24] ^{1}H NMR (400 MHz, $CDCl_3$) *δ*: 4.67 (t, 1H), 3.70-4.08 (m, 3H), 3.43-3.59 (m, 3H), 1.46-1.92 (m, 6H); υ_{max}/cm^{-1} 666, 752, 813, 844, 866, 903, 965, 1003, 1022, 1074, 1120, 1200, 1274, 1351, 1440, 1453, 2868, 2940; MS (*m/z*) Cald for $[C_7H_{14}O_2BrNa]^+$: 230.9991, found: 230.9988.

2,7-dibromo-9,9-di(2-(2-tetrahydropyranyloxy)ethyl)-fluorene

A 50 mL round bottom flask was charged with 2,7-dibromofluorene (5 g, 15.4 mmol, 1.0 eq.), tetrabutylammonium bromide (0.397 g, 1.2 mmol, 0.078 eq.) as a phase-transfer catalyst were and toluene (30 mL). Aqueous NaOH solution (20 mL, 50 wt.%) was added and the reaction was allowed to stir for 1 hour at room temperature**.** 2-(2-Bromoethoxy)tetrahydro-2H-pyran(8.07 g, 15.425 mmol, 1.03) was added and the reaction mixture was thenheated at 70 °C under reflux for 20 h. The reaction mixture was cooled to room temperature (~27^{o}C) and quenched with saturated sodium bicarbonate (10 mL). The mixture was extracted with DCM (2 x 100 mL). The combined organic layers were washed with water (2 x 100 mL) dried over anhydrous sodium sulfate, filtered and the solvent was removed under reduced pressure. The crude product was recrystallized in methanol (20 mL) to give a white solid (5.612 g; 63%).[25] ^{1}H NMR (400 MHz, $CDCl_3$) *δ*: 7.57-7.23 (m, 6H), 4.13 (t, 2H), 3.49-3.46 (m, 2H), 3.28-3.13 (m, 4H), 2.76-2.70 (m, 2H), 2.39-2.35 (m, 4H), 1.47-1.26 (m, 10H); υ_{max}/cm^{-1} 665, 753, 805, 843, 877, 902, 969, 1003, 1031, 1059, 1075, 1134, 1205, 1216, 1228, 1365, 1415, 1449, 1737, 2862, 2939, 2968; MS (*m/z*) Cald for $[C_{27}H_{32}Br_2O_4]^+$: 580.0644, found: 580.0644; T_m=102.43 °C.

9,9-bis(2-(2-tetrahydropyranyloxy)ethyl)-fluorene-2,7-diboronic acid bis(pinacol) ester

A flame dried 100 mL round bottom flask was charged with 2,7-dibromo-9,9-di(2-(2-tetrahydropyranyloxy)ethyl)-fluorene (1.0 g, 1.72 mmol, 1.0 eq.) and dry THF (40 mL) under argon atmosphere and cooled to -78 ^{o}C.*N*-butyllithium (1.6 M in hexane, 2.26 mL, 3.62 mmol, 2.1 eq.) was added andthe mixture was stirred for 1 h at -78 ^{o}C. 2-Isopropoxy4,4,5,5-tetramethyl-[1,3,2]dioxaborolane (0.73 mL, 5.1 mmol, 2.05 eq.) was added and the reaction was left stirring overnight at room temperature. The reaction was quenched with 30 mL of cold waterand the mixture was extracted with chloroform (3 x 50 mL). The combined organic layers were washed with water (2 x 50 mL). The organic layer was dried over anhydrous sodium sulfate, filtered, and the solvent was removed under reduced pressure to afford an off-white solid. The product was recrystallized in methanol to afford a white solid (0.751 g; 63%). ^{1}H NMR (400 MHz, $CDCl_3$) δ: 7.88-7.69 (m, 6H), 4.06 (t, 2H), 3.50-3.44 (m, 2H), 3.20-3.06 (m, 4H), 2.71-2.69 (m, 2H), 2.48-2.44 (m, 4H), 1.30 (m, 36H); υ_{max}/cm^{-1}647, 697, 750, 825, 842, 858, 932, 981, 1031, 1056, 1091, 1132, 1215, 1229, 1322, 1349, 1424, 1475, 1606, 1737, 2869, 2936, 2968; MS (*m/z*) Cald for $[C_{39}H_{56}B_2O_8]^+$: 674.4156, found: 674.4147; T_m=195.67 ^{o}C.

Synthesis of Poly(3-[3,3,4,4,5,5-hexafluoro-2-(2-methyl-3-thienyl)-1-cyclopenten-1-yl]-2-methylthiophene)-*alt*-(9,9-di(2-(2-tetrahydropyranyloxy)ethyl)-fluorene)

A 50 mL Schlenk tube was charged with 2-bis(5′-bromo-2′-methylthien-3′-yl)hexafluoro- cyclopent-1-ene (0.402g, 0.776 mmol, 1.0 eq.), 9,9-bis(2-(2-

tetrahydropyranyloxy)ethyl)-fluorene-2,7-diboronic acid bis(pinacol) ester (0.538 g, 0.776 mmol, 1.0 eq.), THF (25 mL) and aqueous potassium carbonate (8 ml, 2 M). This mixture was purged with nitrogen for 10 min and $Pd(PPh_3)_4$ (0.0106 g, 0.00776 mmol, 0.01 eq.) was added. The mixture was then degassed three times using freeze-pump thaw cycles then covered under a blanket of argon. The mixture was stirred at 60 °C for 144 h. To remove the reactive end-groups, the resultant polymer was treated bromobenzene and phenylboronic acid after 96 and 120 h, respectively. The reaction was quenched with water (20 mL), and the mixture was extracted with dichloromethane (3 x 20 mL). The combined organic layers were washed with water (2 x 50 ml) and brine (20 mL). The organic layer was dried over anhydrous sodium sulfate, filtered, and the solvent was removed under reduced pressure to afford a teal green colored oil. The oil was dissolved in 10 ml of chloroform and precipitated into 50 mL methanol to afford a teal green solid (0.402 g, 64%).λ_{max} (open isomer) (THF)/nm 365 [log(ε/dm^3 mol^{-1} cm^{-1}) (4.64)], λ_{max} (closed isomer) (THF)/nm 642 [log(ε/dm^3 mol^{-1} cm^{-1}) (4.36)]; ^{1}H NMR (400 MHz, $CDCl_3$) δ: 7.34-7.70 (m, 8H), 4.05-4.20 (m, 2H), 3.48-3.52 (m, 4H), 3.24-3.28 (m, 4H), 2.80-2.85 (m, 2H), 2.20-2.26 (m, 4H), 2.02-2.04 (m, 6H), 1.28-1.44 (m, 10H);υ_{max}/cm^{-1}696, 741, 812, 867, 900, 988, 1029, 1053, 1074, 1114, 1188, 1271, 1340, 1428, 2930; GPC: M_w=12.17 kg/mol; PDI=2.44.

6.2.3. Characterization

^{1}H NMR spectra were recorded on Bruker AscendTM 400 MHz spectrometer for samples in $CDCl_3$. Chemical shifts are reported in parts per million (ppm) and are referenced to the residual solvent peak (chloroform, ^{1}H = 7.26 ppm). Peak multiplicities are designated in the following manner: singlet (s), doublet (d), triplet (t), doublet and multiplet (m). The polymer molecular weights were determined using gel permeation chromatography (GPC) (Agilent Technologies 1260 Infinity Series) equipped with a UV absorption and refractive index detectorusing THF as eluent and polystyrene narrow standards. The PLgel 5 µm Mixed–C columns (300×7.5 mm)×2 were calibrated using polystyrene narrow standards in tetrahydrofuran. Infrared spectra were recorded using a Nicolet 6700 FT-IR spectrometer equipped with an attenuated total reflection (ATR) crystal. Absorption spectra were recorded using a Shimadzu UV2600 spectrophotometer.

Solution quantum yields of cyclization ($\Phi_{o\rightarrow c}$)and cycloreversion ($\Phi_{c\rightarrow o}$)were measured by a relative method in THF using 1,2-bis(2-methyl-5-phenyl-3-thienyl)perfluorocyclopentene as the standard, which has a quantum yields of cyclization of 0.574 at 365 nm and quantum yield of cycloreversion of 0.013 at λ>492 nm.[26,27] Acid-catalyzed deprotection was carried out by annealing the films in the presence of 5 mol% acid at 185 °C for 3 min. Thin films for measuring UV–Vis absorption and atomic microscopy analysis were prepared on glass (Sail Brand) by spin coating 20 mg/mL of P7 in toluene or chloroform at 1500 rotations per minute for 45 s using a Chemat KW-4A spincoater. Glass substrates were cleaned prior to use in an ultrasound bath for 10 minutes using soapy water, acetone and ethanol, respectively, and dried under nitrogen atmosphere. The surface morphology and thickness of the films was measured using an NTEGRA TS-150 atomic force microscope (AFM). Microscope images were acquired on an Olympus X60 optical microscope using Image-Pro Plus 7 software. Thermal properties were investigated using an SDT 650 (TA instruments) and DSC 250 (TA instruments). The DSC was equipped with a refrigeration cooling system (RCS) and the heating/ cooling rates were equal at 10 ºC min^{-1}. TGA ramp rate was maintained at 10 ºC min^{-1}.Degradation temperatures were estimated at 5% weight loss. TGA ramp rate was maintained at 10 ºC min^{-1}. Degradation temperatures were estimated at 5% weight loss. Photochemical stability measurements were performed by switching repeatedly between the colored and colorless isomeric forms of the polymers using a handheld UVGL-58 lamp at 365 nm and a visible light lamp (>550 nm) and measuring the absorption spectra. Polymer films (~20 nm) were irradiated with alternate UV and visible light for 600s in air and absorbance was measured and recorded after each switching cycle. The switching cycles were repeated twelve times.

6.3. Results and discussion

6.3.1. Polymer structure

P7 was synthesized by Suzuki-Miyaura polycondensation reaction between 2-bis(5′-bromo-2′-methylthien-3′-yl)hexafluorocyclopent-1-ene and 9,9-bis(2-(2-tetrahydropyranyloxy)ethyl)-fluorene-2,7-diboronic acid bis(pinacol). The dibromide comonomer was synthesized as previously reported.[28,29] 9,9-bis(2-(2-tetrahydropyranyloxy)ethyl)-fluorene-2,7-diboronic acid bis(pinacol) ester was synthesized from 2,7-dibromo-9,9-di(2-(2-tetrahydropyranyloxy)ethyl)-fluorene following a method presented in **Scheme 6.2**(Supporting Information). The polymer was end-capped using phenyl boronic acid and bromobenzene to remove reactive bromide and boronic ester groups.[30,31]

The structure of P7 was confirmed by ^{1}HNMR and FTIR spectroscopy. Resonance peaks observed at 7.34-7.70 ppm were ascribed to the aromatic protons of flourene and thiophene rings. The peak due to methine protons of the THP groups was observed at 4.15 ppm [21–23] and the peak at 2.02 ppm was assigned to the methyl protons on the thiophene rings. The molecular weight of P7 was found to be 12.2 kg/mol with a polydispersity index of 2.44.Molecular weight can be increased by changing the solvent or increasing reaction temperature. The most used solvents for

Suzuki-Miyaura polycondensation reactions are toluene and THF. In this study, THF was chosen as the reaction solvent due to low solubility of 9,9-bis(2-(2-tetrahydropyranyloxy)ethyl)-fluorene-2,7-diboronic acid bis(pinacol) ester in toluene. The reaction temperature was kept at 60 °C to avoid cleaving the THP group.[21]

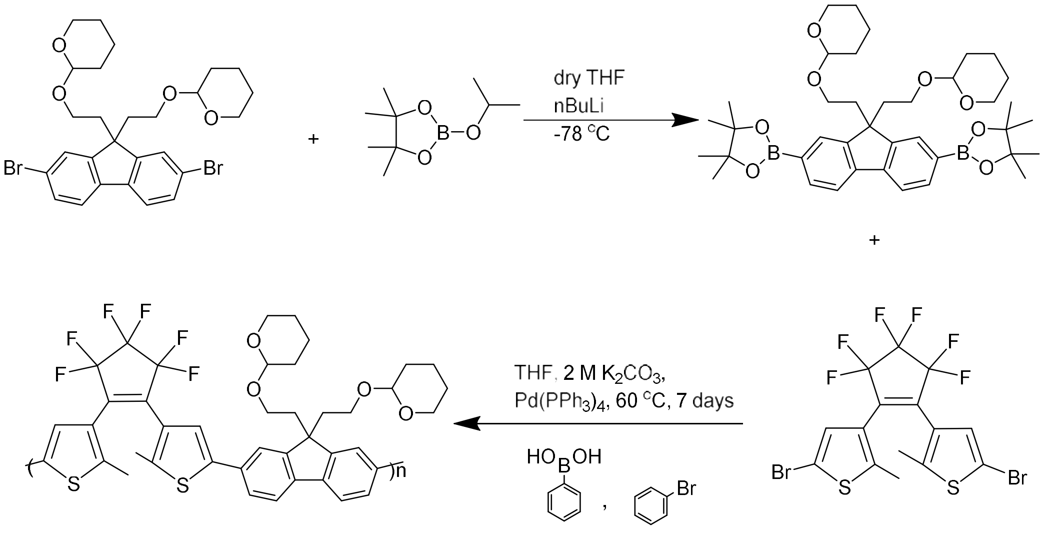

Scheme 6.2: Synthesis protocol of P7.

6.3.2. Thermal properties and solid-state reaction

Thermal properties of P7 were studied using thermogravimetric analysis. In the absence of CSA, P7 is stable up to ~240 °C and undergoes thermolytic decomposition between 240 °C and 325 °C accompanied by a 20.5% weight loss (**Figure 6.1a**). The observed weight change is consistent with the theoretical mass corresponding to the cleavage of THP groups and volatilization of two moles of dihydropyran. Upon addition of 5 mol% CSA, the TGA thermogram showed a 20.5% loss between 154 °C and 250 °C. This weight loss is also consistent with the theoretical value of dihydropyran lost through volatilization. This confirms that the removal of the THP group at 154 °C is due to the presence of 5 mol % CSA thus the reaction is acid-catalyzed. AFM micrographs (**Figure S6.1**) of pristine polymer film and acid catalyzed deprotected film are smooth with root mean square roughnesses of 0.6358 and 0.8851 nm, respectively. The AFM micrograph of P7 annealed at at 325 °C is rough with RMS of 2.008 nm due to crystallization (**Figure S6.1**). This confirms that acid-catalyzed deprotection does not damage the conjugated polymer unlike uncatalyzed thermolytic deprotection. The acid-catalyzed reaction of P7 was further studied using FTIR spectroscopy (**Figure 6.1b**). The FTIR spectrum of pristine P7 do not show peaks corresponding to hydroxyl groups even if it is annealed at 250 °C. The spectrum of P7 + CSA annealed at 200 °C shows a broad peak at 3400 cm^{-1} confirming the formation of hydroxyl groups. The deprotected polymer is insoluble in THF (insert-**Figure S6.2**), chloroform and toluene due to short alky side chains and hydrogen bonding through terminal hydroxyl groups.

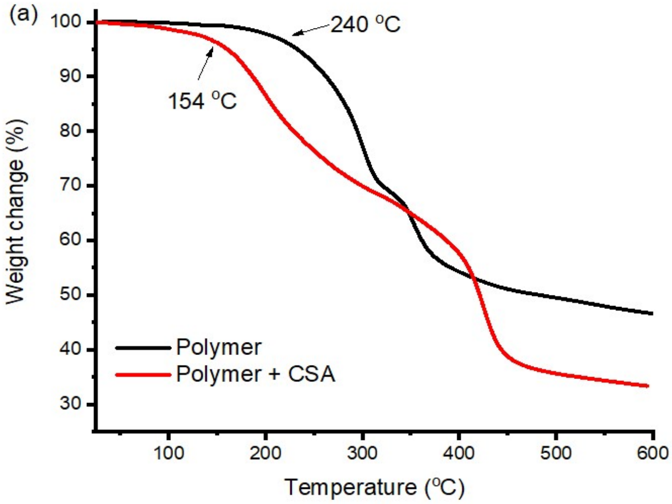

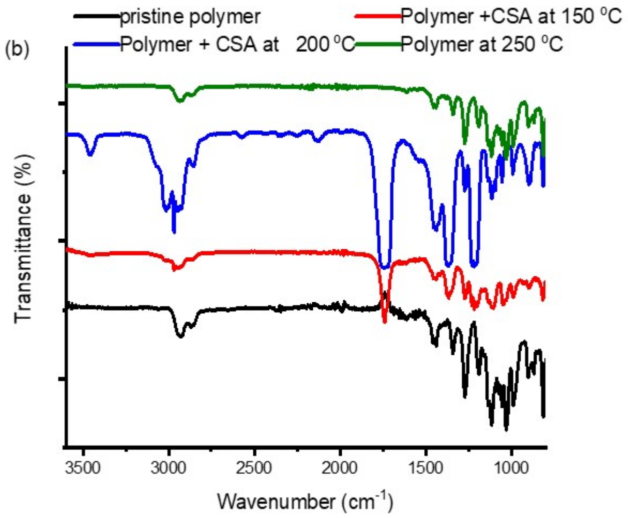

Figure 6.1: TGA thermogram of P7 and P7 +CSA (a), FTIR spectra of P7 and P7 +CSA (b).

6.3.3. Optical properties

Solution optical and photochromic properties were studied by UV-Vis spectroscopy in THF and the results are summarized in **Table 6.1**. **Figure 6.2** shows the absorption spectra of P7 before and after irradiation with UV light. Before irradiation (**Figure 6.2a**), the absorption spectrum (black line) shows a peak at 355 nm due to open-form isomer of P7. Upon irradiation with UV light for 10 seconds a new broad peak at 642 nm emerged due to the formation of the closed form isomer. The closed form isomer is teal green in color. The intensity of the new peak and the color of the solution intensified as the irradiation time increased until photostationary state was reached at 600 seconds. The closed form isomer absorbs at a longer wavelength because upon cyclization the π-conjugation delocalizes throughout the molecule, and the HOMO−LUMO gap becomes small thus shifting the maximum absorption peak to the visible region of the absorption spectrum.[27,32,33] The colored solution was irradiated with visible light (>550 nm) until the peak in the visible region disappeared and solution turned colorless as shown in **Figure 6.2b**. Quantum yields of cyclization and cycloreversion for P7 were found to be 0.55 and 0.0082, respectively. These values are comparable to those of other diarylethene-*alt*-fluorene polymers discussed in **chapter 4**.

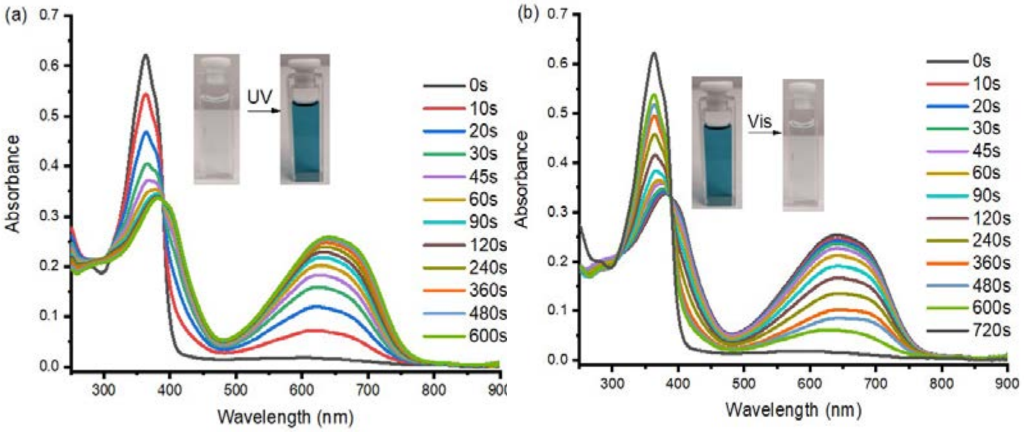

Figure 6.2: Absorption spectra of P7 upon irradiation with UV light (a) and visible light (b). Concentration was 1x10^{-5} M.

Most photochromic polymers have low switching quantum yields in solid state due to the lack of sufficient free volume for molecules to undergo electrocyclization and cycloreversion processes.[5,6,34] This has hindered the practical application of photochromic molecules in organic electronics. Therefore, it is imperative to develop materials with high photoswitching quantum yields in solid states. Photochromic properties of P7 investigated in solid state before and after the removal of the THP group. The spectra are similar to those observed in solution (**Figure 6.3** and **Figure 6.4**) implying that the polymer retains its photochromic properties after deprotection. Interestingly, the photoswitching rates (**Figure 6.5**) for deprotected films are higher than those of pristine films possibly due to reduced side chain bulkiness.[35]

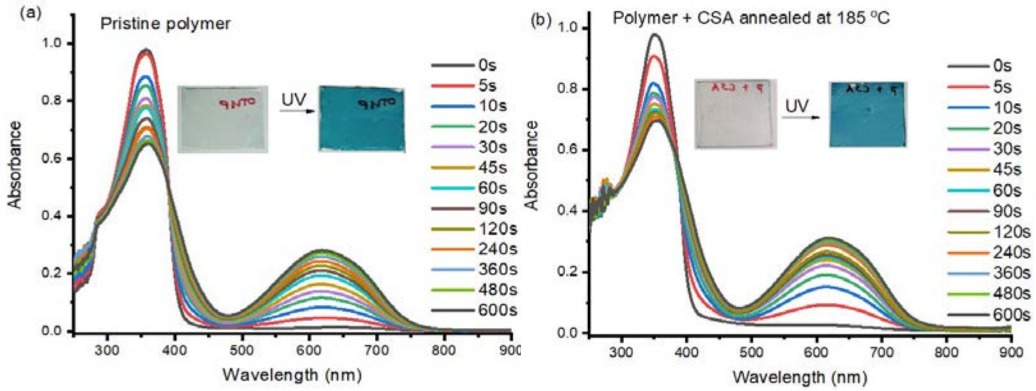

Figure 6.3: Absorption spectra of thin films of P7 (a) and P7 + CSA (b) upon irradiation with UV light (a) and visible light (b).

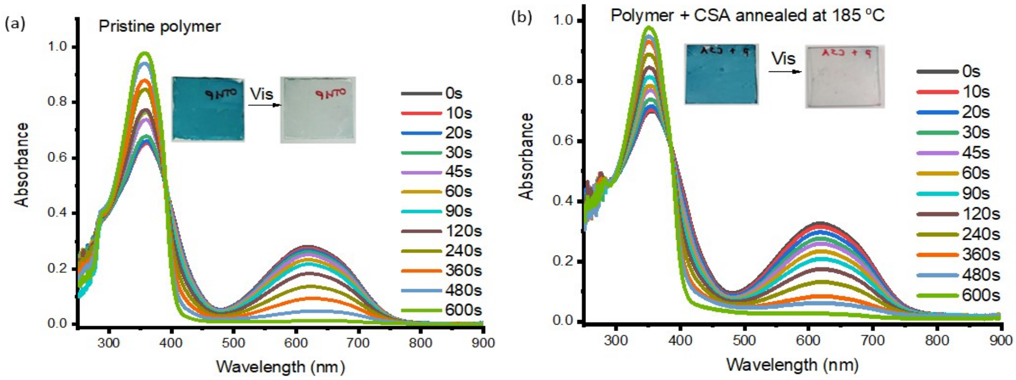

Figure 6.4: Absorption spectra of thin films of P7 (a) and P7 + CSA (b) upon irradiation with visible light.

Table 6.1. Summary of properties of P7

	P7	**P7 + CSA**
Solution		
λ_{max} (open-form)	365	-
ε (M^{-1} cm^{-1}) (open-form)	43606	-
λ_{max}(closed-form)	642	-
ε (M^{-1} cm^{-1}) closed-form	24054	-
$\Phi_{o\rightarrow c}$	0.55	-
$\Phi_{c\rightarrow o}$	0.0082	-
Film		

λ_{max} (open-form)	355	352
ε (M^{-1} cm^{-1}) (open-form)	23158	35787
λ_{max} (closed-form)	618	620
ε (M^{-1} cm^{-1}) closed-form	10945	16628

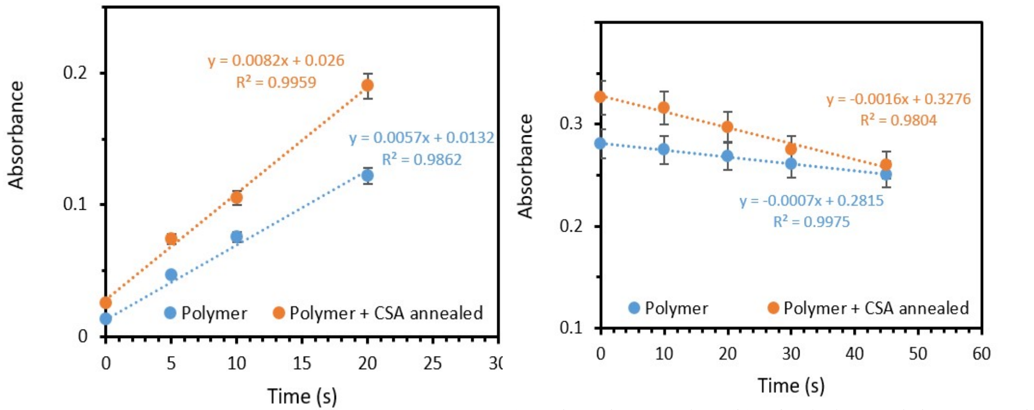

Figure 6.5: Absorbance vs time upon cyclization (a) and cycloreversion (b) of pristine and deprotected films.

6.3.4. Chemically amplified soft lithography

The major advantage of soft lithography over photolithographic patterning techniques is the elimination of possible damage to the conjugation polymer.[36] Chemically amplified soft lithography involving the catalytical removal of solubilizing groups at moderate temperatures is the most appealing technique for patterning microelectronics based on photochromic polymers. **Figure 6.6a** shows the schematic illustration of the procedure followed to demonstrate chemically amplified soft lithography using P7. Film thickness and annealing time were optimized but CSA concentration was maintained at 0.01 M as it has been optimized in another study.[23] A solution of P7 in chloroform was spincast onto a glass substrate resulting in a film approximately 50 nm thick. The patterned surface of a PDMS stamp was immersed in 0.01 M CSA in THF/hexane (50/50) (v/v) for 3 seconds and then dried in air for 30 seconds. The inked stamp was gently pressed onto the polymer film for 10 seconds to allow acid transfer to occur. The film was then thermally heated at 185 °C on hot plate for 5 seconds and allowed to cool to room temperature before development in chloroform. Acid-catalyzed deprotection reaction occurred in the regions where CSA was deposited and resulted in cleavage of the THP group and elimination of dihydropyran. Dihydropyran is reported to vaporize at ~90 °C, so at high temperatures it is expelled from the film.[23] The deprotected regions were insoluble due reduced alkyl side chain length and formation of hydroxyl groups resulting in changes in polarity. After dipping the film in chloroform, unreacted regions dissolved leaving positive images of the PDMS stamp printed on the glass substrate as shown in **Figure 6.6b**.

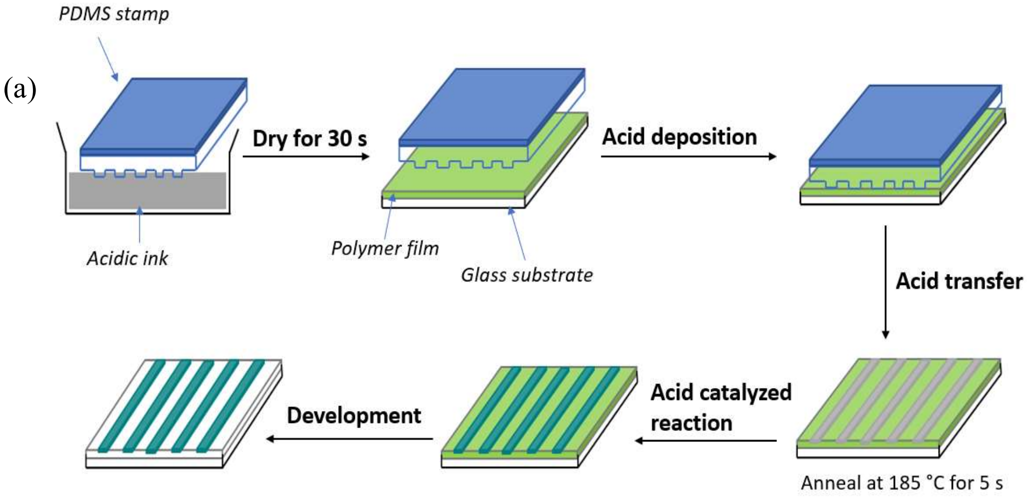

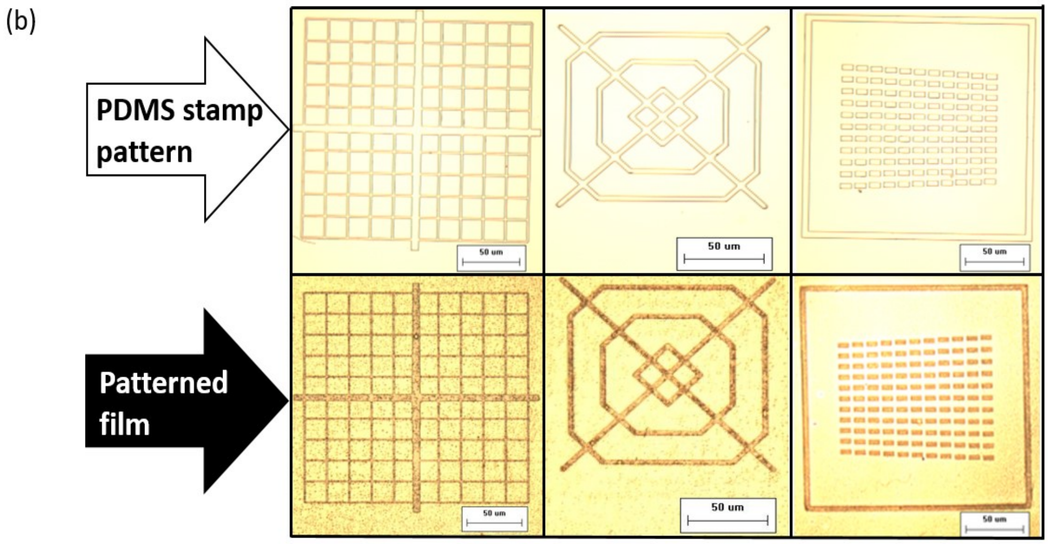

Figure 6.6: Illustration of chemically amplified soft lithography of P7 (a) and micrographs of patterned films with corresponding PDMS stamp patterns (b).

Fatigue resistance of active layer components is an important factor in organic electronics. The photochemical stability of P7 was investigated by irradiating the polymer thin films (both pristine and deprotected) with UV light for 600 s followed by visible light for 600 s 12 times in air which represents 240 min of alternate irradiation with UV and visible light. Electrocyclization and cycloreversion was repeated 12 cycles, no signs of fatigue were observed for both films (**Figure 6.7**).The photochemical stability observed indicates that DTE by-product was not formed [37–39] and fluorenone formation often observed in polyfluorenes does not occur.[40,41]

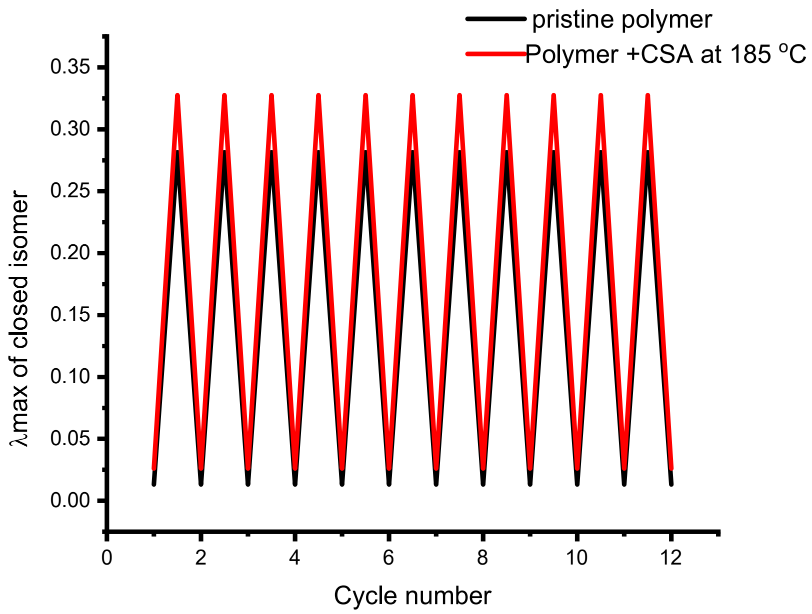

Figure 6.7: Reversible photoswitching P7 before and after deprotection. Films were excited with UV light for 600 s and visible light for 600 s.

6.4. Conclusion

A mainchain photochromic polymer bearing THP side chains was successfully synthesized by Suzuki-Miyaura polycondensation reaction. The polymer is photoswitchable in both solution and solid state. This polymer undergoes, solid state acid-catalyzed removal of THP groups and volatilization as dihydropyran. The removal of the THP groups reduces the length of side chains and causes the formation of terminal hydroxyl groups, thus changing the polarity of the polymer. This causes the polymers to become insoluble thus allowing spatially controlled patterning using chemically amplified soft lithography. The photochromic behavior is retained after deprotection. Based on these exciting results, this polymer is an ideal candidate for the fabrication of multi-functional, light-controlled microelectronic devices such as phototransistors and organic light emitting diodes.

6.5. References

[1] T. Tsujioka, T. Sasa, Y. Kakihara, *Org. Electron.***2012**, *13*, 681.

[2] P. Zacharias, M. C. Gather, A. Köhnen, N. Rehmann, K. Meerholz, *Angew. Chemie - Int. Ed.***2009**, *48*, 4038.

[3] G. Ligorio, G. F. Cotella, A. Bonasera, N. Zorn Morales, G. Carnicella, B. Kobin, Q. Wang, N. Koch, S. Hecht, E. J. W. List-Kratochvil, F. Cacialli, *Nanoscale***2020**, *12*, 5444.

[4] Y. Ishiguro, R. Hayakawa, T. Chikyow, Y. Wakayama, *J. Mater. Chem. C***2013**, *1*, 3012.

[5] T. Kawai, Y. Nakashima, M. Irie, *Adv. Mater.***2005**, *17*, 309.

[6] T. J. Wigglesworth, N. R. Branda, *Adv. Mater.***2004**, *16*, 123.

[7] F. Stellacci, C. Bertarelli, F. Toscano, M. C. Gallazzi, G. Zotti, G. Zerbi, *Adv. Mater.***1999**, *11*, 292.

[8] R. C. Shallcross, P. Zacharias, A. Köhnen, P. O. Körner, E. Maibach, K. Meerholz, *Adv. Mater.***2013**, *25*, 469.

[9] J. S. Choi, K. Y. Cho, J. H. Yim, *Eur. Polym. J.***2010**, *46*, 389.

[10] B. Tasaengtong, Y. Sameenoi, *Microchem. J.***2020**, *158*, 105078.

[11] K. Hong, S. H. Kim, A. Mahajan, C. D. Frisbie, *ACS Appl. Mater. Interfaces***2014**, *6*, 18704.

[12] K. Skarżyński, J. Krzemiński, M. Jakubowska, M. Słoma, *Sci. Rep.***2021**, *11*, 1.

[13] V. R. Feig, H. Tran, M. Lee, K. Liu, Z. Huang, L. Beker, D. G. Mackanic, Z. Bao, *Adv. Mater.***2019**, *31*, 1.

[14] S. Sekine, Y. Ido, T. Miyake, K. Nagamine, M. Nishizawa, *J. Am. Chem. Soc.***2010**, *132*, 13174.

[15] X. Zhang, L. Cox, Z. Wen, W. Xi, Y. Ding, C. N. Bowman, *Polymer.***2018**, *156*, 162.

[16] J. Yu, S. Holdcroft, *Chem. Commun.***2001**, 1274.

[17] J. H. Moon, A. Small, G. R. Yi, S. K. Lee, W. S. Chang, D. J. Pine, S. M. Yang, *Synth. Met.***2005**, *148*, 99.

[18] S. Wang, J. Xu, W. Wang, G. J. N. Wang, R. Rastak, F. Molina-Lopez, J. W. Chung, S. Niu, V. R. Feig, J. Lopez, T. Lei, S. K. Kwon, Y. Kim, A. M. Foudeh, A. Ehrlich, A. Gasperini, Y. Yun, B. Murmann, J. B. H. Tok, Z. Bao, *Nature***2018**, *555*, 83.

[19] Y. Liu, A. F. McGuire, H. Y. Lou, T. L. Li, J. B. H. Tok, B. Cui, Z. Bao, *Proc. Natl. Acad. Sci. U. S. A.***2018**, *115*, 11718.

[20] H. Yuk, B. Lu, S. Lin, K. Qu, J. Xu, J. Luo, X. Zhao, *Nat. Commun.***2020**, *11*, 4.

[21] X. Han, X. Chen, G. Vamvounis, S. Holdcroft, *Macromolecules***2005**, *38*, 1114.

[22] J. Yu, M. Abley, C. Yang, S. Holdcroft, *Chem. Commun.***1998**, 1503.

[23] J. Yu, S. Holdcroft, *Macromolecules***2000**, *33*, 5073.

[24] J. Liu, Y. Zhao, H. Chen, Z. Zhang, W. Zhang, X. Zhu, *React. Funct. Polym.***2017**, *121*, 76.

[25] R. Jagarapu, S. Maddala, I. Mahto, P. Venkatakrishnan, *Asian J. Org. Chem.***2020**, *9*, 2144.

[26] K. Higashiguchi, H. Yotsuji, K. Matsuda, *Chem. Lett.***2017**, *46*, 1564.

[27] M. Irie, T. Lifka, S. Kobatake, N. Kato, *J. Am. Chem. Soc.***2000**, *122*, 4871.

[28] R. Liu, Y. Yang, Q. Cui, W. Xu, R. Peng, L. Li, *Chem. - A Eur. J.***2018**, *24*, 17756.

[29] D. Becker, N. Konnertz, M. Böhning, J. Schmidt, A. Thomas, *Chem. Mater.***2016**, *28*, 8523.

[30] G. L. Gibson, D. Gao, A. A. Jahnke, J. Sun, A. J. Tilley, D. S. Seferos, *J. Mater. Chem. A***2014**, *2*, 14468.

[31] U. Koldemir, S. R. Puniredd, M. Wagner, S. Tongay, T. D. McCarley, G. D. Kamenov, K. Müllen, W. Pisula, J. R. Reynolds, *Macromolecules***2015**, *48*, 6369.

[32] M. Irie, T. Eriguchi, T. Takada, K. Uchida, *Tetrahedron***1997**, *53*, 12263.

[33] M. Irie, T. Fukaminato, K. Matsuda, S. Kobatake, *Chem. Rev.***2014**, *114*, 12174.

[34] Y. C. Jeong, D. G. Park, E. Kim, S. I. Yang, K. H. Ahn, *Macromolecules***2006**, *39*, 3106.

[35] M. El Gemayel, K. Börjesson, M. Herder, D. T. Duong, J. A. Hutchison, C. Ruzié, G. Schweicher, A. Salleo, Y. Geerts, S. Hecht, E. Orgiu, P. Samorì, *Nat. Commun.***2015**, *6*, 1.

[36] R. Kanai, E. Itoh, *Thin Solid Films***2014**, *554*, 127.

[37] K. Higashiguchi, K. Matsuda, S. Kobatake, T. Yamada, T. Kawai, M. Irie, *Bull. Chem. Soc. Jpn.***2000**, *73*, 2389.

[38] H. Jean-Ruel, R. R. Cooney, M. Gao, C. Lu, M. A. Kochman, C. A. Morrison, R. J. D. Miller, *J. Phys. Chem. A***2011**, *115*, 13158.

[39] J. Buntine, E. Carrascosa, J. N. Bull, G. Muller, U. Jacovella, C. Glasson, G. Vamvounis, E. Bieske, *Phys. Chem. Chem. Phys.***2022**, *24*, 16628.

[40] A. P. Kulkarni, X. Kong, S. A. Jenekhe, *J. Phys. Chem. B***2004**, *108*, 8689.

[41] Y. Honmou, S. Hirata, H. Komiyama, J. Hiyoshi, S. Kawauchi, T. Iyoda, M. Vacha, *Nat. Commun.***2014**, *5*, 1.

CHAPTER 7

CONCLUSION AND FUTURE WORK

7.1.General summary and conclusions

The aim of this work was to understand design requirements of photochromic molecules and their potential application in organic electronics. Four independent projects were undertaken, each exploring different themes regarding synthesis and application of photochromic compounds. Each project is presented as an independent chapter.

In the first project **(Chapter 3),** the focus was to improve morphological stability, thermal and optical properties of solar cell blends (P3HT:PCBM)using photochromic additives: 1,3,3-Trimethylindolino-6'-nitrobenzopyrylospiran, azobenzene and 1,2-bis(2,5-dimethyl-3-thienyl)perfluorocyclopentene. Various concentrations of photochromic additives ranging from 0.5%-2.0% (wt.%) were added into P3HT: PCBM (1:1 wt.%) blend. Films were prepared and characterized by UV-Vis spectroscopy, atomic force microscopy (AFM), X-ray diffractometry (XRD) and differential scanning calorimetry (DSC) to study their absorption, morphology, crystallinity and thermal stability. It was envisioned that photochromic additive would interact with P3HT and PCBM through intermolecular π-π interactions and facilitate ordered molecular arrangements, enhance absorptivity and photostability of OSC blends. Results showed that addition of photochromic additives (notably with the spiropyran) decreases the glass transition and melting temperatures implying that these molecules have plasticizing effects. Furthermore, addition of photochromic additives reduced the crystallinity of the active layer which is detrimental for solar cell stability and performance. No photochromic behavior was observed upon irradiating the blends with UV and visible light. This could be attributed to low photochromic additive concentration in the blend. These challenges motivated the development of mainchain photochromic polymers.

The goal of the second project **(Chapter 4)** was to develop synthetic strategies to produce solution-processable mainchain photochromic polymers. The study further explored the effect of alkyl chain length on polymer properties. Polymer syntheses were attempted using various methods such as direct arylation, Stille coupling, and Suzuki-Miyaura cross-coupling polycondensation reactions. Higher molecular weights were obtained from Suzuki-Miyaura cross-coupling reactions between 5-bromo-3-[2-(5-bromo-2-methyl-3-thienyl)-3,3,4,4,5,5-hexafluoro-1-cyclopenten-1-yl]-2-methylthiophene and the corresponding diboronic acid bis(pinacol) esters. A series of alternating copolymers of a dithienylethene with di-*n*-alkyl-fluorene was synthesized and their properties were investigated as a function of alkyl chain length. All the polymers were photoswitchable in both solution and solid state. Photoswitching quantum yields were similar regardless of alkyl chain length. The glass transition temperature of the polymers decreased as the length of the alkyl chain increases due to internal plasticization. The polymer with the shortest alkyl chains had the roughest surface while those with longer alkyl groups resulted in smooth films, which is important for charge transport.

Owing to the successful synthesis of solution processable dithienylethene-*alt*-di-*n*-alkyl-fluorene photochromic polymers there was a need to study the effect of conjugation length on polymer properties. Therefore, the third project **(Chapter 5)** investigated the effect of conjugation length on polymer properties. A series of dithienylethene with di-*n*-hexylphenylene, 9-heptadecanylcarbazole and 4,8-bis(3,5-dioctyl-2-thienyl)-1,5-dithia-*s*-indacene were designed and synthesized by Suzuki-

Miyaura polycondensation reactions. All the polymers were soluble in common organic solvents.All the polymers were thermally stable and showed no signs of photo-degradation after being exposed to UV-light for 120 min in air. The color of the photochromic polymer was tuned according to the comonomer and the maximum absorption wavelength ranged from 569 to 675 nm in the closed isomeric form. It was found that the conjugation length could be controlled to match the specific light source required for the application.

Organic electronic devices require printing/patterning. Therefore, it is crucial to develop materials which can be easily printed or patterned. The fourth and last project (**Chapter 6**) focussed on the design and synthesis of a patternable diarylethene-based photochromic polymer. A mainchain photochromic polymer bearing THP side chains was successfully synthesized by Suzuki-Miyaura polycondensation reaction between 2-Bis(5′-bromo-2′-methylthien-3′-yl)hexafluoro- cyclopent-1-ene and 9,9-bis(2-(2-tetrahydropyranyloxy)ethyl)-fluorene-2,7-diboronic acid bis(pinacol) ester. The polymer was photoswitchable in both solution and solid state. This polymer undergoes, solid state acid-catalyzed removal of THP groups and volatilization as dihydropyran. The removal of the THP groups reduces the length of side chains and causes the formation of terminal hydroxyl groups, thus changing the polarity of the polymer. This causes the polymers to become insoluble thus allowing spatially controlled patterning using chemically amplified soft lithography. The photochromic behavior is retained after deprotection. This polymer may be useful for the fabrication of multi-functional and photoswitchable organic microelectronic devices.

7.2.Future directions

7.2.1. Synthesis methods

It is still a challenge to synthesize mainchain diarylethene-based photochromic polymers with high molecular weights. The highest molecular weight reported so far is M_n=11 600 and M_w=25 000.[1] Molecular weight depends on the type of polymerization reaction which is governed by the functional groups of the reacting monomers. In this study, high molecular weights were obtained when using Suzuki-Miyaura polycondensation reactions between a photochromic dibromide monomer and corresponding boronic esters. Efforts to prepare boronic esters and stannyl-based photochromic units were unsuccessful as the compounds degraded under ambient conditions. Future projects should focus on designing comonomers which can be polymerized with the switching unit to yield mainchain photochromic polymers with high molecular weights.

7.2.2. Low-band gap photochromic polymers for potential application in "smart" solar cells

Low-band polymers which absorb in the near infrared (NIR) region are highly desirable for solar cell applications. Traditional solar cell materials such as P3HT and PCBM could only absorb light up to 650 nm of the electromagnetic spectrum resulting in power conversion efficiencies less than 5%. However, infrared (IR) absorption profiles possess 52% of total energy in the solar spectrum. Harvesting low-energy but abundant IR photons leads to higher short-circuit current density (J_{SC}) and power conversion efficiencies in photovoltaic cells.[2,3] Smart photovoltaic cells with the ability to simultaneously tint, provide shade, power and aesthetical appearance are promising energy sources for building integrated photovoltaics and greenhouses. NIR diarylethene-based mainchain photochromic polymer are ideal materials for fabricating such devices. Extending the conjugation lengths of some of the photochromic polymers reported in Chapter 5 could result in diarylethene-based mainchain polymers which absorb in the NIR. Polymer structures shown in **Figure 7.1** have been designed. Synthesis will commence soon within our group.

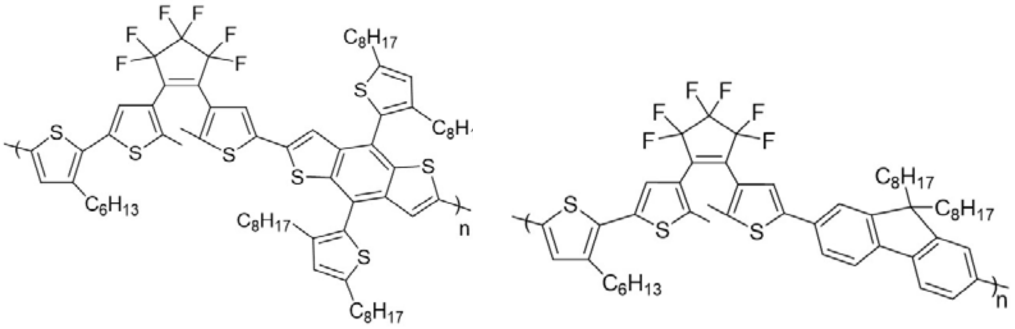

Figure 7.1: Proposed chemical structures of low band-gap mainchain diarylethene-based photochromic polymers.

7.2.3. Diketopyrrolopyrrole-based photochromic polymers for ambipolar OFETs

Diketopyrrolopyrrole-based conjugated polymers have attracted interest in the development of OFETs. Interestingly, this type of semiconductor exhibits ambipolar characteristics. Ambipolar semiconducting polymers characterized by both high electron (μ_e) and hole (μ_h) mobility, and narrow energy gaps offer the advantage of realizing complex complementary electronic circuits with a single semiconducting layer. Current reports on photoswitchable ambipolar transistors involve dispersing photochromic molecules in the semiconducting polymer as dopants, unfortunately, the dopant degrades the host polymer's properties. Low-band gap mainchain photochromic polymers with high μ_e and (μ_h) mobility could enable fabrication of photoswitchable ambipolar transistors with a single semiconducting layer. With this in mind, a low band-gap diarylethene-*alt*-diketopyrrolopyrrole-based polymer was designed (**Figure 7.2**). Its photochromic behavior and performance in ambipolar transistor devices will be investigated. This work is currently underway in collaboration with Professor Prashant Sonar's group at the Queensland University of Technology.

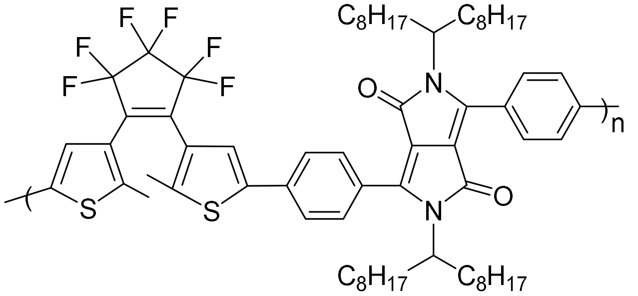

Figure 7.2: Proposed chemical structure of a diarylethene-*alt*-diketopyrrolopyrrole photochromic polymer.

7.3.References

[1] C. Bertarelli, A. Bianco, V. Boffa, M. Mirenda, M. C. Gallazzi, G. Zerbi, *Adv. Funct. Mater.***2004**, *14*, 1129.

[2] D. Meng, R. Zheng, Y. Zhao, E. Zhang, L. Dou, Y. Yang, *Adv. Mater.***2022**, *34*, 2107330.

[3] E. Zhou, K. Hashimoto, K. Tajima, *Polyme.***2013**, *54*, 6501.

APPENDICES

Supplementary figures for chapter 3

Thermogravimetric analysis (TGA) of materials used in chapter 3

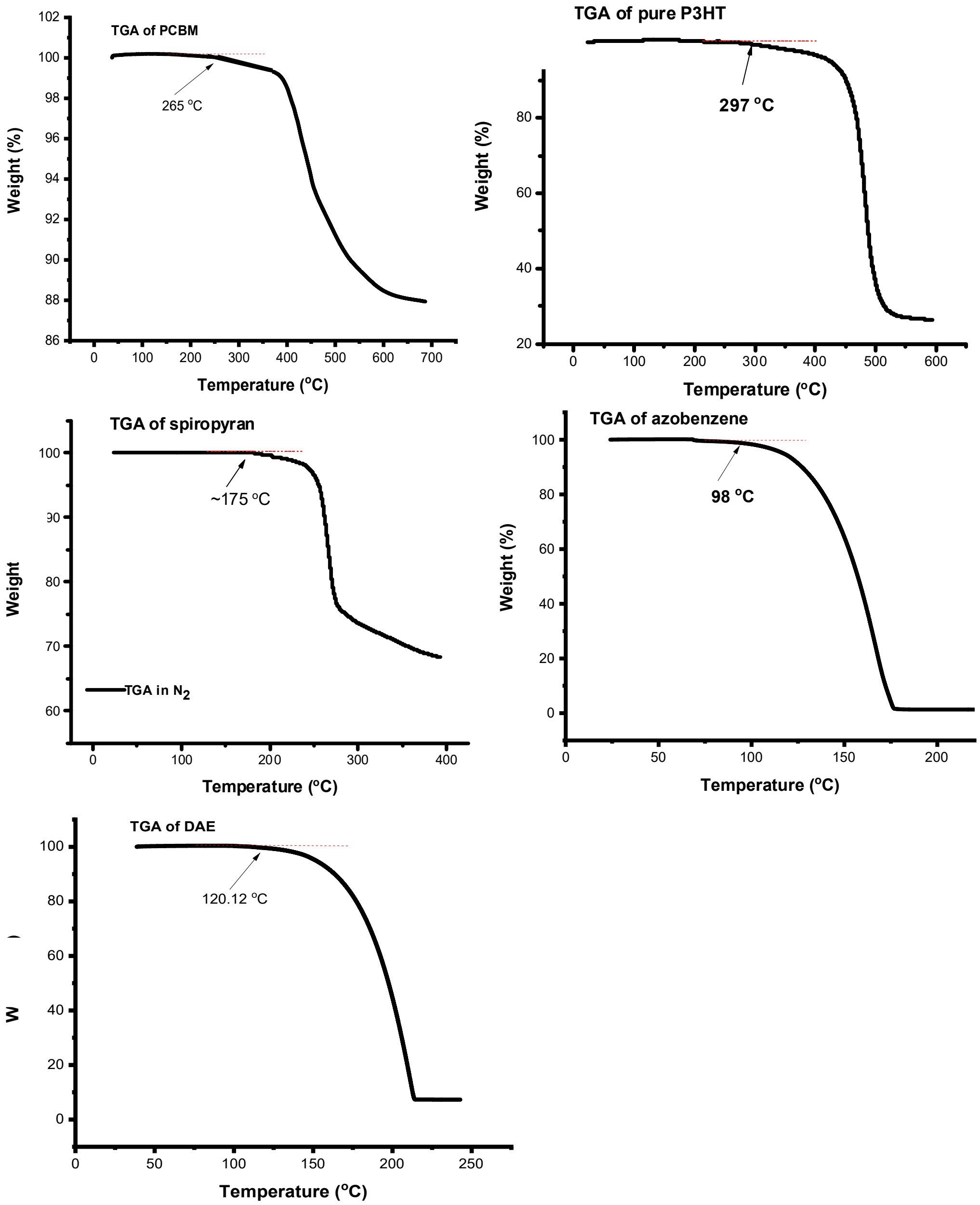

Figure S3.1: Thermogravimetric analysis (TGA) of pure PCBM (a), P3HT (b), Spiropyran (c), Azobenzene (d) and DAE (e).

Differential Scanning Calorimetry (DSC) analysis of materials used in Chapter 3

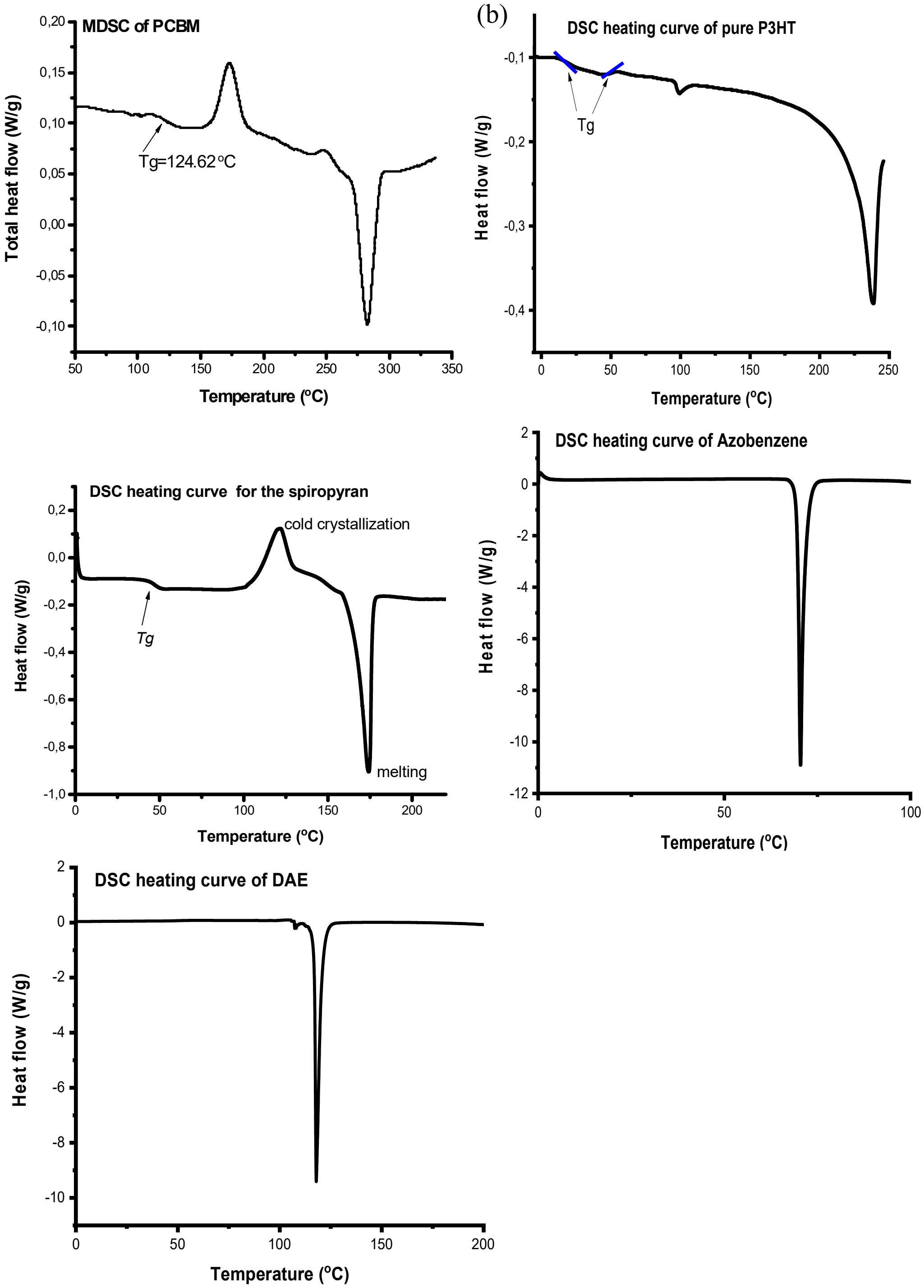

Figure S3.2:MDSC heating curves of pure PCBM (a), DSC heating curves of P3HT (b), Spiropyran (c), Azobenzene (d) and DAE (e).

Atomic force microscope images of blends processed with various additives

(a)

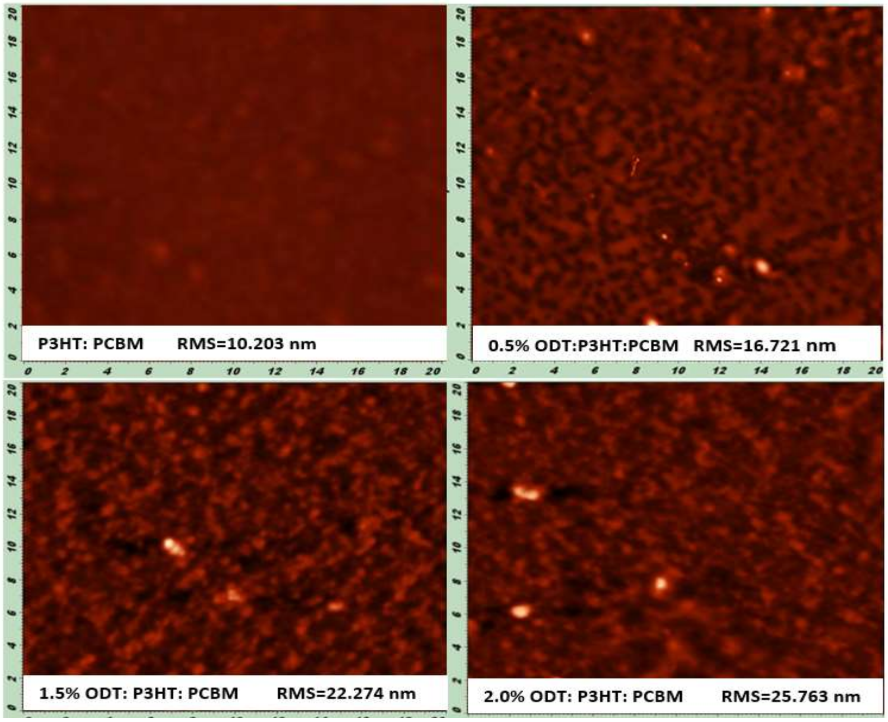

(b)

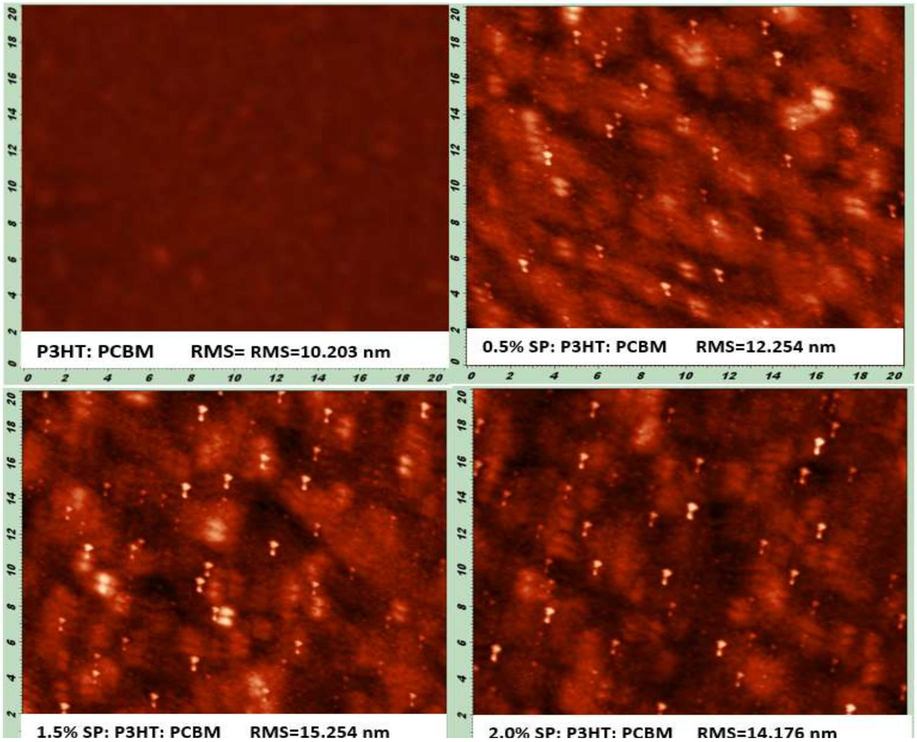

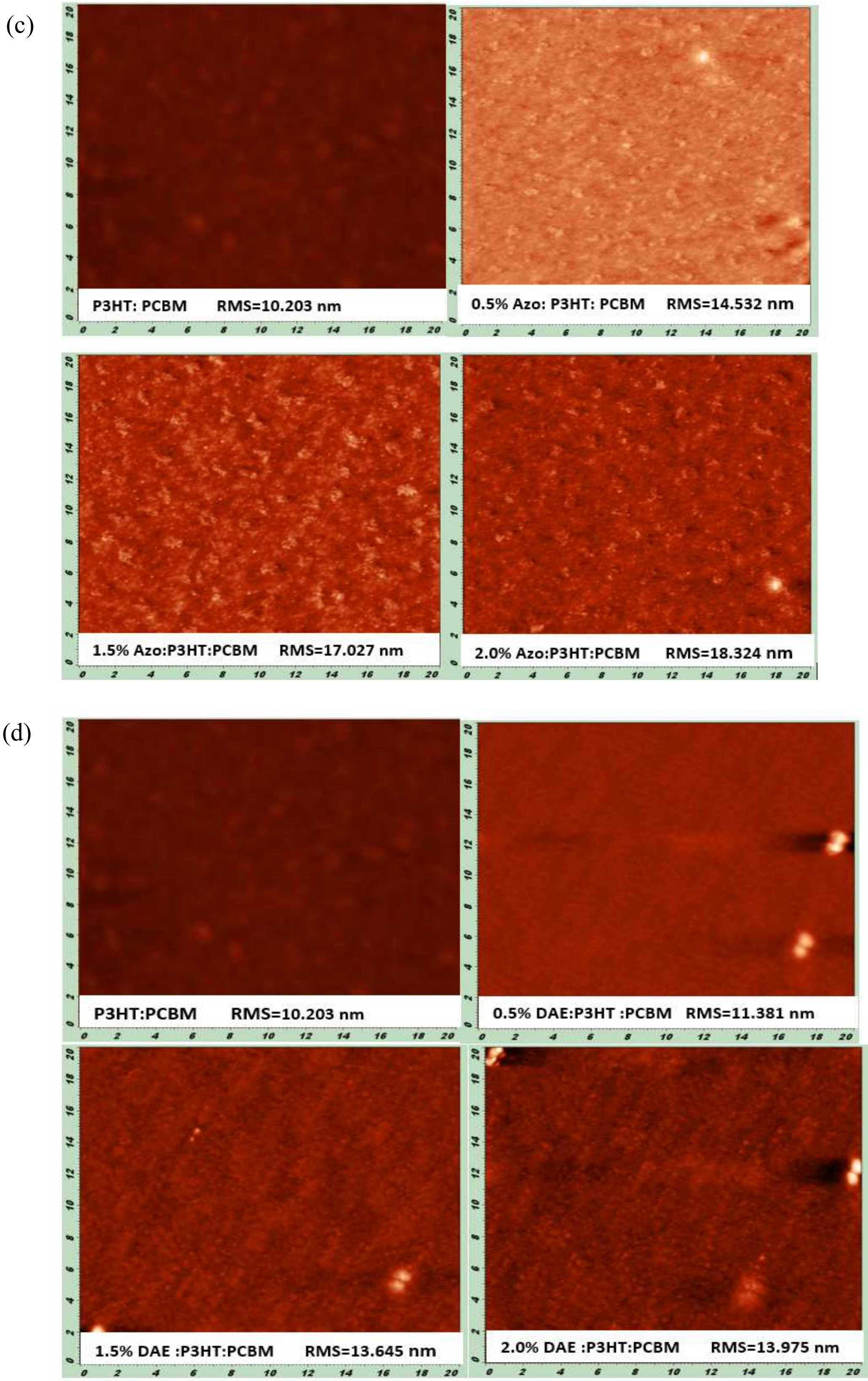

Figure S3.3:AFM images ofP3HT:PCBM blends processed with ODT (a), SP (b), Azo (c), DAE (d).

Absorption properties of pure photochromes in solution and solid states

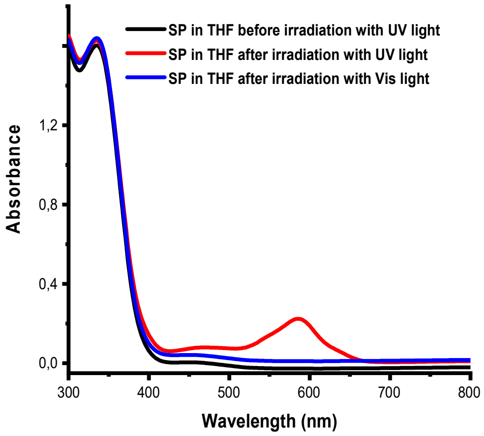

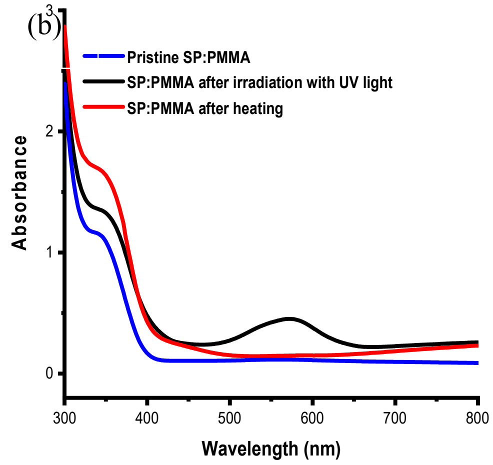

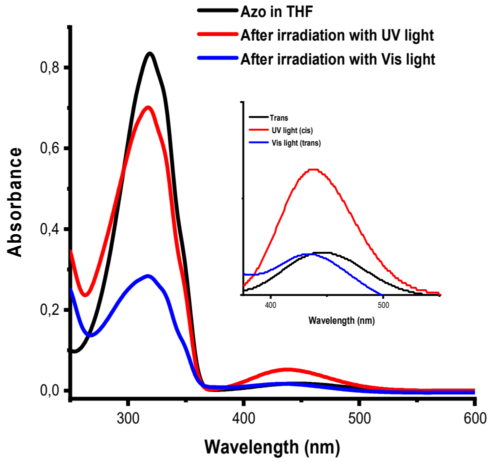

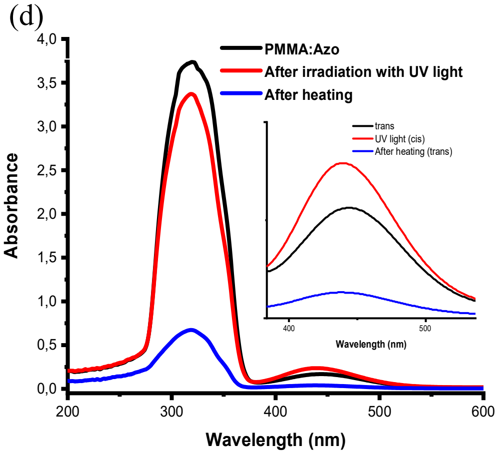

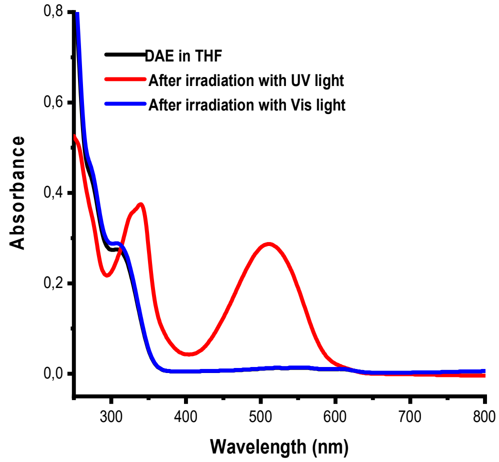

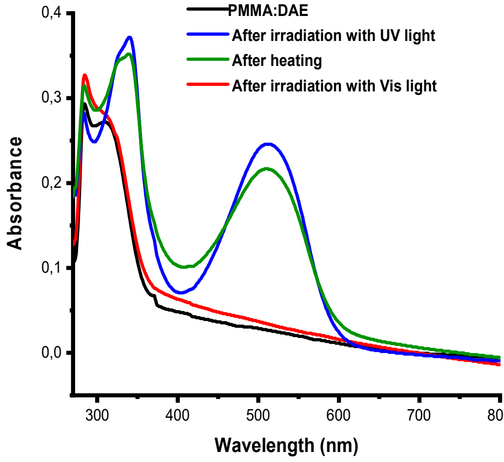

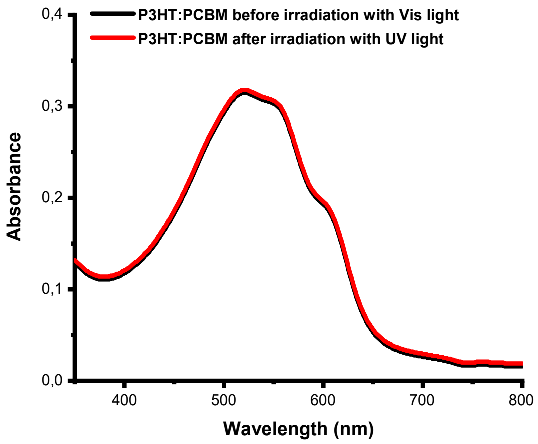

Figure S3.4: Solution and solid-state absorption properties of the spiropyran (a and b), azobenzene (c and d), diarylethene (e and f), P3HT: PCBM (g) upon irradiation with UV and Vis light.

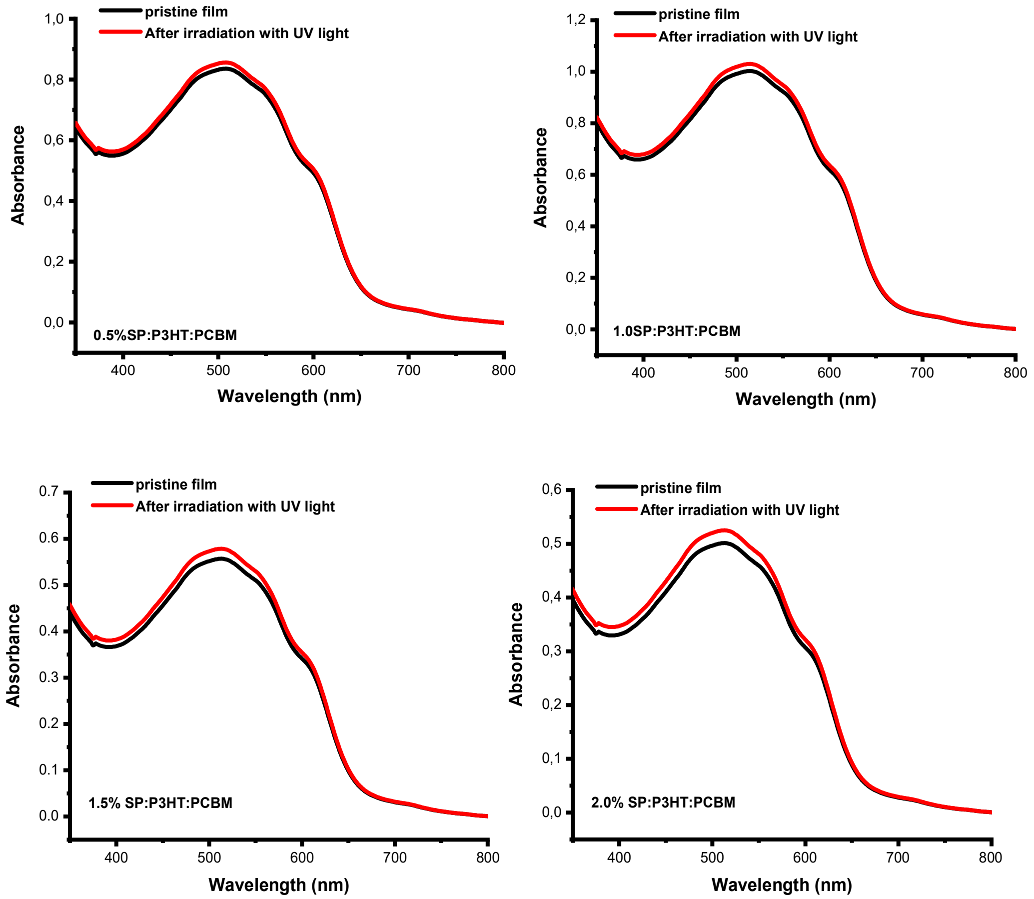

Figure S3.5: Absorption spectra of P3HT: PCBM blends processed with various amounts of SP additive.

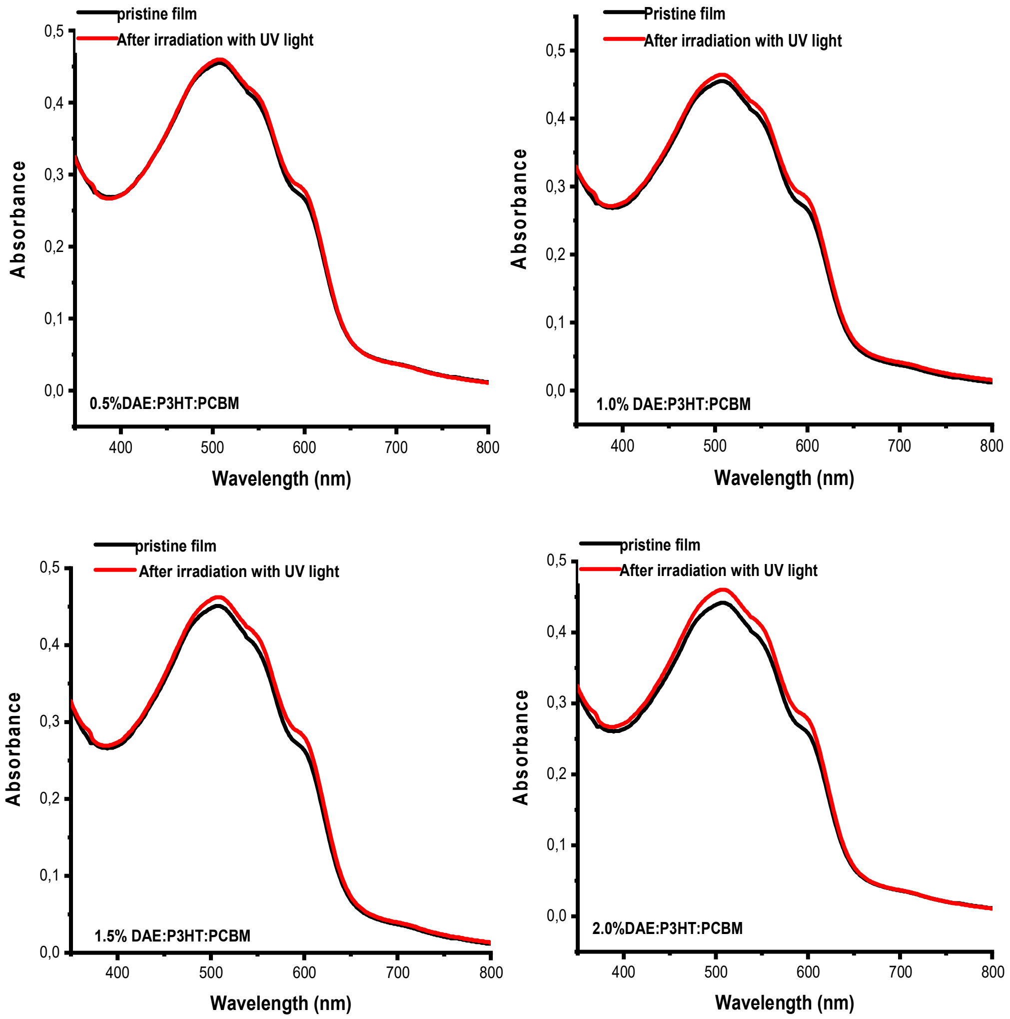

Figure S3.6: Absorption spectra of P3HT: PCBM blends processed with various amounts of DAE additive.

Supplementaryfigures forchapter 4

Analytical data of 3,5-dibromo-2-methylthiophene

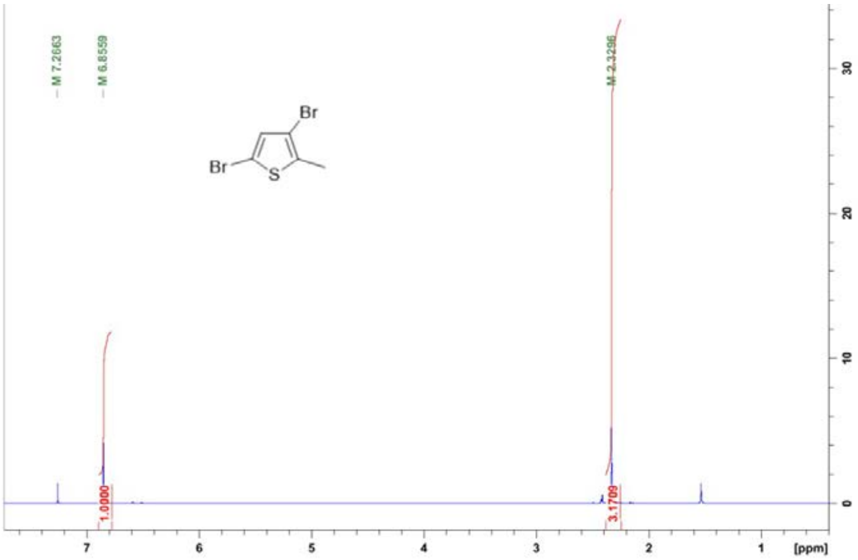

Figure S4.1:^{1}H NMR spectrum of 3,5-dibromo-2-methylthiophene.

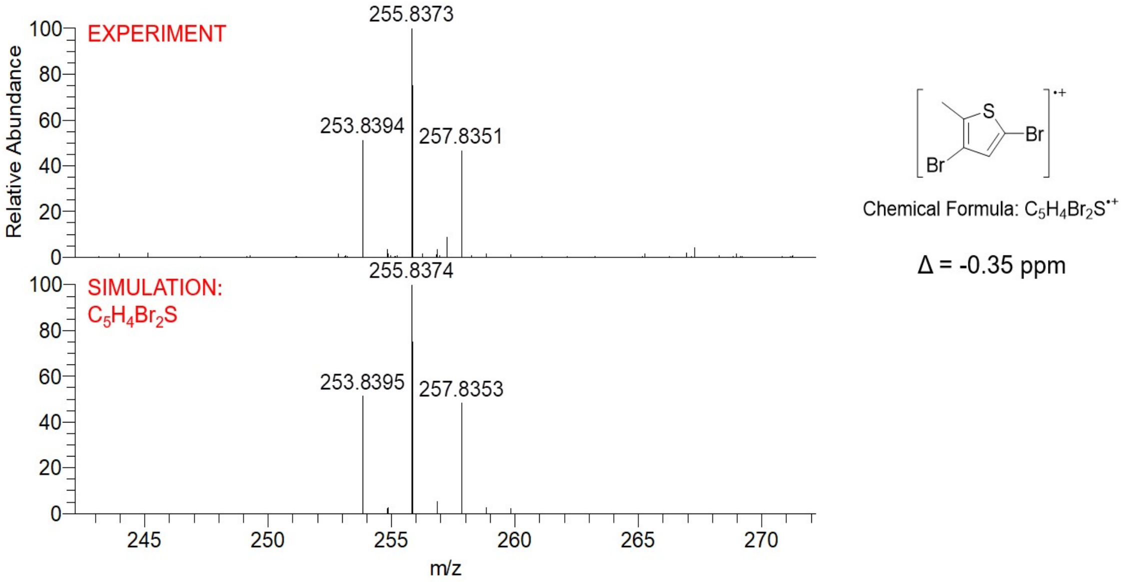

Figure S4.2:MS spectrum of 3,5-dibromo-2-methylthiophene.

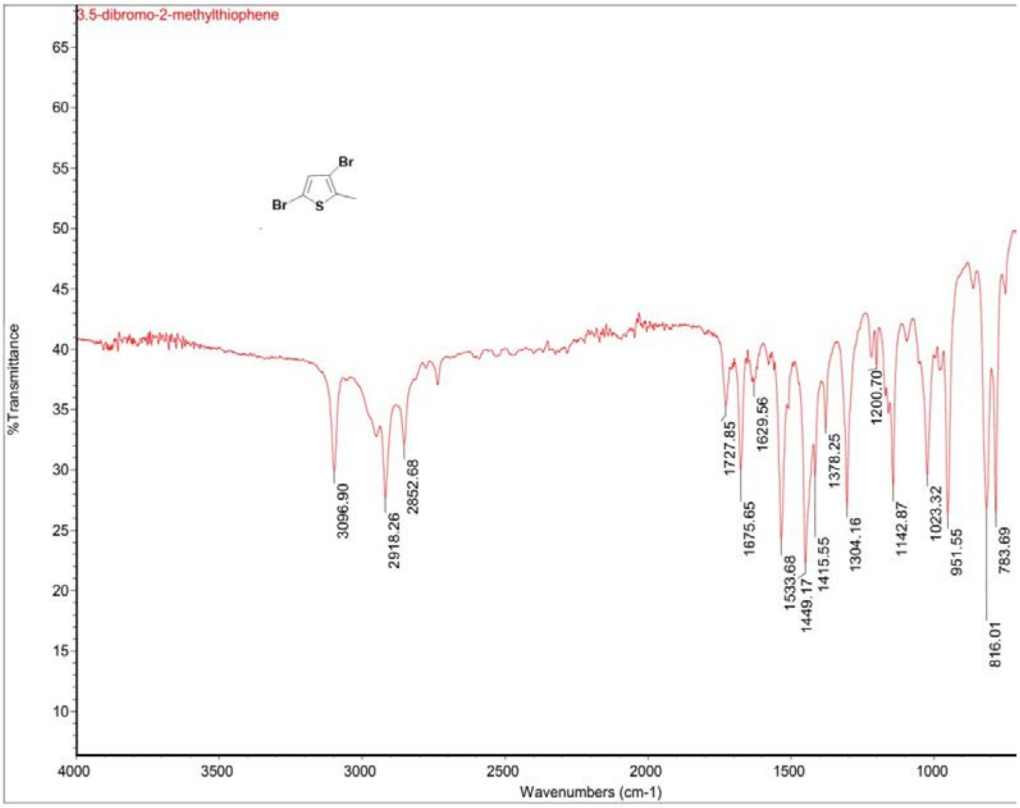

Figure S4.3:FTIR spectrum of 3,5-dibromo-2-methylthiophene.

Analytical data of 3-bromo-2-methyl-5- trimethylsilylthiophene

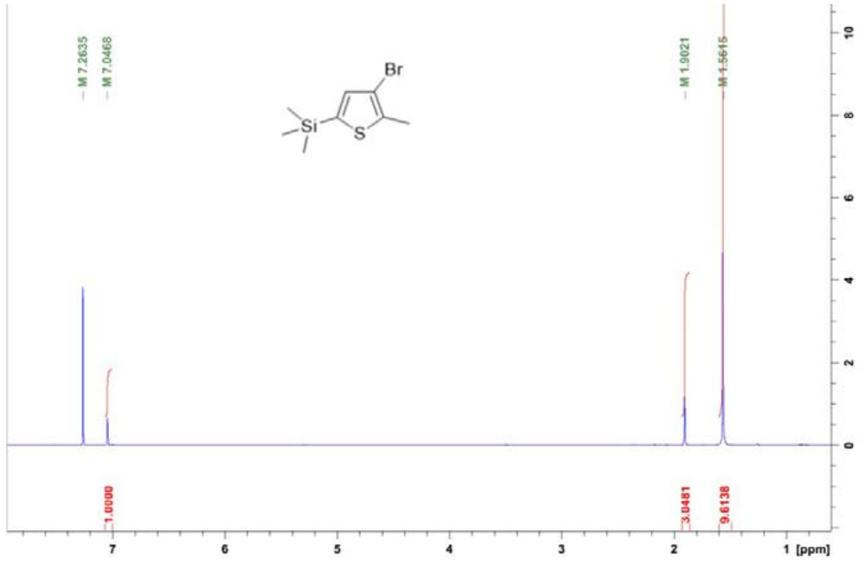

Figure S4.4:^{1}H NMR spectrum of 3-bromo-2-methyl-5- trimethylsilylthiophene.

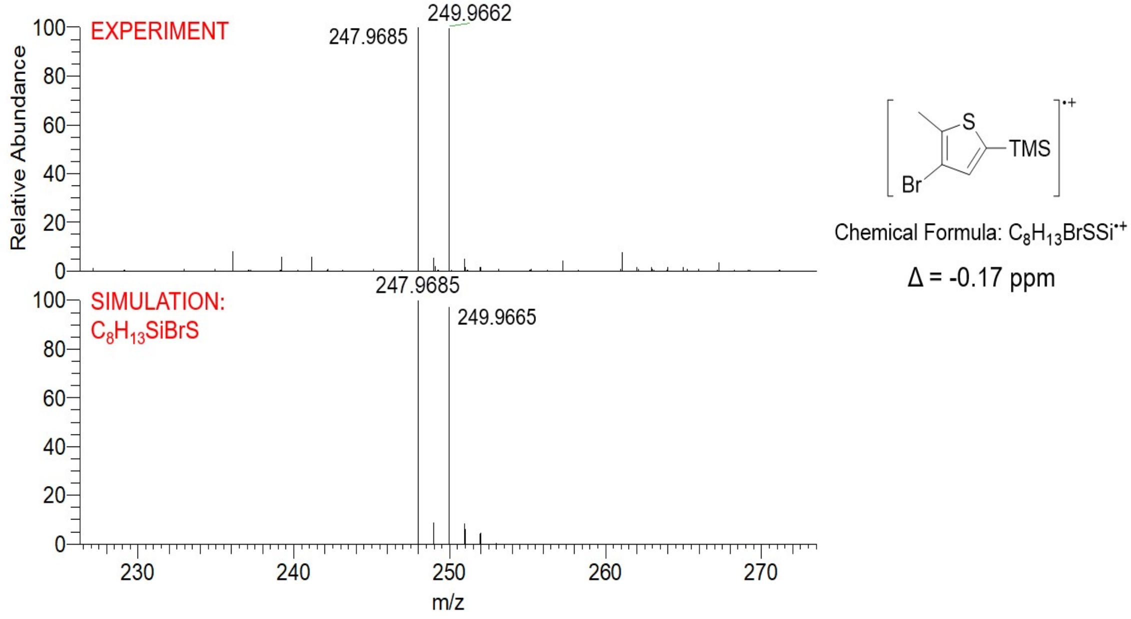

Figure S4.5:MS spectrum of 3-bromo-2-methyl-5- trimethylsilylthiophene.

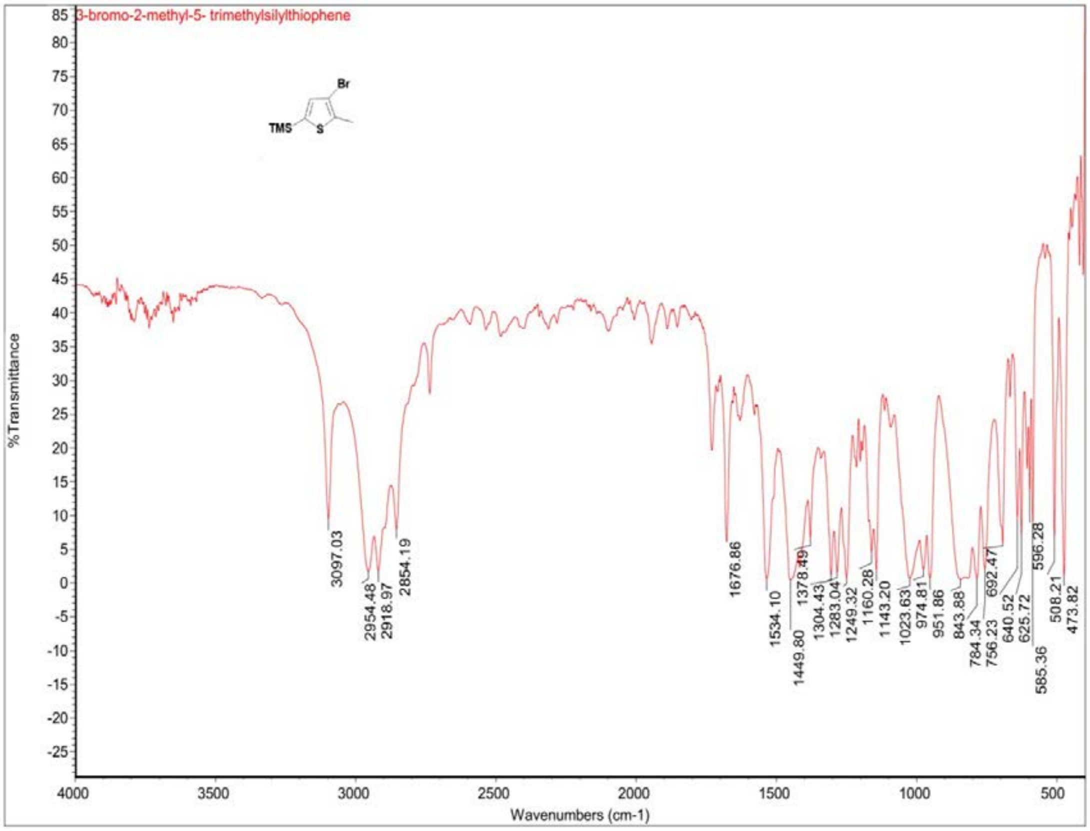

Figure S4.6:FTIR spectrum of 3-b.romo-2-methyl-5- trimethylsilylthiophene.

Analytical data of thiophene, 3,3'-(3,3,4,4,5,5-hexafluoro-1-cyclopentene-1,2-diyl) bis[2-methyl-5-(trimethylsilyl)-

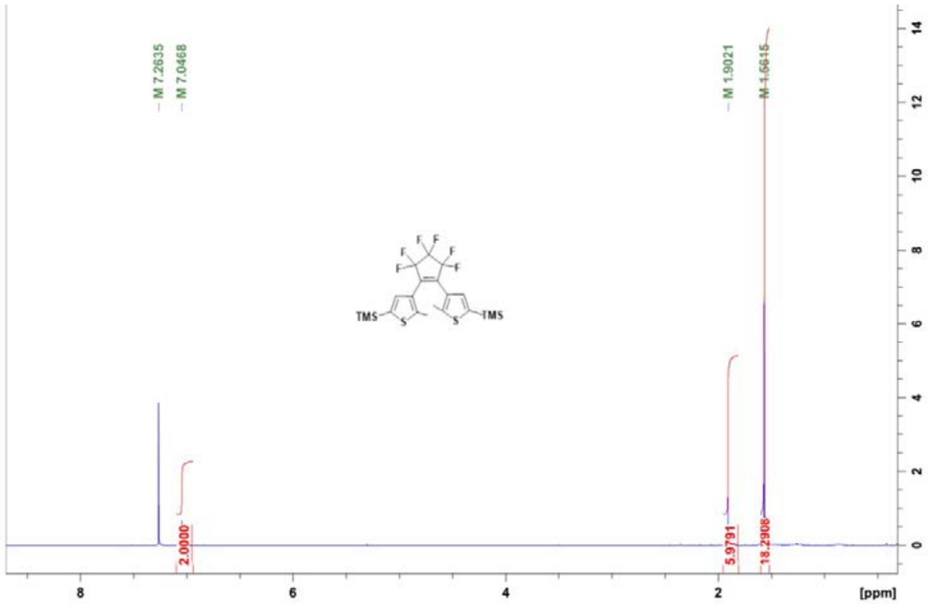

Figure S4.7:^{1}H NMR spectrum of thiophene, 3,3'-(3,3,4,4,5,5-hexafluoro-1-cyclopentene-1,2-diyl) bis[2-methyl-5-(trimethylsilyl)-.

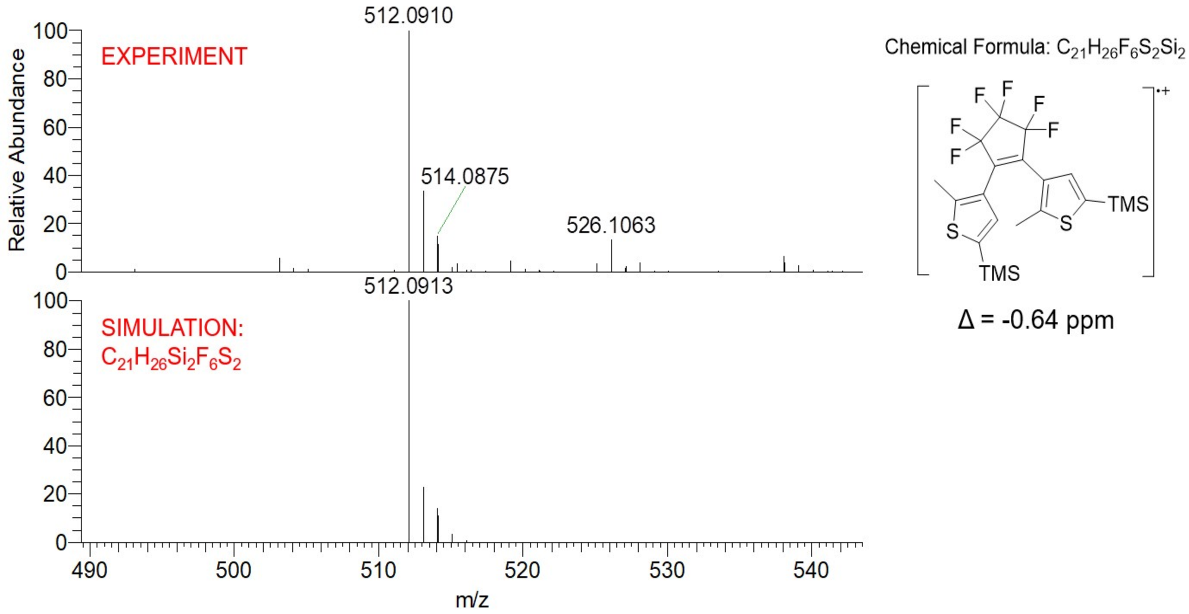

Figure S4.8:MS spectrum of thiophene, 3,3'-(3,3,4,4,5,5-hexafluoro-1-cyclopentene-1,2-diyl)bis[2-methyl-5-(trimethylsilyl)-.

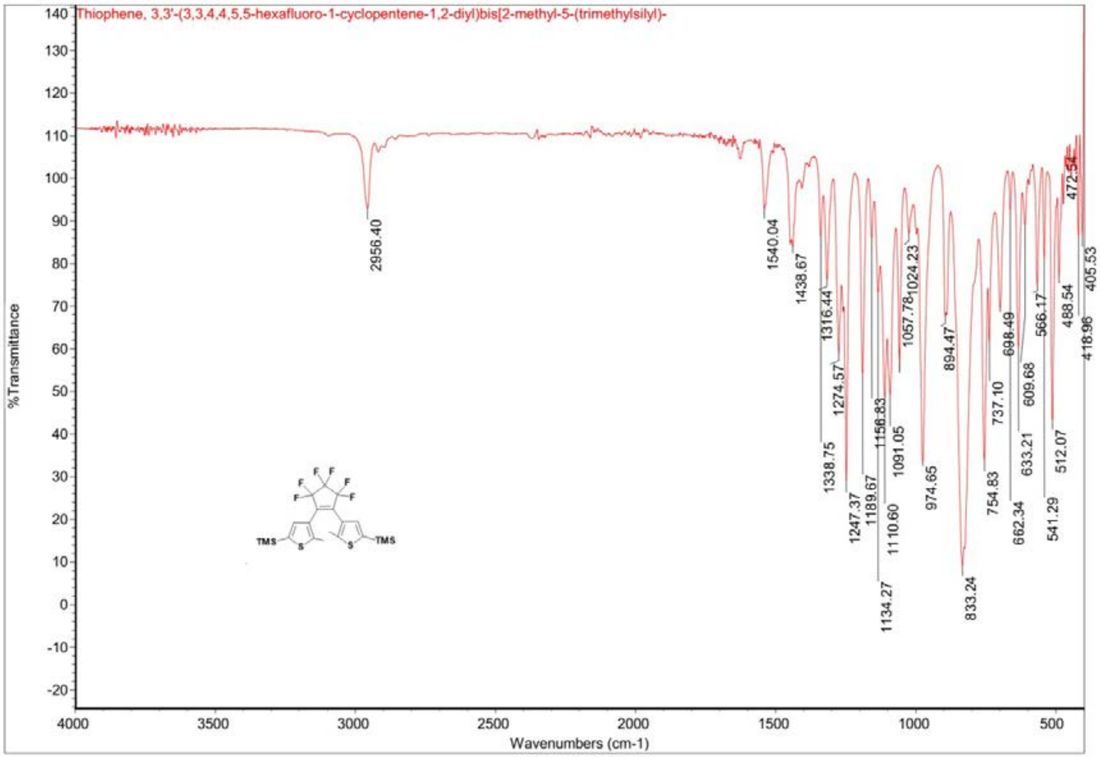

Figure S4.9:FTIR spectrum of thiophene, 3,3'-(3,3,4,4,5,5-hexafluoro-1-cyclopentene-1,2-diyl)bis[2-methyl-5-(trimethylsilyl)-.

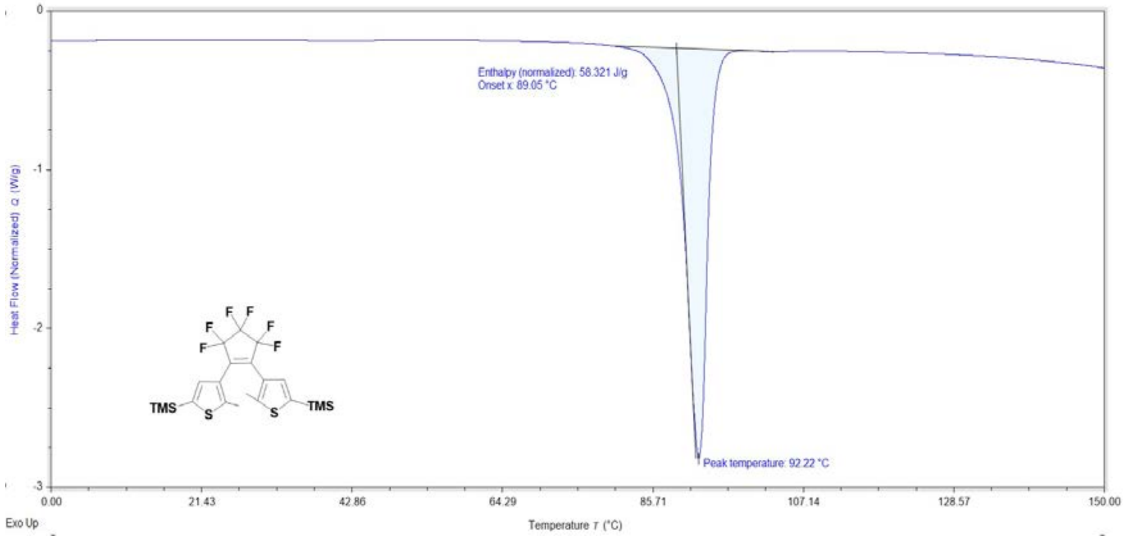

Figure S4.10:DSC heating curve of thiophene, 3,3'-(3,3,4,4,5,5-hexafluoro-1-cyclopentene-1,2-diyl) bis[2-methyl-5-(trimethylsilyl)-.

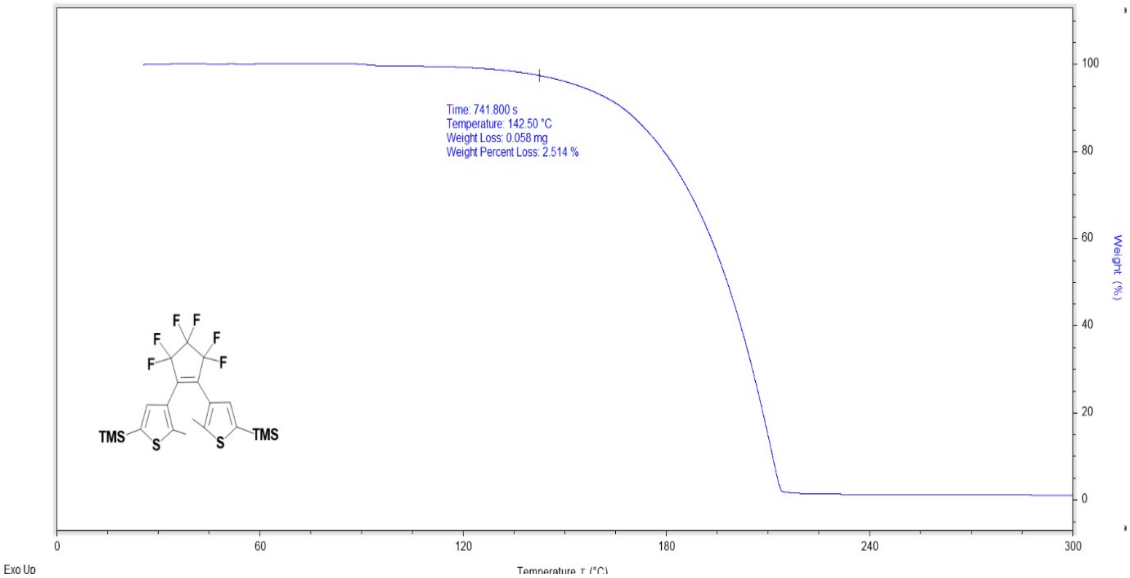

Figure S4.11:TGA thermmogram of thiophene, 3,3'-(3,3,4,4,5,5-hexafluoro-1-cyclopentene-1,2-diyl) bis[2-methyl-5-(trimethylsilyl)-.

Analytical data of 5-bromo-3-[2-(5-bromo-2-methyl-3-thienyl)-3,3,4,4,5,5-hexafluoro-1-cyclopenten-1-yl]-2-methylthiophene

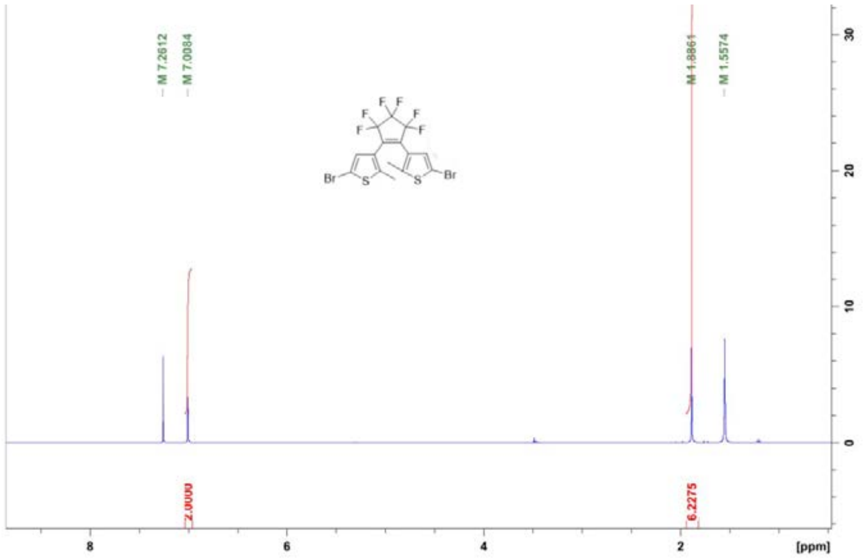

Figure S4.12:^{1}H NMRspectrum of 5-bromo-3-[2-(5-bromo-2-methyl-3-thienyl)-3,3,4,4,5,5-hexafluoro-1-cyclopenten-1-yl]-2-methylthiophene.

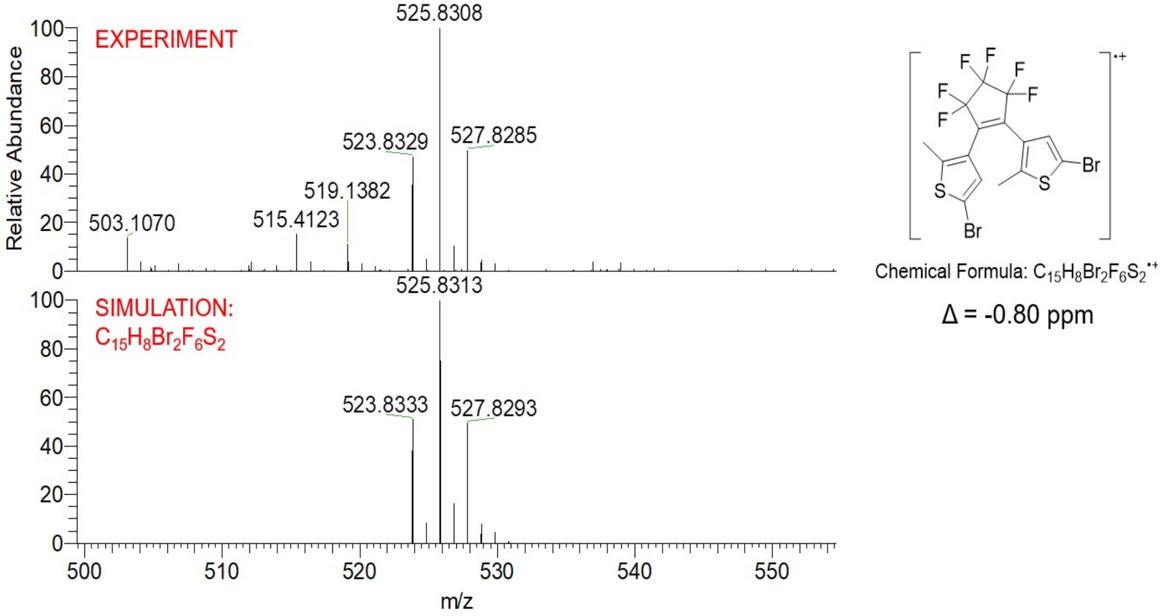

Figure S4.13:MSspectrum of 5-bromo-3-[2-(5-bromo-2-methyl-3-thienyl)-3,3,4,4,5,5-hexafluoro-1-cyclopenten-1-yl]-2-methylthiophene.

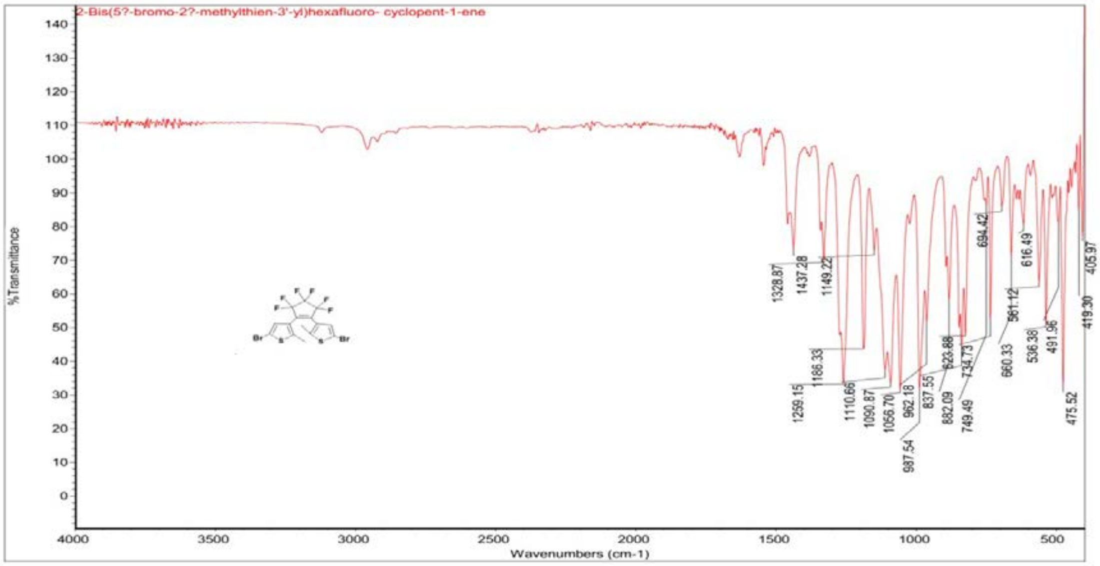

Figure S4.14:FTIRspectrum of 5-bromo-3-[2-(5-bromo-2-methyl-3-thienyl)-3,3,4,4,5,5-hexafluoro-1-cyclopenten-1-yl]-2-methylthiophene.

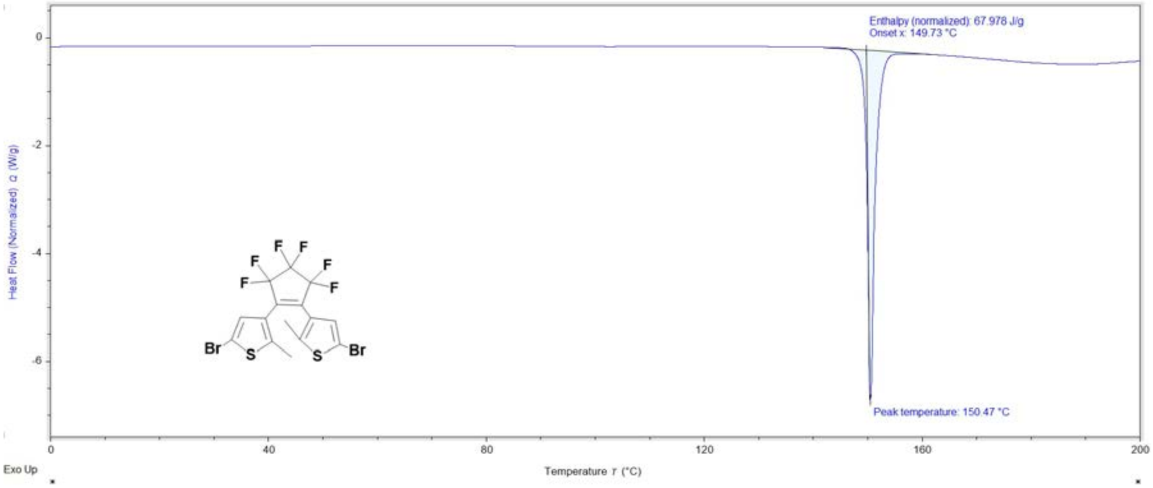

Figure S4.15:DSC heating curve of 5-bromo-3-[2-(5-bromo-2-methyl-3-thienyl)-3,3,4,4,5,5-hexafluoro-1-cyclopenten-1-yl]-2-methylthiophene.

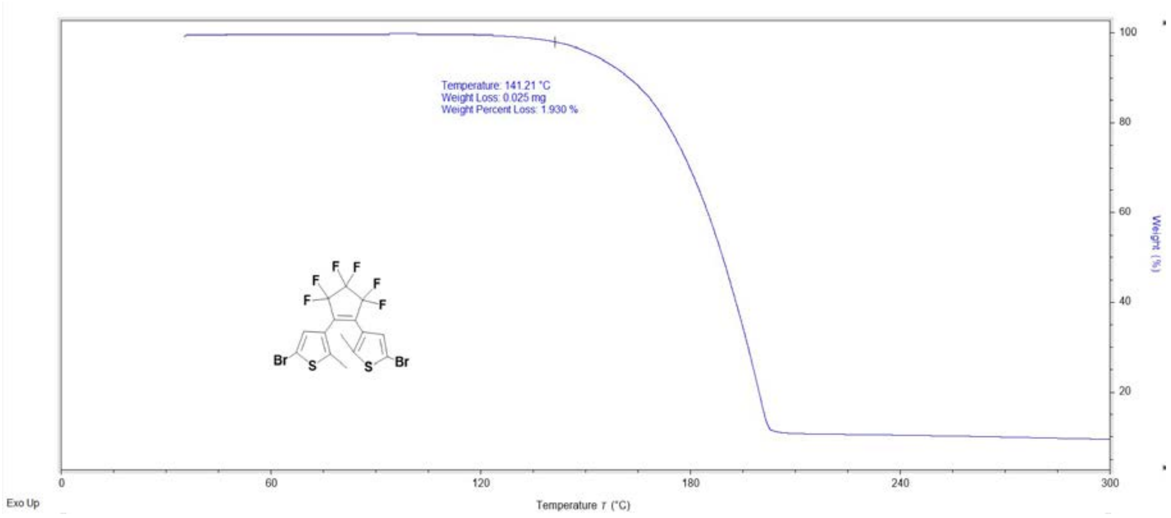

Figure S4.16:TGA thermmogram of 5-bromo-3-[2-(5-bromo-2-methyl-3-thienyl)-3,3,4,4,5,5-hexafluoro-1-cyclopenten-1-yl]-2-methylthiophene.

Analytical data of 2,7-dibromofluorene

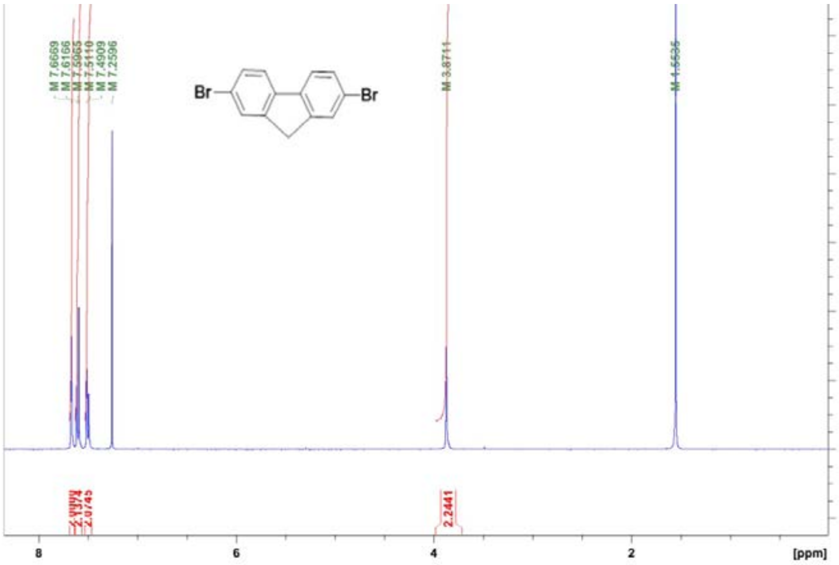

Figure S4.17:1H NMR spectrum of2,7-dibromofluorene.

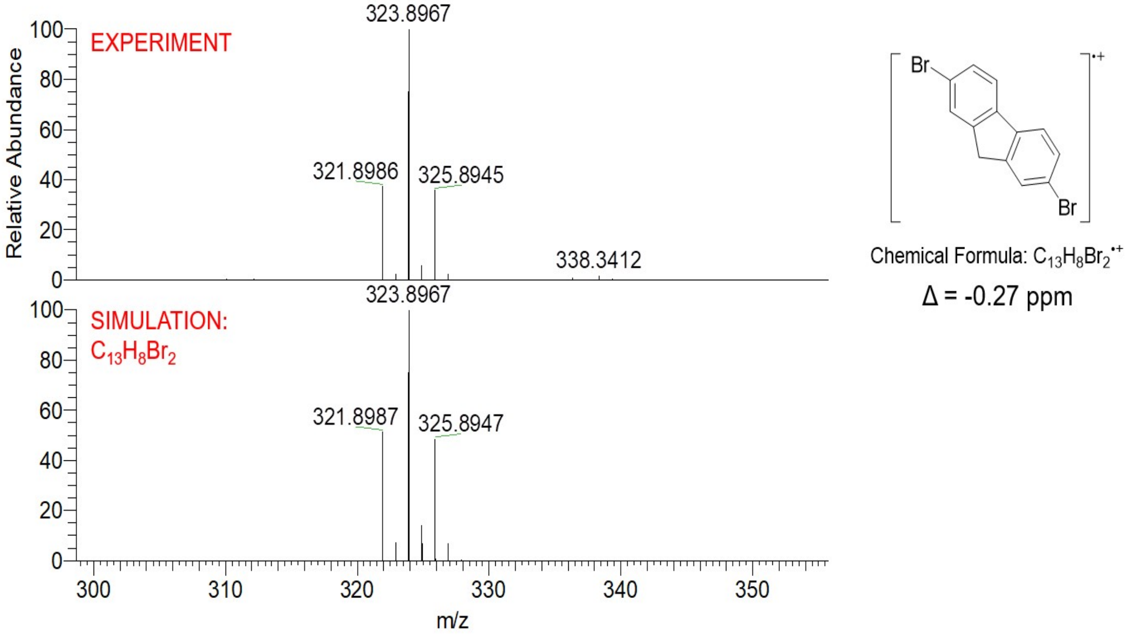

Figure S4.18:MS spectrum of2,7-dibromofluorene.

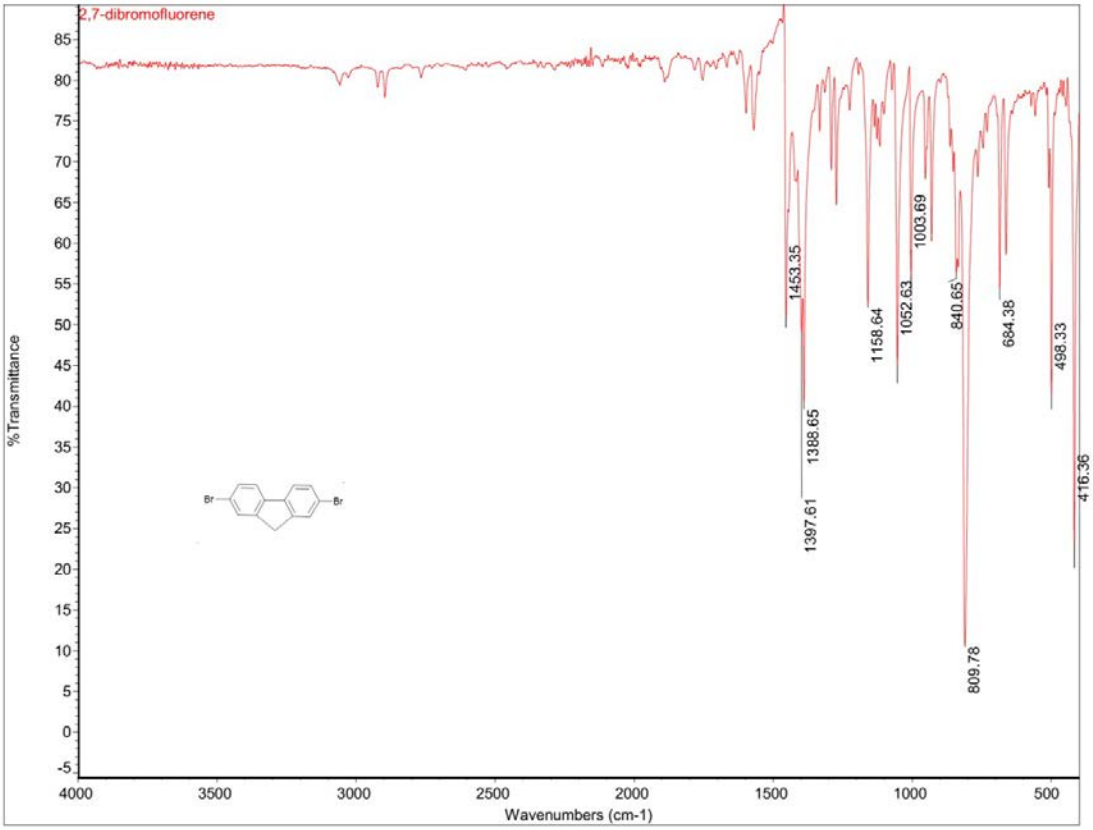

Figure S4.19:FTIR spectrum of2,7-dibromofluorene.

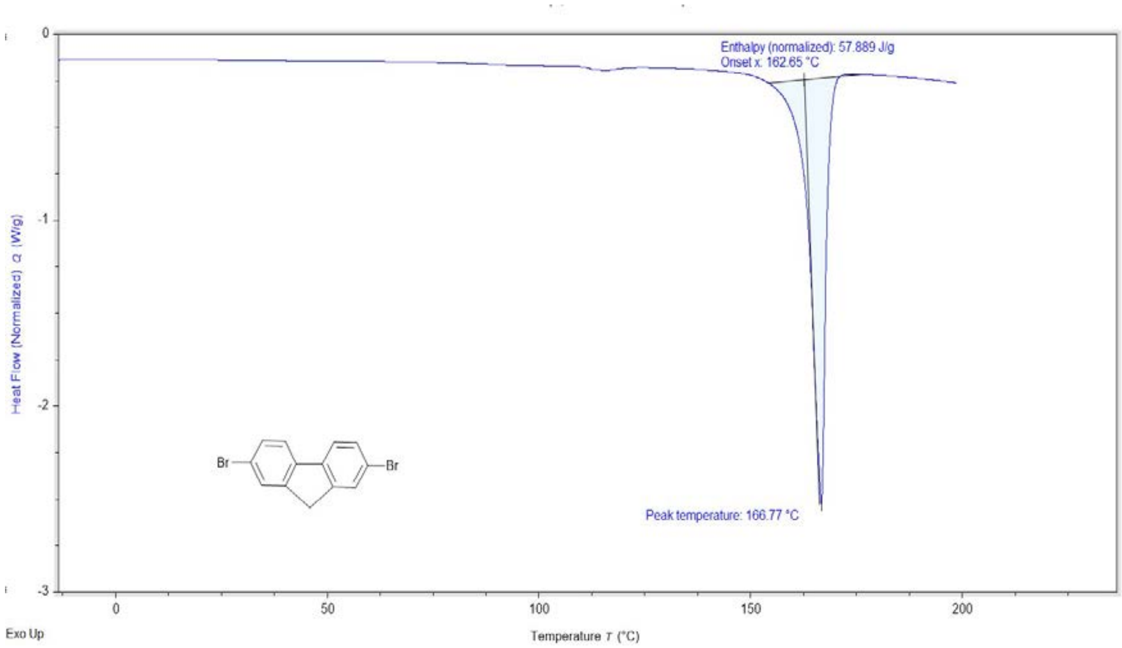

Figure S4.20:DSC heating curve of2,7-dibromofluorene.

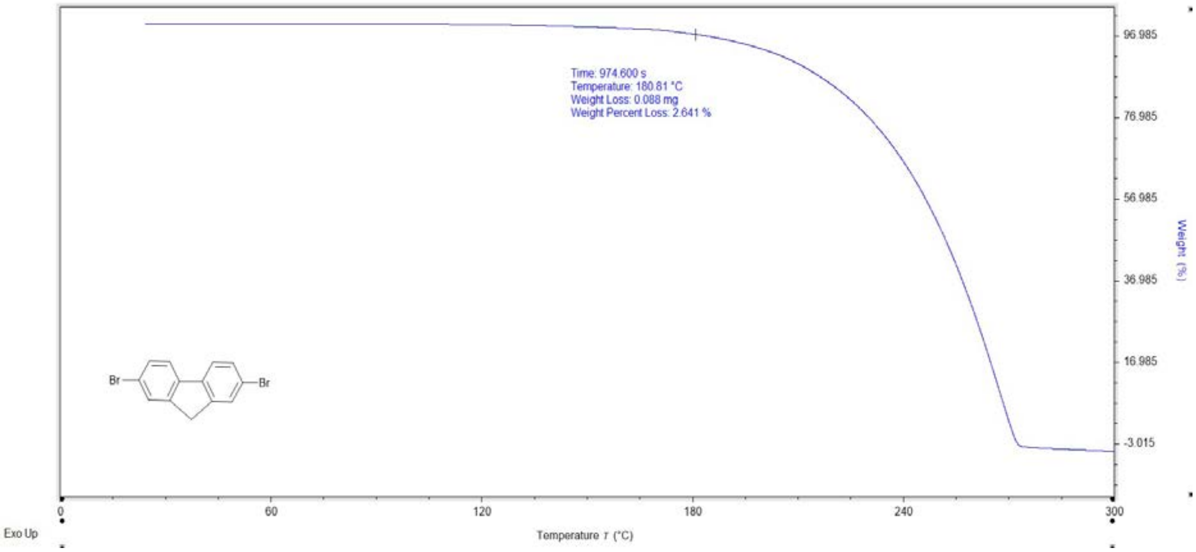

Figure S4.21:TGA thermmogram of2,7-dibromofluorene.

Analytical data of 2,7-dibromo-9,9-dipropylfluorene

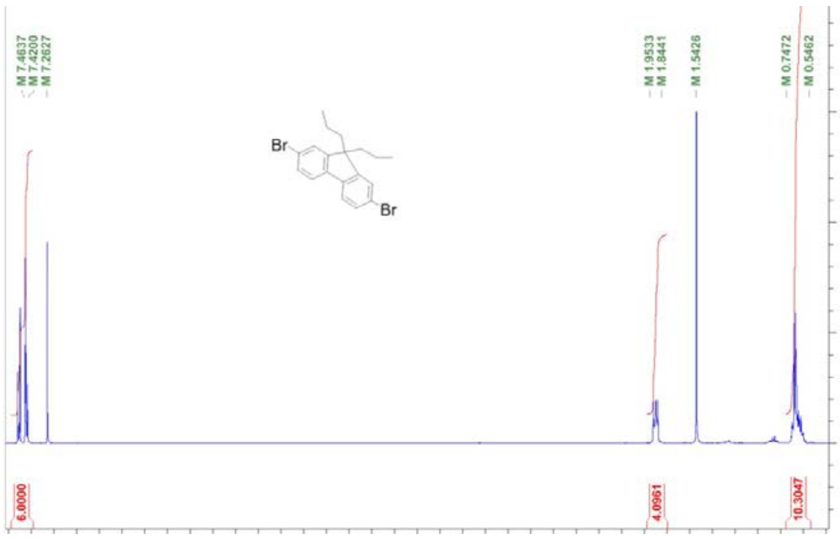

Figure S4.22:^{1}H NMR spectrum of2,7-dibromo-9,9-dipropylfluorene.

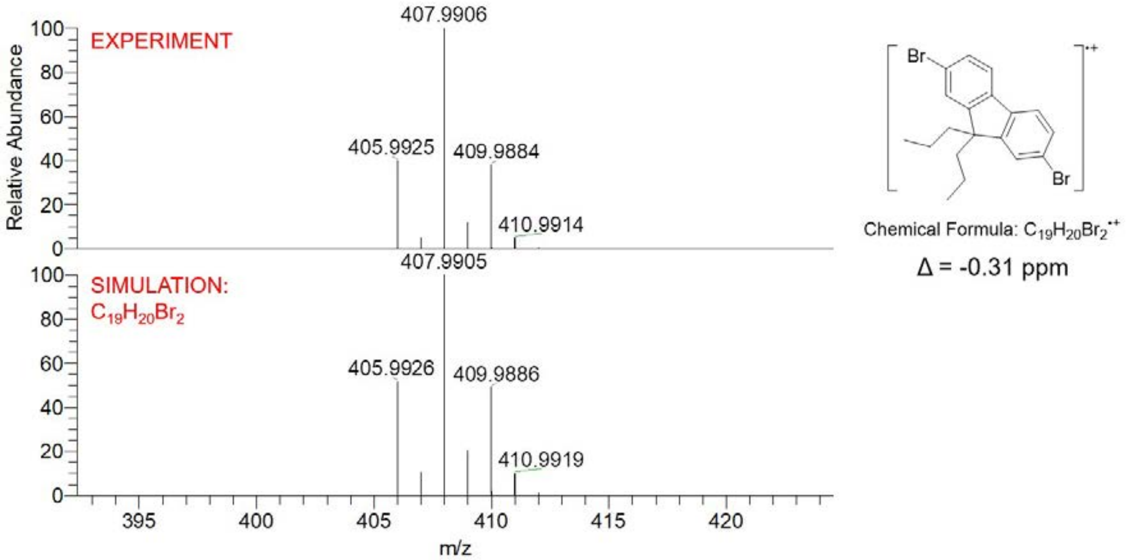

Figure S4.23:MS spectrum of2,7-dibromo-9,9-dipropylfluorene.

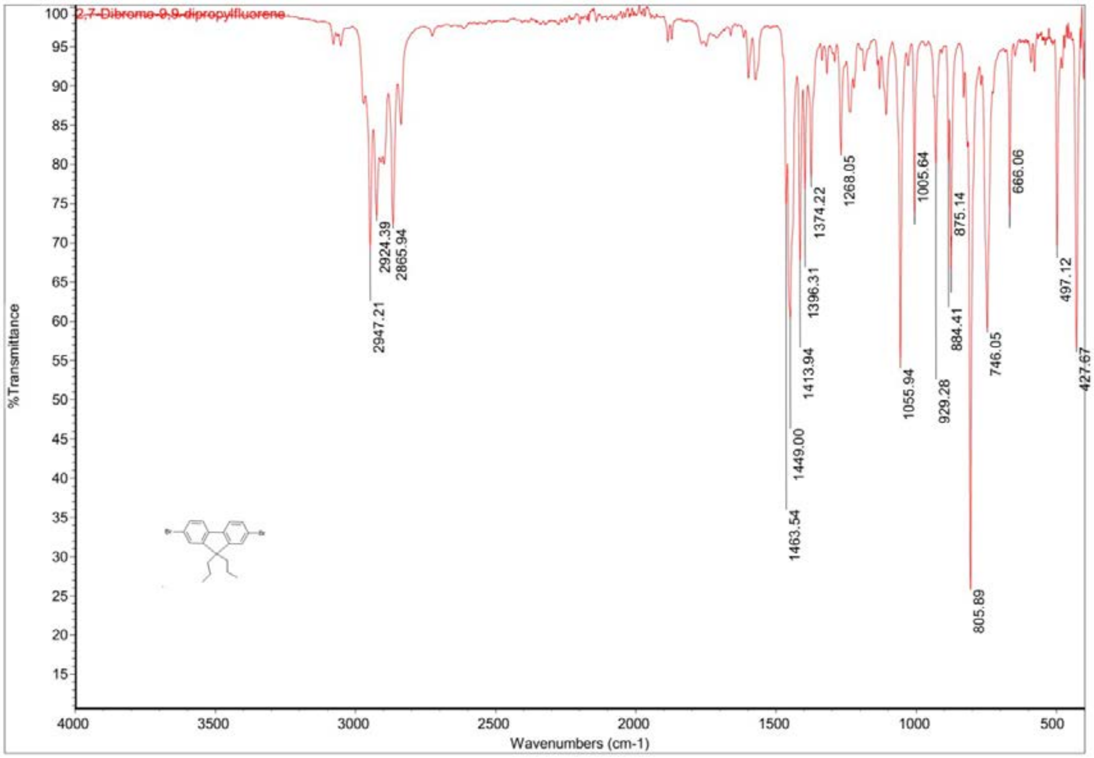

Figure S4.24:FTIR spectrum of2,7-dibromo-9,9-dipropylfluorene.

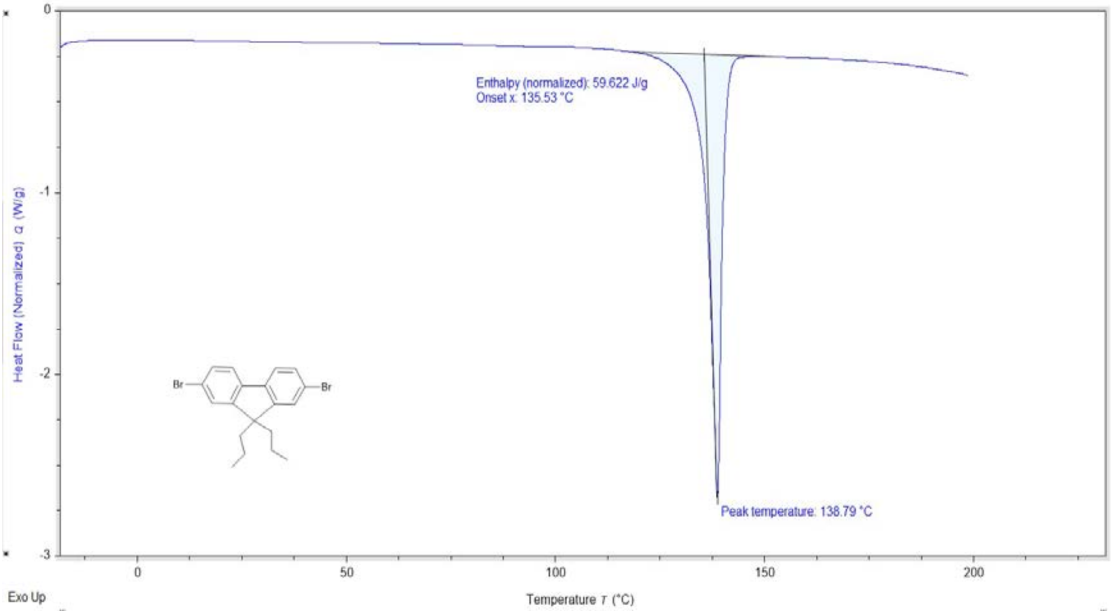

Figure S4.25:DSC heating curve of2,7-dibromo-9,9-dipropylfluorene.

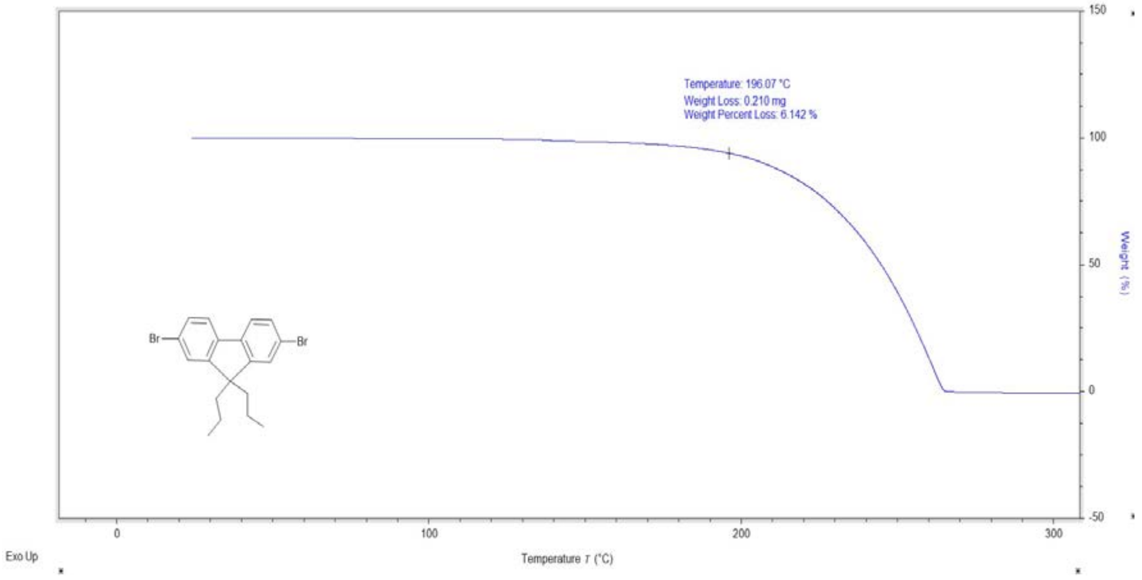

Figure S4.26:TGA thermmogram of2,7-dibromo-9,9-dipropylfluorene.

Analytical data of 9,9-dipropylfluorene-2,7-diboronic acid bis(pinacol) ester

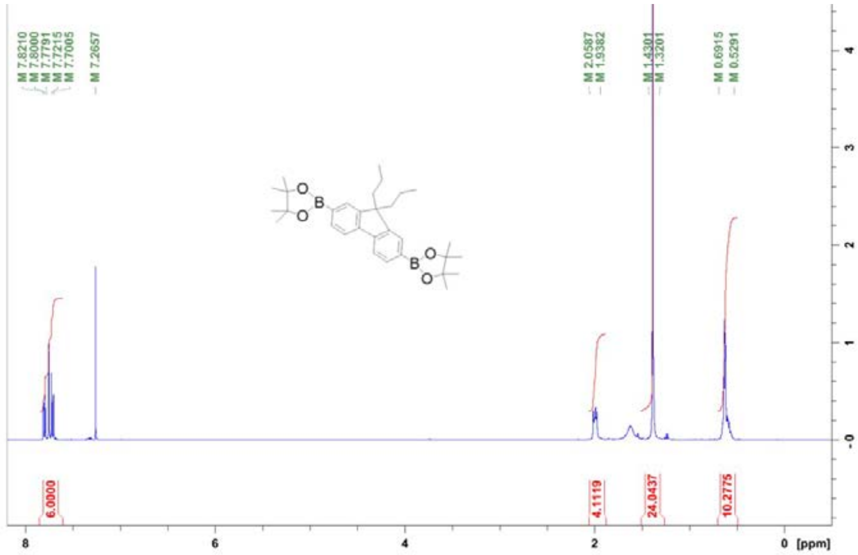

Figure S4.27: ^{1}H NMR spectrum of9,9-dipropylfluorene-2,7-diboronic acid bis(pinacol) ester.

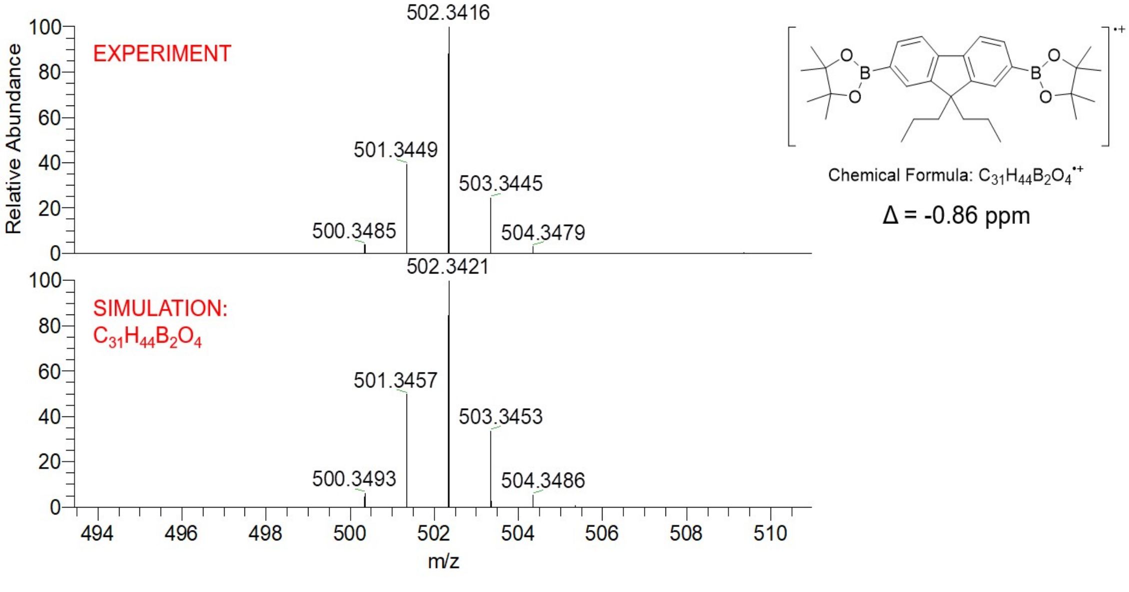

Figure S4.28: MS spectrum of9,9-dipropylfluorene-2,7-diboronic acid bis(pinacol) ester.

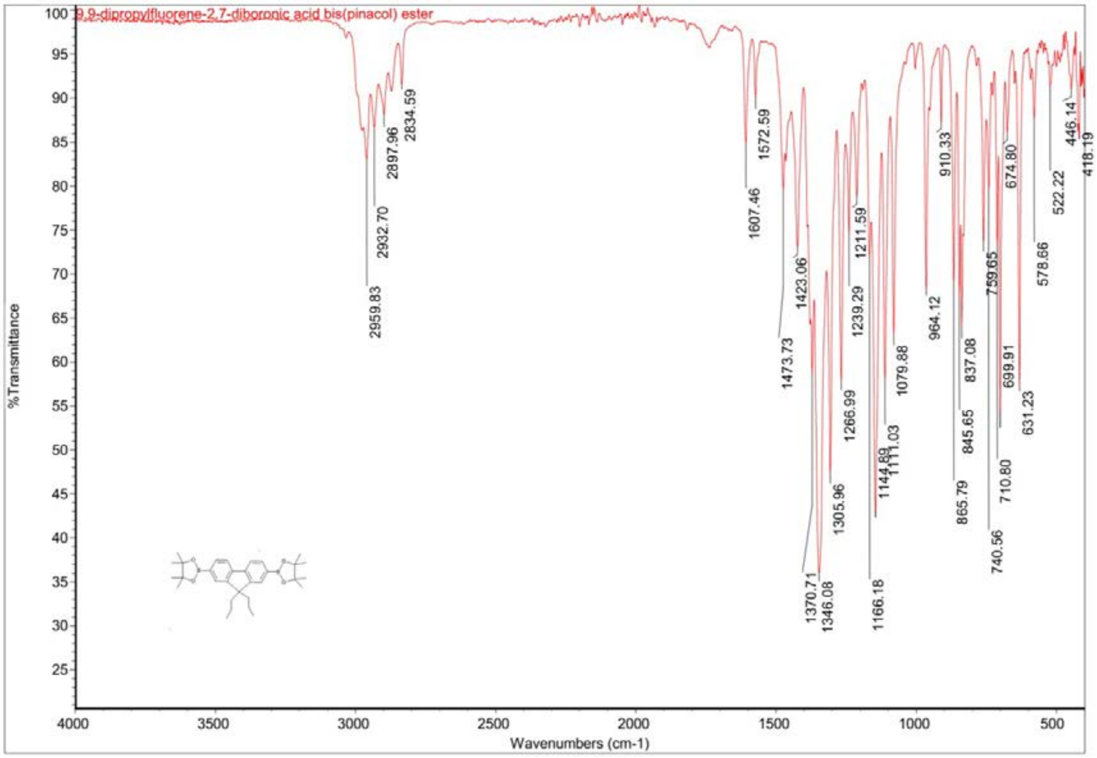

Figure S4.29:FTIR spectrum of9,9-dipropylfluorene-2,7-diboronic acid bis(pinacol) ester.

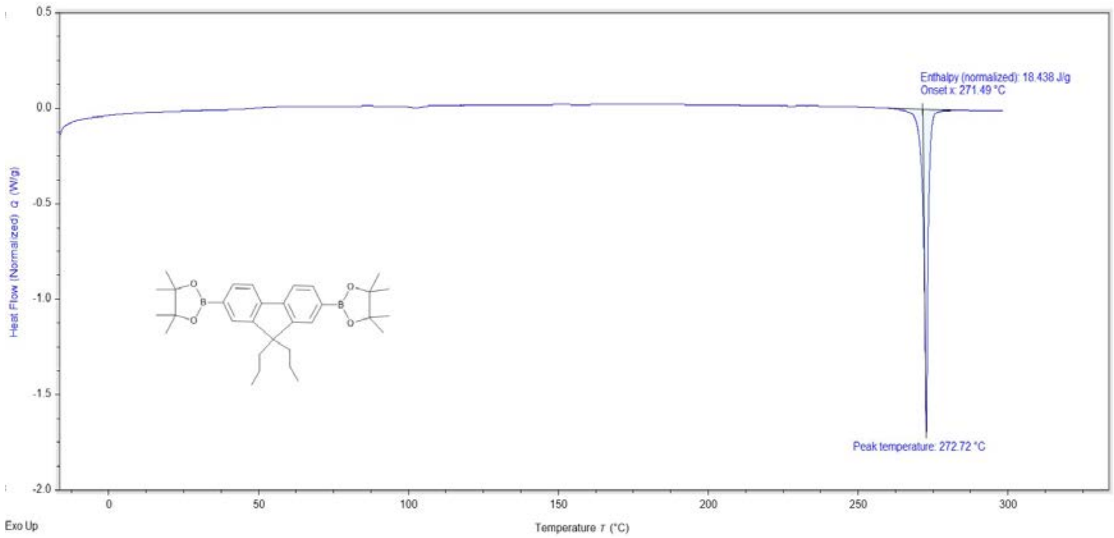

Figure S4.30:DSC heating curve of9,9-dipropylfluorene-2,7-diboronic acid bis(pinacol) ester.

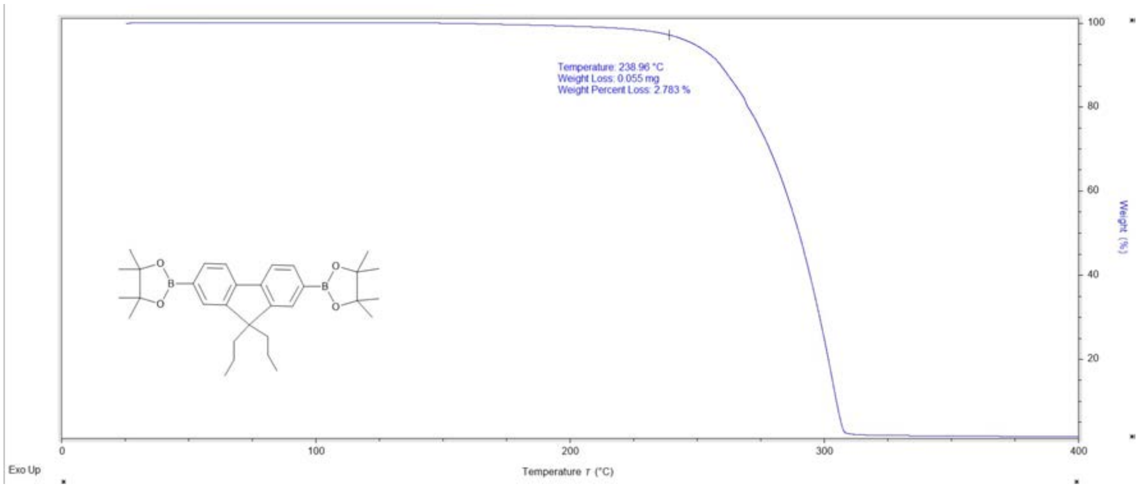

Figure S4.31:TGA thermmogram of9,9-dipropylfluorene-2,7-diboronic acid bis(pinacol) ester.

Analytical data of polymers P1-P3

Analytical data for P1

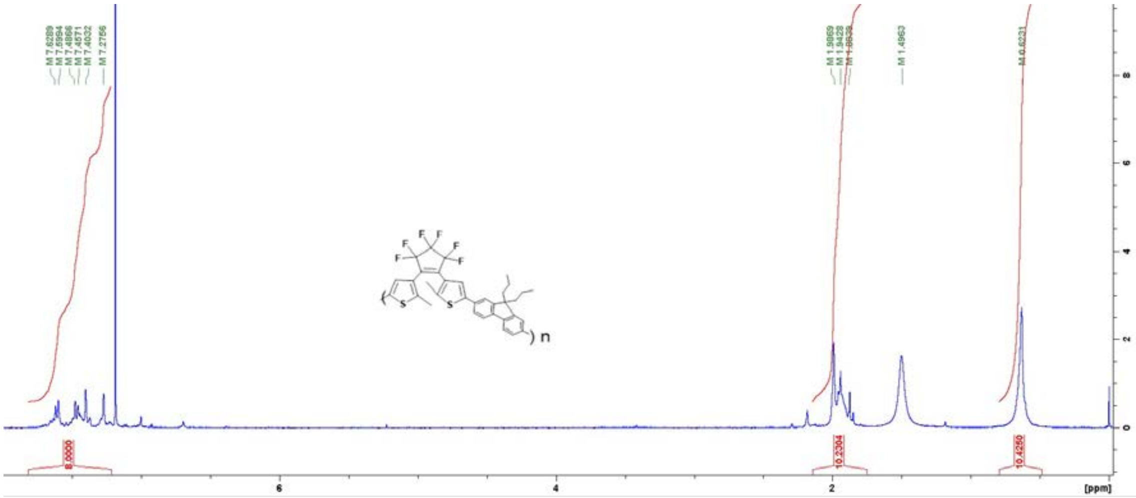

Figure S4.32:^{1}H NMR spectrum ofpoly (3-[3,3,4,4,5,5-hexafluoro-2-(2-methyl-3-thienyl)-1-cyclopenten-1-yl]-2-methylthiophene)-alt-(9,9-di-*n*-propyl-9H-fluorene) (P1).

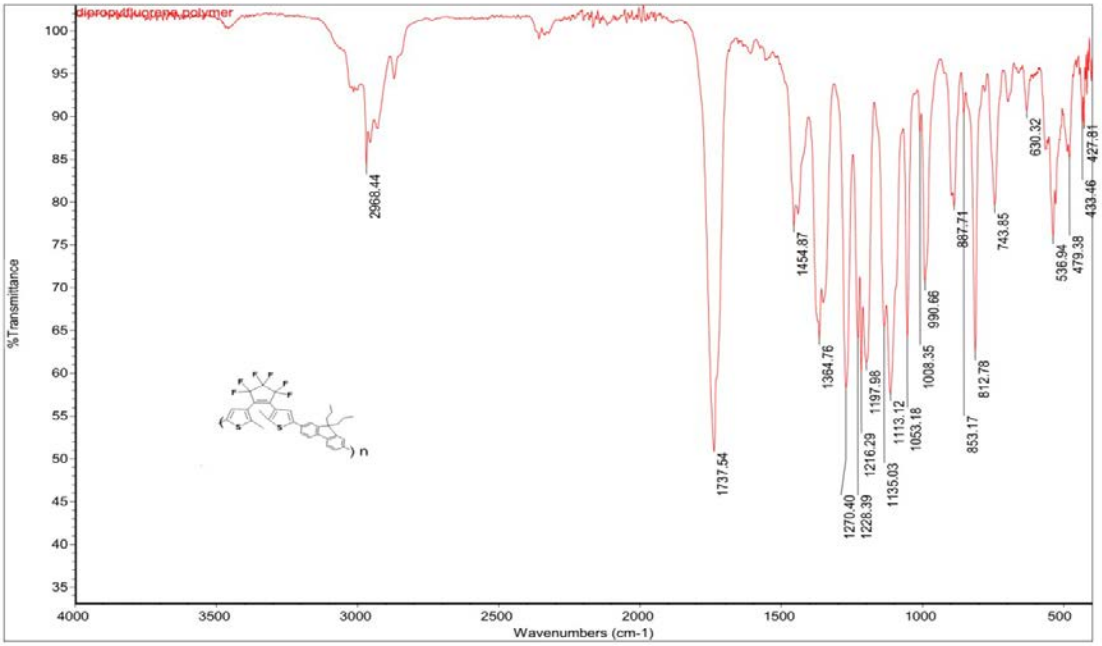

Figure S4.33:FTIR spectrum ofpoly (3-[3,3,4,4,5,5-hexafluoro-2-(2-methyl-3-thienyl)-1-cyclopenten-1-yl]-2-methylthiophene)-alt-(9,9-di-*n*-propyl-9H-fluorene) (P1).

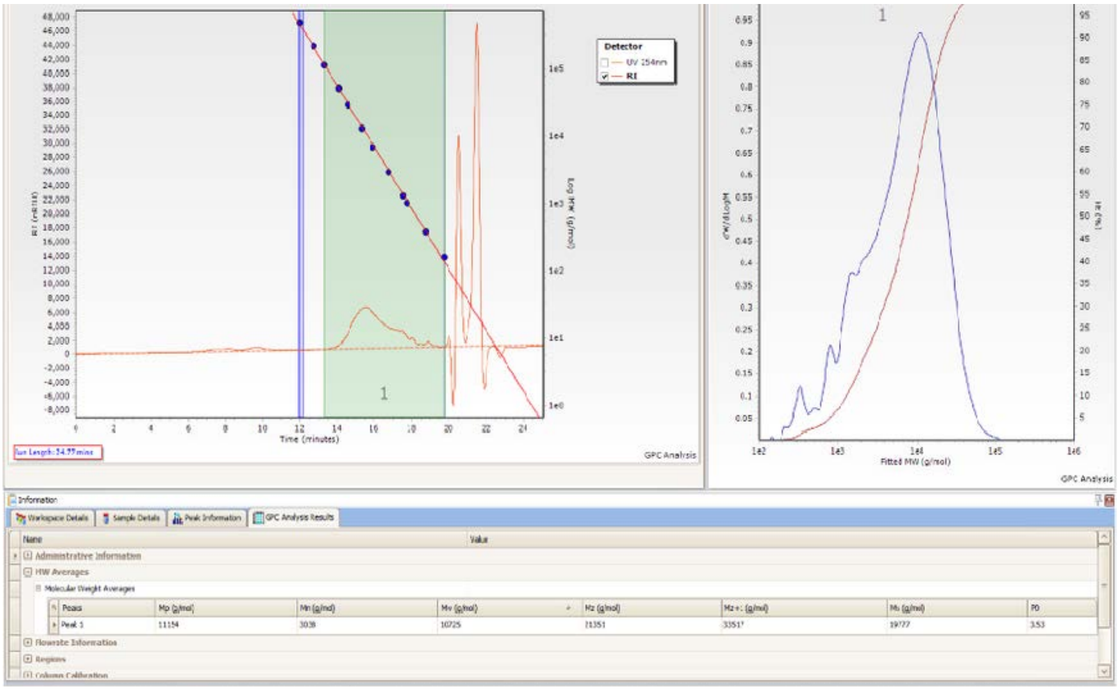

Name	Value
⊞ Administrative Information	
⊟ MW Averages	
⊟ Molecular Weight Averages	

Peaks	Mp (g/mol)	Mn (g/mol)	Mv (g/mol)	Mz (g/mol)	Mz+1 (g/mol)	Mw (g/mol)	PD
Peak 1	11154	3038	10725	21351	33517	19777	3.53

⊞ Flowrate Information

⊞ Regions

⊞ Column Calibration

Figure S4.34:GPC molecular weight distribution ofpoly (3-[3,3,4,4,5,5-hexafluoro-2-(2-methyl-3-thienyl)-1-cyclopenten-1-yl]-2-methylthiophene)-alt-(9,9-di-*n*-propyl-9H-fluorene) (P1).

Analytical data for P2

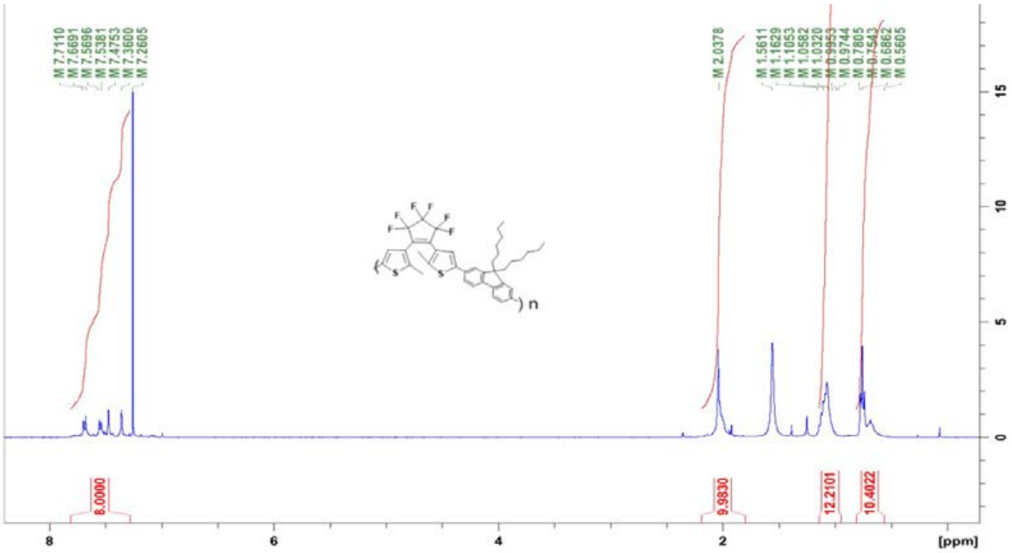

Figure S4.35:^{1}H NMR spectrum ofpoly (3-[3,3,4,4,5,5-hexafluoro-2-(2-methyl-3-thienyl)-1-cyclopenten-1-yl]-2-methylthiophene)-alt-(9,9-di-*n*-hexyl-9H-fluorene) (P2).

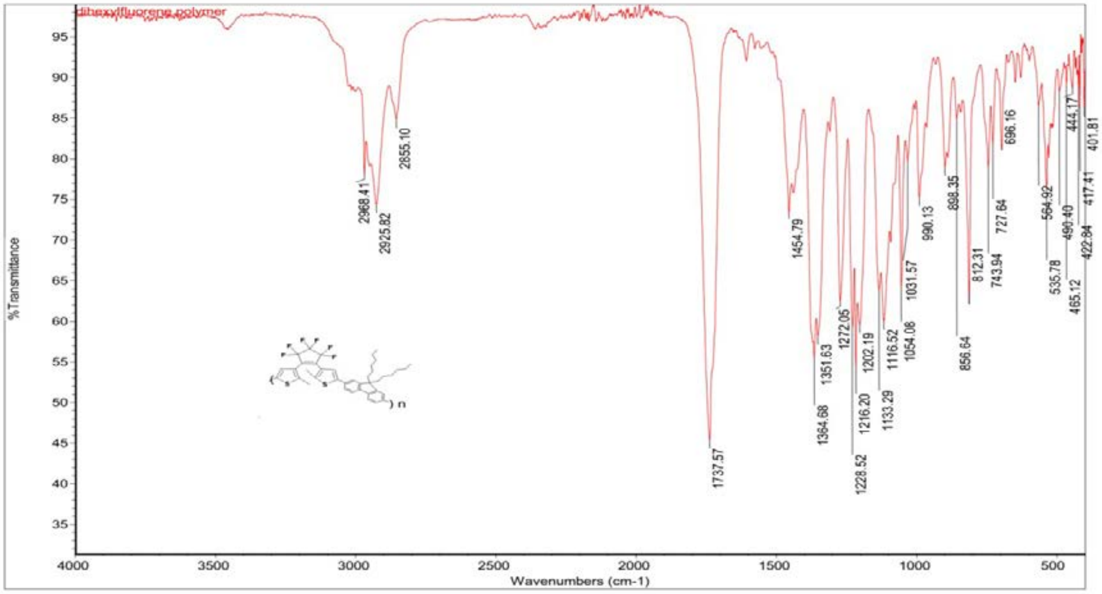

Figure S4.36:FTIR spectrum ofpoly (3-[3,3,4,4,5,5-hexafluoro-2-(2-methyl-3-thienyl)-1-cyclopenten-1-yl]-2-methylthiophene)-alt-(9,9-di-*n*-hexyl-9H-fluorene) (P2).

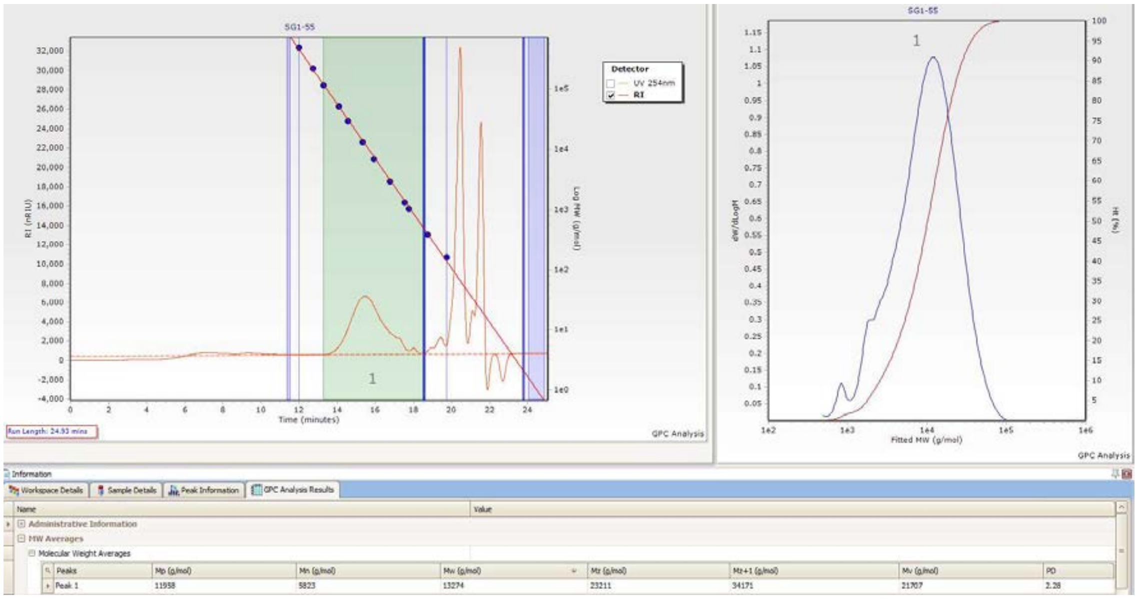

Name	Value
Administrative Information	
MW Averages	
Molecular Weight Averages	

Peaks	Mp (g/mol)	Mn (g/mol)	Mw (g/mol)	Mz (g/mol)	Mz+1 (g/mol)	Mv (g/mol)	PD
Peak 1	11958	5823	13274	23211	34171	21707	2.28

Figure S4.37:GPC molecular weight distribution ofpoly (3-[3,3,4,4,5,5-hexafluoro-2-(2-methyl-3-thienyl)-1-cyclopenten-1-yl]-2-methylthiophene)-alt-(9,9-di-*n*-hexyl-9H-fluorene) (P2).

Analytical data for P3

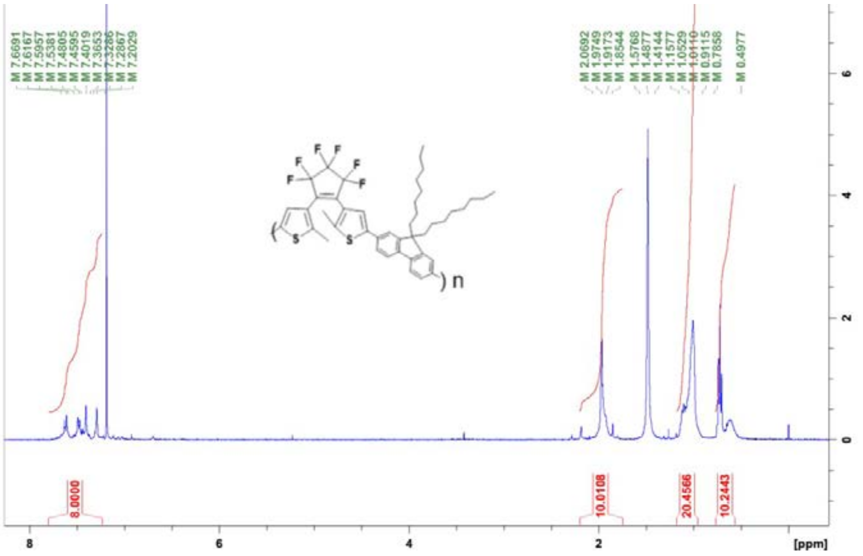

Figure S4.38:^{1}H NMR spectrum ofpoly (3-[3,3,4,4,5,5-hexafluoro-2-(2-methyl-3-thienyl)-1-cyclopenten-1-yl]-2-methylthiophene)-alt-(9,9-di-*n*-octyl-9H-fluorene) (P3).

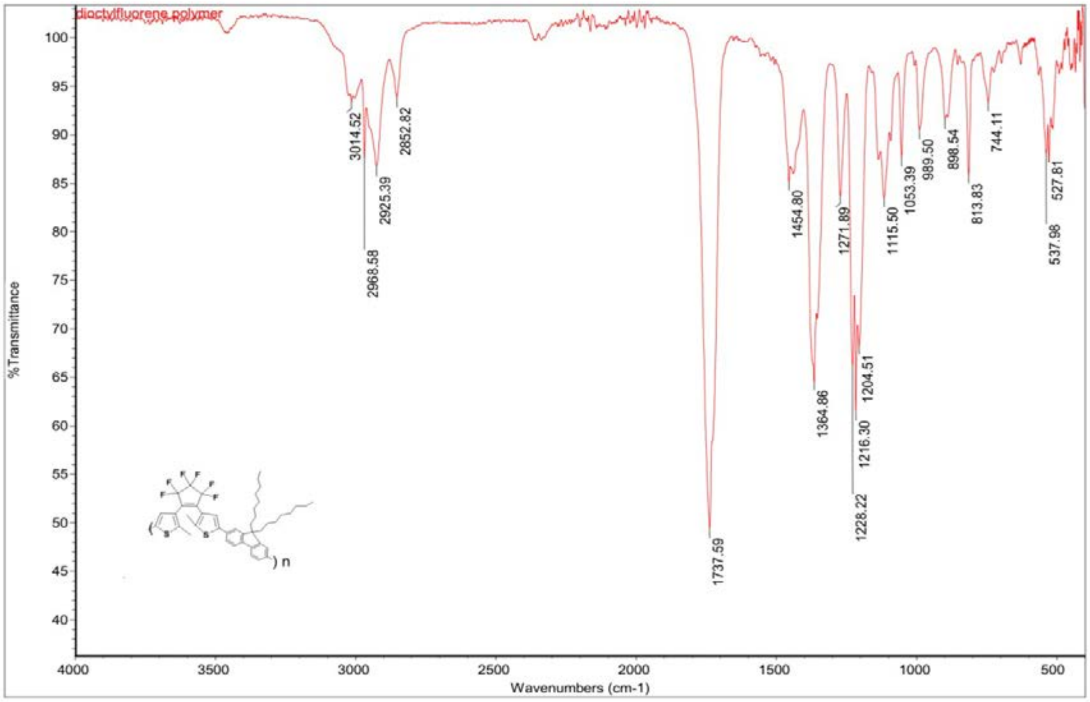

Figure S4.39:FTIR spectrum ofpoly (3-[3,3,4,4,5,5-hexafluoro-2-(2-methyl-3-thienyl)-1-cyclopenten-1-yl]-2-methylthiophene)-alt-(9,9-di-*n*-octyl-9H-fluorene) (P3).

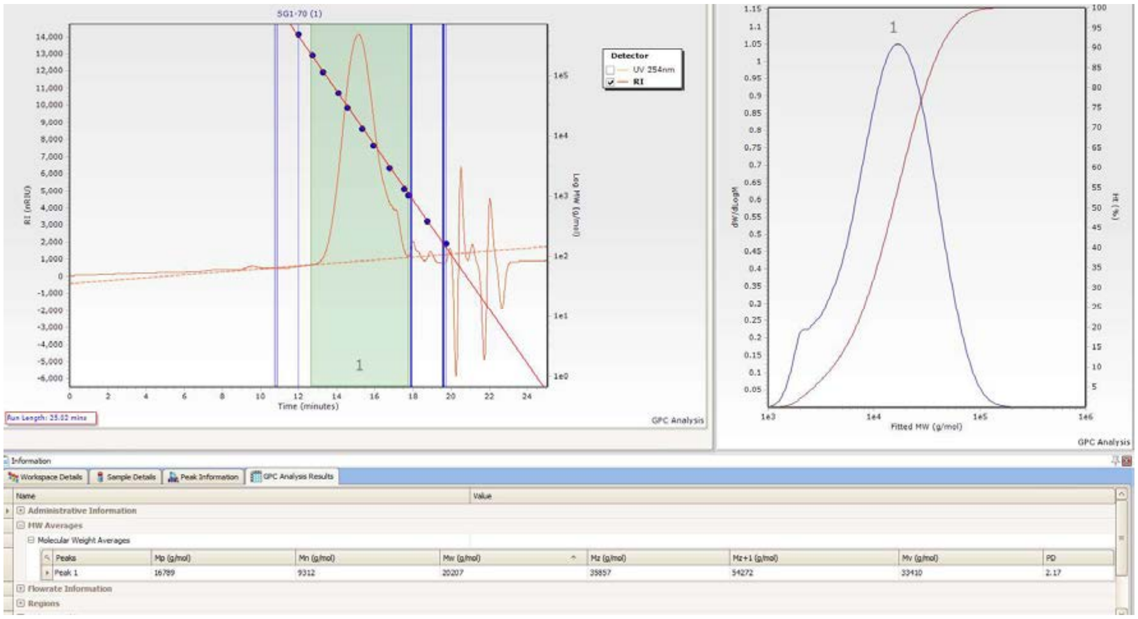

Peaks	Mp (g/mol)	Mn (g/mol)	Mw (g/mol)	Mz (g/mol)	Mz+1 (g/mol)	Mv (g/mol)	PD
Peak 1	16789	9312	20207	35857	54272	33410	2.17

Figure S4.40:GPC molecular weight distribution ofpoly (3-[3,3,4,4,5,5-hexafluoro-2-(2-methyl-3-thienyl)-1-cyclopenten-1-yl]-2-methylthiophene)-alt-(9,9-di-*n*-octyl-9H-fluorene) (P3).

Analytical data of P1-1

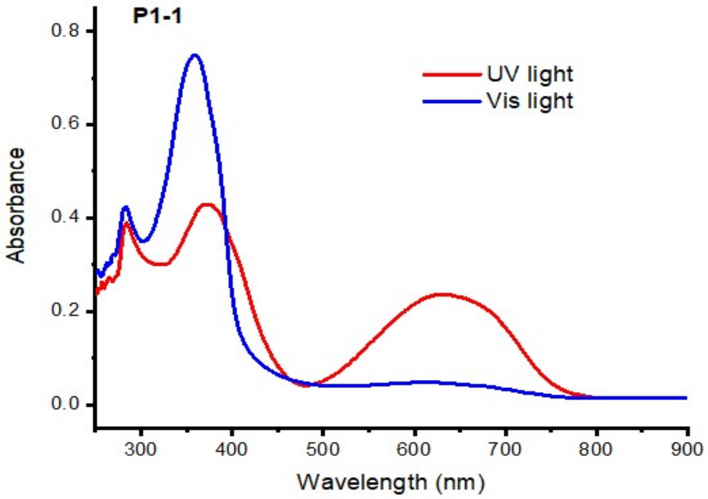

Figure S4.41: Absorption spectra of P1-1.

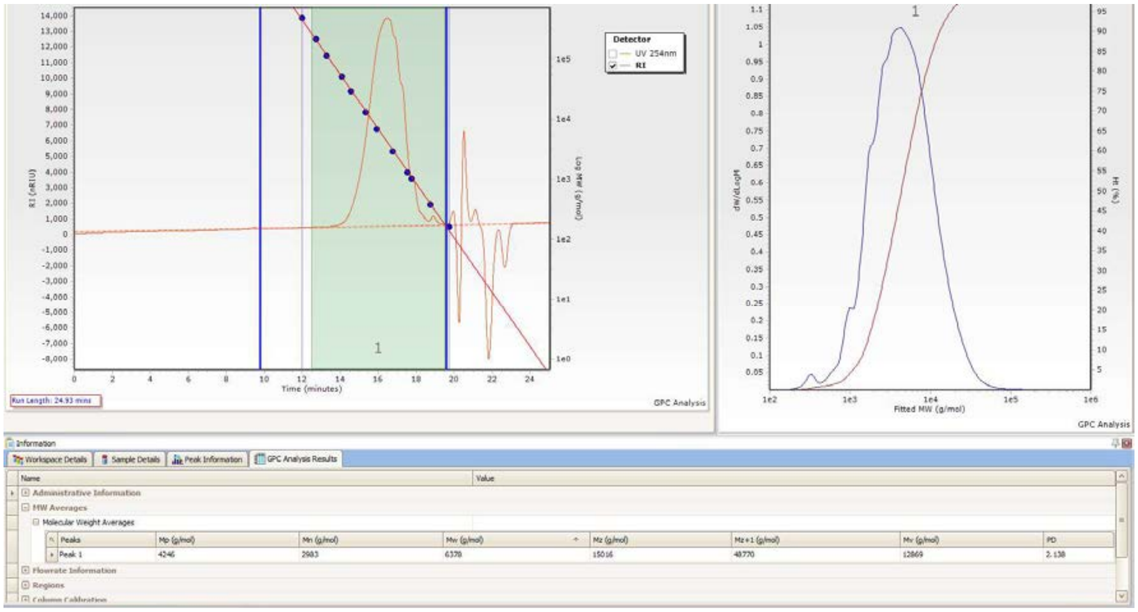

Name	Value
MW Averages	
Molecular Weight Averages	

Peaks	Mp (g/mol)	Mn (g/mol)	Mw (g/mol)	Mz (g/mol)	Mz+1 (g/mol)	Mv (g/mol)	PD
Peak 1	4246	2983	6378	15016	48770	12869	2.138

Figure S4.42:GPC molecular weight distribution of P1-1.

Analytical data of P3-1

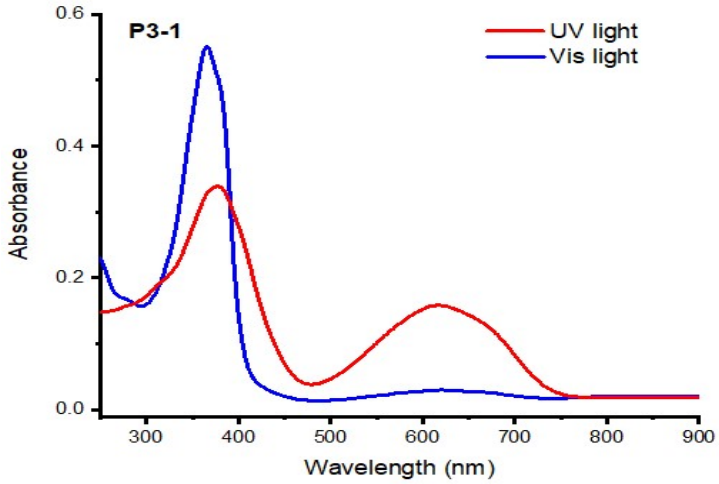

Figure S4.43: Absorption spectra of P3-1.

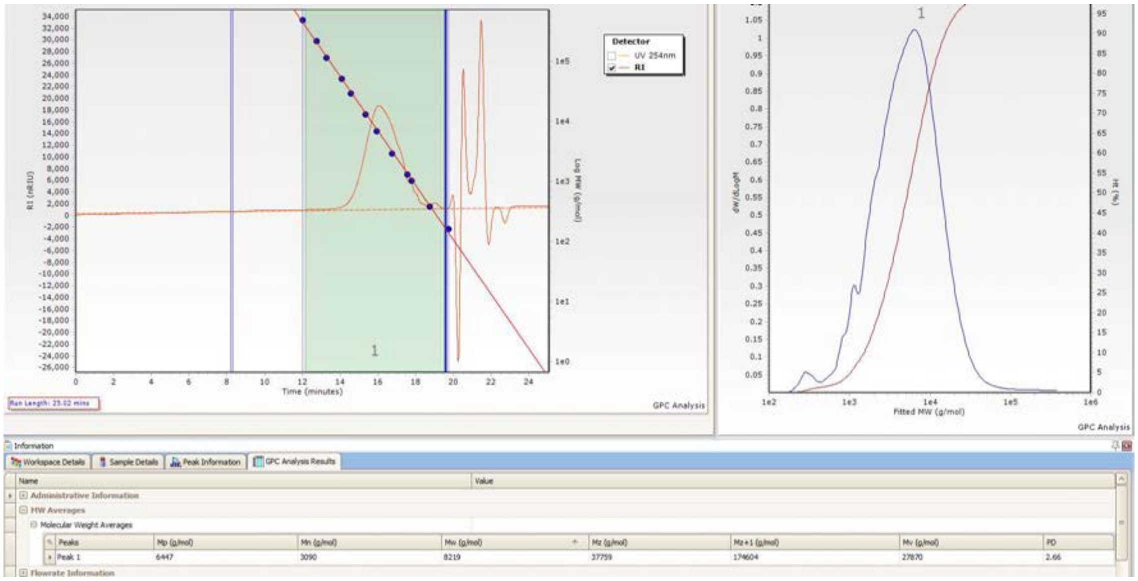

Name	Value
Administrative Information	
MW Averages	
Molecular Weight Averages	

Peaks	Mp (g/mol)	Mn (g/mol)	Mw (g/mol)	Mz (g/mol)	Mz+1 (g/mol)	Mv (g/mol)	PD
Peak 1	6447	3090	8219	37759	174604	27870	2.66

Flowrate Information

Figure S4.44:GPC molecular weight distribution of P3-1.

Supplementary figures for chapter 5

Analytical data of 2,5-Dihexyl-1,4-phenylene-bis(pinacolato boronate)

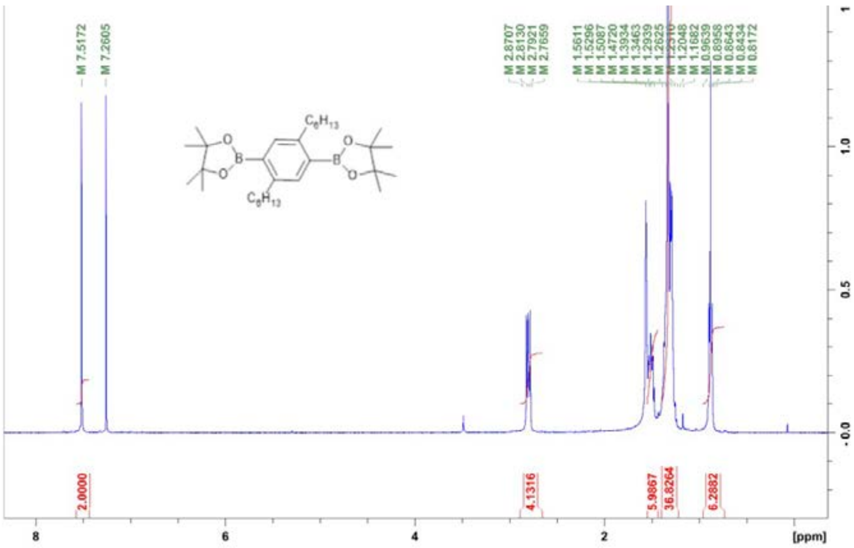

Figure S5.1: ^{1}H NMR spectrum of 2,5-Dihexyl-1,4-phenylene-bis(pinacolato boronate)

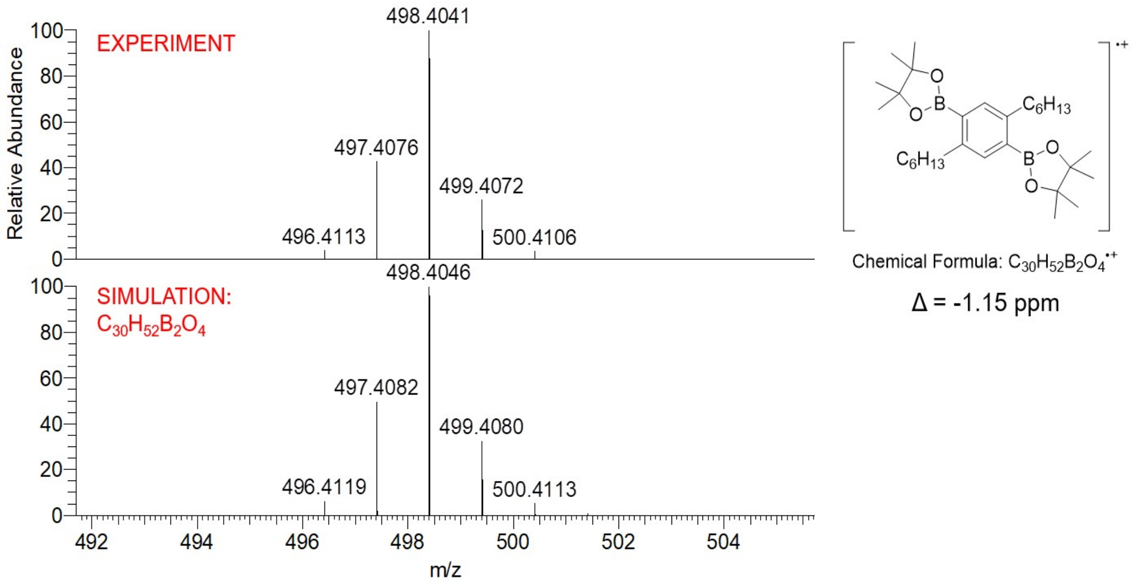

Figure S5.2: MS spectrum of 2,5-Dihexyl-1,4-phenylene-bis(pinacolato boronate)

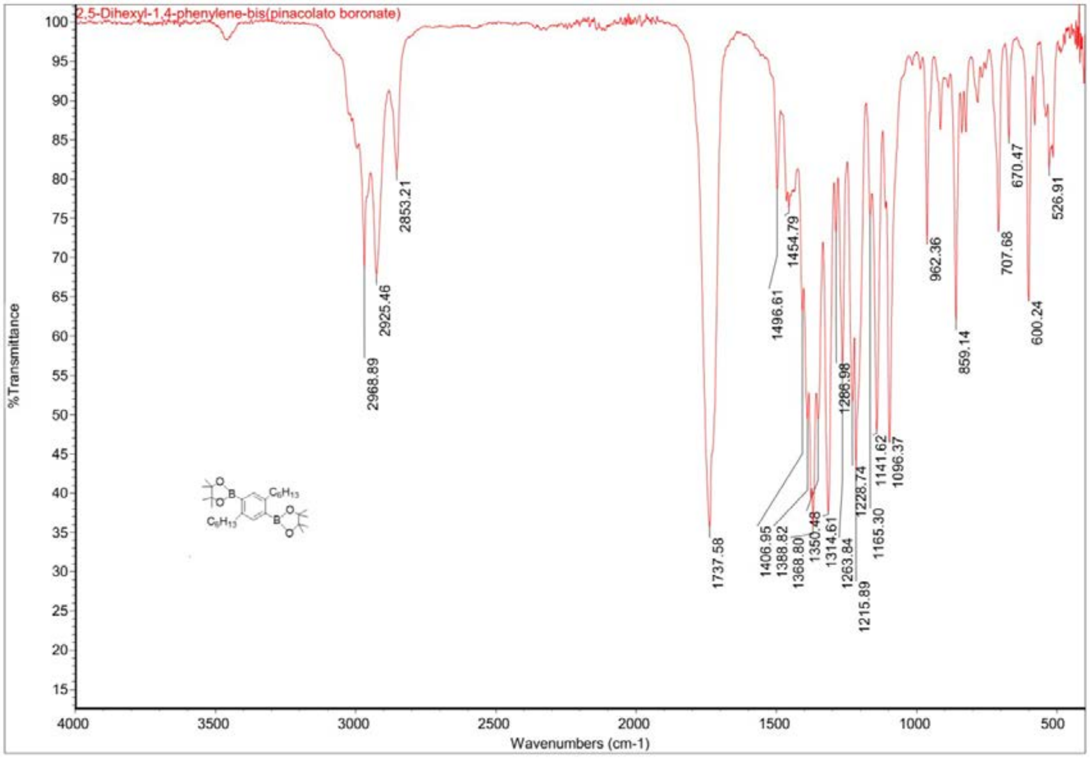

Figure S5.3:FTIR spectrum of 2,5-Dihexyl-1,4-phenylene-bis(pinacolato boronate)

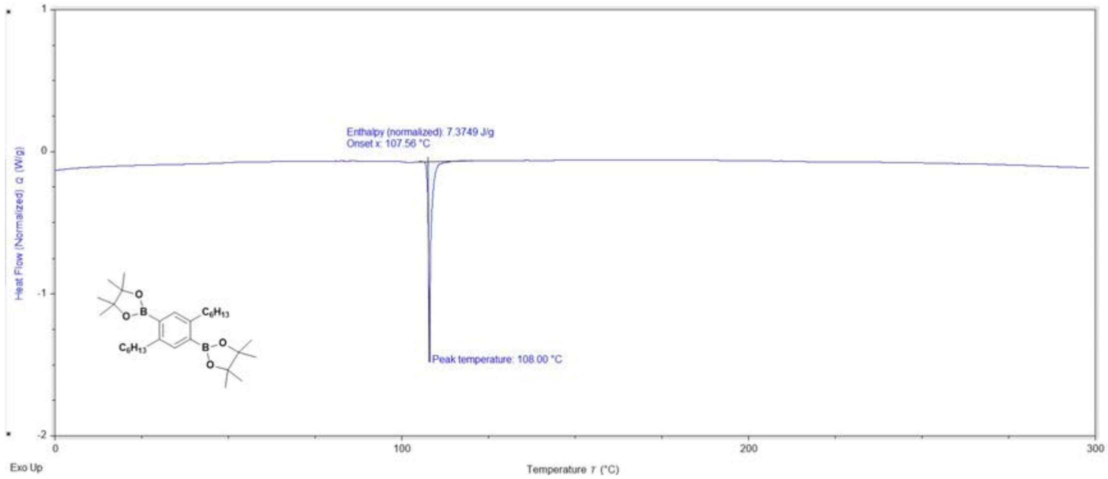

Figure S5.4:DSC heating curve of 2,5-Dihexyl-1,4-phenylene-bis(pinacolato boronate)

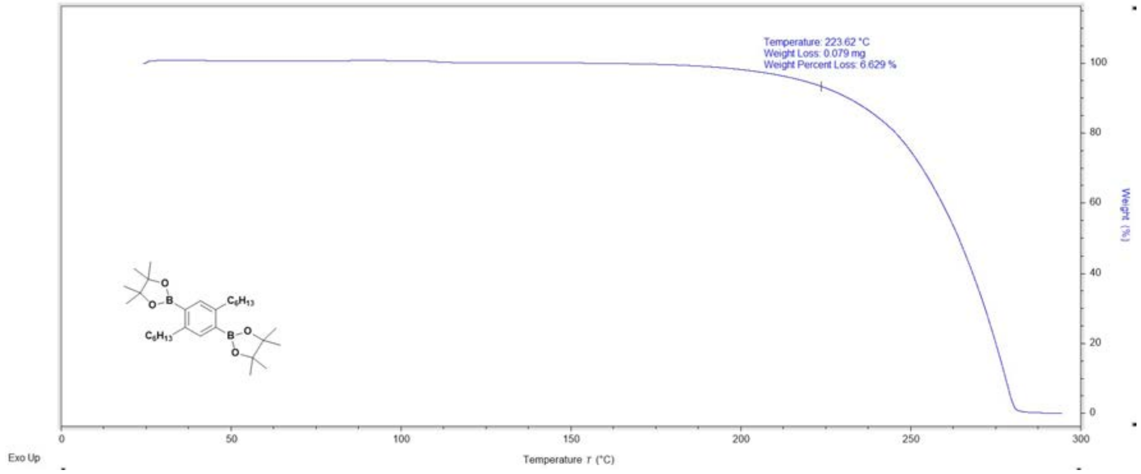

Figure S5.5:TGA thermmogram of 2,5-Dihexyl-1,4-phenylene-bis(pinacolato boronate).

Analytical data of polymers P4-P6

Analytical data for P4

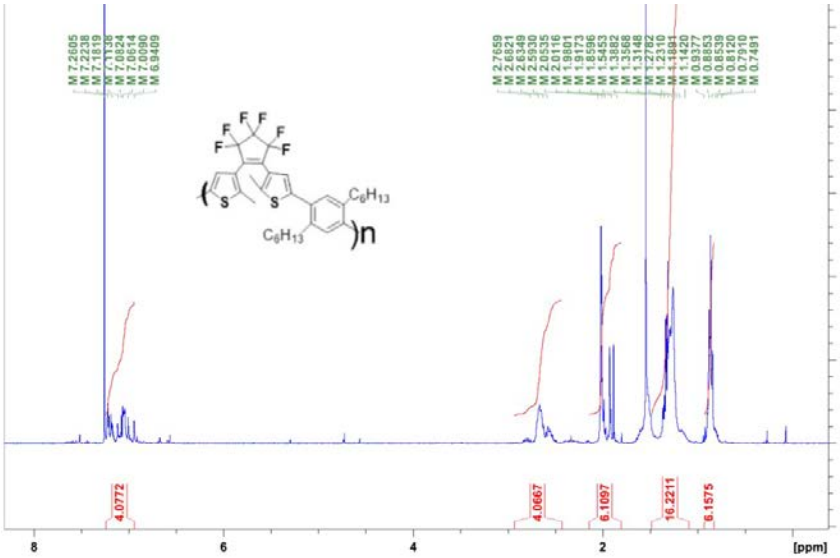

Figure S5.6: ^{1}H NMR spectrum ofpoly(3-[3,3,4,4,5,5-hexafluoro-2-(2-methyl-3-thienyl)-1-cyclopenten-1-yl]-2-methylthiophene)-alt-(di-*n*-hexylphenylene) (P4).

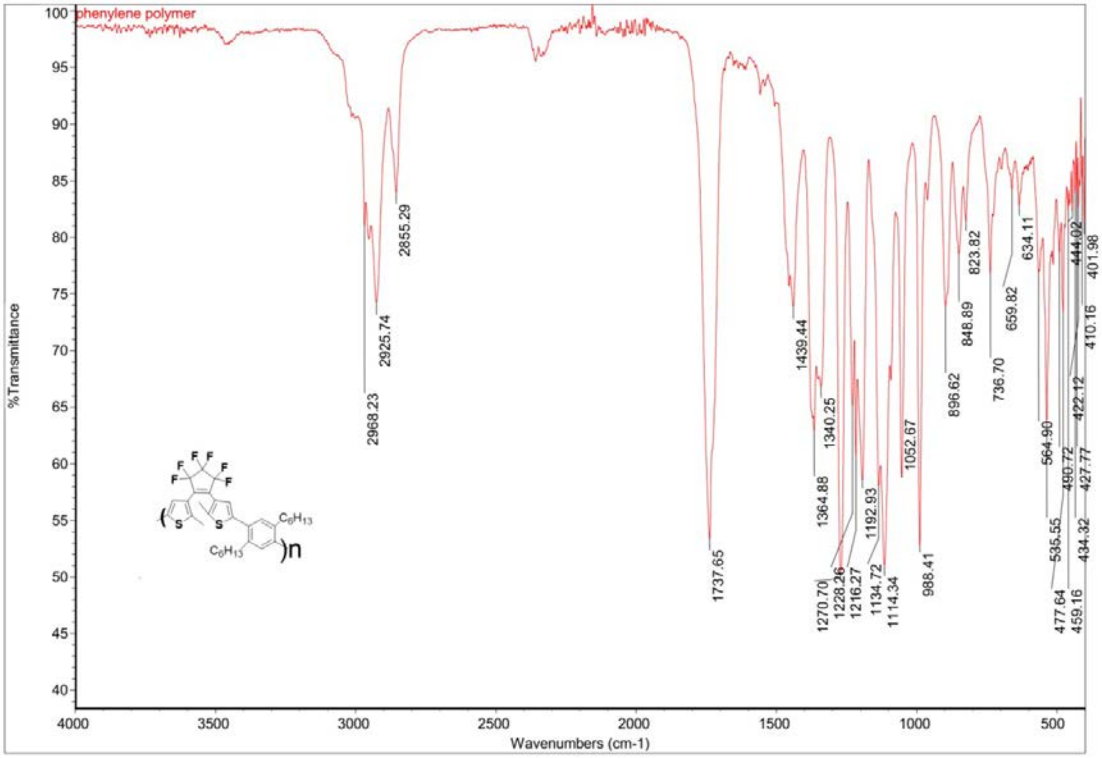

Figure S5.7:FTIR spectrum ofpoly(3-[3,3,4,4,5,5-hexafluoro-2-(2-methyl-3-thienyl)-1-cyclopenten-1-yl]-2-methylthiophene)-alt-(di-*n*-hexylphenylene) (P4).

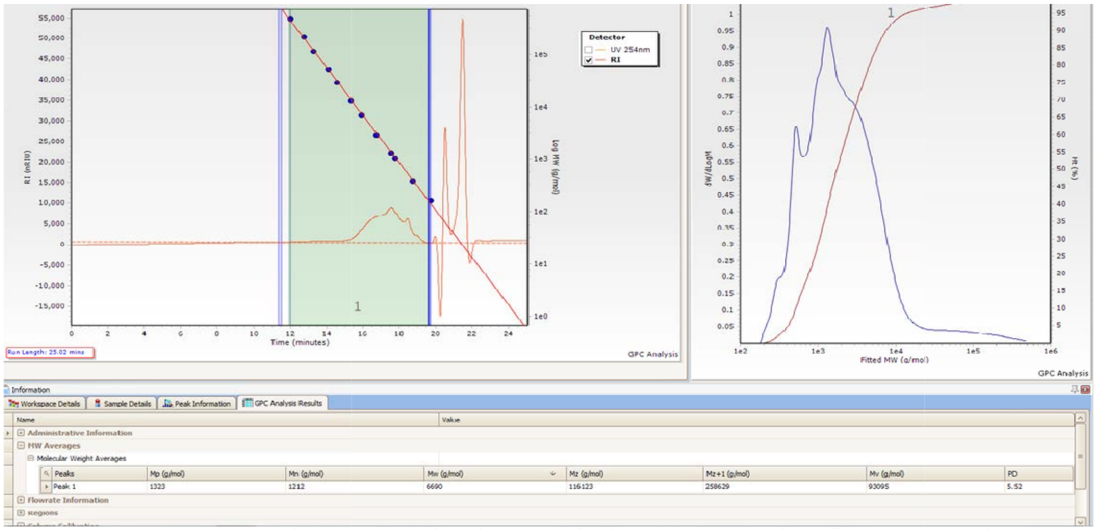

Peaks	Mp (g/mol)	Mn (g/mol)	Mw (g/mol)	Mz (g/mol)	Mz+1 (g/mol)	Mv (g/mol)	PD
Peak 1	1323	1212	6690	116123	258629	93095	5.52

Figure S5.8:GPC molecular weight distribution ofpoly(3-[3,3,4,4,5,5-hexafluoro-2-(2-methyl-3-thienyl)-1-cyclopenten-1-yl]-2-methylthiophene)-alt-(di-*n*-hexylphenylene) (P4).

Analytical data for P5

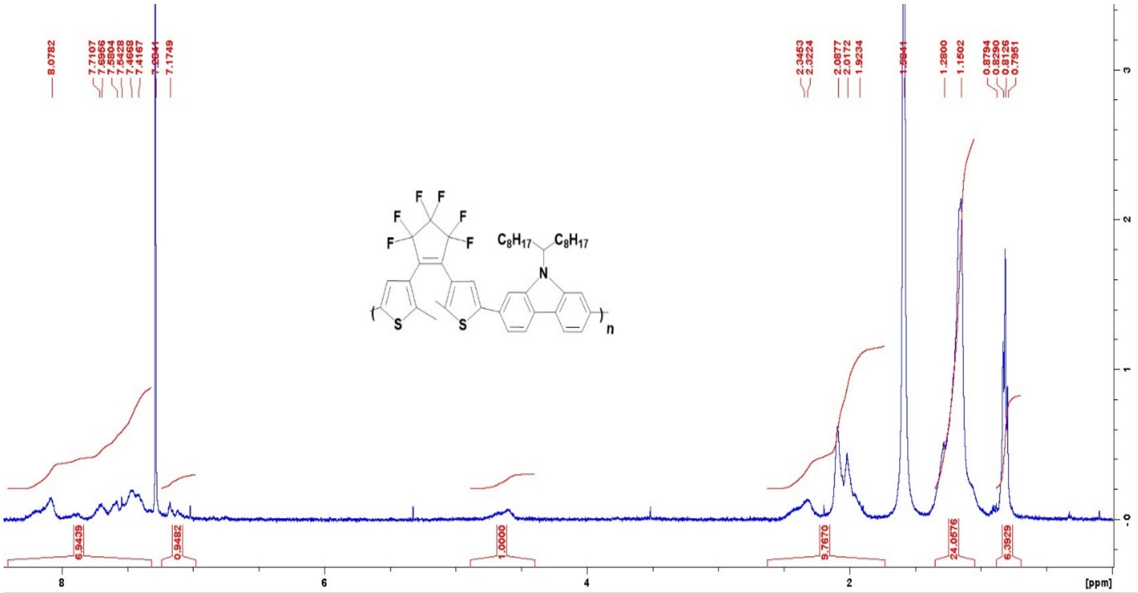

Figure S5.9: ^{1}H NMR spectrum ofpoly(3-[3,3,4,4,5,5-hexafluoro-2-(2-methyl-3-thienyl)-1-cyclopenten-1-yl]-2-methylthiophene)-alt-(9-(1-octylnonyl)carbazole) (P5).

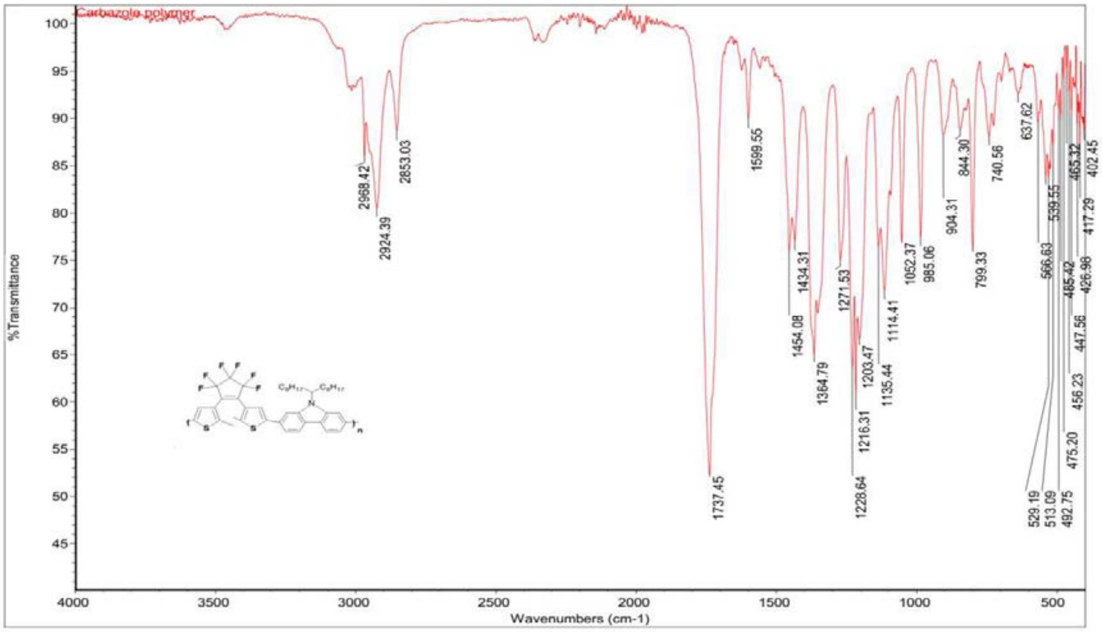

Figure S5.10:FTIR spectrum ofpoly(3-[3,3,4,4,5,5-hexafluoro-2-(2-methyl-3-thienyl)-1-cyclopenten-1-yl]-2-methylthiophene)-alt-(9-(1-octylnonyl)carbazole) (P5).

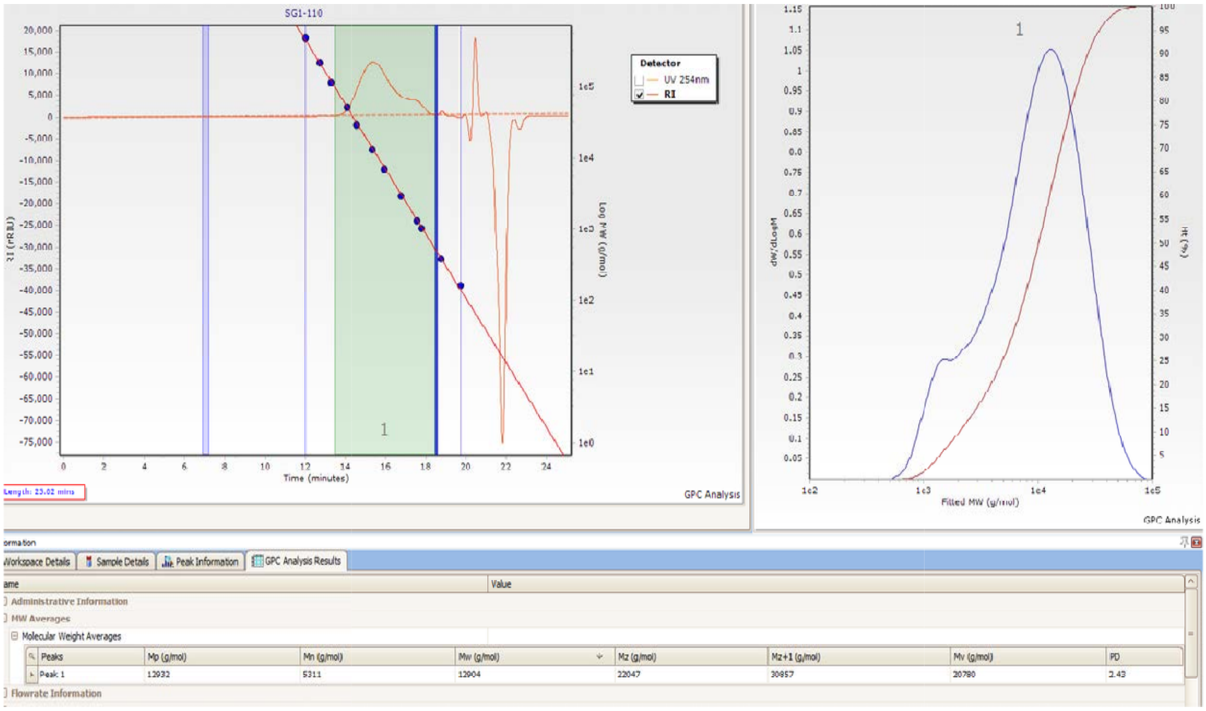

ame	Value
Administrative Information	
MW Averages	
Molecular Weight Averages	

Peaks	Mp (g/mol)	Mn (g/mol)	Mw (g/mol)	Mz (g/mol)	Mz+1 (g/mol)	Mv (g/mol)	PD
Peak 1	12932	5311	12904	22047	30857	20780	2.43

Flowrate Information

Figure S5.11:GPC molecular weight distribution ofpoly(3-[3,3,4,4,5,5-hexafluoro-2-(2-methyl-3-thienyl)-1-cyclopenten-1-yl]-2-methylthiophene)-alt-(9-(1-octylnonyl)carbazole) (P5).

Analytical data for P6

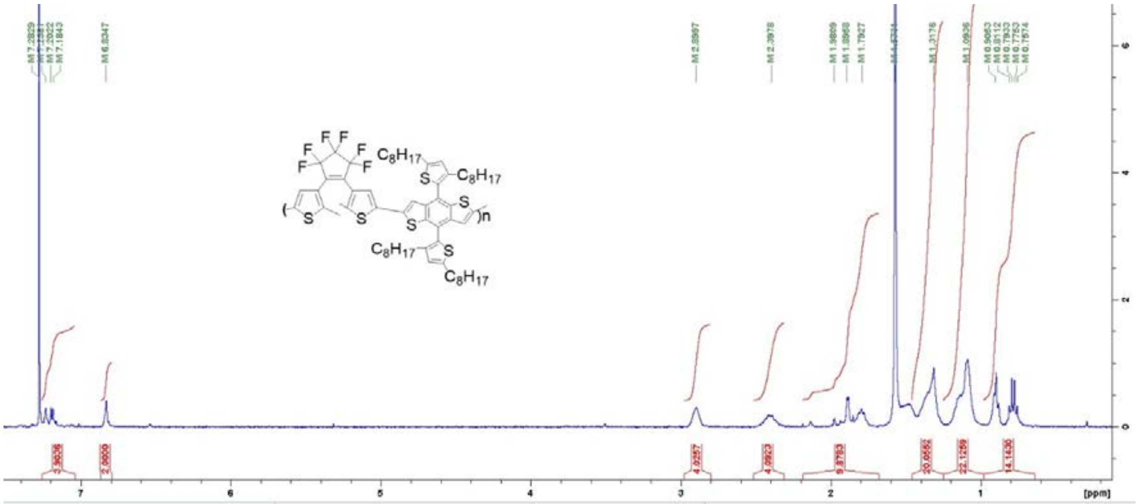

Figure S5.12:^{1}H NMR spectrum ofpoly(3-[3,3,4,4,5,5-hexafluoro-2-(2-methyl-3-thienyl)-1-cyclopenten-1-yl]-2-methylthiophene)-alt-(4,8-bis(3,5-dioctyl-2-thienyl)-1,5-dithia-s-indacene) (P6).

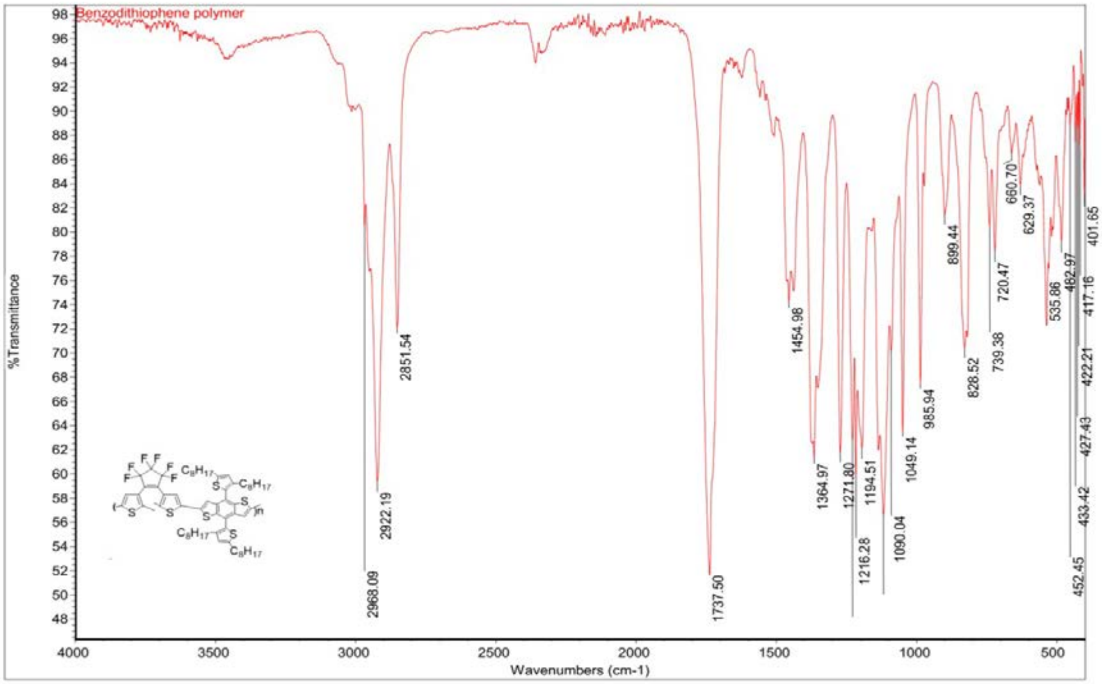

Figure S5.13:FTIR spectrum ofpoly(3-[3,3,4,4,5,5-hexafluoro-2-(2-methyl-3-thienyl)-1-cyclopenten-1-yl]-2-methylthiophene)-alt-(4,8-bis(3,5-dioctyl-2-thienyl)-1,5-dithia-s-indacene) (P6).

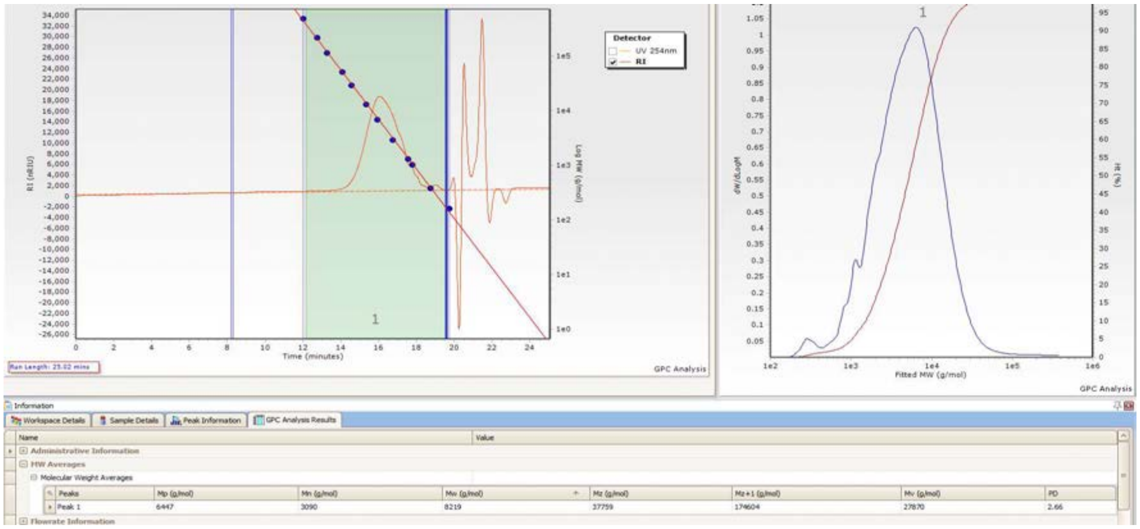

Peaks	Mp (g/mol)	Mn (g/mol)	Mw (g/mol)	Mz (g/mol)	Mz+1 (g/mol)	Mv (g/mol)	PD
Peak 1	6447	3090	8219	37759	174604	27870	2.66

Figure S5.14:GPC molecular weight distribution ofpoly(3-[3,3,4,4,5,5-hexafluoro-2-(2-methyl-3-thienyl)-1-cyclopenten-1-yl]-2-methylthiophene)-alt-(4,8-bis(3,5-dioctyl-2-thienyl)-1,5-dithia-s-indacene) (P6)

Analytical data for P4-1

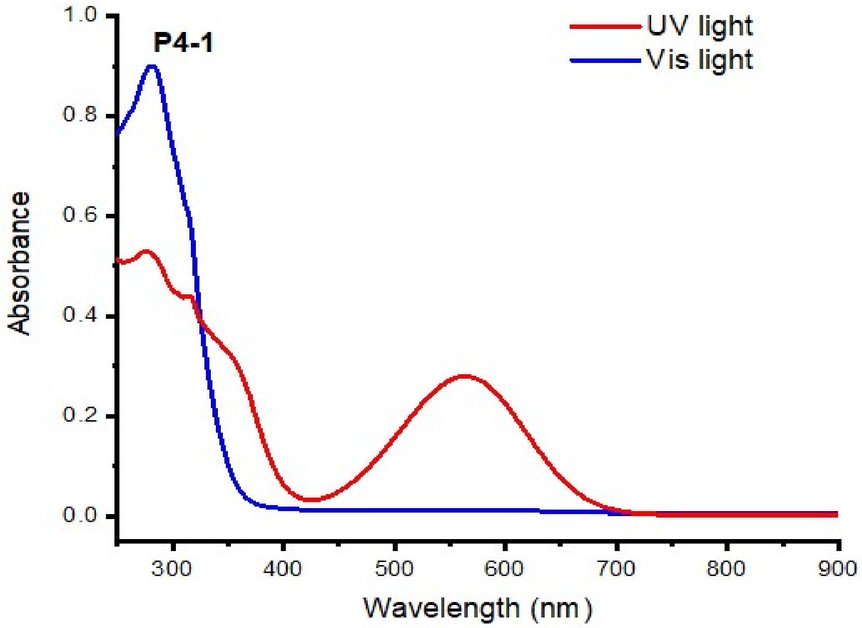

Figure S5.15: Absorption spectra of P4-1.

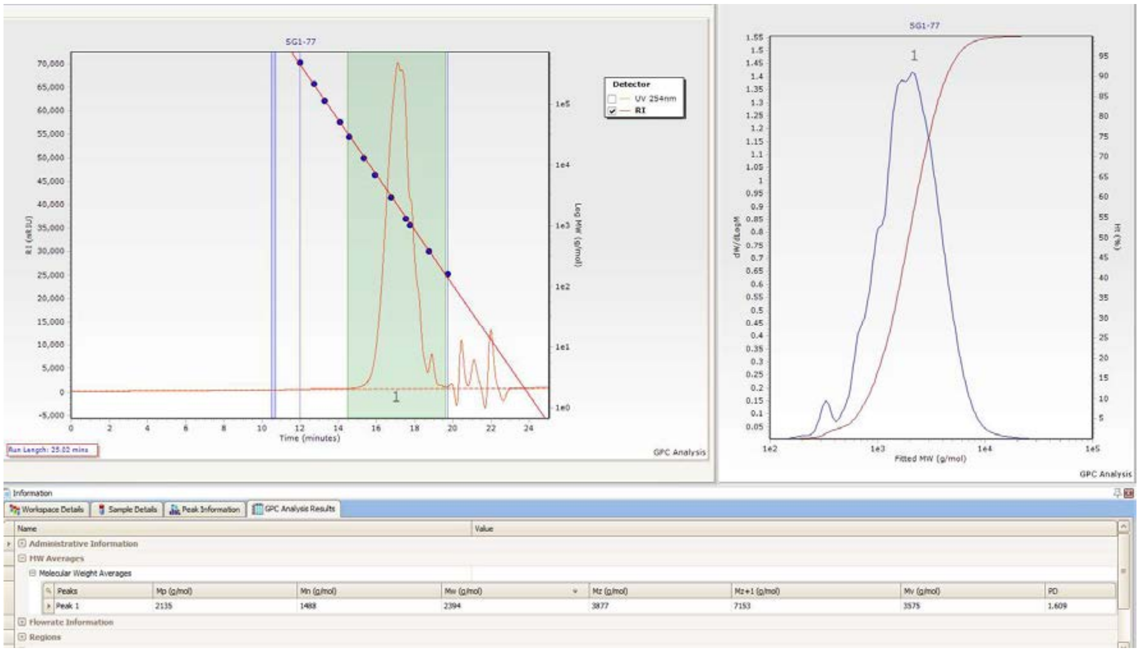

Name	Value
Administrative Information	
MW Averages	
Molecular Weight Averages	
Flowrate Information	
Regions	

Peaks	Mp (g/mol)	Mn (g/mol)	Mw (g/mol)	Mz (g/mol)	Mz+1 (g/mol)	Mv (g/mol)	PD
Peak 1	2135	1488	2394	3877	7153	3575	1.609

Figure S5.16:GPC molecular weight distribution ofP4-1**.**

Supplementary figures for chapter 6

Polymer before deprotection

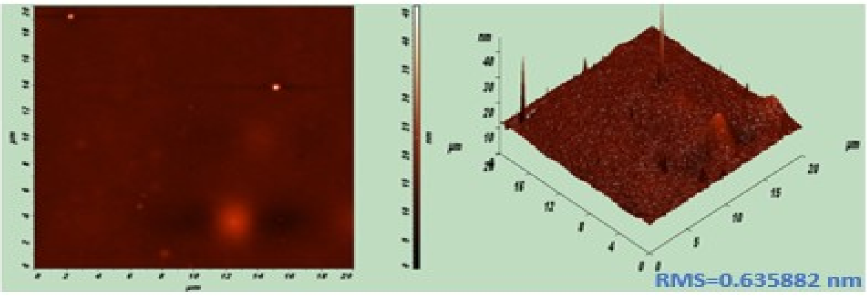

Polymer + CSA

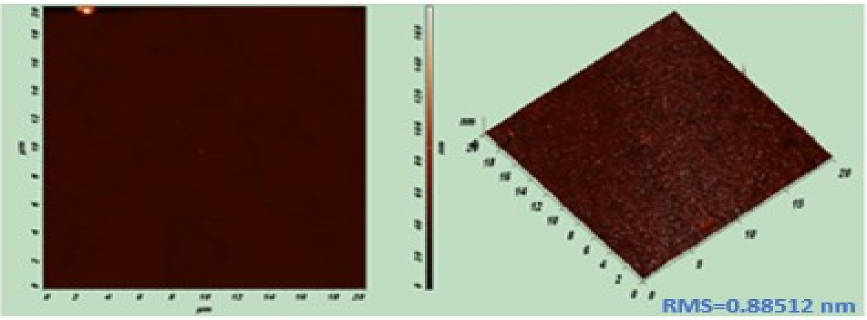

Polymer after thermal deprotection at 325 °C

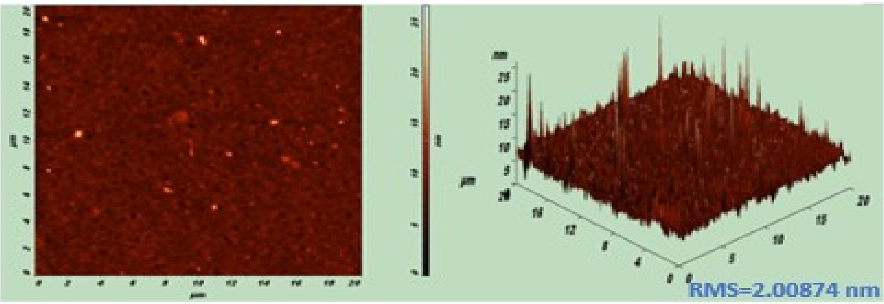

After heating polymer + CSA at 185 °C

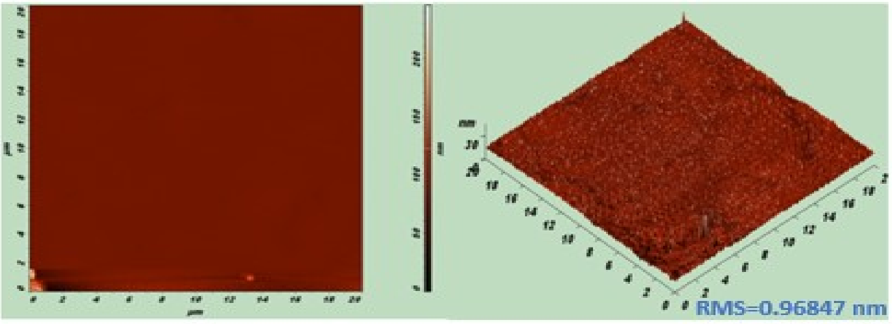

Figure S6.1: AFM images of P1 before deprotection and after thermolytic and acid-catalyzed deprotection.

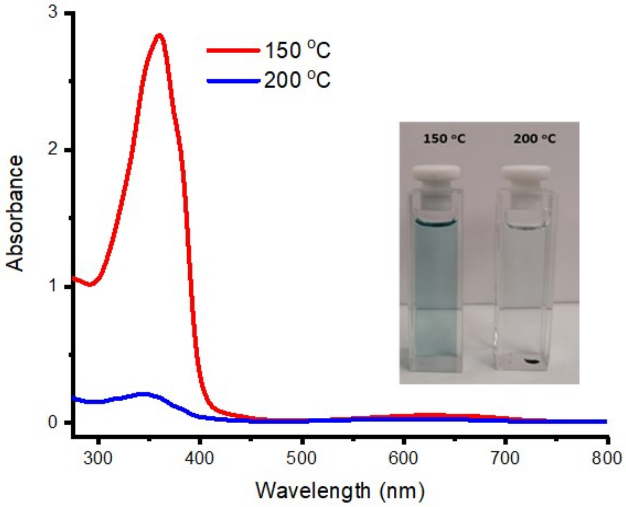

Figure S6.2: Absorption spectra of P1 deprotected at 150 °C and 200 °C (insert-image showing solubility of deprotected films).

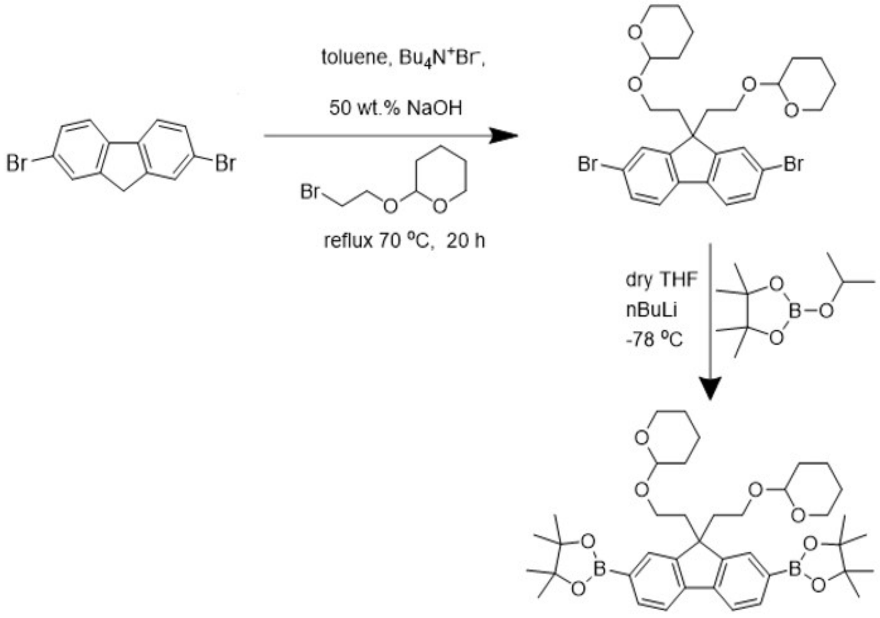

Scheme S6.1: Synthesis protocol of 9,9-bis(2-(2-tetrahydropyranyloxy)ethyl)-fluorene-2,7-diboronic acid bis(pinacol) ester.

Analytical data of 2-(2-Bromoethoxy)tetrahydro-2H-pyran

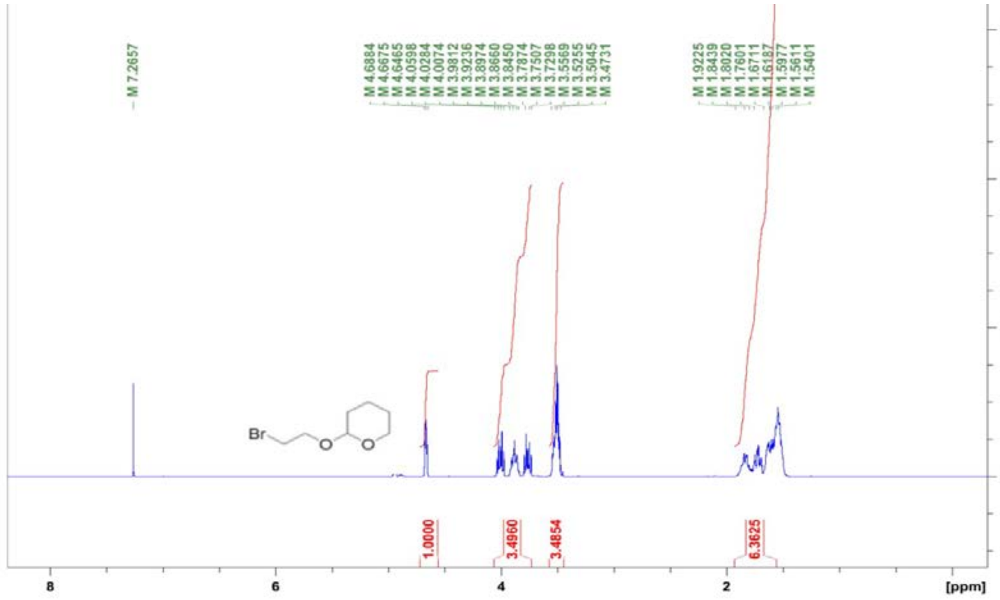

Figure S6.3:^{1}H NMRspectrum of 2-(2-Bromoethoxy)tetrahydro-2H-pyran.

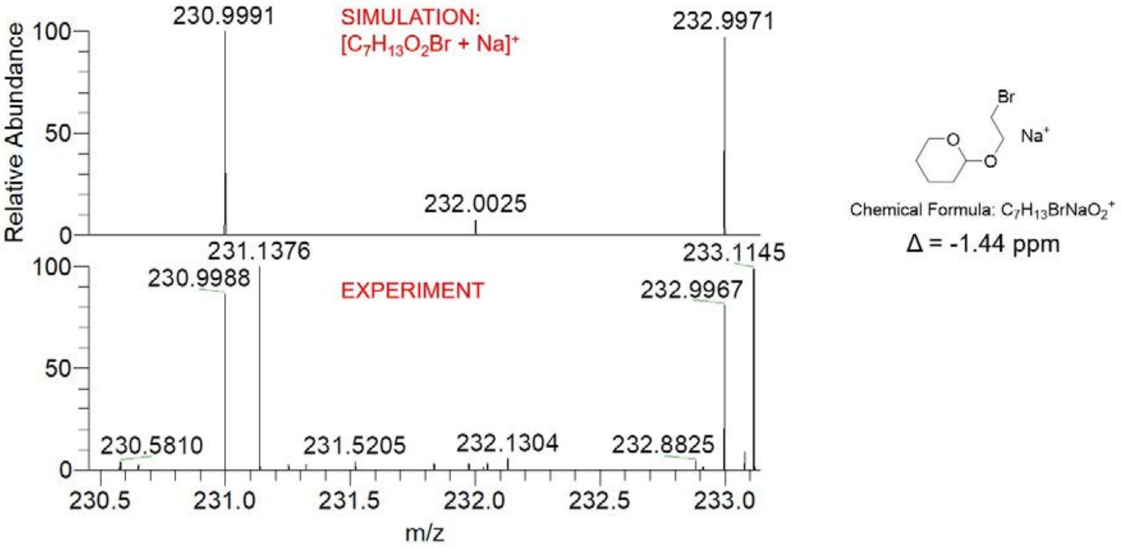

Figure S6.4:MSspectrum of 2-(2-Bromoethoxy)tetrahydro-2H-pyran.

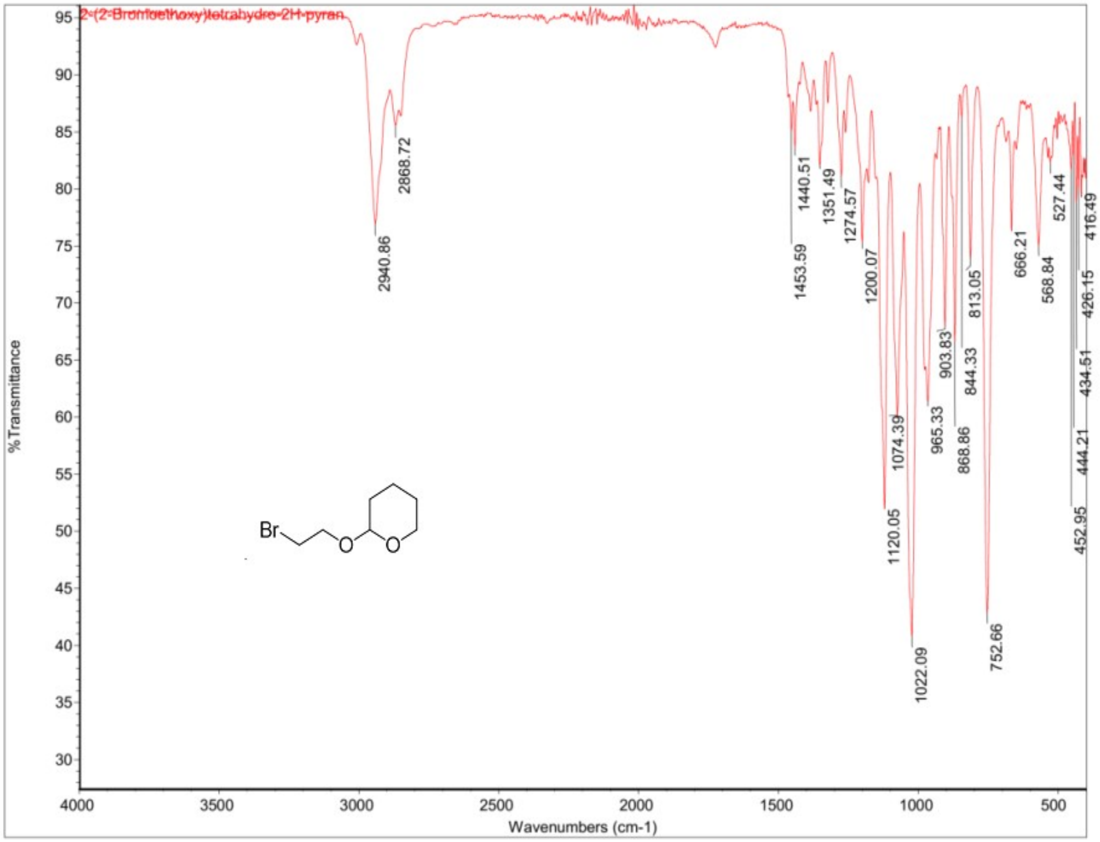

Figure S6.5:FTIRspectrum of 2-(2-Bromoethoxy)tetrahydro-2H-pyran.

Analytical data of 2,7-dibromo-9,9-di(2-(2-tetrahydropyranyloxy)ethyl)-fluorene

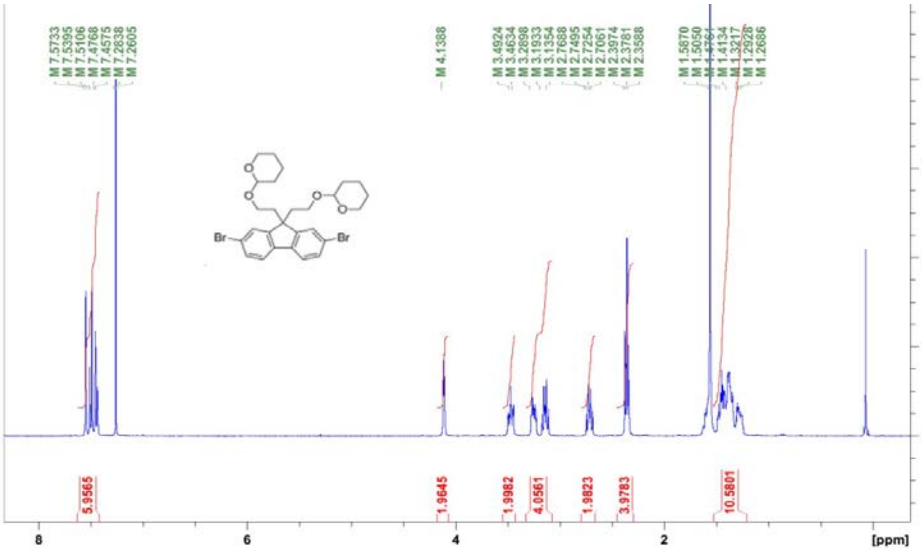

Figure S6.6:^{1}H NMR spectrum of 2,7-dibromo-9,9-di(2-(2-tetrahydropyranyloxy)ethyl)-fluorene.

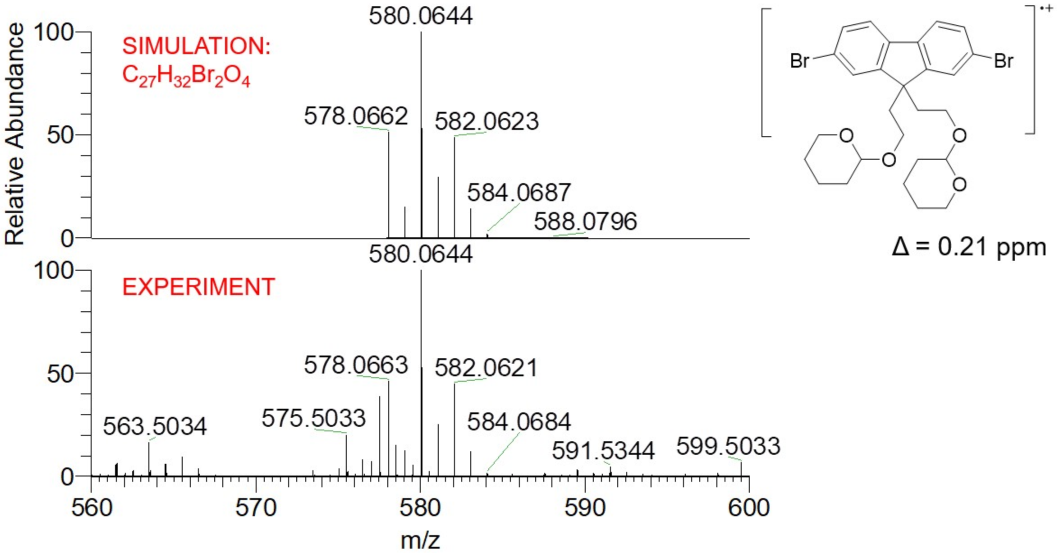

Figure S6.7:MS spectrum of 2,7-dibromo-9,9-di(2-(2-tetrahydropyranyloxy)ethyl)-fluorene.

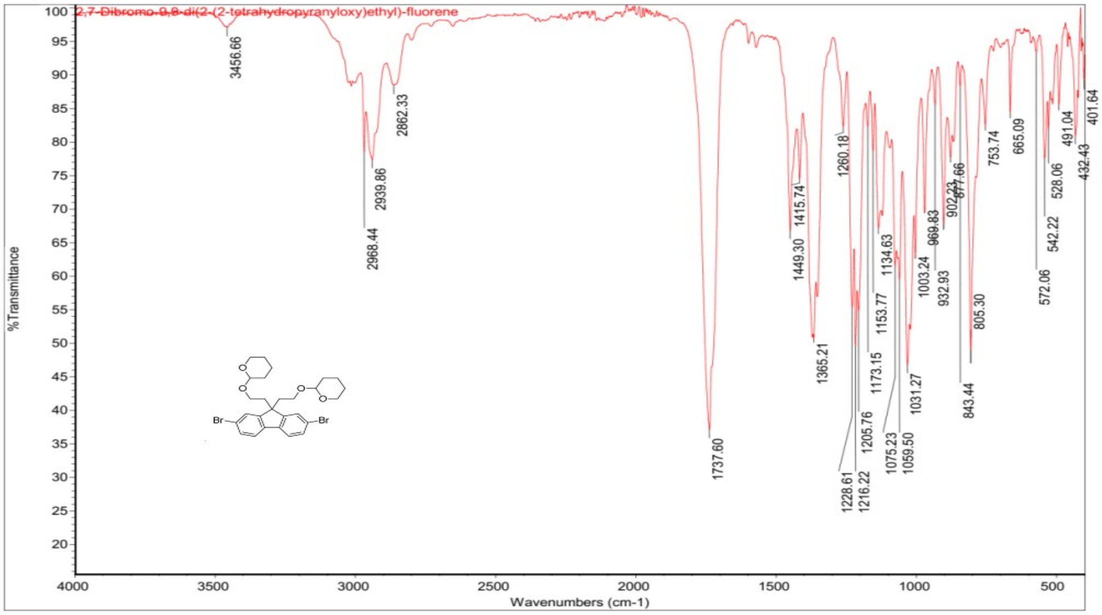

Figure S6.8:FTIR spectrum of 2,7-dibromo-9,9-di(2-(2-tetrahydropyranyloxy)ethyl)-fluorene

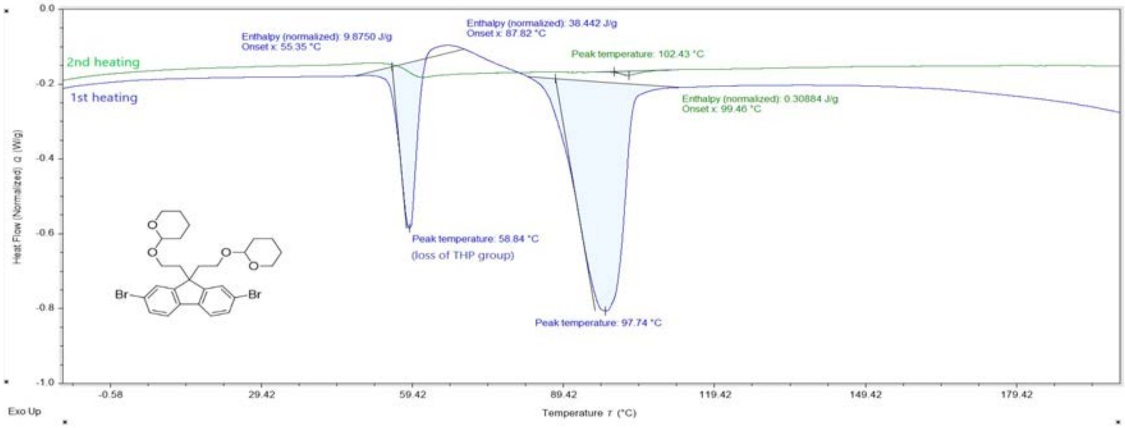

Figure S6.9:DSC heating curves of 2,7-dibromo-9,9-di(2-(2-tetrahydropyranyloxy)ethyl)-fluorene

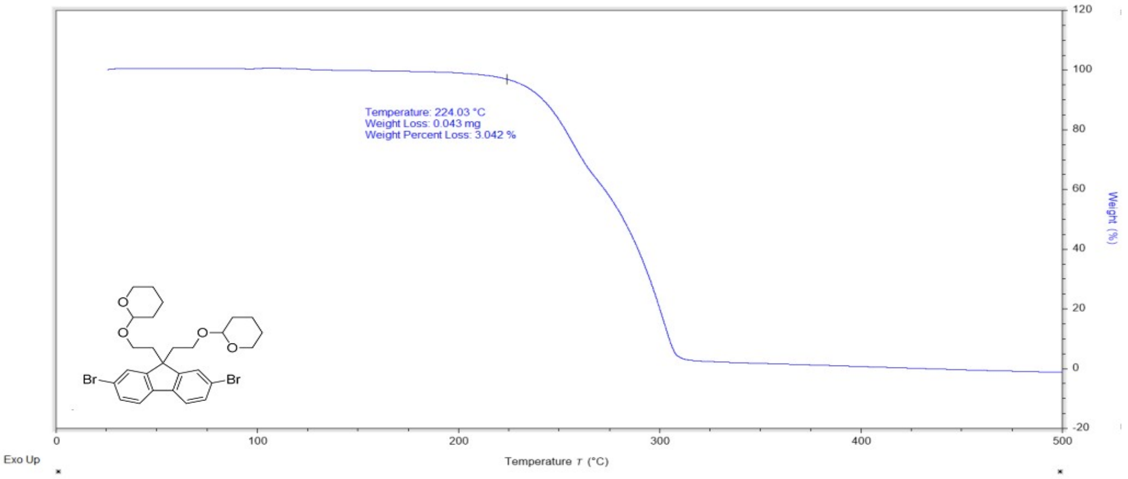

Figure S6.10:TGA thermogram of 2,7-dibromo-9,9-di(2-(2-tetrahydropyranyloxy)ethyl)-fluorene.

Analytical data of 9,9-bis(2-(2-tetrahydropyranyloxy)ethyl)-fluorene-2,7-diboronic acid bis(pinacol) ester

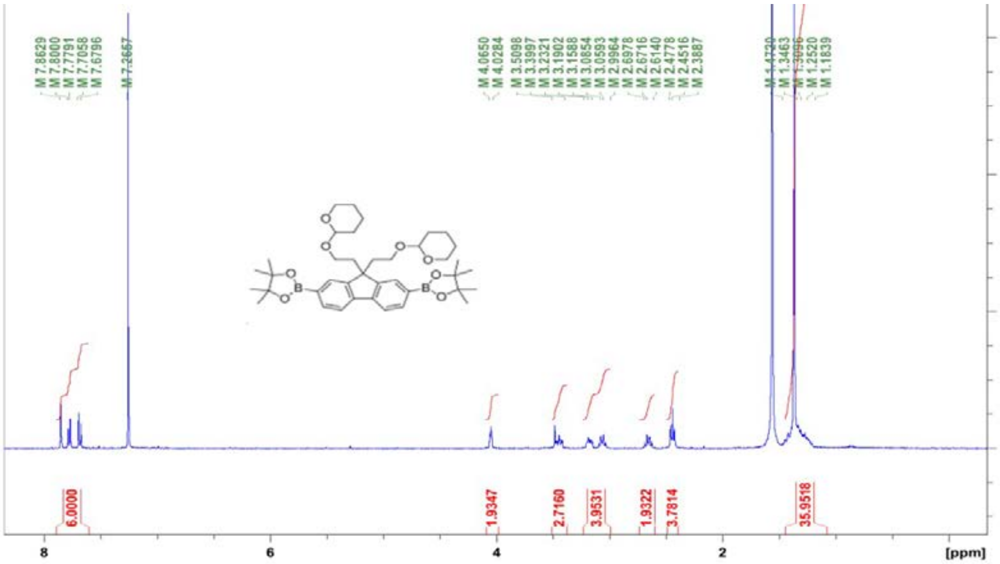

Figure S6.11:^{1}H NMR spectrum of 9,9-bis(2-(2-tetrahydropyranyloxy)ethyl)-fluorene-2,7-diboronic acid bis(pinacol) ester.

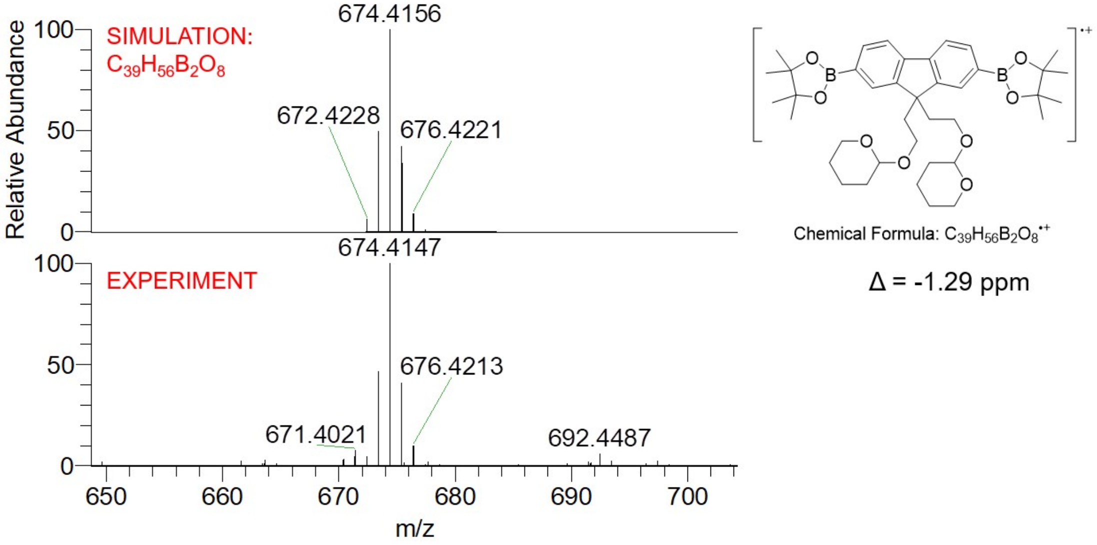

Figure S6.12:MS spectrum of 9,9-bis(2-(2-tetrahydropyranyloxy)ethyl)-fluorene-2,7-diboronic acid bis(pinacol) ester.

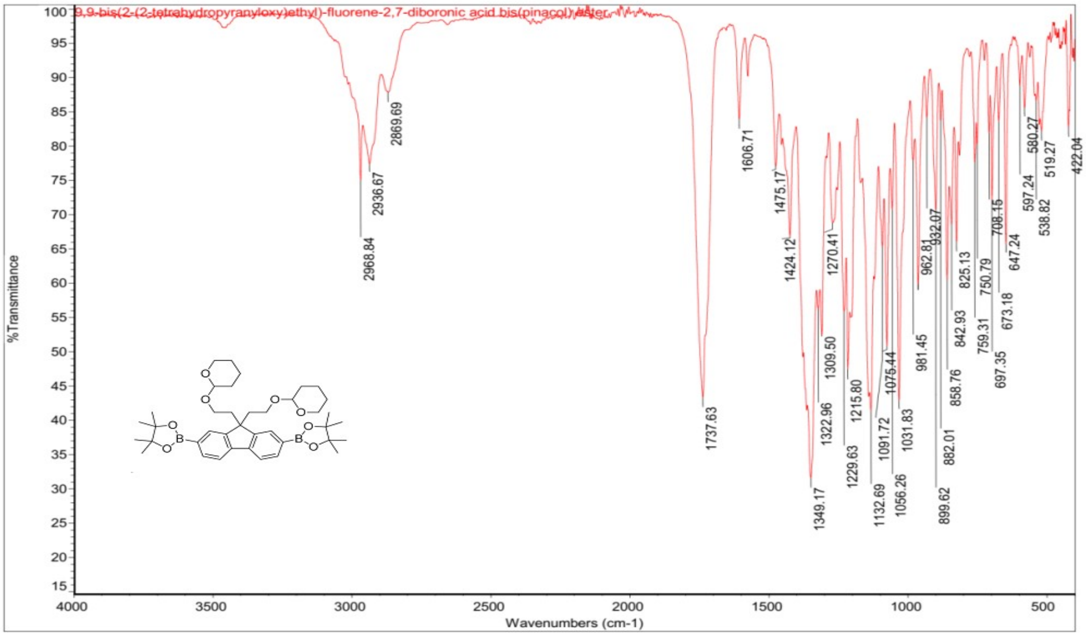

Figure S6.13:FTIR spectrum of 9,9-bis(2-(2-tetrahydropyranyloxy)ethyl)-fluorene-2,7-diboronic acid bis(pinacol) ester.

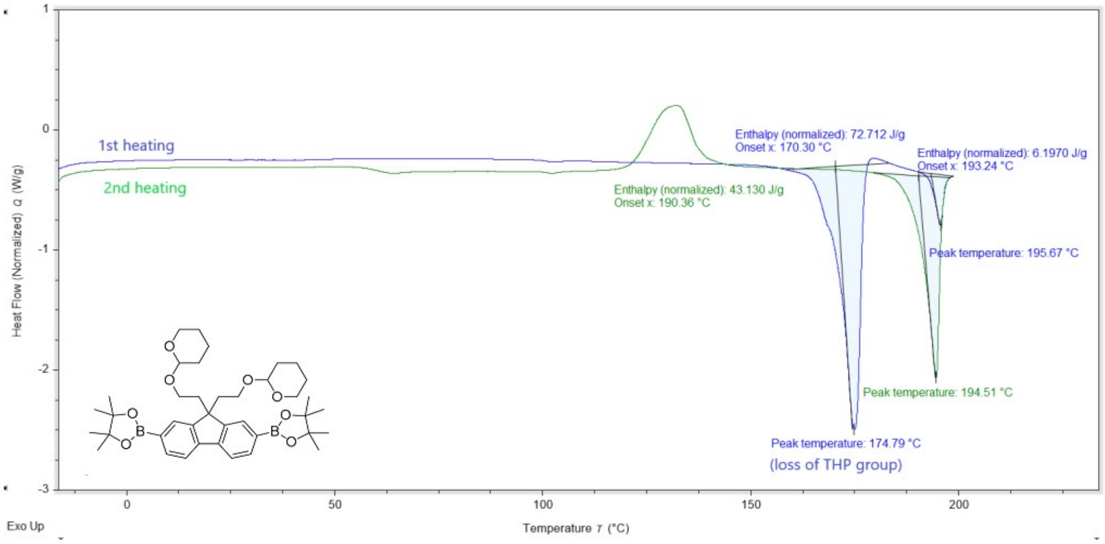

Figure S6.14:DSC heating curves of 9,9-bis(2-(2-tetrahydropyranyloxy)ethyl)-fluorene-2,7-diboronic acid bis(pinacol) ester.

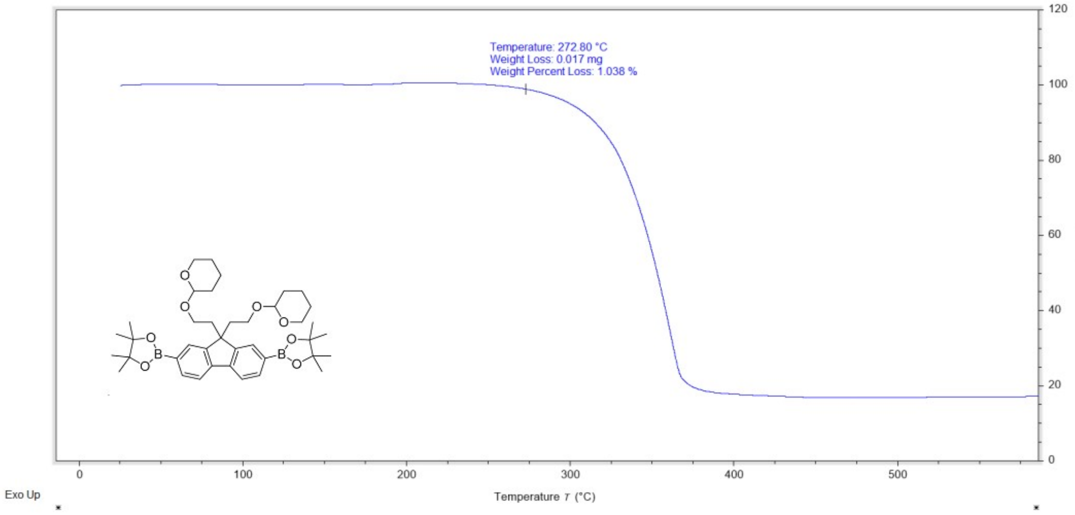

Figure S6.15:TGA thermogram of 9,9-bis(2-(2-tetrahydropyranyloxy)ethyl)-fluorene-2,7-diboronic acid bis(pinacol) ester.

Analytical data of P7

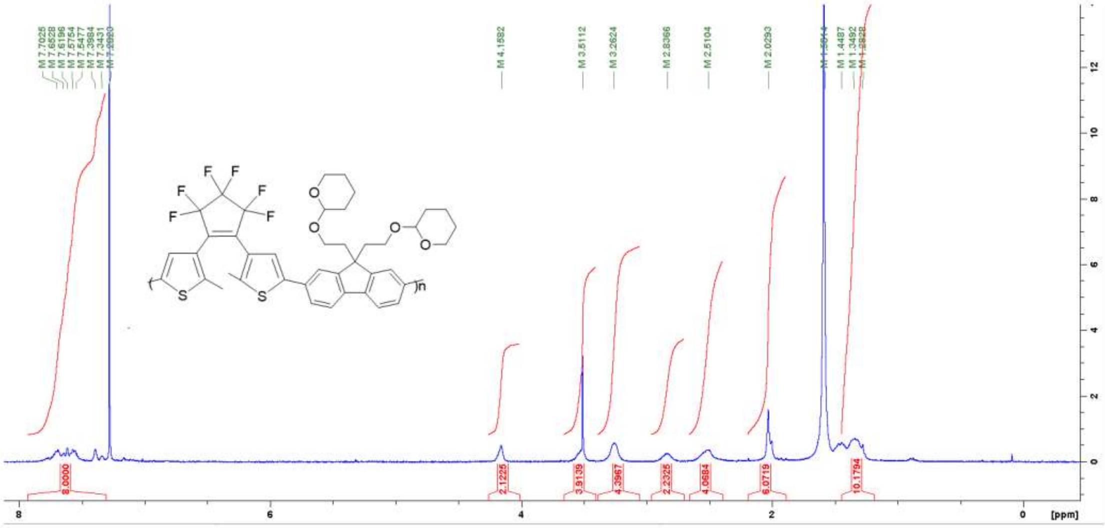

Figure S6.16: 1H NMR spectrum of P7.

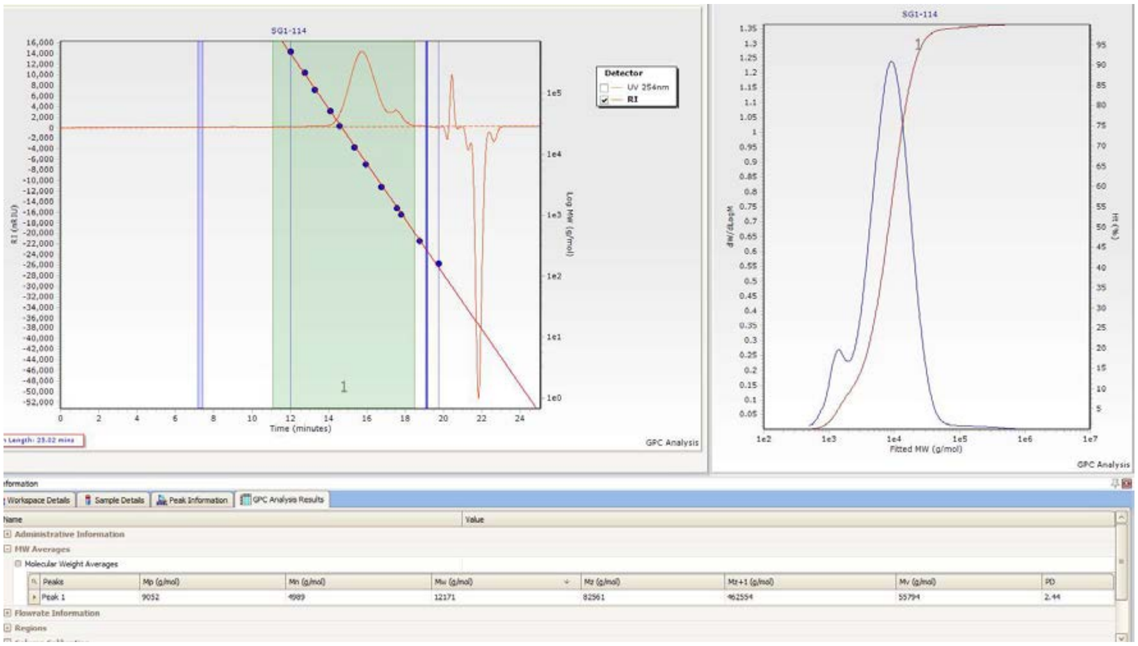

Peaks	Mp (g/mol)	Mn (g/mol)	Mw (g/mol)	Mz (g/mol)	Mz+1 (g/mol)	Mv (g/mol)	PD
Peak 1	9052	4989	12171	82561	462554	55794	2.44

Figure S6.17: 1H NMR spectrum of P7.

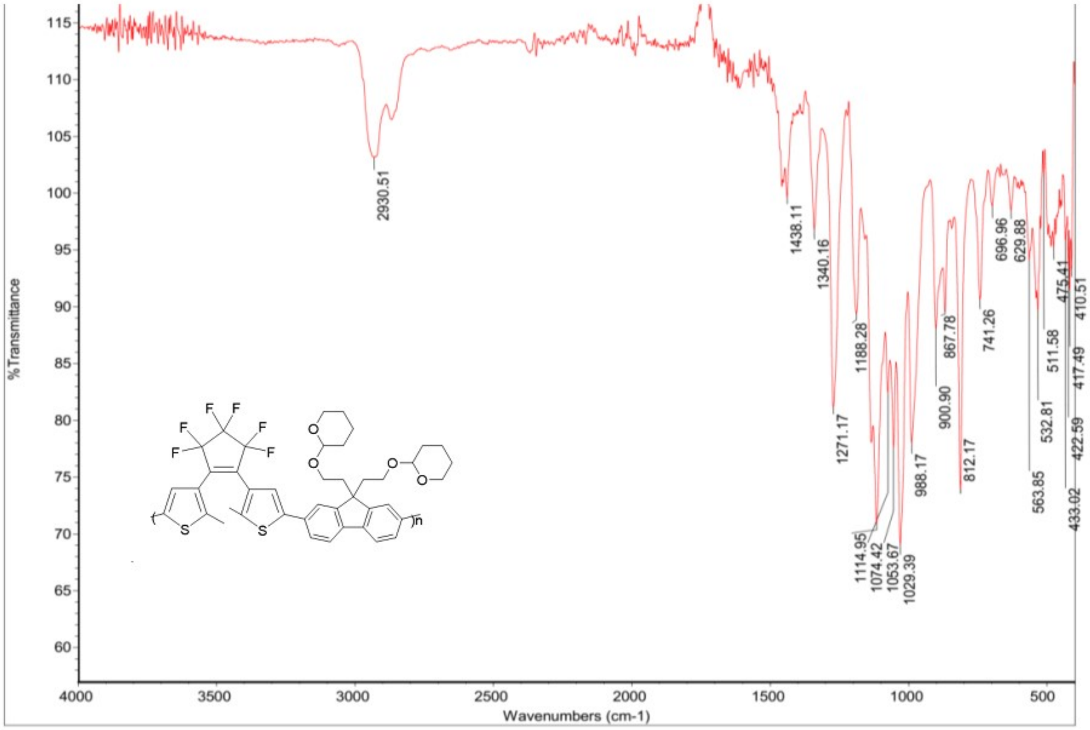

Figure S6.18:FTIR spectrum of P7.